THE HANDBOOK OF RADIOPHARMACEUTICALS

Azuwuike Owunwanne,
Mohan Patel
and
Samy Sadek

CHAPMAN & HALL MEDICAL

The Handbook of
Radiopharmaceuticals

The Handbook of Radiopharmaceuticals

Azuwuike Owunwanne

Department of Nuclear Medicine
Faculty of Medicine, Kuwait University, Kuwait

Mohan Patel

Kuwait Central Radiopharmacy
Kuwait Cancer Control Center
Ministry of Public Health, Kuwait

and

Samy Sadek

Department of Nuclear Medicine
Faculty of Medicine, Kuwait University, Kuwait

CHAPMAN & HALL MEDICAL
London · Glasgow · Weinheim · New York · Tokyo · Melbourne · Madras

Published by Chapman & Hall, 2–6 Boundary Row, London SE1 8HN, UK

Chapman & Hall, 2–6 Boundary Row, London SE1 8HN, UK

Blackie Academic & Professional, Wester Cleddens Road, Bishopbriggs, Glasgow G64 2NZ, UK

Chapman & Hall GmbH, Pappelallee 3, 69469 Weinheim, Germany

Chapman & Hall USA, One Penn Plaza, 41st Floor, New York NY 10119, USA

Chapman & Hall Japan, ITP-Japan, Kyowa Building, 3F, 2-2-1 Hirakawacho, Chiyoda-ku, Tokyo 102, Japan

Chapman & Hall Australia, Thomas Nelson Australia, 102 Dodds Street, South Melbourne, Victoria 3205, Australia

Chapman & Hall India, R. Seshadri, 32 Second Main Road, CIT East, Madras 600 035, India

First edition 1995

Softcover reprint of the hardcover 1st edition 1995

Typeset by EXPO Holdings, Malaysia

ISBN 978-1-4757-0416-7 ISBN 978-1-4757-0414-3 (eBook)
DOI 10.1007/978-1-4757-0414-3

A catalogue record for this book is available from the British Library

Printed on permanent acid-free text paper, manufactured in accordance with ANSI/NISO Z39.48-1992 and ANSI/NISO Z39.48-1984 (Permanence of Paper).

This book is dedicated with gratitude to our parents and families

Contents

Preface

The *Handbook of Radiopharmaceuticals* is intended to bring together the salient features of the chemical, biologic and radiopharmacy aspects of radiopharmaceuticals. It is designed for nuclear medicine technology students, nuclear medicine and radiology residents, radiopharmacists, radiochemists, physicians, physicists and other scientists with an interest in nuclear medicine, for whom the handbook will be a quick reference book. The book emphasizes:

- the practical aspects of preparation, quality control testing and dispensing of radiopharmaceuticals (and therefore is a very useful tabletop reference manual for technologists and radiopharmacists);
- the interrelationship between the effects of chemistry and biology on the biodistribution and elimination of administered radiopharmaceuticals;
- the uses and radiation absorbed doses of each radiopharmaceutical.

The book is divided into four parts that can be read independently. In Part One we describe the theoretical considerations of the production, quality control testing, design and biologic disposition of administered radiopharmaceuticals. In Part Two, we describe and discuss the chemistry, practical aspects of in-house preparation, quality control testing, biologic behavior, uses and dosimetry of each radiopharmaceutical. The information on biologic behavior is derived mainly from human data. In Part Three, we discuss a system approach for good radiopharmacy practice. And in Part Four, relevant theoretical and practical information is given as appendices.

To fully understand and appreciate Chapter 1, we recommend prior knowledge of radiation physics. We have tried as much as possible to include all the available latest materials, but as is always the case we might have missed out a few radiopharmaceuticals that are currently under development.

To our readers, we will appreciate any comments you may have both on the format and content of this handbook.

A. Owunwanne
M. Patel
S. Sadek
Kuwait

Acknowledgments

Many people have contributed to the writing of this handbook. We would like to thank all of them, especially Drs Hussein Abdel-Dayem, David Weber, Mathew Thakur, Abdelhamid Elgazzar, Fawaz Al-Huda, Raghuveer Halkar, Iman Al-Shammary and Qansy Salako and Mr Jacob George Tharayillthu for reading and reviewing the manuscript while it was in preparation. We appreciated their comments and contributions. We would like to thank the Faculty of Medicine, Kuwait University, for the relevant facilities used in the preparation of this book. We would also like to thank Mrs Delphine D'Souza for her untiring secretarial assistance and our editors Ms Linda Yelverton, Dr Peter Altman, Ms Lynne Maddock and the Production Department, Chapman & Hall. We would also like to thank our colleagues with whom we discussed different portions of this book; technologists for their technical drawings; students and residents on whom we tried out different portions of this handbook as teaching materials; and personal friends whose moral support and encouragement kept us going when we felt otherwise. Finally, we would like to thank our wives and children for their support and understanding during the writing of this handbook.

Part One

Radiobiopharmaceutics

The term radiobiopharmaceutics includes the theoretical consideration of the production, quality control and fate of administered radiopharmaceuticals. Radionuclide production, particularly nuclear reactor and accelerator reactions, are described briefly. However, the ^{99}Mo–^{99m}Tc generator is described in detail because of the central role of ^{99m}Tc in radionuclide imaging. In Chapter 5, The fate of administered radiopharmaceuticals, we take a new approach to discussing uptake and clearance mechanisms and the biologic behavior of administered radiopharmaceuticals from a holistic perspective. Chapter 6, Drug–radiopharmaceutical interactions, is written from a practical perspective.

1

Preparation of radiopharmaceuticals

The preparation of radiopharmaceuticals involves three basic steps: production of the radionuclides, synthesis of the non-radioactive compound and reaction of the radionuclide with the non-radioactive compound.

PRODUCTION OF RADIONUCLIDES

The first step in the preparation of radiopharmaceuticals is the production of an appropriate radionuclide. There are two main sources for the production of radionuclides which are useful for nuclear medicine procedures. These are primary and secondary sources. The primary source involves the direct production of radionuclides from either a nuclear reactor or a particle accelerator. The secondary source involves an indirect method of producing a radionuclide from a system known as radionuclide generator.

PRIMARY SOURCE

Nuclear reactors

In a nuclear reactor, a stable nucleus of a chemical compound is bombarded with low-energy or thermal neutrons. By absorbing the neutrons, the nucleus of the bombarded atom is rearranged and thus becomes unstable (radioactive). This instability is followed by emission of particles (protons or alpha particles), gamma rays or fission. This nuclear reaction can be symbolically represented as

$$(n,p),(n,{}^4He),(n,\gamma) \text{ or } (n,f)$$

where n is a neutron, p is a proton, ^{4}He is an alpha particle or helium nucleus, γ is a gamma ray and f is fission. In nuclear medicine procedures, the (n,γ) and (n,f) reactions are the most important methods of producing radionuclides in a nuclear reactor.

(n,γ) process

This process can be depicted schematically as

$$^A_Z X(n,\gamma)^{A+1}_Z X$$

where X is an element and A and Z are its mass number and atomic number respectively. The process is exemplified by

$$^{98}Mo(n,\gamma)^{99}Mo \xrightarrow{\beta^-} {}^{99m}Tc.$$

The above (n,γ) reaction involves irradiation of molybdenum-98 to produce molybdenum-99. The natural abundance of ^{98}Mo is 24.13% and the cross-section of thermal neutrons is 0.13 barns. Irradiation is done in a neutron flux of 10^{13} n/cm^2/s for 3–7 days. In order to produce ^{99}Mo with high specific activity and fewer radionuclidic contaminants, it is important to use highly enriched ^{98}Mo, and the preferred chemical form is the trioxide (MoO_3). Associated radionuclidic impurities are listed in Table 1.1.

Table 1.1 Radionuclidic impurities in $^{98}Mo(n,\gamma)$ ^{99}Mo process

Radionuclide	*Half-life*
^{60}Co	5.3 years
^{95}Zr	65.5 days
^{95}Nb	35.6 days
^{110m}Ag	249.9 days
^{124}Sb	60.4 days
^{134}Cs	2.1 days
^{185}W	75.1 days
^{187}W	23.8 hours
^{186}Re	90.6 hours
^{188}Re	17.0 hours
^{192}Ir	74.3 days

Note: When highly enriched MoO_3 is irradiated, the level of impurity due to each radionuclide is of the order of 1×10^{-5}% and therefore is of no practical consequence.

Other examples of (n,γ) reactions which are useful in nuclear medicine procedures are:

$$^{50}Cr(n,\gamma)\,^{51}Cr;\ ^{58}Fe(n,\gamma)\,^{59}Fe$$

$$^{130}Te(n,\gamma)\,^{131}Te \xrightarrow{\beta^-} {}^{131}I$$

$$^{124}Xe(n,\gamma)\,^{125}Xe \xrightarrow{EC} {}^{125}I$$

Note that the starting material and products have the same chemical identity in these (n,γ) reactions. (EC = electron capture.)

(n,f) process

This is exemplified by

$$^{235}U(n)\,^{236}U(f) \rightarrow {}^{99}Mo + {}^{135}Sn + 2n$$
$$^{131}I + {}^{102}Y + 3n$$
$$^{137}Cs + {}^{97}Rb + 2n$$

The above (n,f) reaction involve irradiation of uranium-235 in the form of the dioxide (UO_2) to produce ^{236}U, which fissions into other radionuclides with lower atomic numbers, as in the examples above. High specific activity ^{99}Mo in the form of ammonium molybdate is chemically separated from the other fission products and is used for the production of ^{99}Mo–^{99m}Tc generators. Other radionuclides produced by (n,f) reactions and which are useful in nuclear medicine procedures include ^{87m}Sr, ^{113m}Sn, ^{131}I, ^{133}Xe and ^{137}Cs. Note that

- for fission reaction to occur, the nucleus of the element will have a mass number equal to or greater than 200;
- the starting material and products have different chemical identity in (n,f) reactions.

Particle accelerators

There are two types of particle accelerators: linear and cyclotron. The stable nucleus of the chemical compound is bombarded with charged particles such as electrons, protons, deuterons and alpha particles. In a linear accelerator, the bombarding particles are accelerated along a linear path using an electric current and voltage for control, while in a cyclotron the bombarding particles are accelerated along a circular path using an electric current and magnetic field for control. The charged particles are provided with sufficient energy to overcome the barrier surrounding the nucleus (Coulomb barrier). A summary of nuclear reactor and cyclotron processes is given in Table 1.2.

Examples

$$^{68}Zn(p,2n)\,^{67}Ga;\ ^{201}Hg(d,2n)\,^{201}Tl$$

$$^{203}Tl(p,3n)\,^{201}Pb \xrightarrow{\beta^+ \text{or EC}} {}^{201}Tl$$

$$^{205}Tl(p,5n)\,^{201}Pb \xrightarrow{\beta^+ \text{or EC}} {}^{201}Tl$$

Note that

- the ^{203}Tl is enriched while ^{205}Tl is naturally occurring;
- the starting material and product have different chemical identities.

Table 1.2 Summary of nuclear reactor and cyclotron processes

Property	*Nuclear reactor*	*Cyclotron*
Mode of production	Neutron bombardment	Charged particle bombardment
Major reactions	(n, γ),(n, p),(n, d), (n, f)	(d, n),(α, d),(α, np), (p, n)
Neutron–proton ratio	Neutron excess Proton deficient	Neutron deficient Proton excess
Mode of decay of daughter radionuclide	β^-	β^+, EC
Specific activity	(n, γ) low (n, f) high	High
Cost of production	Low	High
Chemical identity of starting material and product	(n, γ) same (n,f) different	Different

SECONDARY SOURCE

This is the indirect method of producing radionuclides using a generator system which is constructed in such a way that it is chemically easy to separate the daughter from the parent radionuclide at local hospitals or central radiopharmacies. The ideal characteristics of a radionuclide generator are as follows:

- The design and construction of the generator should be such that it is portable and surface radiation exposure should not exceed 200 mR/h at any point.
- The generator should be able to be stored at room temperature.
- The separation technique of the daughter from the parent radionuclide should be easy to perform.
- The separated product should be sterile, pyrogen free and preferably in physiologic solution.
- The yield of separation should not be less than 80%, the specific activity and activity concentration should be high.
- No parent radionuclide or other radionuclidic impurity should be present in the final product.
- The half-life of the parent radionuclide should be short enough for the daughter to grow in but long enough to be practically useful.
- The daughter radionuclide should have ideal gamma energy for imaging.
- The chemistry of the daughter radionuclide should allow for in-hospital preparation of other radiopharmaceuticals.
- The grand-daughter radionuclide should have a stable nucleus or a very long half-life so as not to cause any radiation dose when administered to a patient.

Various generators are commercially available, and these include molybdenum-99–technetium-99m (^{99}Mo–^{99m}Tc), tin-113–indium-113m (^{113}Sn–^{113m}In), rubidium-81–krypton-81m (^{81}Rb–^{81m}Kr), strontium-82–rubidium-82 (^{82}Sr–^{82}Rb) and germanium-68–gallium-68 (^{68}Ge–^{68}Ga). Of these, the most important and the most frequently used is the

Table 1.3 Other generators

Daughter radionuclides	^{113m}In	^{81m}Kr	^{82}Rb	^{68}Ga
Half-life (min)	100	0.22	1.33	68
Gamma energy (keV)	393	193	511, 777	511
Mode of decay	IT	IT	β^+	β^+
Parent radionuclides	^{113}Sn	^{81}Rb	^{82}Sr	^{68}Ge
Half-life (days)	118	0.20	25	275
Mode of production	^{112}Sn (n,γ)	^{79}Br (α,2n)	^{80}Kr (α,2n)	^{69}Ga (p,2n)
Type of generator	Column	Column	Column	Column
Adsorbent material	Hydrous zirconium oxide, alumina	None	Hydrous stannic oxide	Alumina
Eluent	0.05 N HCl or HNO_3	Humidified oxygen or air	Physiologic saline	1 N HCl

IT, isomosic transition.

Notes:
1. Because of the long half-lives of ^{113}Sn (118 days) and ^{68}Ge (275 days) both generators may be bought once or twice a year.
2. The short half-life of ^{81}Rb (4.7 h) poses many practical handling problems. As a result, the ^{81}Rb–^{81m}Kr generator is not commonly used.
3. With recent advancements in positron emission tomographic (PET) imaging, both ^{82}Sr–^{82}Rb and ^{68}Ge–^{68}Ga generators are commercially available and may find wide use at PET centers.

^{99}Mo–^{99m}Tc generator, which is described in detail. The salient features of other generators are given in Table 1.3.

^{99}Mo–^{99m}Tc generator systems

The rapid development of nuclear medicine is due in part to the development of the technology of this generator. There are various types: column, sublimation and solvent extraction [1–3].

COLUMN GENERATOR

A schematic diagram of a column generator is given in Figure 1.1. Listed below are radiochemicals and chemicals involved in the construction and operation of the ^{99}Mo–^{99m}Tc generator.

Parent radionuclide	^{99}Mo
Parent radiochemical	$^{99}MoO_4^{2-}$ (molybdate ion)
Daughter radionuclide	^{99m}Tc
Daughter radiochemical	$^{99m}TcO_4^-$ (pertechnetate ion)
Eluent	0.9% NaCl (physiologic saline)
Adsorbent material	Alumina (aluminum oxide, Al_2O_3)
Eluate	$^{99m}TcO_4^-$

The relative difference in the affinity of MoO_4^{2-} and TcO_4^- for alumina is the basis for the separation of ^{99m}Tc from ^{99}Mo in a column generator. When physiologic saline is passed through an alumina column containing adsorbed $^{99}MoO_4^{2-}$ and $^{99m}TcO_4^-$, the latter is selectively

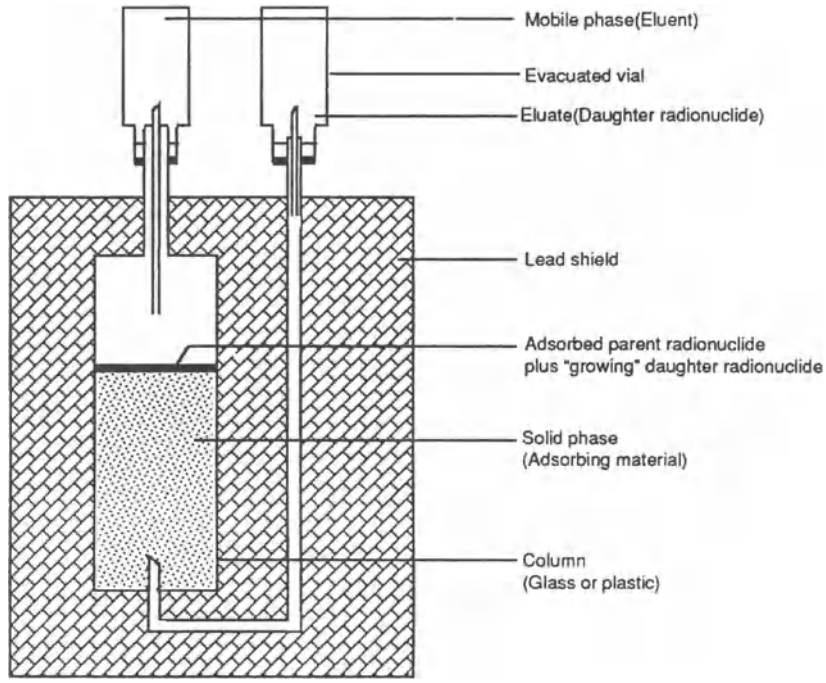

Figure 1.1 A ^{99}Mo–^{99m}Tc column generator.

eluted. High specific activity ^{99}Mo obtained from either the fission product of ^{236}U or neutron activation of enriched ^{98}Mo can be used in column generators. The column size is small, therefore it requires small shielding, which makes the generator easily portable. Its radiochemical, radionuclidic and biologic impurities are checked and controlled by the manufacturers before shipping to the local hospital or central radiopharmacy. The column-type generator is the most widely used ^{99}Mo–^{99m}Tc generator, of which there are two types: wet and dry generators.

Wet generator The top of the column is attached to reservoir of the eluent. It is eluted with an evacuated vial by opening a spigot. Between elutions the column is always wet.

Dry generator The column is not attached to reservoir of eluent. To elute, a vial containing the eluent is placed onto another port which is attached to the bottom of the column. Between elutions, the column is dry. The dry-type generator may trap air bubbles. To get rid of the air bubbles, a dry elution should be done with an evacuated vial.

Equation for calculating the yield from a column generator

$$(A_{99m_{Tc}}) = 0.956(A_{99_{Mo}})_t$$

where $(A_{99_{Mo}})_t = (A_{99_{Mo}})_0\ (e^{-0.0103t})$, $(A_{99_{Mo}})_0$ is the radioactivity of ^{99}Mo at time zero or the last elution and t is the time elapsed after the last elution.

Example of calculation A 14.8 GBq ^{99}Mo–^{99m}Tc generator calibrated for Wednesday, 12.00 noon, was delivered on Sunday. Assume that transient equilibrium has been established and that the elution efficiency is 80%:

1. Calculate the amount of $^{99m}TcO_4^-$ radioactivity to be eluted on Thursday, 12.00 noon.
2. Suppose that the generator was eluted on Monday, preceding the calibration date, calculate the amount of $^{99m}TcO_4^-$ eluted at 08.00 am.

Solution

1. Amount of ^{99}Mo on Thursday 12.00 noon will be

$$A_{^{99}Mo} = (14.8 \times e^{-0.0103 \times 24}) \text{ GBq}$$
$$= 11.56 \text{ GBq}$$
$$A_{^{99m}Tc} = (11.56 \times 0.956 \times 0.8) \text{ GBq}$$
$$= 8.84 \text{ GBq}$$

2. Amount of ^{99}Mo on Monday 08.00 am preceding calibration date will be

$$A_{^{99}Mo} = (14.8 \times e^{+0.0103 \times 52}) \text{ GBq}$$
$$= 25.28 \text{ GBq}$$
$$A_{^{99m}Tc} = (25.28 \times 0.956 \times 0.8) \text{ GBq}$$
$$= 19.33 \text{ GBq}$$

Probable impurities in the eluate Probable impurities are ^{99}Mo and aluminum ion, Al^{3+}. ^{99}Mo comes from the parent radionuclide. It is necessary by law to check its presence in administered ^{99m}Tc radiopharmaceuticals. The United States Pharmacopeia limit is 0.15 μCi of ^{99}Mo per mCi of ^{99m}Tc and the total in any administered dose should not exceed 2.5 μCi^{99}Mo. The $A1^{3+}$ ion comes from the the absorbent material. The US Pharmacopeia limit is 10 μg/ml in administered solution. Its presence may interfere with the preparation of colloids.

Advantages Column generators are portable and simple to operate. The $^{99m}TcO_4^-$ is in a physiologic solution, does not need any further processing, is separated with high efficiency (80%) and has an excellent elution profile.

Disadvantages Initial high capital investment for fission processing plant is required. There are special problems associated with the processing of fission products to separate carrier-free ^{99}Mo from other radionuclides. There is also the problem of disposing of the unwanted radionuclides. The cost per mCi of ^{99m}Tc is high.

SUBLIMATION GENERATOR

Parent radionuclide	^{99}Mo
Parent radiochemical	$^{99}MoO_3$(molybdenum trioxide)
Daughter radionuclide	^{99m}Tc
Daughter radiochemical	$^{99m}Tc_2O_7$ (ditechnetium heptaoxide)
Boiling point of Tc_2O_7	310.6°C
Melting point of MoO_3	795°C
Boiling point of MoO_3	1150°C

The difference in volatility between Tc_2O_7 and MoO_3 is the basis for the separation of ^{99m}Tc from ^{99}Mo in a sublimation generator. Irradiated $^{99}MoO_3$ is loaded into a horizontal tube furnace and heated to a temperature of 850°C in a stream of oxygen. Technetium-99m in the form of Tc_2O_7 is separated from the molten MoO_3 and is condensed on a cold

surface. The condensed $^{99m}Tc_2O_7$ is dissolved in physiologic saline and sterilized.

Probable impurities A trace amount of MoO_3 may be present.

Advantages Inexpensive low specific activity ^{99}Mo can be used. No chemical processing is required. It has high chemical purity. The cost per mCi of ^{99m}Tc is low.

Disadvantages It is not commonly used in hospitals. Its separation efficiency is poor (25–50%).

SOLVENT EXTRACTION GENERATOR

Parent radionuclide	^{99}Mo
Parent radiochemical	$^{99}MoO_4^{2-}$
Daughter radionuclide	^{99m}Tc
Daughter radiochemical	$^{99m}TcO_4^-$
Organic solvent	Methyl ethyl ketone (MEK)
Aqueous solvent	Potassium hydroxide (KOH)

The relative difference in the solubility coefficients of and MoO_4^{2-} and TcO_4^- in MEK is the basis for separation of ^{99m}Tc from ^{99m}Mo in a solvent extraction generator. The TcO_4^- is preferentially extracted into MEK from an alkaline solution of MoO_4^{2-}. Low specific activity ^{99}Mo in 5 N KOH is brought into vigorous contact with MEK. The ^{99}Mo in aqueous alkaline solution in the lower layer is separated and stored for re-use, while the (organic) upper layer of MEK containing $^{99m}TcO_4^-$ is passed through a small Al_2O_3 column for purification. The MEK solution is carefully evaporated to dryness. The residue is reconstituted in physiologic saline and subjected to membrane filtration (0.22 μm).

Probable impurities ^{99}Mo and other radionucides listed in Table 1.1 may be present. Radiolytic products of MEK, polymeric organic impurities and the Al^{3+} ion may be also be found.

Advantages Inexpensive low specific activity ^{99}Mo can be used. It is an extremely useful method of obtaining low-cost ^{99m}Tc in developing countries. It has high separation efficiency (85–90%).

Disadvantages Highly trained personnel are required. There is a possibility of fire hazard owing to the use of MEK. The polymeric organic impurities may interfere with the labeling procedure and lead to undesirable biologic distribution.

A comparison of various types of ^{99m}Mo–^{99m}Tc generators is given in Table 1.4.

SYNTHESIS OF THE NON-RADIOACTIVE COMPOUND

The second step in the preparation of radiopharmaceuticals is the organic/inorganaic synthesis of the non-radioactive compound. The synthesis may be a simple one-step mixing and refluxing of the appropriate reagents or a complex, multistep procedure involving different physicochemical conditions. Depending on the nature of the clinical study, the non-radioactive compound may function as a 'carrier compound' (methylene diphosphonate) which transports the radionuclide to the target organ/tissue, or it may be a complexing or chelating agent (ligand) which upon reaction with the radionuclide forms a 'new compound' with different chemical and biologic properties (iminodiacetate derivatives). Brief descriptions of the chemistry of

Table 1.4 Comparison of various types of ^{99}Mo–^{99m}Tc generators

	Column		*Sublimation*	*Solvent extraction*
	Mo-99 separated from fission	*Mo-99 obtained from enriched Mo-98*		
Operation of generator	Simple	Simple	Complex	Complex
Portable	Yes	Yes	Feasible	No
Radiation dose to personnel	Low	Low	High	High
Yield of $^{99m}TcO_4^-$	High (80%)	High (80%)	Low (25–50%)	High (85%–90%)
Probable impurity in $^{99m}TcO_4^-$	Low	Low	Low	Low
Specific activity of ^{99}Mo	Carrier-free	Not carrier-free	Not carrier-free	Not carrier-free
Waste disposal problems associated with production of ^{99}Mo	High	Low	Low	Low
Overall cost	High	Very high	Low	Low
Potential for large-scale production	High	Low	Low	Low

the synthesis of these non-radioactive compounds are given in Part Two. However, a few comments are in order. The non-radioactive compound should be such that it

- is amenable to 'kit' formulation;
- can provide a 'backbone' molecule suitable for chemical modification and/or substitution;
- can maximize the *in vivo* stability of the final product unless biotransformation is required to produce either a long residence time or fast transit through the target organ;
- is not toxic and does not have any adverse effects at the milligram dose level;
- can stabilize any of the lower oxidation states of technetium in an aqueous medium for the preparation of ^{99m}Tc radiopharmaceuticals;
- can be radiolabeled by simple exchange reaction in the final step of the preparation of iodine radiopharmaceuticals.

The non-radioactive compound should be characterized both chemically and structurally using both chemical and physical methods. These methods include melting point determination, elemental analysis, polarography, paper chromatography, thin-layer chromatography (TLC), high-performance liquid chromatography (HPLC), electrophoresis, ion exchange, ^{1}H- and ^{13}C-nuclear magnetic resonance (NMR), infrared (IR), UV–visible and magnetic susceptibilities, field desorption mass spectroscopies and X-ray crystal analysis.

Note that it is important when synthesizing the non-radioactive compound to keep in mind the end use of the final product; i.e. to

take into account the biologic behavior of the radiopharmaceutical.

REACTION OF THE RADIONUCLIDE WITH THE NON-RADIOACTIVE COMPOUND

The final step in the preparation of radiopharmaceuticals involves the reaction between a radionuclide and non-radioactive compound. The procedure may involve addition of $^{99m}TcO^-_4$ or $^{111}InCl_3$ to a vial containing the non-radioactive compound, exchange reaction between radioactive and non-radioactive iodide in a molecule, substitution of radioactive iodide for a leaving group in an organic compound or on-line synthesis of positron-emitting radiopharmaceuticals. Although in practice this final step may be a simple procedure, it does involve complicated chemical reactions and some of these are described briefly below.

CHEMISTRY OF THE PREPARATION OF ^{99M}Tc RADIOPHARMACEUTICALS

The preparation of all ^{99m}Tc radiopharmaceuticals except $^{99m}TcO^-_4$ and ^{99m}Tc-sulfur colloid involves the reduction of Tc(VII) to a lower oxidation state in the presence of a ligand. Many reducing agents have been used, and these include stannous chloride/fluoride, a combination of ferric chloride and ascorbic acid, ferrous chloride, sodium borohydride, concentrated hydrochloric acid, aldehyde and electrolysis. Of these, the most frequently used reducing agent is the stannous ion, Sn^{2+}, in the form of stannous chloride/fluoride ($SnCl_2$ or SnF_2). In order to avoid the hydrolysis of Sn^{2+} ion to stannous hydroxide [$Sn(OH)_2$], the $SnCl_2$ or SnF_2 is dissolved in a solution of hydrochloric acid prior to addition to the ligand for the freeze-drying procedure. For the preparation of ^{99m}Tc radiopharmaceuticals in basic medium, stannous acetate/tartrate is the reducing agent of choice. Because technetium exhibits various oxidation states and has several coordination numbers, different ligands have been used to produce many organ-specific ^{99m}Tc radiopharmaceuticals such as Tc(V) in ^{99m}Tc-MAG_3 and ^{99m}Tc-1, 1-ECD [4, 5]; Tc(III) in ^{99m}Tc-IDAs [6]; and Tc(I) in ^{99m}Tc-sestamibi [7]. Depending on the oxidation state of technetium and the charge on the ligand, the final product may be neutral, negative or positive. A simplistic scheme summarizing the chemical reactions involved in the preparation of ^{99m}Tc complexes or chelates is given in Figure 1.2.

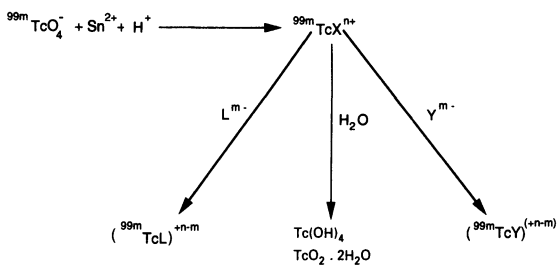

Figure 1.2 Chemical reactions involved in the preparation of ^{99m}Tc radiopharmaceuticals. n, the charge on reduced Tc; X, oxygen atom associated with reduced Tc; L, ligand; Y, impurity in ligand or saline containing a preservative (benzyl chloride).

Note the following points:

- *n* is always positive [8].
- *m* may be zero or negative.
- The net charge on $(^{99m}TcL)^{(+n-m)}$ or $(^{99m}TcY)^{(+n-m)}$ is determined by the sum of *n* and *m*. Thus, when *n* and *m* are equal, a neutral complex such as ^{99m}Tc-1, 1-ECD is produced [4, 9]; when *n* is less than *m*, a negatively charged complex such as $(^{99m}$Tc-IDA$)^-$ is produced [6, 10]; and when *n* is greater than *m* a positively charged complex such as $(^{99m}$Tc-sestamibi$)^+$ is produced [7, 11].
- The $^{99m}Tc(OH)_4$ or $^{99m}TcO_2$ is a hydrolysis product when $^{99m}TcO^-_4$ is reduced in the absence of a ligand. This is the impurity

that stays at the origin when radiochemical analysis of non-particulate ^{99m}Tc radiopharmaceutical is performed using paper chromatography or instant TLC.

- The $(^{99m}TcY)^{(+n-m)}$ is a radiochemical impurity which may be due to impurity in the ligand or saline. It is because of this impurity that saline-containing preservatives are not used in the elution of ^{99m}Mo–^{99m}Tc generator or in the preparation of ^{99m}Tc radiopharmaceuticals.
- The $^{99m}TcO_4^-$ is always the last reagent to be added to the reaction vial in order to minimize the formation of reduced hydrolyzed technetium ($^{99m}TcO_2$).

CHEMISTRY OF THE PREPARATION OF IODINE RADIOPHARMACEUTICALS

Direct and indirect methods are used for the radioiodination of compounds to produce iodine radiopharmaceuticals. The direct method involves either the oxidation of iodide to cationic iodine followed by direct substitution of a hydrogen atom or exchange of radioactive iodide for a leaving group in a molecule. The indirect method involves either the conjugation of a radioiodinated compound to a large molecule in order to preserve its biologic activity or a recoil labeling technique. Iodine radiopharmaceuticals involve a carbon–iodine bond which, unless stabilized by an electron cloud such as in a benzene ring, is weak and generally dissociates easily. If a molecule containing such a weak carbon–iodine bond is administered to a patient, it quickly dissociates *in vivo*, and this process is referred to as deiodination. Deiodination is a major problem with the use of labeled iodine radiopharmaceuticals. Both the direct and indirect methods of radioiodination will be described briefly.

Direct methods

Oxidative radioiodination method

This method involves the use of an oxidizing agent and radioactive sodium iodide to produce the cationic iodine (electrophilic iodine species) that reacts with an activated aromatic ring such as phenol, aniline or imidazole [12]. A variety of oxidizing agents and methods have been used, and these include nitrite, iodate, persulfate, hydrogen peroxide, chloramine-T, iodogen, hydrogen oxidases (peroxidase, lactoperoxidase and glucose oxidase) and electrolysis [13–20]. Nitrite, iodate and persulfate are strong oxidizing agents and hence are not suitable for labeling biologic compounds. However, chloramine-T, iodogen and lactoperoxidase are relatively mild oxidizing agents and are more suitable for labeling biologic compounds. High specific activity iodine radiopharmaceuticals can be produced using these reagents.

Exchange radioiodination method

This method produces iodine radiopharmaceuticals that are labeled at specific sites. This is achieved by activating a site in the molecule where an appropriate leaving group exists. Leaving groups include iodine, bromine, diazotized aniline and derivatives of tin, boron, trisilicon and thallium. The exchange of radioactive iodine with a stable iodine is the simplest of these techniques and is the most amenable to 'kit' formulation [21,22]. Extensive heating to produce a melt condition or the presence of a catalyst such as copper or ammonium sulfate may be required for the exchange reaction. Since the radioactive iodine is intended to replace all the stable iodine, it is not possible to prepare iodine radiopharmaceuticals of very high specific activity by an iodine exchange reaction. At any rate, this technique has been used

for the radioiodination of *o*-iodohippurate and *m*-iodobenzylguanidine.

Indirect methods

Conjugation technique

The radiodination of the biologic compound is achieved by first radioiodinating an organic compound with an activated ring and then covalently binding (conjugating) it to the biologic compound (carrier molecule). The *N*-hydroxysuccinimide ester of *o*-iodohippurate is conjugated to antibodies to produce radioactive iodine-labeled antibodies [23]. This technique is also amenable to kit formulation because in the final step of the preparation of the iodine radiopharmaceutical only simple addition of a properly prepared radioactive iodine compound to the molecule is required.

Recoil radioiodination method

When a radioactive nucleus decays by electron capture, ionization of the atom occurs through the loss of Auger electrons, thereby producing highly positively charged species (referred to as recoil atoms). This phenomenon is used in the recoil radioiodination method to produce iodine radiopharmaceuticals. Therefore, the recoil technique involves the reaction between highly positively charged iodine species produced by the radioactive decay (electron capture) of the corresponding xenon radionuclide with the compound to be radioiodinated. This labeling technique is exemplified by the commercial preparation of ^{123}I-(*S*)-(–)-3-iodo-2-hydroxy-6-methoxy-*N*-[(1-ethyl-2-pyrrolidinyl) methyl] benzamide (^{123}I-BZM) (a D-2 dopamine receptor radiopharmaceutical) through the use of ^{123}Xe [24].

CHEMISTRY OF THE PREPARATION OF INDIUM RADIOPHARMACEUTICALS

The aqueous chemistry of indium is dominated by the +3 oxidation state, which reacts with ligands to form strong complexes and chelates [25, 26]. In acidic medium, the +3 oxidation (In^{3+}) is stable and reacts readily with various ligands to form indium radiopharmaceuticals such as ^{111}In-DTPA, ^{111}In-antimyosin and ^{111}In-antifibrin [26–28] or starting materials such as ^{111}In-oxinate or ^{111}In-tropolonate for labeling white blood cells [29, 30]. In the absence of a ligand, complexing or stabilizing agent at pH above 2.5, In^{3+} is hydrolyzed to indium hydroxide [$In(OH)_3$], which does not react with ligand, and at pH higher than 4 the $In(OH)_3$ is precipitated out. Hence, care must be taken not to dilute the solution of radioactive $InCl_3$ (the starting material for making most indium radiopharmaceuticals) with water or saline.

Note that the paper chromatographic technique used in radiopharmacy for quality control of ^{111}In antibodies does not distinguish between the ^{111}In-labeled antibody and $^{111}In(OH)_3$. Therefore when 100% labeling efficiency is indicated it may not guarantee obtaining the expected biologic behavior of the injected ^{111}In antibodies.

REFERENCES

1. Molinski, V.J. (1982) A review of ^{99m}Tc generator technology. *Int. J. Appl. Radiat. Isot.*, **33**, 811–19.
2. Boyd, R.E. (1982) Technetium-99m generators – the available options. *Int. J. Appl. Radiat. Isot.*, **33**, 801–9.
3. Steigman, J. (1982) Chemistry of alumina column. *Int. J. Appl. Radiat. Isot.*, **33**, 829–34.
4. Cheesman, E.H., Blanchette, M.A., Ganey, M.V *et al.* (1988) Technetium-99m ECD: ester-derivatized diaminedithiol Tc complexes for imaging brain perfusion (abstract). *J. Nucl. Med.*, **29**, 788.
5. Fritzberg, A.R., Kasina, S., Eshima, D. *et al.* (1986) Synthesis and biological evaluation of technetium-99m-MAG_3 as a hippuran replacement. *J. Nucl. Med.*, **27**, 111–16.

6. Loberg, M.D. and Fields, A.T. (1978) Chemical structure of Tc-99m labeled N-(2,6-dimethylphenylcarbamoylmethyl) iminodiacetic acid (Tc-HIDA). *Int. J. Appl. Radiat. Isot.*, **29**, 167–73.
7. Jones, A.G., Abrams, M.J., Davison, A. *et al.* (1984) Biological studies of a new class of technetium complexes: the hexakis (alkylisonitrile) technetium (I) cations, *Int. J. Nucl. Med. Biol.*, **11**, 225–34.
8. Owunwanne, A., Marinsky, J., and Blau, M. (1977) Charge and nature of technetium species produced in the reduction of pertechnetate by stannous ion. *J. Nucl. Med.*, **18**, 1099–105.
9. Vallabhajosula, S., Zimerman, R.E., Picard, M. *et al.* (1989) Technetium-99m ECD: a new brain imaging agent: in vivo kinetics and biodistribution studies in normal human subjects. *J. Nucl. Med.*, **30**, 599–604.
10. Nunn, A.D., Loberg, M.D. and Conley, R.A. (1983) A structure–distribution relationship approach leading to the development of Tc-99m mebrofenin: an improved cholescintigraphic agent. *J. Nucl. Med.*, **24**, 423–30.
11. Jones, A.G., Dronauge, G.F. and Davison, A. (1985) Biological distribution and structure function relationships of hexakis isonitrile Tc (1) complexes (abstract). *J. Nucl. Med. All. Sci.*, **29**, 200.
12. Hughes, W.L. (1957) The chemistry of iodination. *Ann. NY Acad. Sci.*, **70**, 3–18.
13. Veall, N., Pearson, J.D., and Hanley, T. (1955) The preparation of ^{132}I- and ^{131}I-labeled human serum albumin for clinical tracer studies. *Br. J. Radiol.*, **28**, 633–35.
14. Taurog, A., and Chaikoff, I.L. (1957) Synthetic and analytic procedures: isolation and degradation methods, in *Methods in Enzymology, Vol. 4* (eds S.P. Colowick and N.O. Kaplan), Academic, San Diego, pp. 856–82.
15. Hunter, W.M. and Greenwood, F.C. (1962) Preparation of iodine-131-labeled growth hormone of high specific radioactivity. *Nature*, **194**, 495–96.
16. Bolton, R.M. and Hunter, W.M. (1986) Radioimmunoassays and related methods, in *Handbook of experimental immunology, Vol. 1. Immunochemistry.* 4th edn (ed. D.M. Weir), Blackwell Scientific Publications, Oxford, pp. 26.1–26.56.
17. Fraker, P.J. and Speck, J.C. (1978) Protein and cell membrane iodinations with a sparingly soluble chloramide 1,3,4,6-tetrachloro-3α, 6α-diphenylglycauril. *Biochem. Biophys. Res. Commun.*, **80**, 849–57.
18. Marchalonis, J.J. (1969) An enzymatic method for the trace iodination of immunoglobulin and other proteins. *Biochem. J.*, **113**, 299–305.
19. Thorell, J.I. and Johanson, B.G. (1972) Enzymatic iodination of polypeptides with ^{125}I to high specific activity. *Biochem. Biophys. Res. Commun.*, **48**, 464–71.
20. Rosa, V., Pennise, F., Bianchi, R., *et al.* (1969) Chemical and biological effects of iodination on human albumin. *Biochim. Biophys. Acta*, **133**, 486–98.
21. Sinn, H.J., Schrenk, H.M. and Mainer-Borst, W. (1985) A new radioiodine exchange labeling technique. *Int. J. Radiat. Appl. Instrum. (A)*, **37**, 17–21.
22. Mangner, T.J., Wu, J. and Wieland, D.M., (1982) Solid phase exchange radioiodination of aryl iodides. Facilitation by ammonium sulfate. *J. Organic Chem.*, **47**, 1484–88.
23. Bhargava, K.K. and Chervu, L.R. (1987) N-Hydroxysuccinimide hippuran ester: application for radiolabeling of macromolecules. *Biochem. Biophys. Res. Commun.*, **144**, 323–28.
24. Product information (1993) ^{123}I-IBZM, Cygne Eindhoven University of Technology, Eindhoven, The Netherlands.
25. Welch, M.J. and Welch, T.J. (1975) Solution chemistry of carrier-free indium, in *Radiopharmaceuticals* (eds G. Subramaniam, B.A. Rhodes, J.F. Cooper and V.J. Sodd), The Society of Nuclear Medicine, New York, pp. 73–9.
26. Goodwin, D.A., Sundberg, M.W., Diamanti, C.I. and Meares, C.F. (1975) ^{111}In-labeled radiopharmaceuticals and their clinical use, in *Radiopharmaceuticals* (eds G. Subramanian, R.A. Rhodes, J.F. Cooper and V.J. Sodd), The Society of Nuclear Medicine, New York, pp. 80–101.
27. Khaw, B.A., Strauss, H.W., Moore, R. *et al.* (1987) Myocardial damage delineated by indium-111 antimyosin fab and technetium-99m pyrophosphate. *J. Nucl. Med.*, **28**, 76–82.

28. Knight, L.C., Maurer, A.H., Ammar, I.A. *et al.* (1988) Evaluation of ^{111}In-labeled antifibrin antibody for imaging vascular thrombi. *J. Nucl. Med.*, **29**, 494–502.
29. Thakur, M.L., Welch, M.J., Joist, J.H. and Coleman, R.E. (1976) Indium-111 labeled platelets: studies on preparation and evaluation of in vitro and in vivo function. *Thromb. Res.*, **9**, 345–57.
30. Dewanjee, M.K., Rao, S.A. and Didisheim, P. (1981) Indium-111 tropolone, a new high affinity label. Preparation and evaluation of labeling parameters. *J. Nucl. Med.*, **22**, 981–87.

2

Ideal characteristics of radiopharmaceuticals

Radiopharmaceuticals are used for imaging, therapy and hematologic studies, and they have both common and different ideal characteristics for these studies. The common ones include availability, cost, ease of preparation and biologic behavior, while the different requirements are those associated with the radionuclide.

AVAILABILITY AND COST

The radiopharmaceutical should be easily available and inexpensive.

PREPARATION

The final step in the preparation of radiopharmaceutical (involving the incorporation of radionuclide into the non-radioactive compound) should be an easily performed procedure with very minimal or no purification required prior to administration.

BIOLOGIC BEHAVIOR

The target to non-target ratio should be very high. Any administered radiopharmaceutical that is not extracted by the target organ/tissue should be eliminated not only from circulation but also completely from the body. The amount of radioactivity in the body is determined by the effective half-life according to the equation given below:

$$T_e = T_p T_b / T_p + T_b$$

where T_e is the effective half-life, T_p is the physical half-life and T_b is the biologic half-life. Note that

- when $T_p \gg T_b$, $T_e = T_b$; $T_b \gg T_p$, $T_e = T_p$;
- radiopharmaceuticals with a long effective half-life deliver high radiation dose to the patient.
- for imaging and hematologic studies, radiopharmaceuticals should have a short effective half-life, which should not be much longer than the time required to complete the study.
- for therapy, longer effective half-life is required to maximize delivery of radiation to the target organ/tissue.

Once administered, a radiopharmaceutical should not metabolize or react *in vivo* prior to accumulation in the target organ. For some radiopharmaceuticals biotransformation [e.g. ^{99m}Tc-*I*, *I*-ECD and ^{18}FDG) is required for retention in the target organ.

RADIONUCLIDIC CHARACTERISTICS

Because the ideal radionuclidic characteristics for imaging, therapeutic and hematologic studies are different, these characteristics will be considered separately for each study.

IMAGING

- The radionuclide should decay by either isomeric transition (IT) or electron capture (EC).

- The gamma energies should be in the range of 100–510 keV, however, the optimum range for an Auger camera is 100–200 keV.
- The photon abundance should be high in order to obtain good counting statistics.
- The half-life should be long enough to allow for complete preparation of the radiopharmaceutical and imaging but short enough not to give high radiation dose to the patient and personnel.

THERAPY

- The radionuclide should decay by β^- or α emission with high linear energy transfer in order to deliver maximum radiation dose to the target organ/tissue.
- The associated gamma or Bremsstrahlung radiation can be used for imaging purposes.
- The half-life should be long enough to allow delivery of maximum radiation to the target organ.

HEMATOLOGY

- The radionuclide should decay by IT or EC. The gamma energies may range from 25 keV to 1 MeV because the samples are assayed in a well counter.
- The half-life may be a few hours or days depending upon the type of study.
- For blood volume estimation, a radionuclide with a half-life of a few hours is preferred, while for cell survival studies a few days half-life is necessary.

3

Quality control of radiopharmaceuticals

In hospitals, most radiopharmaceuticals are prepared by reconstituting ready-to-use kits with appropriate radionuclide. This reconstitution procedure results in the formation of a 'new' chemical compound. Therefore quality control tests must be performed after the final step of the preparation of the radiopharmaceutical in addition to those required for non-radioactive drugs. The quality control tests associated with the 'kits' formulation and production of radionuclides from primary sources are performed by manufacturers, while those associated with the final step of the preparation of the radiopharmaceutical are performed in the radiopharmacy. Broadly, two classes of quality control tests are performed: biologic and physicochemical.

BIOLOGIC TESTS

The biologic tests include sterility, pyrogenicity, toxicity and biologic distribution.

STERILITY

Sterility is the absence of viable micro-organisms in the radiopharmaceutical and it is achieved through prior sterilization of all preparative materials and solutions by autoclaving and/or membrance filtration of the radiopharmaceutical using 0.22-μm millipore filters. Two methods (colony culture and radiorespirometry) are used for sterility testing.

Colony culture

The sample of radiopharmaceutical is incubated in thioglycolate medium (30–35°C) for aerobic and anaerobic bacteria or in soyabean casein medium (20–25°C) for fungi, molds, aerobic and facultative anaerobic bacteria. The test medium is observed for 7–14 days. The presence or absence of micro-organism in the sample is determined by bacterial growth or lack of it in the culture [1]. This procedure takes a long time to accomplish and the result is only available after the radiopharmaceutical has been administered. Therefore, colony culture technique is not adequate for testing sterility of radiopharmaceuticals.

Radiorespirometry

The sample of radiopharmaceutical is incubated in a culture medium containing ^{14}C-glucose or ^{14}C-acetate at 37°C for 3–24 h. If bacteria are present in the sample, they metabolize the ^{14}C-glucose or ^{14}C-acetate to $^{14}CO_2$, which is measured in a liquid scintillation counter [2,3]. Radiorespirometry is a faster technique for sterility testing of radiopharmaceuticals.

PYROGENICITY

Pyrogens are either polysaccharides or proteins produced by the metabolism of micro-

organisms or debris of cell membrane. They are soluble in water, heat stable and filterable. They are found in distilled water, solutes, chemicals, glassware tubing and needles. In order to prevent pyrogen contamination of the radiopharmaceutical, all glassware and equipment should be heated at 200°C for 2 h, double-distilled water should be used to prepare solutions and whenever possible solutions be passed through a sterile Al_2O_3 column. Intravenous injection of solutions containing pyrogens produce fever, chills, leukopenia, pain in the joints, flushing, sweating and headache 0.5–2 h after injection.

United States Pharmacopeia (USP) test

The sample of the radiopharmaceutical is injected intravenously in three rabbits and the temperature is recorded every hour for 3 h. If there is a rise in temperature that is less than 0.6°C for each rabbit or less than 1.4°C for all three rabbits, the sample is assumed to be pyrogen free. However, if the rise in temperature is greater than 1.4°C, the test is repeated using five rabbits. The results of all eight rabbits are pooled. The sample is assumed to be pyrogen free if for any three rabbits the rise in temperature of each is not more than 0.6°C or if the total increase in temperature of all eight rabbits does not exceed 3.7°C [4].

Limulus Amebocyte Lysate (LAL) test

A 0.1-ml volume of buffered sample (pH 6–8) of the radiopharmaceutical is added to 0.1 ml of lysate. The sample is observed for 15 min to 1 h for positive gel formation [5,6]. The method is very sensitive for endotoxins and convenient to perform but requires meticulous handling because minute contamination may lead to a false-positive result.

TOXICITY

Toxicity is the negative pharmacologic response of the tissue to the administered drug. Radiopharmaceuticals do not evoke a pharmacologic response because only a trace amount of the chemical compound is used. However, the manufacturer is required to assure that the non-radioactive component of the radiopharmaceutical is not toxic at the milligram level.

BIODISTRIBUTION

Biodistribution studies are essential quality control tests for batch preparation of radiopharmaceuticals to assure their *in vivo* suitability (retention and elimination). A sample of the radiopharmaceutical is injected into a predesignated animal model. The animals are sacrificed at fixed time intervals, the organs dissected out and the activity in each organ is assayed. The percentage administered dose in each organ and the target to non-target ratio are calculated and compared with the results obtained from previous preparations. If the results are in good agreement, then the preparation is assumed to be suitable for human use.

PHYSICOCHEMICAL TESTS

The physicochemical tests include physical appearance, particle size, pH and chemical, radionuclidic and radiochemical purity. There are two divergent opinions as to whether all or some of the physicochemical tests are to be performed daily or only as an aid to trouble-shooting. Even those who advocate performing these tests daily do not agree on whether or not the tests should be performed prior to or after administration of the radiopharmaceutical because of time constraints. The authors advocate that these quality control tests should be performed daily prior to administration of the radiopharmaceutical and should be an integral

part of the daily schedule. Where additional tests are required for trouble-shooting, these should also be done.

Physical appearance

Prior to intravenous injection, the radiopharmaceutical is visually examined to assure that it is either particulate or a true solution. Particulates include colloids, macroaggregated albumin, microspheres and blood cells. True solutions include all other liquid radiopharmaceuticals. If a true solution contains particles or if a change in color is observed, it should not be administered to humans.

Particle size

The particle size of colloids is checked with an ultramicroscope and should be 1–100 nm, while the size of aggregates is checked with a light microscope and should be 10–100 μm. Radiopharmaceutical aggregate preparations with a particle size greater than 150 μm should be discarded to avoid blockage of pulmonary arterioles.

pH

The pH of radiopharmaceuticals varies from 2 to 9 and is checked with pH paper.

RADIONUCLIDIC PURITY

This is the fraction of total radioactivity in the form of desired radionuclide present in the radiopharmaceutical. In the radiopharmacy, it is the presence of the undesired radionuclide that is checked, for example ^{99}Mo in ^{99m}Tc radiopharmaceuticals, $^{202}Tl^{+}$ in ^{201}TlCl and ^{124}I in ^{123}I radiopharmaceuticals. The US pharmacopeia limits are 0.15 μCi of ^{99}Mo per mCi of ^{99m}Tc and 2% ^{202}Tl in ^{201}Tl at the time of administration.

The presence of undesired radionuclides can be detected and determined by gamma spectroscopy using a multichannel analyzer with a NaI(Tl) crystal or Ge(Li) semiconductor detector and measurement of the half-lives of the radionuclides.

- The presence of radionuclidic impurities will cause an increase in radiation dose to patient and personnel and lead to the degradation of the image.
- In practice, radionuclidic impurity is not a significant problem. However, routine monitoring of ^{99}Mo is required for ^{99m}Tc radiopharmaceuticals and is usually performed on the eluate ($^{99m}TcO_4^-$).

RADIOCHEMICAL PURITY

This is the fraction of total radioactivity in the desired chemical form present in the radiopharmaceutical. In the radiopharmacy, it is the presence of the undesired radiochemical impurities that is checked. These impurities are due to decomposition of the radiopharmaceutical caused by solvent, temperature, light or radiolysis; or labeling of a chemical impurity with the same radionuclide. Examples include the presence of $^{99m}TcO_4^-$ and reduced hydrolyzed ^{99m}Tc in other ^{99m}Tc radiopharmaceuticals; ^{131}I or ^{123}I iodide in other ^{131}I or ^{123}I radiopharmaceuticals. More than 90% purity of the desired radiochemical form is recommended. However, in practice, acceptance of the degree of purity is dependent on the clinical study performed. While 90% purity of ^{99m}Tc-MAA is adequate for lung imaging, 90% purity of ^{99m}Tc-RBCs is inadequate for a gastrointestinal bleeding study.

Radiochemical purity can be determined by liquid chromatography, either planar or column chromatography. In planar chromatography, the stationary phase can be a paper strip or a thin layer of adsorbent on a plate. The separated fractions appear as spots behind the solvent front on the stationary phase. In column chromatography, the stationary phase (alumina, ion-exchange resins or Sephadex) is contained in a cyclindrical tube

(the column). The sample components elute from the column at different time intervals.

In the radiopharmacy, planar chromatography is the technique that is routinely used for radiochemical analysis of radiopharmaceuticals, while column chromatography is used mostly for research and development. When high inlet pressure and small-diameter particles are used in columns, the technique is known as high-performance liquid chromatography (HPLC) to distinguish it from the gravity flow technique. A radiation detector is usually attached to the HPLC system in addition to a UV detector. HPLC can be used to separate sample components that are closely related in structure, such as isomers.

In planar chromatography, a drop (1–10 μl) of the radiopharmaceutical is spotted on a miniaturized paper or instant thin-layer chromatography (ITLC) strip, and developed in a solvent by ascending method under atmospheric conditions [7]. Generally, the solvents are selected in such a way that the radiopharmaceutical and impurity will be widely separated. The developed strips are dried and cut into two segments, referred to as the origin and the solvent front, as shown in Figure 3.1.

Each segment is assayed separately in a dose calibrator. Background radioactivity is subtracted and percentages are calculated as follows.

$$\text{Radioactivity at origin (\%)} = \frac{\text{Radioactivity at origin}}{\text{Radioactivity (at origin + at solvent front)}} \times 100$$

$$\text{Radioactivity at solvent front (\%)} = \frac{\text{Radioactivity at solvent front}}{\text{Radioactivity (at origin + at solvent front)}} \times 100$$

The radiochemical impurity present at the origin or at the solvent front depends upon the solvent system and the type of radiopharmaceutical.

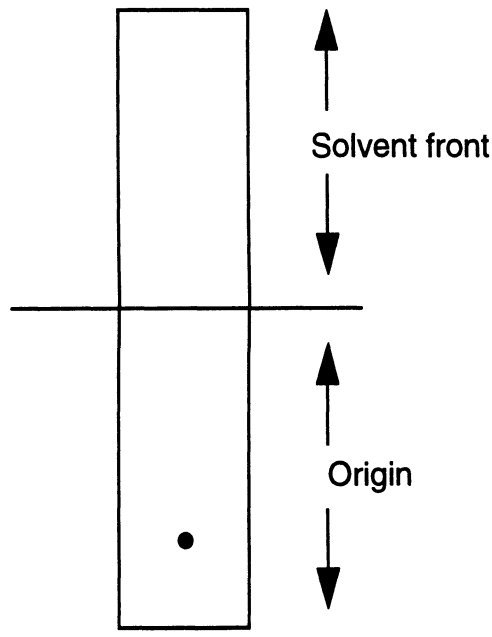

Figure 3.1 Paper or ITLC strip indicating segments referred to as the origin and the solvent front. In practice, the segments are not always cut equally.

For ^{99m}Tc radiopharmaceuticals, in most cases, two solvent systems are used: organic and aqueous solvents. The organic solvent (acetone, methyl alcohol or MEK) is used to separate the ^{99m}Tc-labeled radiopharmaceutical (at the origin) from $^{99m}TcO_4^-$ (at the solvent front), while aqueous solvent (saline) is used to separate it (at the solvent front) from reduced hydrolyzed $^{99m}TcO_2$ (at origin). The radiochemical purity of the ^{99m}Tc-labeled radiopharmaceutical (percentage labeling efficiency) is then determined by material balance as follows:

$$\text{Labeling efficiency (\%)} = 100 - \%\ ^{99m}TcO_4^- - \%\ ^{99m}TcO_2$$

REFERENCES

1. (1975) *The United States Pharmacopeia*, 19th revision, United States Pharmacopeial Convention, Rockville, M.A., pp. 592–93.
2. Deland, F.H. and Wagner Jr, H.N. (1969) Early detection of bacterial growth with carbon-14 labelled glucose. *Radiology*, **92**, 154–55.
3. Ganatra, R.D., Buddemeyer, E.U., Deodhar, M.N. *et al.* (1980) Modifications in biphasic liquid-scintillation vial system for radiometry. *J. Nucl. Med.*, **21**, 480–83.
4. (1975) *The United States Pharmacopeia*, 19th revision, United States Pharmacopeial Convention, Rockville, MA, p. 613.
5. Cooper, J.F., Hochstein, H.D. and Selligman, E.B. (1972) The limulus test for endotoxins in radiopharmaceuticals. *Bull. Parent Drug Assoc.*, **26**, 809.
6. Cooper, J.F. (1975) Principles and applications of limulus test for pyrogens in parenteral drugs. *Bull. Parent Drug Assoc.*, **29**, 809.
7. Zimmer, A.M. and Pavel, D.G. (1977) Rapid miniaturized chromatographic quality control procedures for ^{99m}Tc-radiopharmaceuticals. *J. Nucl. Med.*, **18**, 1230–33.

4

Design of radiopharmaceuticals

The major objective in the design of a radiopharmaceutical is to assure that it accumulates in and is eliminated from the target organ/tissue, blood and whole body. Since a radiopharmaceutical is made up of two components – radionuclide and non-radioactive compound – the design criteria must take into account the biologic activity not only of the individual component but also of the product, the radiopharmaceutical. When the biologic activity resides only in the radionuclide, the radiopharmaceutical is either an element (^{133}Xe) or a completely ionized molecule ($^{99m}TcO_4^-$, $^{123}I^-$ or $^{201}Tl^+$), in which case the non-radioactive component serves as a co-ion (Na^+ or Cl^-). When the biologic activity resides only in the non-radioactive component (antibodies, MDP, colloids or MAA), the radionuclide serves only as a tag (^{99m}Tc) for external monitoring. When the biologic activity is shared by both the radionuclide and the non-radioactive compound, a coordinated complex with the radionuclide as the central atom is formed (^{99m}Tc-IDA derivates, ^{99m}Tc-*d,l*-HMPAO or ^{99m}Tc-sestamibi). To design the above categories of radiopharmaceuticals rationally, a number of processes are involved, and these are grouped together under radionuclide, chemistry, biology, human studies and registration.

RADIONUCLIDE

The production, characteristics and quality control of radionuclides have been previously described.

CHEMISTRY

Three major steps are involved: synthesis of the non-radioactive compound, preparation of the radiochemical compound and formulation of 'cold kit'. The synthesis of the non-radioactive compound has been discussed previously.

The radiochemical preparation of a test sample is done for initial trial studies in animals and humans to demonstrate accumulation in or fast transit through the organ of interest. To optimize accumulation or elimination of the tracer, physicochemical parameters (pK_a, pH, molecular size, charge, protein binding, lipophilicity and isomerism) are modified and further biostudies are carried out. These series of chemical modification–biodistribution studies are referred to as structure–distribution relationships, exemplified by ^{99m}Tc-IDA derivatives, which led to the development of ^{99m}Tc-mebrofenin for hepatobiliary imaging [1]; ^{99m}Tc-PnAO, which led to the development of ^{99m}Tc-*d,l*-HMPAO, a brain perfusion radiopharmaceutical [2]; and the ^{99m}Tc-hexakis isonitrile series, which led to the development of ^{99m}Tc-sestamibi for myocardial perfusion [3].

The 'cold kit' is formulated and the radiochemical quality control technique is developed for ease of use in the hospital.

BIOLOGY

Both *in vivo* and *in vitro* models are used.

IN VIVO MODEL

Animals are used for studying biologic distribution, mechanism of accumulation and elimination, dosimetry and toxicity.

Biologic distribution

This study is aimed at determining whether or not there is sufficient radioactivity in the target organ(s) by calculating the percentage administered dose of the radiopharmaceutical in each organ and uptake ratios of the target to non-target (particularly adjacent) organ(s). This objective is achieved by either killing or imaging the animal. For experiments involving killing, smaller animals, particularly mice and rats, are used because of their size, low-cost maintenance and ease of handling. When imaging is required, larger animals such as rabbits, dogs and cats, and at times baboons and monkeys, are used.

It is important to point out that the initial animal experimentation should be done in different animal species and detailed biostudies should be performed on the species that most closely resembles humans in the way that the radiopharmaceutical accumulates in and is eliminated from the target organ/tissue. Owing to the differences in physiology and biochemistry, the same radiopharmaceutical can behave differently in animal species and in humans. The ^{99m}Tc-phosphino complexes [such as ^{99m}Tc-$(DMPE)_2Cl_2$ and ^{99m}Tc-$(DEPE)_2Cl_2$] show good accumulation in the canine heart but poor myocardial uptake in humans [4]. On the other hand, ^{99m}Tc-HMPAO and ^{123}-*o*-iodophenylheptadecanoic acid show poor accumulation in rat and higher uptake in human brain and heart respectively [5,6]. Hence, the most suitable animal species for detailed biostudies should be selected prior to embarking on detailed chemical studies of the new radiopharmaceutical.

Endogenous or exogenous compounds whose mode of actions are well known are used to study the mechanism of accumulation and elimination of the radiopharmaceuticals. Sulfbromophthalein (BSP), which has the same pathway as bilirubin, and bilirubin itself have been used to study the mode of uptake and excretion of ^{99m}Tc-IDA derivatives in dogs [7] and rabbits [8] respectively. Depletion of glutathione with diethylmaleate in a rat model [9] was used to study the mechanism of uptake of ^{99m}Tc-HMPAO and was shown not to be dependent on the concentration of glutathione. Treatment of mice with probenecid showed that ^{99m}Tc-MAG_3 is excreted through the renal tubules [10].

Dosimetry

The uptake values (percentage injected dose) for each organ obtained from biodistribution studies are used in conjunction with the published 'S' factors [11] to calculate the radiation dose to each organ. This calculation is particularly important because the critical organ (the organ bearing the most radiation burden) may not be the target organ, as exemplified by the ^{99m}Tc lipophilic tracers.

Example

Estimate the radiation absorbed dose to liver from intravenous administration of 5 mCi (5000 μCi) of ^{99m}Tc-sulfur colloid

The equation for estimating absorbed dose is

$$\overline{D}_{r_k \leftarrow r_h} = \overline{A}_r S_{r_k \leftarrow r_h}$$

where D is the mean absorbed dose expressed in rad/h, r_k is the target organ, r_h is the source organ, A is the accumulated activity in source organ expressed in microcuries and S is the absorbed dose per unit of accumulated activity for a particular radionuclide and source–target configuration as given in Ref. 11.

The normal biologic distribution of ^{99m}Tc-sulfur colloid is as follows: liver (85%), spleen

(7%), bone marrow (5%) and the rest of the body (3%) [12]. The accumulated activity in each organ is calculated from the expression

$$\overline{A} = 1.44\, A_{So} T_{eff}\ \mu\text{Ci h}$$

where 1.44 is a constant that relates A_s to the fractional uptake in the source organ(s) and T_{eff} is the effective half-life and for ^{99m}Tc-sulfur colloid is assumed to be equal to the physical half-life of ^{99m}Tc (6 h).

$$\overline{A}_{li} = 1.44 \times 0.85 \times 5000 \times 6 = 3.672 \times 10^4$$

$$\overline{A}_{sp} = 1.44 \times 0.07 \times 5000 \times 6 = 3.02 \times 10^3$$

$$\overline{A}_{bm} = 1.44 \times 0.05 \times 5000 \times 6 = 2.16 \times 10^3$$

where li is liver, sp is spleen and bm is bone marrow. The $\overline{D}$ to the liver estimated using S values is given by

$$\begin{aligned}
\overline{D}_{li} &= \overline{A}_{li}.S_{li \leftarrow li} + \overline{A}_{sp}.S_{li \leftarrow sp} + \overline{A}_{bm}.S_{li \leftarrow bm} \\
&= (3.672 \times 10^4 \times 4.6 \times 10^{-5}) + \\
&\quad (3.02 \times 10^3 \times 9.87 \times 10^{-7}) + \\
&\quad (2.6 \times 10^3 \times 1.6 \times 10^{-6}) \\
&= 1.69\,\text{rad}/5\,\text{mCi} \\
&= 0.34\,\text{rad/mCi} \\
&= 0.092\,\text{mGy/MBq}
\end{aligned}$$

Factors affecting radiation absorbed dose

These factors include the amount of administered radioactivity, the decay mode of the radionuclide and the chemical nature and biologic behavior of the radiopharmaceutical.

Amount of administered radioactivity The radiation absorbed dose is directly related to the amount of administered radioactivity. Hence the administered amount should not exceed what is necessary to obtain optimal study.

Decay mode of the radionuclide The type of radiation emitted and physical half-life of the radionuclide affect the amount of radiation absorbed dose. In radionuclide imaging, mostly low-energy gamma rays are used, while in therapeutic nuclear medicine mostly beta particles are used. Gamma rays are penetrating radiation, while beta particles are nonpenetrating, hence more radiation is absorbed from beta particles. To decrease radiation for diagnostic purposes, it is preferable to use a pure gamma emitter (isomeric transition) without any beta particles. The physical half-life of the radionuclide affects the amount of radioactivity administered. In general, the longer the half-life, the less the amount administered, particularly if the radiopharmaceutical has a long retention time in the body.

Chemical nature The biologic disposition and radiation absorbed dose depend on the chemical nature of the radiopharmaceutical. Lipophilic radiopharmaceuticals diffuse freely into tissues and may undergo intracellular biotransformation or binding to the tissues that leads to long retention in the organ. Examples include ^{99m}Tc-HMPAO, ^{99m}Tc-ECD, ^{99m}-Tc-sestamibi and ^{18}FDG. Most hydrophilic radiopharmaceuticals are readily eliminated from the body and would have a lower radiation absorbed dose. Particulate radiopharmaceuticals are either trapped in the pulmonary capillaries or phagocytosed by the recticuloendothelial system and hence retained in the organs. Gaseous radiopharmaceuticals are easily exhaled. Therefore, to minimize the absorbed radiation dose, it is important that the radiopharmaceutical is in the desired chemical form.

Biologic behavior To estimate the absorbed radiation dose of any radiopharmaceutical adequately its time course of distribution and elimination must be known. Total elimination depends on both the physical and biologic

half-lives. The physical half-life is a known quantity, but there is considerable difficulty in determining the biologic half-life. The blood clearance half-life is not the same as the biologic half-life. The biologic half-life varies from organ to organ. In many cases the biologic data are obtained from experimental animals and extrapolated to humans. In some cases it is possible to obtain the biologic data in humans, but these are obtained from normal volunteers instead of patients. Even then there is considerable variation in the organ sizes. Hence radiation absorbed dose is estimated for a standard human weighing 70 kg.

Toxicity

Generally toxicity is assessed using the non-radioactive compound in both male and female animals (mostly rats and rabbits) following single and repeated intravenous administration. Toxicity is not a 'serious' problem in the design and development of radiopharmaceuticals because the amount used does not elicit a pharmacologic response.

IN VITRO MODELS

These are highly specific systems used for studying the mechanisms of uptake, retention, elimination and biochemical events associated with the radiopharmaceuticals. Perfused organs/tissues (heart, liver, pancreas and lungs), cell cultures (myocytes and hepatocytes) and organ slices (liver) are most frequently used for these studies, as shown in Table 4.1. The *in vitro* model is relatively inexpensive and easily manipulated.

Although *in vitro* studies can provide information on what the transport mechanism of a radiopharmaceutical might be *in vivo*, an *in vitro* model is not a substitute for animal studies because the interplay of physiologic and biochemical events taking place *in vivo* cannot be adequately mimicked in an *in vitro* model.

HUMAN STUDIES

These studies are done in volunteers (both normal and patients) to evaluate the effectiveness and safety of the radiopharmaceutical. The volunteers are given either single or repeated injections at different dose levels. Written informed consent is obtained from each volunteer and the protocols are approved by the appropriate committee(s) of the institution. The radiopharmaceutical is usually administered intravenously and any adverse reactions are noted. Vital signs (temperature, blood pressure, respiratory and heart rates), urine and blood chemistries (haemoglobin, hematocrit, blood count, creatinine, urea, (serum glutamate exaloacetate transaminate (SGOT), sodium potassium, calcium and chloride) are monitored up to 24 hrs after injection.

Whole-body and spot view images are obtained. The rates of extraction and elimination of the radiopharmaceutical in the organ of interest, blood and excretory organs are calculated. These data are sometimes used to estimate radiation dose.

REGISTRATION

This is the process through which the radiopharmaceutical developer (academic institution or company) presents its radiochemical, biologic and human studies data to the appropriate regulatory agency in the country for approval for routine human use. The requirements vary from country to country. In general, the developer must assure that the radiopharmaceutical is safe, efficacious and effective.

REFERENCES

1. Nunn, A.D., Loberg, M.D. and Conley, R.A. (1983) A structure–distribution relationship approach leading to the development of ^{99m}Tc mebrofenin: an improved cholescintigraphic agent. *J. Nucl. Med.*, **24**, 423–30.

Table 4.1 In vitro models for studying transport mechanisms or site of localization of radiopharmaceuticals

Radiopharmaceutical	*Biologic systems*	*Transport/ localization*	*Reference*
$^{99m}TcO_4^-$, $^{131}I^-$	Thyroid sections; metabolic inhibitors	Active	13, 14
$^{201}Tl^+$, $^{22}Na^+$ $^{42}K^+$, ^{99m}Tc-$(DMPE)_2Cl_2$	Isolated erythrocyte membrane; ouabain	Na^+-K^+ATPase Diffusion	15, 16, 17
^{99m}Tc-sestamibi	Isolated pig heart slices and subcellular organelles; ouabain, hypoxic media	Diffusion and binding to cytosol	18
^{99m}Tc-TBI, ^{99m}Tc-IPI ^{99m}Tc-$(DMPE)_2Cl_2$ $^{42}K+$, $^{201}Tl^+$	Neonatal rat myocyte and human erythrocyte; ouabain	Diffusion Na^+-K^+ATPase	19, 20
^{99m} Tc-teboroxime ^{99m}Tc-sestamibi	Cultured chick embryo or rat heart; culture media and metabolic inhibitors	Diffusion and binding to cytosol for ^{99m}Tc-sestamibi	21, 22
^{99m}Tc-pyrophosphate ^{99m}Tc-glucoheptonate ^{99m}Tc-tetracyclin	Perfused fetal mouse heart; culture media	Irreversibly damaged myocardium	23
^{99m}Tc-HMPAO	Human whole blood, red cells; mice brain slices; RPMI medium	Inconclusive data	24
^{99m}Tc-Mebrofenin	Isolated hepatocyte; BSP	Shares common anionic transport with BSP	1
^{125}I-HIPDM	Isolated perfused lung; Krebs–Ringer bicarbonate buffer	Diffusion and binding to pulmonary endothelial cell membranes	25

2. Cumming, S.A. Nechvatal, G., Canning, L.R. *et al.* (1985) Development of ^{99m}Tc regional cerebral blood flow agents based upon the propyleneamine oxime (PnAO). (abstract). *Eur. J. Nucl. Med.*, **11**, 107.
3. Jones, A..G, Dronauge, G.F., Davison, A. *et al.* (1985) Biological distribution and structure function relationships of hexakisisonitrile Tc(l) complexes (abstract). *J. Nucl. Med. All. Sci.*, **29**, 200.
4. Ketring, A.R., Deutsch, E., Libson, K. *et al.* (1983) The Noah's ark experiment. A search for a suitable animal model for evaluation of cationic ^{99m}Tc myocardial imaging agents (abstract). *J. Nucl. Med.*, **24**, 9.
5. Neirinckx, R.D., Canning, L.R., Piper, I.M. *et al* (1987) ^{99m}Tc d, l- HM-PAO: a new radiopharmaceutical for SPECT imaging of regional cerebral blood perfusion. *J. Nucl. Med.*, **28**, 191–202.
6. Schon, H.R., Senekowitsch, R., Berg, D. *et al.* (1986) Measurement of myocardial fatty acid metabolism: kinetics of iodine-123 heptadecanoic acid in normal dog hearts. *J. Nucl. Med.*, **27**, 1449–55.
7. Harvey, E., Loberg, M., Ryan, J. *et al.* (1979). Hepatic clearance mechanism of ^{99m}Tc-HIDA and its effect on quantitation of hepatobiliary function. *J. Nucl. Med.*, **20**, 310–13.

8. Jansholt, A.L., Vera, D.R., Krohn, K.A. *et al.* (1979) *In-vivo* kinetics of hepatobiliary agents in jaundiced animals, in *Radiopharmaceuticals, Vol. 11* (eds V.J. Sodd, D.R. Allen, D.C. Hoogland and R.D. Ice), The Society of Nuclear Medicine, New York, pp. 555–64.
9. El-Shirbiny, A.M., Sadek, S., Owunwanne, A, *et al.* (1989) Is ^{99m}Tc hexamethyl propyleneamine oxime uptake in tissues related to glutathione cellular content? *Nucl. Med. Commun.*, **10**, 905–11.
10. Fritzberg, A.R., Kasina, S. Johnson, D.L. *et al.* (1985) Comparison of a new ^{99m}Tc renal function agent, ^{99m}Tc mercaptoacetyltriglycine, with I-131 OIH (abstract). *J. Nucl. Med.*, **26**, P56.
11. Snyder, W.S., Ford, M.R., Walner, G.O. and Watson, S.B. (1975) 'S' absorbed dose per unit accumulated activity for selected radionuclides and organs, *MIRD Pamphlet No. 11*, The Society of Nuclear Medicine, New York.
12. Atkins, H.L., Cloutier, R.J., Lathrop, K.A., *et al.* (1975) MIRD Report No. 3. Technetium-99m-sulfur colloids in various liver conditions. *J. Nucl. Med.* **16**, 108A.
13. Wolf, J. and Maurey, J.R. (1962) Thyroid iodide transport III. Comparison with anions of periodic group VII A. *Biochim. Biophys. Acta*, **57**, 422–26.
14. Wolf, J. (1964) Transport of iodide and other anions into the thyroid gland. *Physiol. Rev.*, **44**, 45–90.
15. Gehring, P.J. and Hammond, P.B.. (1964) The uptake of thallium by rabbit erythrocytes. *J. Pharmacol. Exp. Ther.*, **145**, 215–21.
16. Sand, H., Delano, M.L., Camin, L.L. *et al.* (1985) Comparison of the transport of $^{42}K^+$, $^{22}Na^+$, $^{201}Tl^+$ and $[^{99m}Tc(DMPE)_2Cl_2]^+$ using human erythrocytes. *Biochim. Biophys. Acta*, **812**, 665–70.
17. Mousa, S.A., Williams, S.J. and Sands, H. (1987) Characterization of *in vivo* chemistry of cations in the heart. *J. Nucl. Med.* **28**, 1351–57.
18. Mousa, S.A. and Williams, S.J. (1986) Myocardial uptake and retention of Tc-99m-hexakis aliphatic isonitriles: evidence for specificity (abstract). *J. Nucl. Med.* **27**, 995
19. Sands, H., Delano, M.L. and Gallagher, B.M. (1986) Uptake of hexakis (t-butylisonitrile) technetium (I) and hexakis (isopropylisonitrile) technetium (I) by neonatal rat myocytes and human erythrocytes. *J. Nucl. Med.* **27**, 404–8.
20. Delano, M.L,. Sands, H. and Gallagher, B.M. Transport of $^{42}K^+$, $^{201}Tl^+$ and $[^{99m}Tc\ (DMPE)_2Cl_2]^+$ by neonatal rat myocyte cultures. *Biochem. Pharmacol.*, **34**, 3377–80.
21. Kronauge, J.F., Chiu, M.L., Cone, J.S. *et al.* (1992) Comparison of neutral and cationic myocardial perfusion agents: characteristics of accumulation in cultured cells. *Nucl. Med. Biol.*, **19**, 141–48.
22. Maublant, J.C., Moins, N., Gachon, P. *et al.* (1993) Uptake of technetium-99m-teboroxime in cultured myocardial cells: comparison with thallium-201 and technetium-99m sestamibi. *J. Nucl. Med.*, **34**, 255–59.
23. Schelbert, H.R., Ingwall, J.S., Sybers, H.D. and Ashburn, W.L. (1976) Uptake of infarct-imaging agents in reversibly and irreversibly injured myocardium in cultured fetal mouse heart. *Circ. Res.*, **39**, 860–68.
24. Nakamura, K., Tukatani, Y., Kubo, A. *et al.* (1989) The behaviour of ^{99m}Tc-hexamethyl-propyleneamineoxime (^{99m}Tc-HMPAO) in blood and brain. *Eur. J. Nucl. Med.*, **15**, 100–107.
25. Slosman, D.O., Brill, A.B., Polla, B.S. and Alderson, P.O. (1987) Evaluation of [Iodine-125] N, N, N'-trimethyl N' [2-hydroxy-3-methyl-5-iodobenzyl]-1, 3-propanediamine lung uptake using an isolated-perfused lung model. *J. Nucl. Med.*, **28**, 203–8.

5

The fate of administered radiopharmaceuticals

The biologic fate of administered radiopharmaceutical is depicted in Figure 5.1 and depends mostly on distribution and elimination because most radiopharmaceuticals are administered by intravenous injection. Absorption plays a minimal role and affects only those few procedures in which radiopharmaceuticals are given intradermally (lymphoscintigraphy), orally (thyroid uptake), intrathecally (cisternography) and by inhalation (ventilation). Both distribution and elimination are influenced by blood flow, capillary permeability, intracellular interaction and degree of binding to blood components. The residence time in the organ is in turn influenced by any biotransformation that occurs intracellularly. Other factors such as the quality of the radiopharmaceutical and the health status of the patient also affect the distribution and elimination of the administered radiopharmaceutical.

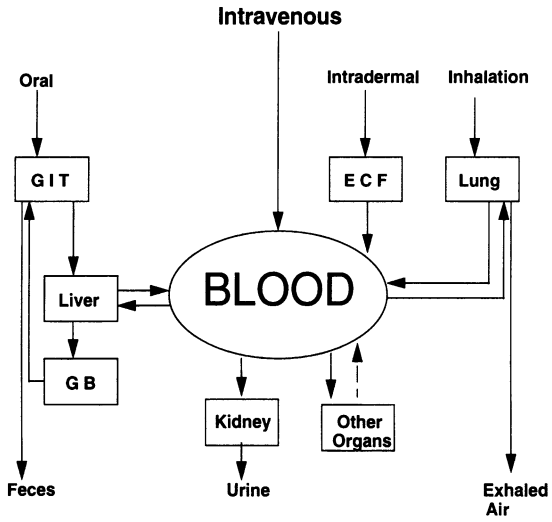

Figure 5.1 Routes of administration, distribution and elimination of radiopharmaceuticals (modified from [1]). ECF, extracellular fluid; GIT, gastrointestinal tract; GB, gallbladder.

A time course of the distribution and elimination of an intravenously injected radiopharmaceutical is shown in Figure 5.2. Qualitatively, it is possible to deduce that the radiopharmaceutical has a long residence (curve A) or fast transit time (curve B), as exemplified by ^{99m}Tc-MDP, ^{99m}Tc-*l*, *l*-ECD, ^{99m}Tc-*d*, *l*-HMPAO and ^{99m}Tc-sestamibi for curve A or ^{99m}Tc-IDA, ^{99m}Tc-teboroxime and ^{99m}Tc-MAG_3 for curve B. Quantitatively, pharmacokinetic parameters such as rates of extraction, elimination and volumes of distribution can be calculated and used to answer the following questions:

- How much of the radiopharmaceutical is in the target organ(s) at various times after its administration?
- How quickly is the radiopharmaceutical excreted by each excretory organ (kidney/liver)?

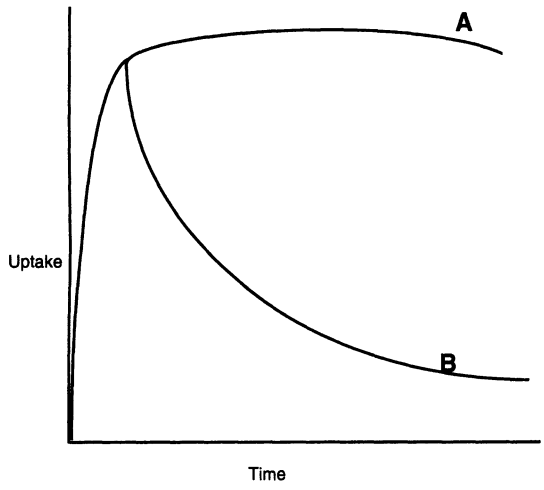

Figure 5.2 The uptake of radiopharmaceuticals in and elimination from the target organ(s). Curve A represents radiopharmaceuticals with long residence time, while curve B represents those with fast transit time through the target organ(s).

To describe the distribution and elimination of the intravenously injected radiopharmaceutical adequately, a brief description of membrane transport systems is helpful.

MEMBRANE TRANSPORT SYSTEMS

There are two basic transport systems: passive and specialized.

PASSIVE TRANSPORT SYSTEMS

Passive transport does not involve expenditure of energy and there are two types: diffusion and filtration.

Diffusion

Small hydrophilic molecules such as $^{99m}TcO^-_4$ pass across lipid membranes through aqueous channels or pores, whereas the lipophilic radiopharmaceuticals such as ^{99m}Tc-*d,l*-HMPAO pass through the lipid bilayer. The rate of transfer across the cell membrane is dependent on the lipid solubility of the radiopharmaceutical, as measured by lipid–water partition coefficient. If the lipophilic radiopharmaceutical exists in both ionized and non-ionized form, it is the non-ionized form or neutral molecule that crosses the membrane. For example, newly prepared ^{99m}Tc-*d*, *l*-HMPAO is neutral and upon injection can cross the blood–brain barrier and enter the central nervous system; however, when it is left standing for more than 30 mins after preparation, there is an increase, in the amount of the ionized form, which does not cross the blood brain–barrier [2]. Therefore, preparations of ^{99m}Tc-*d*, *l*-HMPAO should not be used after 30 mins.

Filtration

When water flows in bulk across a porous membrane, it carries solutes that are small enough to pass through pores. These pores have a relatively small diameter (4 nm), and therefore only radiopharmaceuticals with small molecular weight of approximately 100–200 can pass through them. However, in the glomeruli of the kidney, where the pores are much larger (70 nm), hydrophilic radiopharmaceuticals with a molecular weight less than that of albumin (60 000) can pass through and be filtered. These radiopharmaceuticals include ^{99m}Tc-DTPA, ^{99m}Tc-glucoheptonate, ^{99m}Tc-phosphorus complexes and metabolized ^{99m}Tc *l*, *l*-ECD.

SPECIALIZED TRANSPORT SYSTEMS

Active transport, facilitated transport and phagocytosis are described as specialized transport systems.

Active transport

This describes a transport system characterized by movement of substances across elec-

trochemical gradients at high substrate concentration. It is both saturable and selective, and therefore open to competitive inhibition. It also requires expenditure of energy. The transport of $^{201}Tl^+$ from blood to myocardium is based on the Na^+–K^+ ATPase system [3, 4]. Both $^{123/131}I^-$ and $^{99m}TcO_4^-$ ions are concentrated in the thyroid by an active transport system, as shown in an *in vitro* experiment using a metabolic inhibitor such as 1-methyl-2-mercaptoimidazole or propylthiouracil [5, 6].

Facilitated transport

This is a carrier-mediated transport system that is thought to have the characteristics of active transport in which the substance is not moved across a concentration gradient and expenditure of energy is not involved, as exemplified by the transport of ^{18}FDG from blood to tissue [7].

Phagocytosis

This is a transport system in which the cell membrane flows around a particle to engulf it either from the bloodstream by the reticuloendothelial system of liver, spleen and bone marrow or in the alveoli by the alveolar phagocytes. The particulate radiopharmaceuticals such as ^{99m}Tc-sulfur colloid are transported from the blood to liver by phagocytosis [8].

DISTRIBUTION

Upon intravenous injection, the radiopharmaceutical is available for distribution throughout the body. It is diluted in the bloodstream to the total blood volume if the radiopharmaceutical can easily and freely penetrate into the red cells, otherwise it is limited to the plasma volume. The rate at which a radiopharmaceutical enters various tissues depends on the relative rate of blood flow, its permeability across the capillaries and any intracellular interaction.

BLOOD FLOW

Blood flow to various organs differs widely depending on the capillary density of the tissues and the physiologic roles and metabolic rates of the organs. Hence varying amounts of the radiopharmaceutical are delivered to each organ where extraction may occur. Blood flow can be measured in two different units: the flow through a vessel is measured in volume per unit time (ml/min), while the flow to the regional tissue of interest (perfusion) is measured in volume per unit time per unit mass (ml/min/g). The flow through a vessel can be measured using microspheres [9, 10], while perfusion can be estimated either qualitatively or quantitatively using a perfusion agent such as $^{201}Tl^+$ for myocardium [11] and ^{99m}Tc-*d*, *l*-HMPAO or ^{99m}Tc-*l*, *l*-ECD for brain [12, 13].

CAPILLARY PERMEABILITY

Lipophilic radiopharmaceuticals diffuse freely through the capillary walls, and the rate of transfer depends on the lipid solubility of the radiopharmaceutical as measured by the lipid–water partition coefficient. Because the transfer rate is rapid, it is presumed that the entire capillary endothelial surface is available for diffusion. However, for hydrophilic molecules only a small fraction of the capillary wall is available for diffusion and filtration [14]. The rate of transfer is dependent on the molecular size of the radiopharmaceutical.

Capillaries of various tissues differ in their permeability characteristics. The glomerular capillaries are large and therefore allow the diffusion of large molecules. The sinusoidal capillaries of the liver seem to lack an endothelial wall and hence allow the passage of large molecules. In general, the capillaries of most tissues, except those of brain, allow relatively easy passage of radiopharmaceuticals from circulation to the interstitial fluid. In the brain, however, the permeability to

hydrophilic radiopharmaceuticals of all sizes is very restricted.

As mentioned previously, the rate of transcapillary transfer depends on lipid solubility, molecular size and whether or not the radiopharmaceutical is bound to blood components. Radiopharmaceuticals that are strongly bound to blood components remain in the circulation for a long time and thereby affect the amount that is extracted by the target organs. For example gallium-67 citrate is strongly bound to transferrin and haptoglobin and thus less of the injected tracer is available to tumor cells and inflammatory reactive sites [15]. In general, hydrophilic radiopharmaceuticals are more extensively bound to plasma proteins ($^{111}InCl_3$, $^{89}SrCl_2$), while lipophilic radiopharmaceuticals penetrate into blood cells (^{99m}Tc-*d*, *l*-HMPAO, ^{99m}Tc-*l*, *l*-ECD) [2, 13].

INTRACELLULAR INTERACTION

The final distribution of a radiopharmaceutical with respect to the organ of interest depends on the extent to which it is retained by the tissues. This retention depends on intracellular interaction, which may involve biotransformation, trapping or adsorption.

Biotransformation

In this process the radiopharmaceutical is transported into the tissues, where a biochemical reaction takes place, and the product cannot diffuse out of the cell. Both $^{99m}TcO_4^-$ and Sn^{2+} diffuse into erythrocytes, where $^{99m}TcO_4^-$ is reduced and reacts with hemoglobin to form ^{99m}Tc-hemoglobin, which does not diffuse out. ^{123}I-IMP is presumed to be retained in the brain as the result of a specific neuroreceptor reaction [16], while ^{123}I-HIPDM is protonated in the brain tissue because of the difference between blood and brain pH [17]. The brain retention of ^{99m}Tc-*l*, *l*-ECD is due to the intracellular hydrolysis of its ester groups to an acidic form [18], while that of ^{99m}Tc-*d*, *l*-HMPAO is presumed to be due to its reaction with brain glutathione [19, 20]. However, there are other reports that brain uptake of ^{99m}Tc-*d*, *l*-HMPAO is independent of glutathione concentration [21, 22]. ^{18}FDG, upon crossing the blood–brain barrier into the brain tissue, is phosphorylated to ^{18}FDG-6-PO_4, which does not diffuse out of the brain tissue [7, 23]. The retention of the receptor radiopharmaceuticals is due to their binding to receptor sites: ^{123}I-IBZM and ^{11}C-*N*-methylspiperone bind to dopamine D_2 receptors [24] and ^{111}In-octreotide binds to somatostatin receptor-positive tissues [25].

Mechanical trapping

The mechanical trapping of radiopharmaceuticals by organs is dependent on the size and shape of the molecules and the biologic environment. The trapping of $^{99m}TcO_4^-$ by thyroid is presumed to be due to the similarity between the tetrahedral shape of $^{99m}TcO_4^-$ and I^- ion, with the thyroid mistaking $^{99m}TcO_4^-$ for the I^- ion. However, *in vitro* studies have shown that the transport of $^{99m}TcO_4^-$ to the thyroid is an active process [5, 6]. The trapping of macroaggregated albumin or microspheres in the lung is the result of capillary blockade.

Physical adsorption

This is the process whereby radiopharmaceuticals are selectively adsorbed onto various forms of tissue calcium stores, including amorphous calcium phosphate, crystalline hydroxyapatite and calcium complexed with myofibrils and other macromolecules, for example the accumulation of ^{99m}Tc-phosphorus radiopharmaceuticals (^{99m}Tc-pyrophosphate, ^{99m}Tc-MDP and ^{99m}Tc-HMDP) on bone and acutely infarcted myocardium [26, 27].

ELIMINATION

Upon intravenous injection, radiopharmaceuticals are either extracted by target organ(s) or cleared from the bloodstream by the excretory organs.

The clearance of radiopharmaceuticals from the blood can be represented by a semilogarithmic plot of radioactivity versus time. If the plot is a straight line, it is assumed that the radiopharmaceutical is rapidly distributed in one compartment and that elimination is by first-order kinetics (that is the amount eliminated is proportional to the amount present in the compartment). Although the assumption that the radiopharmaceutical is rapidly distributed is an oversimplification, it does provide an accurate description of the plasma radioactivity–time profile. This profile can be used to calculate pharmacokinetic parameters such as half-life, volume of distribution and clearance. The first-order rate constant for elimination (k_e) can be calculated from the slope of the graph (Figure 5.3) as slope $=-k_e/2.303$. The half-life is a constant for a given rate; it is independent of the initial amount and can be calculated from k_e as $t_{1/2} = 0.693/k_e$.

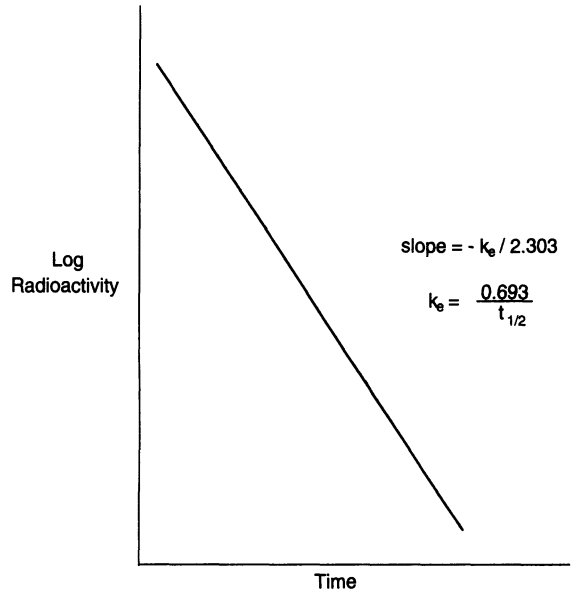

Figure 5.3 Semilogarithmic plot of radioactivity in the blood after intravenous administration of a radiopharmaceutical: one-compartment model.

If the semilogarithmic plot of radioactivity versus time is best described by an exponential curve, then a multicompartmental analysis is required. In the case of two compartments (Figure 5.4) the exponential curve can be resolved into two straight lines by the curve-stripping method and the rate constants are calculated as shown in Figure 5.5. The elimination rate is particularly useful for radiopharmaceuticals with fast transit through the target organ and is used for intercomparison of radiopharmaceuticals when structure–distribution relationship studies are being carried out, as exemplified by ^{99m}Tc-IDA derivatives and the ^{99m}Tc-hexakis isonitrile series.

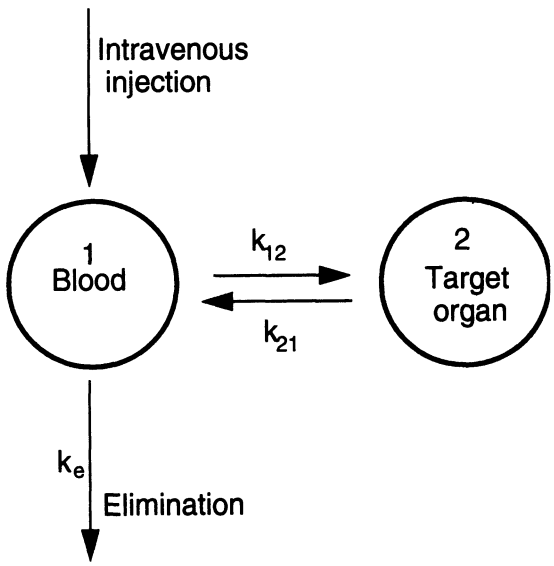

Figure 5.4 Two-compartment model.

It is important to point out that the half-life determined from the blood clearance

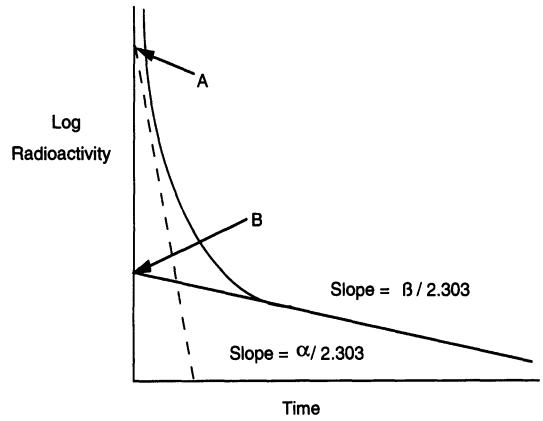

Figure 5.5 Semilogarithmic plot of radioactivity in the blood after intravenous administration of a radiopharmaceutical for an open two-compartment model as shown in Figure 5.4. The dashed line is obtained by the method of stripping. The rate constants are calculated as follows:

$$k_{21} = \frac{\alpha B + \beta A}{A + B};\ k_e = \frac{\alpha\beta}{k_{21}};\ k_{12} = \alpha + \beta - k_{21} - k_e$$

curve does not necessarily represent the actual half-life of the radiopharmaceutical in the organs or tissue. In classical pharmacokinetics, half-life is generally determined from blood clearance because it is difficult to sample the concentration of the drug in other tissues. However, in nuclear medicine, because it is technically feasible to measure the amount of radioactivity in each organ using an external detector, it is possible to determine the biologic half-life of the radiopharmaceutical in that organ, as shown in Table 5.1.

Several factors influence the blood clearance of radiopharmaceuticals, and these include the volume of distribution, degree of binding to plasma protein or tissue, the extent of biotransformation and the effectiveness of both renal and hepatobiliary excretion.

Table 5.1 Blood clearance and target organ half-lives of some radiopharmceuticals

Radiopharmaceutical	*Blood* $t_{1/2}$	*Target organ*		*Reference*
		$t_{1/2}$	*Organ*	
$^{99m}TcO_4^-$	50 min	60 min (85%) 600 min (15%)	Thyroid	28
^{99m}Tc-*d, l*-HMPAO	< 10 min	71 h	Brain	29
^{99m}Tc-*l, l*-ECD	0.8 min	1.3 h (40%) 42.3 h (40%)	Brain	13
^{99m}Tc-MRP-20	> 4 h	> 24 h	Brain	30
^{99m}Tc-MAA	< 1 min	6 h (85%) 3 days (15%)	Lung	31
^{99m}Tc-albumin microspheres	< 1 min	1.8 h (60%)	Lung	32
^{99m}Tc-aerosols (DTPA)	–	79.2 min	Lung	33, 34
^{99m}Tc-RBC	60 h	–	Heart	8
^{99m}Tc-denatured RBC	3 h	∞	Spleen	35
^{99m}Tc-sestamibi	4.3 min	7 h	Heart	36
^{99m}Tc-teboroxime	0.79 min	5.2 min (60%) 3.8 h (33%)	Heart	37, 38
^{99m}Tc-PYP	54 min	∞	Bone	39
^{99m}Tc-MDP	44 min	∞	Bone	39
^{99m}Tc-HMDP	50 min	∞	Bone	39
^{99m}Tc-HEDP	44 min	∞	Bone	39
^{99m}Tc-colloids	< 5 min	∞	Liver	40

Table 5.1 (cont.)

Radiopharmaceutical	*Blood $t_{1/2}$*	*Target organ*		*Reference*
		$t_{1/2}$	*Organ*	
^{99m}Tc-EHIDA	3.12 min	37.3 min	Liver	41, 42
^{99m}Tc-mebrofenin		17.01 min	Liver	41
^{99m}Tc-DISIDA	1.77 min	19.0 min	Liver	41, 42
^{99m}Tc-BIDA	3.09 min	107.6 min	Liver	41, 42
^{99m}Tc-DTPA	25 min	12 min	Kidneys	43, 44
^{99m}Tc-DMSA	63.5 min	60 min (50%)	Kidneys	45, 46
^{99m}Tc-glucoheptonate	< 10 min	45 min (15%) > 24 h (85%)	Kidneys	45, 47
^{99m}Tc-MAG$_3$	22.1 min	3–5 min	Kidneys	48, 49
^{99m}Tc-human serum albumin	6.8 h (40%) 1.29 days (22%) 15.4 days (38%)	–	Heart	50
^{125}/^{131}I-sodium iodide		80 days	Thyroid	51
^{123}/^{131}I-hippuran	4.34 min 15.7 min	4–6 min	Kidneys	52
^{111}In-oxine leukocytes	7.5 h	70 days	Spleen	53, 54
^{111}In-oxine platelets	4 days (60%)	70 days	Spleen	55, 56, 57
^{111}In-DTPA (intrathecal)	67 min	12 hrs	Cerebrospinal fluid	58
^{201}Tl$^+$	2.9 min	4 h	Heart	59, 60
^{67}Ga citrate	8.5 h	1.25 days 25.5 days	Tumor	61, 62
^{18}FDG	0.2–0.3 min 11.6±1.1 min	∞	Brain and heart	63
^{153}Sm-EDTMP	14 min 11.5 hrs	∞	Bone	64

Note: When the target $t_{1/2}$ is determined by the physical half-life of the radionuclide, the target $t_{1/2}$ is presumed to be infinity (∞).

Volume of Distribution

The volume of distribution (V_d) is a useful concept for describing the distribution of radiopharmaceutical between plasma and tissue; it does not correspond to any anatomic space and it is mathematically defined as the ratio between the amount of radioactivity in the body and plasma:

$$V_d = D_{iv} / D_p$$

where D_{iv} is the injected dose and D_p is the amount in plasma. Experimentally, it is calculated from the expression

$$V_d = \text{Dose}/\text{AUC}.k_e = \text{Dose} \times t_{1/2} / \text{AUC}.\ 0.693$$

where AUC is the area under the plasma curve of radioactivity versus time (Figure 5.5). A high V_d indicates that the amount of radiopharmaceutical present in the tissue is more than that in the plasma and therefore less is available for excretion. A low V_d indicates that more radiopharmaceutical is present in the plasma than in the tissue and therefore more is available for excretion, as exemplified by the elimination of ^{99m}Tc-MAG$_3$.

Binding

The extent of plasma protein or tissue binding affects the amount of radiopharmaceutical cleared from blood or eliminated from the body and the rate at which excretion occurs. The blood clearance of ^{99m}Tc-PYP is relatively slower than that of ^{99m}Tc-HEDP, ^{99m}Tc-MDP, or ^{99m}Tc-HMDP. The slower clearance of ^{99m}Tc-PYP is attributed to its higher binding to plasma protein [65, 66]. The blood clearance of ^{67}Ga citrate is very slow; it binds strongly to transferrin and haptoglobin and loosely to albumin [67]. The labeled blood components (RBCs with ^{99m}Tc; leukocytes and platelets with ^{111}In-oxine or ^{111}In-tropolone) remain in circulation for a very long time. The ^{99m}Tc-RBCs are cleared biexponentially with half-lives of 2.5 ± 0.7 and 176.6 ± 163.6 hs [53]; ^{111}In-oxine (free of red cells) and ^{111}In-tropolone leukocytes have blood clearance half-lives of 7.5 and 9.0 ± 2.5 hs respectively [53]. ^{111}In-oxine platelets and ^{111}In-tropolone platelets have mean survival times of 230.0 ± 2.5 and 226.0 ± 13 hrs respectively [54].

Biotransformation

Radiopharmaceuticals may be excreted in metabolized or unmetabolized form. Hydrophilic and lipophilic radiopharmaceuticals are generally excreted in the renal and biliary systems respectively. Biochemical transformation of radiopharmaceuticals, particularly neutral molecules, may occur in the plasma prior to excretion and the metabolite may be excreted via the renal instead of the biliary system. ^{99m}Tc-1, 1-ECD is lipophilic; however, after intravenous injection, the ester group is hydrolyzed in plasma to a carboxylic group and the metabolite is excreted in urine [13]. On the other hand the conversion of ^{99m}Tc-*d*, *l*-HMPAO to a hydrophilic secondary form probably occurs in the liver, and it is excreted mostly in the bile [12]. ^{123}IMP, through a series of biochemical reactions, is metabolized to *p*-iodohippuric acid, which is excreted in the urine [68]. Hence the extent of biotransformation affects the excretory route of the injected radiopharmaceutical.

ROUTES OF EXCRETION

Most radiopharmaceuticals are excreted in urine and/or bile.

Urinary excretion

Radiopharmaceuticals are excreted from plasma to urine by passive glomerular filtration, tubular diffusion and active tubular secretion. Filtration occurs at the glomerulus and, since the glomerular capillaries have large pores, most hydrophilic radiopharmaceuticals can be filtered unless they are protein bound. If the radiopharmaceutical is not reabsorbed, its clearance will be equal to the glomerular filtration rate (GFR). However, most radiopharmaceuticals are partially reabsorbed and therefore the estimated GFR will be less than the volume of plasma cleared. For the radiopharmaceuticals that are actively secreted from the plasma to urine, the volume of plasma cleared is greater than GFR because theoretically all substances reaching the kidney can be cleared by active secretion and the renal plasma flow (660 ml/min) is much greater than GFR (125 ml/min). Also, unlike filtration, both the protein-bound and unbound radiopharmaceuticals are available for secretion.

Both $^{99m}TcO_4^-$ and ^{99m}Tc-DTPA are filtered at the glomeruli [43,44,69]. ^{99m}Tc-glucoheptonate is cleared from blood by both glomerular filtration and tubular secretion transport systems [45]. ^{99m}Tc-MAG_3 and $^{123/131}$I-hippuran are excreted mostly by tubular secretion, however 20% of $^{123/131}$I-hippuran is cleared by glomerular filtration [48, 49, 52].

Biliary excretion

Radiopharmaceuticals are transported from plasma to hepatocytes, from where they are excreted into bile via bile canaliculi. The negatively charged radiopharmaceuticals (^{99m}Tc-IDA derivates) have been shown to share the same pathway as bilirubin, BSP and other dye anions. It is presumed that ^{99m}Tc-*d,l*-HMPAO and ^{99m}Tc-teboroxime use the pathways for neutral compounds while the positively charged ^{99m}Tc-sestamibi and ^{99m}Tc-tetrofosmin use the pathway for cations in the sinusoidal membrane of the liver. Once the radiopharmaceutical is excreted into bile and enters the intestine, it can be either reabsorbed or eliminated with feces.

URINARY OR BILIARY EXCRETION?

The factors which determine whether a radiopharmaceutical is excreted in urine or bile are not well known. It has been suggested that molecular weight and polarity may be important. Polar radiopharmaceuticals with low molecular weight (≤ 325) are excreted in urine, while those with higher molecular weight and which are lipid soluble are excreted in bile. However, there are radiopharmaceuticals that are partially excreted in urine and bile as either a parent or metabolite (Table 5.2). If the biotransformation occurs in plasma, the metabolite is excreted in urine, as exemplified by hydrolysis of ^{99m}Tc-1,1-ECD and metabolism of ^{123}IMP. If it occurs in the liver, the metabolite is excreted in bile, as shown by the suggested reaction between ^{99m}Tc-*d,l*-HMPAO and glutathione.

THE QUALITY OF THE RADIOPHARMACEUTICAL

The chemical integrity of the radiopharmaceutical influences its biodistribution and subsequent elimination. An unstable radiopharmaceutical or one that contains more

Table 5.2 Summary of urinary and biliary excretion of some radiopharmaceuticals

Radiopharmaceutical	*Molecular weight*	*Nature of complex*	*Excretion (%)*		*Reference*
			Urinary	*Biliary*	
^{99m}Tc-*d,l*-HMPAO	383	Neutral, biotransformed complex: polar	29 (4 h)	23 (4 h)	12
^{99m}Tc-*l,l*-ECD	435	Neutral, metabolite in plasma: polar	65% (4 h)	11.2±6.2% (48 h)	13
^{99m}Tc-sestamibi	815	Positively charged, lipophilic	37 (48 h)	27 (24 h)	13
^{99m}Tc-tetrofosmin	930	Positively charged, lipophilic	39±3.7 (48 h)	34.2±4.3 (48 h)	70
^{99m}Tc-EHIDA	753	Negatively charged and extent of lipophilicity depends on *p* or *0* substitution	17.1±3.2	82.3[a]	41, 42
^{99m}Tc-disofenin	787		11.1±1.5	88.0[a]	71
^{99m}Tc-mebrofenin	860		1.5±0.3	98.1[a]	
^{99m}Tc-MAG_3	418	Negatively charged, hydrophilic	73 (30 min)	3[a]	48, 49

[a] Hepatic uptake.

than 'one radiochemical compound' will result in an altered biologic behavior. Immediately after preparation, lipophilic ^{99m}Tc-*d,l*-HMPAO is formed, but upon standing it converts to a more hydrophilic form which upon injection is not extracted by the brain. Antioxidants such as gentisic acid are added to some ^{99m}Tc radiopharmaceutical preparations to stabilize them *in vitro* [72]. Iodinated long-chain fatty acids are readily dehalogenated *in vivo*, releasing radioactive iodide, which complicates imaging and renders quantitation of cardiac metabolism of free fatty acid difficult to perform [73,74]. To overcome this problem, an iodinated phenyl group is attached to the fatty acids, for example 15-(-*p*-^{123}I-iodophenyl)pentadecanoic acid and its ortho isomer, 15-(-*o*-^{123}I-iodophenyl)pentadecanoic acid [75, 76].

To ensure the chemical integrity of the tracer, radiochemical quality control procedures are performed on the radiopharmaceutical preparations.

THE HEALTH STATUS OF THE PATIENT

Various conditions contribute to the clinical status of the patient, and these include disease state, blood chemistry, the presence of chemotherapeutic agents and/or other drugs, body surface area (weight and height) and age. Radiopharmaceuticals are designed to have specific patterns of biodistribution and

Table 5.3 Effect of health condition on the biologic behavior of some administered radiopharmaceutical

Health condition	*Radiopharmaceutical*	*Altered biologic behavior*	*Reference*
Compromized blood–brain barrier	$^{99m}TcO_4^-$, ^{99m}Tc DTPA ^{99m}Tc-GHA	Able to enter the brain	44
Poor/inadequate hydration	^{99m}Tc-DTPA, ^{99m}Tc-MAG_3 ^{99m}Tc-GHA, $^{123/131}$I-hippuran and all other radiopharmaceuticals excreted in urine	Prolonged elimination	43, 44
Poor functioning hepatocytes and cholestasis	^{99m}Tc-IDA derivatives	Poor uptake and delayed excretion	41, 71 77
Compromized phagocytic function of spleen	^{99m}Tc colloids	Non-visualization of spleen but ability to visualize spleen with heat-denatured ^{99m}Tc-RBCs	78
Ingestion of iodine-containing food and/or administration of radiologic contrast media containing iodine	$^{123/131}I^-$ ion	Decreased uptake	79
Cigarette smoking	^{99m}Tc-DTPA aerosol	Increased permeability through alveolar membrane	33
Drugs[a]			

[a] The examples are included in Tables 6.1–6.3.

elimination when administered to normal subjects. In the presence of any or a combination of the above conditions, these patterns may be altered (Table 5.3). It is this altered pattern that helps a physician make a diagnosis. It is therefore important, in order to make optimal interpretation of the altered biodistribution and/or elimination of the administered radiopharmaceutical, that the health status of the patient be fully known.

REFERENCES

1. Klassen, C.D. (1986) Distribution, excretion and absorption of toxicants, in *Casarett and Doul's Toxicology. The Basic Science of Poisons*, 3rd edn (eds C.D. Klaassen, M.D. Amdur and J. Doul), Macmillan Publishing, New York, pp. 33–63.
2. Neirinckx, R. D., Canning, L.R., Riper, I.M. *et al.* (1987) Technetium-99m d, *l*-HMPAO: a new radiopharmaceutical for SPECT imaging of regional cerebral blood perfusion. *J. Nucl. Med.* **28**, 191–202.
3. Gehring, P.J. and Hammond, P.B. (1967) The interrelationship between thallium and potassium in animals. *J. Pharmacol. Exp. Ther.*, **55**, 187–201.
4. Gelbart, A., Doherty, P.W., McLaughlin, P.R. *et al.* (1976) Na^+, K^+-ATPase and coronary blood flow as determinants of thallium-201 uptake by ischemic myocardium. *Circulation*, **54**, 11–70.
5. Wolff, J. and Maurey, J.R. (1962) Thyroid iodide transport. III. Comparison with anions of periodic group VII A. *Biochim. Biophys. Acta*, **57**, 422–26.
6. Wolff, J. (1964) Transport of iodide and other anions into thyroid gland. *Physiol. Rev.*, **44**: 45.
7. Gallagher, B.M., Fowler, J.S., Gutterson, N.L. *et al.* (1978) Metabolic trapping as a principle of radiopharmaceutical design: some factors responsible for the biodistribution of [^{18}F] 2-deoxy-2-fluoro-D-glucose. *J. Nucl. Med.*, **19**, 1154–61.
8. Atkins, H.L., Richards, P., Schiffer L. (1966) Scanning liver, spleen and bone marrow with colloidal ^{99m}technetium. *Nucl. Applic.*, **2**, 27–32.
9. Heymann, M.A., Payne, B.D., Hoffman, J.I.E. and Rudolph, A.M. (1977) Blood flow measurements with radionuclide-labeled particles. *Prog. Cardiovasc. Dis.*, **20**, 55–79.
10. Wagner Jr, H.N., Rhodes, B.A., Sasaki, Y. *et al.* (1969) Studies of the circulation with radioactive microspheres. *Invest. Radiol.*, **4**, 374–86.
11. Strauss, H.W. and Pitt, B. (1977) Thallium-201 as a myocardial imaging agent. *Semin. Nucl. Med.*, **7**, 49–58.
12. Sharp, P.F., Smith, F.W., Gemmell, H.G. *et al.* (1986) Technetium-99m HM-PAO stereoisomers as potential agents for imaging regional cerebral blood flow: human volunteer studies, *J. Nucl. Med.*, **27**, 171–77.
13. Vallabhajosula, S., Zimmerman, R.E., Picard, M. *et al.* (1989) Technetium-99m ECD: a new brain imaging agent: *in vivo* kinetics and biodistribution studies in normal human subjects. *J. Nucl Med.*, **30**, 599–604.
14. Pratt, W.B. (1990) The entry, distribution and elimination of drugs, in *Principles of Drug Action: The Basis of Pharmacology*, 3rd edn (eds W.B. Pratt and P. Taylor), Churchill Livingstone, New York, pp. 201–97.
15. Hartman, R.E. and Hayes, R.L. (1969) The binding of gallium by blood serum. *J. Pharmacol. Exp. Ther.*, **168**, 193–98.
16. Winchell, H.S., Horst, W.D., Brau L *et al.* (1980) N-isopropyl (^{123}I) *p*-iodoamphetamine: single-pass brain uptake and washout; binding to brain synaptosomes and localization in dog and monkey brain. *J. Nucl. Med.*, **21**, 947–52.
17. Kung, H.F., Tramposch, K.M., Blau, M. (1983) A new brain perfusion agent: ^{123}I-HIPDM: N, N, N'-trimethyl-N' -[2-hydroxy-3-methyl-5-iodobenzyl]-1, 3-propanediamine. *J. Nucl. Med.*, **24**: 66–72.
18. Van Nerom, C., Bormans, G., De Beukelaer, C. *et al.* (1990) Metabolism of ^{99m}Tc-ECD in organ homogenates of baboon, in *Nuclear Medicine: Quantitative Analysis in Imaging and Function* (ed. H.A.E. Schmidt), Schattauer, Stuttgart, pp. 87–9.
19. Neirinckx, R.D., Burke J.F., Harrison, R.C. *et al.* (1988) The retention mechanism of technetium-99m HMPAO: intracellular reaction with glutathione. *J. Cereb. Blood Flow Metab.*, **8** (Suppl. 1), S4–S12.

20. Suess, E., Malessa, S., Ungersbock, K. *et al.* (1991) Technetium-99m d, l-hexamethylpropyleneamine oxime (HMPAO) uptake and glutathione content in brain tumors. *J. Nucl. Med.*, **32**, 1675–81.
21. El-Shirbiny, A.M., Sadek, S., Owunwanne, A. *et al.* (1989) Is Tc-99m-hexamethylene-propyleneamine oxime uptake in the tissues related to glutathione cellular content? *Nucl. Med. Commun.*, **10**, 905–11.
22. Rowell, N.P., McCready, V.R., Cronin, B. *et al.* (1989) Tc-99m-labeled meso-HMPAO and glutathione content of human lung tumours. *Nucl. Med. Commun.*, **10**, 503–8.
23. Phelps, M.E. (1981) Positron computed tomography of cerebral glucose metabolism in man: theory and application in nuclear medicine. *Semin. Nucl. Med.*, **11**, 32–49.
24. Kung, H.F., Guoy, Z., Billings, D. *et al.* (1988) Preparation and bodistribution of [^{123}I] IBZM: a potential CNS D_2 dopamine receptor imaging agent. *Nucl. Med. Biol.*, **15**, 195–201.
25. Bakker, W.H., Albert, R., Bruns, C. *et al.* (1991) [^{111}In-DTPA-D-Phe'] -octreotide, a potential radiopharmaceutical for imaging somatostatin receptor-positive tumours: Synthesis, radiolabeling and *in vitro* validation. *Life Sci.*, **49**, 1583–91.
26. Jones, A.G., Francis, M.D. and Davis, M.A. (1976) Bone scanning: radionuclide reaction mechanisms. *Semin. Nucl. Med.*, **6**, 3–18.
27. Buja, L.M., Tofe, A.J., Kulkarni, P.V. *et al.* (1977) Sites and mechanisms of localization of technetium-99m phosphorus radiopharmaceuticals in acute myocardial infarcts and other tissues. *J. Clin. Invest.*, **60**, 724–40.
28. MIRD dose estimate report No. 8. (1976) Summary of current radiation dose estimate to normal human from ^{99m}Tc as sodium pertechnetate. *J. Nucl. Med.*, **17**, 74–7.
29. Demonceau, G., Leveille, J. *et al.* (1988) Comparison of ^{99m}Tc-ECD and ^{99m}Tc-HMPAO: first human results (abstract). *J. Nucl. Med.*, **29**, 747.
30. Bossuyt, A., Morgan, G.F., Deblaton, M. *et al.* (1991) Technetium-99m MRP-20, a potential perfusion agent: in vivo biodistribution and SPECT studies in normal male volunteers. *J. Nucl. Med.*, **32**, 399–403.
31. ICRP Publication 53 (1990) *Radiation Dose to Patients from Radiopharmaceuticals*, Pergamon, Oxford, pp. 223.
32. Blau, M., Wicks, R., Thomas, S.R. and Lathrop, K.A. (1982) MIRD dose estimate report No. 10. Radiation absorbed dose from albumin microspheres labeled with technetium-99m. *J. Nucl. Med.*, **23**, 915–17.
33. Coates, G. and O'Brodovich, H. (1986) Measurement of pulmonary epithelial permeability with ^{99m}Tc DTPA aerosol. *Semin. Nucl. Med.*, **16**, 275–84.
34. ICRP Publication 53 (1990) *Radiation Dose to Patients from Radiopharmaceuticals*, Pergamon, Oxford, p. 209.
35. Atkins, H.L., Goldman, A.G., Fairchild, R.G. *et al.* (1980) Splenic sequestration of ^{99m}Tc labeled heat denatured red blood cells. *Radiology*, **136**, 501–3.
36. Wackers, F.J.T., Berman, D.S., Maddahi, J. *et al.* (1989) Technetium-99m hexakis 2-methoxy isobutyl isonitrile: human biodistribution, dosimetry, safety and preliminary comparison to thallium-201 for myocardial perfusion imaging. *J. Nucl. Med.*, **30**, 301–11.
37. Nara, R.K., Nunn, A.D., Kuczynski, B.L. *et al.* (1989) A neutral technetium-99m complex for myocardial imaging. *J. Nucl. Med.*, **30**, 1830–37.
38. Johnson, L.L. and Seldin, D.I.N. (1990) Clinical experience with technetium-99m teboroxime, a neutral, lipophilic myocardial perfusion imaging agent. *Am. J. Cardiol.*, **66**, 63E–67E.
39. Weber, D.A., Makler, P.T., Watson, E.E. *et al.* (1989) MIRD dose estimate report no. 13. Radiation absorbed dose from technetium-99m labeled bone imaging agents. *J. Nucl. Med.*, **30**, 1117–22.
40. ICRP Publication 53 (1990) *Radiation Dose to Patients from Radiopharmaceuticals*, Pergamon, Oxford, p. 179.
41. Krishnamurthy, G.T. and Turner, F.E. (1990) Pharmacokinetics and clinical application of technetium-99m labeled hepatobiliary agents. *Semin. Nucl. Med.*, **22**, 130–49.
42. Brown, P.H., Krishnamurthy, G.T., Bobba, V.R. *et al.* (1982) Radiation dose calculation for five Tc-99m IDA hepatobiliary agents. *J. Nucl. Med.*, **23**, 1025–30.

43. Walter, D.G., Keast, C.M., Fleming, J.S. *et al.* (1987) Measurement of glomerular filteration rate with technetium-99m DTPA: comparison of plasma clearance techniques. *J. Nucl. Med.*, **28**, 372–77.
44. Hauser, W., Atkins, H.L., Nelson, K.G. and Richards, P. (1970) Technetium-99m-DTPA: a new radiopharmaceutical for brain and kidney scanning. *Radiology*, **94**, 679–84.
45. Arnold, R.W., Subramanian, G., McAfee, J.G. *et al.* (1975) Comparison of ^{99m}Tc complexes for renal imaging. *J. Nucl. Med.*, **16**, 357–67.
46. ICRP Publication 53 (1990) *Radiation Dose to Patients from Radiopharmaceuticals*, Pergamon, Oxford, p. 185.
47. ICRP Publication 53 (1990) *Radiation Dose to Patients from Radiopharmaceuticals*, Pergamon, Oxford, p. 193.
48. Prenem, J.A.C., deKlerk, J.H.H., Vanhet Schip, A.D. and Van Rijk, P.P. (1991) Technetium-99m MAG_3 versus iodine-123-OIH: renal clearance and distribution volume as measured by a constant infusion technique. *J. Nucl. Med.*, **32**, 2057–60.
49. Verbruggen, A.M. (1990) Radiopharmaceuticals: state of the art. *Eur. J. Nucl. Med.*, **17**, 346–64.
50. ICRP Publication 53 (1990) *Radiation Dose to Patients from Radiopharmaceuticals*, Pergamon, Oxford, p. 173.
51. ICRP Publication 53 (1990) *Radiation Dose to Patients from Radiopharmaceuticals*, Pergamon, Oxford, pp. 259–62.
52. Taylor, A., Eshima, D. and Fritzberg, A.R. (1986) Comparison of Iodine-131 OIH and Technetium-99m MAG_3 renal imaging in volunteers. *J. Nucl. Med.*, **27**, 795–803.
53. Thakur, M.L., Lavender, J.P., Rosemary, N. *et al.* (1977) Indium-111 labeled autologous leucocytes in man. *J. Nucl. Med.*, **18**, 1014–19.
54. ICRP Publication 53 (1990) *Radiation Dose to Patients from Radiopharmaceuticals*, Pergamon, Oxford, pp. 255–56.
55. Wessels, P., Heyns, A., Pieters, H. *et al.* (1985) An improved method for the quantification of the *in vivo* kinetics of a representative population of ^{111}In labelled platelets. *Eur. J. Nucl. Med.*, **10**, 522–27.
56. Robertson, J.S., Dewanjee, M.K., Brown, M.L. *et al.* (1981) Distribution and dosimetry of ^{111}In platelets. *Radiology*, **140**, 169–76.
57. ICRP Publication 53 (1990) *Radiation Dose to Patients from Radiopharmaceuticals*, Pergamon, Oxford, pp. 253–54.
58. Goodwin, D.A., Song, C.H., Finston, R. and Matin, P. (1973) Preparation, physiology and dosimetry of ^{111}In-labeled radiopharmaceuticals for cisternography. *Radiology*, **108**, 91–8.
59. Chevru, L.R. (1979) Radiopharmaceuticals in cardiovascular nuclear medicine. *Semin. Nucl. Med.*, **4**, 241–56.
60. Saha, G.B., Go, R. and MacIntyre, W.J. (1992) Radiopharmaceuticals for cardiovascular imaging. *Nucl. Med. Biol.*, **19**, 1–20.
61. McAfee, J.G. and Subramanian, G. (1984) Radioactive agents for imaging, in *Freeman and Johnson's Clinical Radionuclide Imaging*. Grune & Stratton, New York, pp. 55–177.
62. ICRP Publication 53 (1990) *Radiation Dose to Patients from Radiopharmaceuticals*, Pergamon Press, Oxford, p. 141.
63. Phelps, M.E., Hoffman, E.J., Selin, C. *et al.* (1978) Investigation of [^{18}F] 2-fluoro-2-deoxyglucose for the measure of myocardial glucose metabolism. *J. Nucl. Med.*, **19**, 1311–19.
64. Mehdi, F., Holmes, R.A., Volkert, W.A. *et al.* (1992) Samarium-153 EDTMP: pharmacokinetic, toxicity and pain response using an escalating dose schedule in treatment of metastatic bone cancer. *J. Nucl. Med.*, **33**, 1451–58.
65. Owunwanne, A., O'Mara, R.E. and Wilson, G.A. (1979) Factors influencing blood clearance of bone scanning radiopharmaceuticals: a review. Teaching exhibit presented at the 26th annual meeting of the Society of Nuclear Medicine, Atlanta, GA, June 26–29.
66. Subramanian, G., McAfee, J., Blair, R.J. and Thomas, F.D. (1975) An evaluation of ^{99m}Tc labeled phosphate compounds as bone imaging agents, in *Radiopharmaceuticals* (eds G. Subramanian, B.A. Rhodes, J.F. Cooper and V.J. Sodd), The Society of Nuclear Medicine, New York, pp. 319–28.
67. Edwards, C.L., Hayes, R.L., Nelson, B.M. *et al.* (1970) Clinical investigation of ^{67}Ga for tumor scanning (abstract). *J. Nucl. Med.*, **11**, 317.

68. Baldwin, R.M. and Wu, J.L. (1988) *In-vivo* chemistry of iofetamine HCI ^{123}Iodine (IMP). *J. Nucl Med.*, **29**, 122–24.
69. Dayton, D.A., Maher, F.T., Elveback, L.R. (1969) Renal clearance of technetium (^{99m}Tc) as pertechnetate. *Mayo Clin. Proc.*, **44**, 539.
70. Kelly, J.D., Forster, A.M., Higley, B. *et al.* (1993) Technetium-99m tetrofosmin as a new radiopharmaceutical for myocardial perfusion imaging. *J. Nucl. Med.*, **34**, 222–27.
71. Nunn, A.D., Loberg, M.D. and Conley, R.A. (1983) A structure–distribution relationship approach leading to the development of Tc-99m mebrofenin: an improved cholescintigraphic agent. *J. Nucl. Med.*, **24**, 423–30.
72. Owunwanne, A., Church, L.B. and Blau, M. (1977) Effect of oxygen on the reduction of pertechnetate by stannous ion. *J. Nucl. Med.*, **18**, 822–26.
73. Schelbert, H.R., Henze, H., Schon, H. *et al.* (1983) C-11 labeled palmitic acid for non invasive evaluation of regional myocardial fatty acid metabolism with positron computed tomography. III. *In vivo* demonstration of the effect of substrate availability on myocardial metabolism. *Am. Heart J.*, **105**, 492–504.
74. Stocklin, G. (1992) Tracers for metabolic imaging of brain and heart. *Eur. J. Nucl. Med.*, **19**, 527–51.
75. Machulla, H.-J., Marsmann, M., Dutschka, K.P. (1980) Radiopharmaceuticals. Synthesis of radioiodinated phenyl fatty acids for studying myocardial metabolism. *J. Radional. Chem.*, **56**, 253–61.
76. Kaiser, K.P., Geuting, B., Grobmann, K. *et al.* (1990) Tracer kinetics of 15-(ortho-$^{123/131}$I-phenyl)-pentadecanoic acid (OPPA) and 15-(p-$^{123/131}$I -phenyl)-pentadecanoic acid (*p*PPA) in animals and man. *J. Nucl. Med.*, **31**, 1608–16.
77. Owunwanne, A., Shihab-Eldeen, A., Sadek, S. *et al.* (1990) The study of the effect of cyclosporin-A on bile flow in experimental animal using technetium-99m EHIDA. *Am. J. Physiol. Imag.*, **5**, 30–5.
78. Owunwanne, A., Halkar, R., Al-Rasheed, A.A. *et al.* (1988) Radionuclide imaging of the spleen with heat denatured Tc-99m RBC when the splenic reticuloendothelial system seems impaired. *J. Nucl. Med.*, **29**, 320–23.
79. dos Remedios, L.V., Weber, P.M. and Jasko, I.A. (1971) Thyroid scintigraphy in 1000 patients: Rational use of ^{99m}Tc and ^{131}I compounds *J. Nucl. Med.*, **12**, 673–77.

6

Drug–radiopharmaceutical interactions

Radiopharmaceuticals are designed to have specific biodistribution and/or elimination patterns when administered to normal subjects. In the presence of biochemical and/or pathophysiologic changes, the normal biodistribution and elimination pattern may be altered. It is this altered biologic behavior that helps a physician make a diagnosis. Altered biologic behavior may also be due to interferences caused by pharmacodynamic effects of drug(s). Hence, drug–radiopharmaceutical interaction will be defined as altered biologic behavior due to tissue response of administered drug. When the altered biologic behavior is desired, the alteration is used for diagnostic intervention or drug therapy monitoring; when it is undesired, it may be due to toxicity or direct interaction. Although there are various classifications for drug–radiopharmaceutical interactions, [1–3] the most practical approach is the one summarized in Figure 6.1.

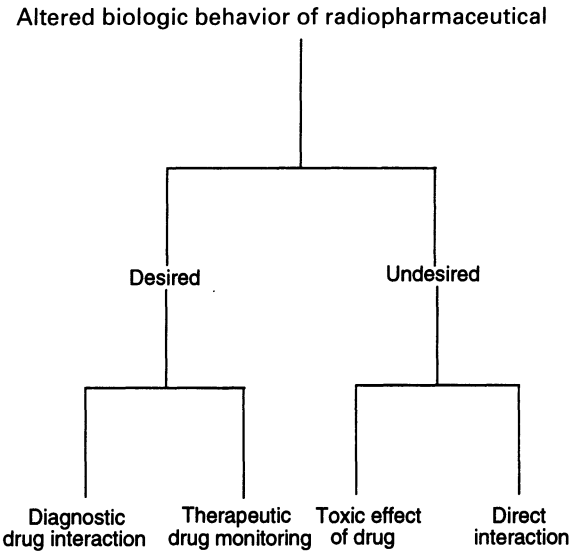

Figure 6.1 Classification of drug–radiopharmaceutical interaction. Note that altered biologic behavior caused by undesired drug–radiopharmaceutical interaction could lead to a wrong or missed diagnosis.

DESIRED DRUG–RADIOPHARMACEUTICAL INTERACTION

A drug is used to induce a pharmacologic response that influences the functional performance of an organ in such a way that the altered biologic behavior of the radiopharmaceutical is used to increase the sensitivity of a diagnosis or monitor the efficacy of therapeutic drug.

DIAGNOSTIC DRUG INTERVENTION

The altered biologic behavior is used to identify a physiologic dysfunction. This is exemplified by the presence of ischemia in cardiac perfusion stress imaging using $^{201}Tl^{+}$ or ^{99m}Tc-sestamibi and pelvicalyceal retention of urine prior to administration of furosemide during renal imaging. The use of drug intervention in the following imaging procedures is described: cardiac, cerebral, renal, thyroid and hepatobiliary studies.

Myocardial perfusion studies

Dipyridamole, adenosine and dobutamine are used for pharmacologic intervention in cardiac studies. They are used as an alternative in patients who cannot be exercised for diagnosis of coronary artery disease involving myocardial perfusion radiopharmaceuticals ($^{201}Tl^{+}$, ^{99m}Tc-sestamibi and ^{99m}Tc-teboroxime).

Dipyridamole

Mode of action Dipyridamole is a potent coronary vasodilator. It acts by blocking the re-uptake process that transports adenosine into heart cells (adenosine receptors), thereby resulting in a higher availability of endogenous adenosine to produce vasodilation of normal but not significantly stenosed coronary arteries [4]. Hence, myocardial perfusion of regions supplied by normal coronary arteries is enhanced [5,6]. Dipyridamole has a plasma half-life of 15–30 min. Its adverse effect(s) may be suppressed by intravenous administration of aminophylline, which blocks adenosine receptors [4–7].

Procedure Patients must fast for at least 3 h and abstain from coffee, tea, chocolate and medications containing caffeine for at least 12 h and stop all theophylline medications 24–36 h prior to the study. The dipyridamole is infused at the rate of 0.142 μg/kg/min over 4 min. The appropriate radiopharmaceutical is injected 2–5 min following the cessation of the dipyridamole infusion.

Adenosine

Mode of action Adenosine acts directly by activating the adenosine A_2 receptors, which relaxes the smooth muscles, leading to vasodilation that results in increased blood flow in normal coronary arteries but not in significantly stenosed arteries [8, 9]. Adenosine has a plasma half-life of less than 10 s [4, 8]. The side-effects of adenosine disappear within 2 mins of cessation of the infusion owing to its ultrashort duration of action. Hence, aminophylline is rarely required.

Procedure Patients should refrain from medications and caffeine-containing food, as mentioned previously, and also from oral dipyridamole. A dose of 0.142 μg/kg/min is infused intravenously over 6 min with simultaneous injection of the appropriate radiopharmaceutical 2–3 min after beginning the adenosine infusion.

Dobutamine

Mode of action Dobutamine is a sympathomimetic amine and acts by increasing myocardial contraction and left ventricular oxygen consumption by direct stimulation of the

myocardial beta-1 receptors. It has a plasma half-life of 2 min [10]. The effect of dobutamine may be suppressed by intravenous administration of esmolol (beta-blocker).

Procedure Patients must fast for at least 3 hs and refrain from taking beta-blockers for 24–48 h. A dose of 5 μg/kg/min is infused intravenously over 3 min and is followed by stepwise increases of 10, 20, 30 and 40 μg/kg/min for each consecutive 3 min. The appropriate radiopharmaceutical is injected and the infusion is continued at the rate of 40 μg/kg/min for another 2 min.

Cerebral perfusion studies

Acetazolamide (Diamox) is used for pharmacologic intervention studies in brain imaging. As a cerebral vasodilator it increases cerebral perfusion of normal tissues while minimal or no increase is produced in regions supplied by vessels with significant stenosis. Therefore, the use of acetazolamide in brain imaging would increase the sensitivity of detection of cerebrovascular diseases and help to identify patients who might benefit from internal–external carotid artery bypass surgery (endarterectomy).

Mode of action The mechanism of action of acetazolamide is not fully understood but it is thought to be due to (a) inhibition of carbonic anhydrase in brain parenchyma and cerebral vasculature leading to cerebral vasodilation [11–13] or (b) the direct effect of acetazolamide on smooth muscle of the cerebral vasculature [14]. Its effect on cerebral perfusion can be detected within 2 min of injection, with a maximum response at 25 min and half-life of 90 min [14].

Procedure Acetazolamide is administered intravenously at a dose of 500–1000 mg, 20 mins before injection of the radiopharmaceutical (^{99m}Tc-*d*, *l*-HMPAO, ^{99m}Tc-*l*, *l*-ECD, ^{123}I-IMP or ^{123}I-HIPDM).

Renal studies

Diuretics (furosemide) or angiotensin converting enzyme inhibitors (captopril, lisinopril or enalopril) are used in renal studies.

Furosemide (Lasix)

Furosemide is used for evaluation of obstructive uropathy (urine outflow obstruction).

Mode of action Furosemide is thought to act by inhibiting the active reabsorption of Cl^- ions (and therefore of NaCl) in the ascending limb of the loop of Henle, leading to loss of Na^+ ions and water [15]. Hence, when furosemide is administered during renal studies, the diuresis that it induces is used to differentiate functional from mechanical obstructive uropathy.

Procedure Patients are properly hydrated by being asked to drink 2–3 glasses of liquid. Furosemide (0.5 mg/kg) may be injected 15 min prior to or after injection of the radiopharmaceutical (^{99m}Tc-DTPA, ^{99m}Tc-MAG_3 or $^{123/131}$I-*o*-IH).

Captopril

Captopril is used for evaluation of renovascular hypertension.

Mode of action Captopril is thought to act by inhibiting the conversion of angiotensin I to angiotensin II, thereby lowering the blood pressure in patients with renovascular hypertension [16]. This inhibition also exaggerates the asymmetry in renal uptake and excretion of ^{99m}Tc-DTPA, ^{99m}Tc-MAG_3 or $^{123/131}$I-*o*-IH

between the abnormal and normal kidneys in patients with unilateral renal artery stenosis [17–23]. It has been reported that the GFR of the kidney with renal artery stenosis may drop while effective renal plasma flow (ERPF) may remain unchanged or even be elevated [24].

Procedure Two studies may be performed with and without captopril administration. Patients are properly hydrated by being asked to drink 2–3 glasses of liquid 30 min prior to the study. If the patient is already on captopril, no further captopril is given; otherwise 25 mg is given orally 1 h prior to injection of the radiopharmaceutical, followed by performance of the routine renal studies.

Thyroid studies

Thyroid-stimulating hormone (TSH), 3, 5, 3′ - triiodothyronine (T_3) suppression and perchlorate discharge tests are the pharmacologic interventions done for thyroid studies.

TSH test

The TSH stimulation test with radioiodine thyroid uptake and/or imaging is used in the diagnosis of thyroid disease, especially in patients with borderline thyroid function, or to determine whether or not a cold nodule (which has been depressed by autonomous toxic nodules) is functioning.

Mode of action Although TSH enhances all processes (transport of iodide, organification, coupling and proteolysis of thyroglobulin and release of thyroxine) leading to the synthesis and secretion of thyroid hormone when administered for iodide uptake or imaging, the effect most probably reflects the transport mechanism only [25]. Therefore it is used to differentiate normal from abnormal borderline thyroid function and to distinguish normal cold area(s) depressed by autonomous toxic nodules from abnormal cold areas.

Procedure Measurement of baseline thyroid uptake of radioiodine and/or imaging is performed. TSH is given intramuscularly for 1–3 days in doses of 5–10 units/day, and the uptake and/or imaging study is repeated. A 50% increase above the baseline uptake value is considered normal.

T_3 suppression test This test involves the suppression of TSH by administering T_3. The increase of T_3 level in the blood inhibits the secretion of TSH by the pituitary gland. This leads to a decrease in thyroid uptake of radioiodine. The test is used to detect autonomous thyroid function and euthyroid patients with Graves' ophthalmopathy [26].

Procedure Baseline thyroid radioiodine uptake is measured. T_3 is given orally at a dose of 75 μg/ day for 8 days. The uptake test is repeated. A decrease of less than 50% of the baseline uptake value is considered normal.

Perchlorate discharge test

This test detects defects in the organification of iodide by the thyroid gland.

Mode of action Owing to similarity between the molecular shape of iodide and perchlorate, they share the same mechanism of transport [27]. Therefore perchlorate acts as a competitive inhibitor of iodide transport.

Procedure Radioiodide is given orally and thyroid uptake is measured every 30 min for 2 h; 500 mg of potassium perchlorate is administered orally and measurement of the thyroid uptake of the radioiodide is continued

for 2 h (every 30 min). If the measurement indicates a decrease ≥ 20% of the 2-hour uptake, it is assumed that the organification process is impaired because potassium perchlorate was able to displace the radioiodide.

Hepatobiliary studies

Cholecystokinin or sincalide, morphine and phenobarbital are used for pharmacologic intervention in hepatobiliary studies.

Cholecystokinin or Sincalide

Cholecystokinin (CCK) or sincalide is used in hepatobiliary studies for confirming chronic acalculous biliary disease by determining the maximal response of gallbladder to exogenous CCK measured as ejection fraction. Patients with a partially obstructed, chronically inflamed or functionally impaired gallbladder have a reduced ejection fraction (<35%) [28–30].

To perform CCK or sincalide hepatobiliary imaging, patients should fast for at least 3–4 h. For determination of gallbladder ejection fraction CCK or sincalide (0.02 μg/kg) is intravenously infused over 3 min, 1 h after ^{99m}Tc-IDA administration or after the gallbladder is seen to be maximally filled with radioactivity (little or no activity remains within the major hepatic biliary radicles). CCK or sincalide must never be given as a bolus injection because it causes spasm of the neck of the gallbladder, which results in a falsely low ejection fraction.

Sincalide or CCK is also used to prepare patients who have fasted longer than 24–48 h and as a means of reducing the time required to confirm the clinical impression of acute cholecystitis from 4 to 1.5 h. In patients who have fasted longer than 24–48 h, there is increased intraluminal gallbladder pressure, which reduces bile flow to the gallbladder. When sincalide or CCK is administered, it causes the gallbladder to contract and eject, and cleans it of its sludge, thereby eliminating the increased intraluminal pressure that permits more bile flow into the bladder if the cystic duct is patent [31].

Morphine

Morphine intervention is used to decrease the time required to determine cystic duct patency. Following intravenous administration, morphine enhances the tone of the sphincter of Oddi and increases intraluminal common bile duct pressure. This increase in pressure is high enough to overcome the resistance of bile flow into the gallbladder provided the cystic duct is patent [31].

If the gallbladder is not visualized up to 60 min after the administration of ^{99m}Tc-IDA and radioactivity is seen in the small intestine, morphine sulfate (0.04 mg/kg) is infused intravenously over 3 min. If the gallbladder is still not visualized cystic duct obstruction is confirmed.

Phenobarbital

Phenobarbital is used to increase the accuracy of differentiating neonatal hepatitis from biliary atresia. Phenobarbital enhances the uptake and excretion of substances that use the hepatic transport system for organic anions, such as BSP, bilirubin and ^{99m}Tc-IDA derivatives [31].

Patients are premedicated with 5 mg/kg phenobarbital in two divided doses for 5 consecutive days before intravenous administration of ^{99m}Tc-IDA. If the hepatobiliary image demonstrates passage of radioactivity into the bowel, the diagnosis of biliary atresia is excluded.

THERAPEUTIC DRUG MONITORING

The altered biologic behavior of the radiopharmaceutical is used to measure the tissue

Table 6.1 Examples of drug–radiopharmaceutical interaction involving therapeutic drug monitoring

Drug	*Radiopharmaceutical*	*Effect on biologic behavior*	*Reference*
Anticancer agents Bleomycin Cyclophosphamide Doxorubicin Vincristine	^{99m}Tc-phosphorus complexes (^{99m}Tc-PYP, ^{99m}Tc-MDP, ^{99m}Tc-HMDP)	Increased bone uptake during the early phase of treatment (3 months) (flare phenomenon) Decreased bone uptake during the later phase of treatment (~6 months)	32–38
	^{18}FDG	Decreased uptake may occur in some tumours, particularly in CNS cancer	39–41
	^{67}Ga citrate	Decreased uptake in the tumor site	42–44
Antithyroid agents Carbimazole, methimazole, PTU	$^{123/131}I^-$ ion	Decreased 24-h uptake and residence time in the thyroid	45–47
Dichloromethylene diphosphonate, Etidronate	^{99m}Tc-phosphorus complexes	Generalized decreased bone uptake in Paget's disease	48, 49
Gamma globulin	^{99m}Tc-*d,l*-HMPAO white blood cells	Markedly decreased uptake in myocardium	50
Hormonal agents	^{99m}Tc-phosphorus complexes	Dramatic increase in bone uptake during the early phase of treatment (2–3 months) Dramatic decrease in bone uptake tending towards normal pattern during the late phase of treatment (6 months)	32, 37
Hormonal agents	^{67}Ga citrate	Decreased lung uptake in pulmonary fibrosis and sarcoidosis	51–52
Labetalol	^{131}I-mIBG	Decreased uptake in pheochromocytoma site	53
Metoclopromide	^{99m}Tc colloid-solid meal	Decreased gastric emptying time	54
Thrombolytic agents	^{99m}Tc-sestamibi,$^{201}Tl^+$	Increased perfusion	55, 56, 57
^{131}I-sodium iodide	$^{123/131}I^-$ ion	Decreased uptake and/or decreased number of metastatic site	58–60
^{153}Sm-EDTMP	^{99m}Tc-phosphorus complexes	Decreased uptake and/or decreased number of localizations at metastatic site	58, 61, 62

Table 6.1 (cont.)

Drug	*Radiopharmaceutical*	*Effect on biologic behavior*	*Reference*
^{186}Re-HEDP	^{99m}Tc-phosphorus complexes	Decreased uptake and/or decreased number of localization at metastatic site	58, 62, 63
^{131}I-mIBG	^{131}I-mIBG	Partial decrease in pheochromocytoma uptake as measured by more than 50% decrease in tumor volume	58, 64

response to the desired pharmacologic effect produced by the drug. The drug may be either non-radioactive or radioactive, such as $^{131}I^-$ ion in the treatment of thyroid cancer and metastasis. Prior to administration of the drug, a baseline abnormal study is obtained, which serves as a reference point for comparison with subsequent studies. The change in the biologic behavior or pattern of the radiopharmaceutical after treatment with the drug is assumed to reflect the tissue response to the pharmacologic effect of the drug as exemplified by monitoring the prognosis of Paget's disease treated with etidronate disodium. Examples of drug–radiopharmaceutical interactions in monitoring drug therapy are given in Table 6.1. In general, the altered biologic behavior is from an abnormal pattern to a normal pattern.

UNDESIRED DRUG–RADIOPHARMACEUTICAL INTERACTION

The undesired drug–radiopharmaceutical interaction is either due to the pharmacodynamic effects induced by a drug whose effect has exceeded its therapeutic value or is a direct result of an *in vivo* chemical reaction between drug and radiopharmaceutical; these are referred to as toxic and direct interactions respectively. Either case results in an altered biologic behavior that might interfere with the interpretation of the radionuclide study.

TOXIC EFFECTS OF DRUGS

The altered biologic behavior is used to measure the undesired tissue response to adverse effects induced by a drug. The extent of the toxicity will depend on blood flow to the organs/tissues, permeability of the drug across capillary/tissue membranes (lipophilicity of the drug), and tissue/plasma protein binding. It is therefore possible for a drug to produce multiorgan toxicity as exemplified by cyclosporin A, an immunosuppressant. Because the amount of radioactivity in each organ can be measured separately using a biodistribution technique or directly using an external monitoring device (gamma camera or probe), radiopharmaceuticals are very useful agents for studying drug toxicity in either animals or humans. In addition to using organ-specific radiopharmaceuticals, radioactive tracers that freely diffuse into various biologic tissues (such as ^{125}I-HIPDM) can be used as screening agents. Examples of drug–radiopharmaceutical interactions involving toxic effects of drugs are listed in Table 6.2. In general, the altered biologic behavior is from a normal pattern to an abnormal pattern.

Table 6.2 Examples of drug–radiopharmaceutical interaction involving toxic effect of drugs

Drug	*Radiopharmaceutical*	*Effect of biologic behavior*	*Reference*
Amphetamine	^{123}IMP	Multiple defects involving mainly the occipital and parietal lobes and the cerebellum	65
	^{99m}Tc-PYP,	Increased soft-tissue uptake	66
Anti-cancer agents, Adriamycin (doxorubicin)	^{99m}Tc-PYP,^{111}In-antimyosin, ^{67}Ga citrate	Uptake in adriamycin-damaged myocardium	57, 67–71
	^{99m}Tc-sestamibi	Reduced myocardial uptake and retention	72
	^{99m}Tc-RBC	Decreased labeling efficiency	73
	^{123}I-mIBG	Decreased myocardial retention	74, 75
	^{201}Tl^{+}	Decreased washout	76
Actinomycin D and melphalan	^{99m}Tc-phosphorus complexes	Diffuse increased uptake in bone and soft tissue	77
Bleomycin, cyclophosphamide, nitrosoureas	^{67}Ga citrate	Diffuse bilateral uptake in lungs owing to interstitial pulmonary inflammation	78, 79
	^{99m}Tc-DTPA aerosol	Patchy lung uptake	80
Doxorubicin, cyclophosphamide, vincristine, methotrexate, gentamycin	^{99m}Tc-phosphorus complexes	Intense renal parenchymal uptake	81
Cisplatin, isostamide	^{99m}Tc-DMSA	Low renal uptake	82, 83
Methotrexate, 6-mercaptopurine	^{99m}Tc colloid	Patchy uptake in liver	84
Interleukin 2	^{99m}Tc-*d*, *l*-HMPAO	Decreased frontal and parietal cortical perfusion and increased perfusion in basal ganglia	85
Alcohol (chronic)	^{99m}Tc-*d*, *l*-HMPAO	Decreased frontal flow and more perfusion in the left than right hemisphere	86
Halothane	^{99m}Tc-sulfur colloid	Reversal of the normal liver–spleen colloid distribution pattern	87
Antihypertensive agent, prazosin	^{99m}Tc-RBC	Decreased labeling efficiency	88
Chloroquine	^{67}Ga citrate	Myocardial and renal uptake	89
Cyclosporin A	^{99m}Tc-IDAs	Prolonged biliary excretion	90
	^{99m}Tc-PYP, ^{111}In-antimyosin	Uptake in myocardium	91

Table 6.2 (cont.)

Drug	*Radiopharmaceutical*	*Effect of biologic behavior*	*Reference*
	^{99m}Tc-DTPA, ^{131}I-hippuran	Decreased renal parenchymal uptake	92–94
	^{125}I-HIPDM	Prolonged retention in liver and kidney Decreased splenic uptake	95
	^{111}In-oxine platelets	Deposition in renal cortical arteries	96
Cocaine	^{99m}Tc-phosphorus complexes	Marked soft-tissue accumulation	97
	^{123}IMP	Decreased rate of cerebral perfusion. Foci of reduced uptake in the frontal and parieto-occipital cortex	98, 99
Diethylstilbestrol	^{99m}Tc-PYP	Bilateral uptake in the breast of male patient with prostatic carcinoma	100
Estrogens	^{67}Ga citrate	Uptake in male breast	101
Iodinated contrast agents	$^{123/131}$I	Decreased thyroid uptake	102, 103
Steroids	^{99m}Tc-phosphorus complexes	Generalized decrease in bone uptake due to depletion of bone mineral	104
Vitamin D_3	^{99m}Tc-PYP	Decreased bone uptake	105

Table 6.3 Examples of drug–radiopharmaceutical interaction involving direct reactions

Drug	*Radiopharmaceutical*	*Effect on biologic behavior*	*Reference*
Aluminum hydroxide	^{99m}Tc colloids	Aggregation of colloid in the lungs	106
Iron dextran (intramuscular)	^{99m}Tc-phosphorus complexes	Accumulation at the site of injection	107, 108
Iron colloid solution (intravenous)	^{99m}Tc-phosphorus complexes	Diffuse liver uptake	109
Digoxin	^{99m}Tc-RBC	Decreased labeling efficiency	88
Heparin	^{99m}Tc-RBC	Decreased labeling efficiency and increased renal uptake excretion	110

DIRECT INTERACTION

The altered biologic behaviour is a direct consequence of an *in vivo* reaction between a drug and a radiopharmaceutical exemplified by the reaction between reduced ^{99m}Tc and heparin during the *in vivo* labeling of red blood cells. The altered biologic behavior results in poor uptake of the radiopharmaceutical in

the organ of interest, high uptake in non-target organ(s) and/or prolonged elimination, as listed in Table 6.3.

REFERENCES

1. Hladik III, W.B., Nigg, K.K. and Rhodes, B.A. (1982) Drug-induced changes in the biological distribution of radiopharmaceutical. *Semin. Nucl. Med.*, **12**, 184–218.
2. Lentle, B.C., Scott, J.R., Noujaim, A.A. *et al.* (1979) Iatrogenic alterations in radionuclide biodistributions. *Semin. Nucl. Med.*, **9**, 131–43.
3. Olmos, R.A.V., Hoefnagel, C.A. and Van der Schoot, J.B. (1993) Nuclear medicine in the monitoring of organ function and the detection of injury related to cancer therapy. *Eur. J. Nucl. Med.*, **20**, 515–46.
4. Klabunde, R.E. (1983) Dipyridamole inhibition of adenosine metabolism in human blood. *Eur. J. Pharmacol.*, **93**, 21–6.
5. Verani, M.S. and Mahmarian, J.J. (1991) Myocardial perfusion scintigraphy during maximal coronary artery vasodilatation with adenosine. *Am. J. Cardiol.*, **67**, 12D–17D.
6. Iskandrian, A.S. (1991) Single-photon emission computed tomographic thallium imaging with adenosine, dipyridamole, and exercise. *Am. Heart J.*, **122**, 279–84.
7. Smits, P., Corstens, F.H.M., Aengevaeren, W.R.M. *et al.* (1991) False-negative dipyridamole-thallium 201 myocardial imaging after caffeine infusion. *J. Nucl. Med.*, **32**, 1538–41.
8. Wilson, R.F., Wyche, K., Christensen, B. *et al.* (1990) Effects of adenosine on human coronary arterial circulation. *Circulation*, **82**, 1595–606.
9. Rossen, J.D., Quillen, J.E., Lopez, J.A. *et al.* (1991) Comparison of coronary vasodilation with intravenous dipyridamole and adenosine. *J. Am. Coll. Cardiol.*, **18**, 485–91.
10. Hurwitz, R.A., Siddiqui, A., Caldwell, R.L. *et al.* (1990) Assessment of ventricular function in infants and children. Response to dobutamine infusion. *Clin. Nucl. Med.*, **15**, 556–59.
11. Giacobini, E. (1962) A cytochemical study of the localization of carbonic anhydrase in the nervous system. *J. Neurochem.*, **9**, 169–77.
12. Ridderstrale, Y. and Hanson, M. (1985) Histochemical study of the distribution of carbonic anhydrase in the cat brain. *Acta Physiol. Scand.*, **124**, 557–64.
13. Ehrenreich, D.L., Burns, R.A., Alman, R.W. *et al.* (1961) Influence of acetazolamide on cerebral blood flow. *Arch. Neurol.*, **5**, 227–32.
14. Hauge, A., Nicolaysen, G. and Thoresen, M. (1983) Acute effects of acetazolamide on cerebral blood flow in man. *Acta Physiol. Scand.*, **117**, 233–39.
15. Berndt, W.O. and Stitzel, R.E. (1990) Water, electrolyte metabolism and diuretic drugs, in *Modern Pharmacology*, 3rd edn. (eds C.R. Craig and R.E. Stitzel), Little Brown, Boston, pp. 248–70.
16. Hodson, G.P., Isles, C.E., Murray, G.D. *et al.* (1983) Factors related to first dose hypotensive effect of captopril prediction and treatment. *BMJ*, **286**, 832–34.
17. Wenting, G.J., Tan-Tjiong, H.L., Dereks, F.H.M. *et al.* (1984) Split renal function after captopril in unilateral renal artery stenosis. *BMJ*, **288**, 886–90.
18. Majd, M., Potter, B.M., Guzzetta, P.C. *et al.* (1983) Effect of captopril on efficiency of renal scintigraphy in detection of renal artery stenosis (abstract). *J. Nucl. Med.*, **24**, 23.
19. Oei, H.Y., Geyskes, G.G., Roos, G.L. *et al.* (1984) Diagnosis of unilateral renal artery stenosis by captopril renography (abstract). *Eur. J. Nucl. Med.*, **9**, A24.
20. Miyamori, I., Yasuhara, S., Takeda, Y. *et al.* (1986) Effects of converting enzyme inhibition on split renal function in renovascular hypertension. *Hypertension*, **8**, 415–21.
21. Geyskes, G.G., Oei, H.Y., Puylaert, C.B.A.J. *et al.* (1986) Renography with captopril: changes in a patient with hypertension and unilateral renal artery stenosis. *Arch. Intern. Med.*, **146**, 1705–708.
22. Fommei, E., Ghione, S., Palla, L. *et al.* (1987) Renal scintigraphic captopril test in the diagnosis of renovascular hypertension. *Hypertension*, **10**, 212–20.
23. Sfakianikis, G.N., Baergoignie, J.J., Jaffe, D. *et al.* (1987) Single dose captopril scintigraphy in the diagnosis of renovascular hypertension. *J. Nucl. Med.*, **28**, 1383–92.
24. Fine, E.J. (1991) Intervention in renal scintigraphy. *Semin. Nucl. Med.*, **21**, 116–27.

25. Antar, M.A. (1984) Interventional studies of the thyroid, in *Interventional Nuclear Medicine* (ed. R.P. Spencer), Grune & Stratton, Orlando, FL, pp. 337–407.
26. Hurley, J.R. and Becker, D.V. (1981) Thyroid supression and stimulation testing: the place of scanning in the evaluation of nodular thyroid disease. *Semin. Nucl. Med.*, **11**, 149–60.
27. Ingbar, S.H. and Woeber, K.A. (1981) The thyroid gland, in *Textbook of Endocrinology*, 7th edn (eds R.H. Williams and D.W. Foster), W.B. Saunders, Philadelphia, pp. 682–815.
28. Bobba, V.R., Krishnamurthy, G.T., Kingston, E. *et al.* (1984) Gallbladder dynamics induced by a fatty meal in normal subjects and patients with gallstones: concise communication. *J. Nucl. Med.*, **25**, 21–4.
29. Krishnamurthy, G.T., Bobba, V.R., McConnel, D. *et al.* (1983) Quantitative biliary dynamics: introduction of a new non invasive scintigraphic technique. *J. Nucl. Med.*, **24**, 217–23.
30. Krishnamurthy, G.T., Bubba, V.R. and Kingston, E. (1981) Radionuclide ejection fraction: a technique for quantitative analysis of motor function of human gallbladder. *Gastroenterology*, **80**, 482–90.
31. Fink-Bennett, D. (1991) Augmented cholescintigraphy: its role in detecting acute and chronic disorders of the hepatobiliary tree. *Semin. Nucl. Med.*, **21**, 128–39.
32. Coleman, R.E., Mashiter, G., Whitaker, K.B. *et al.* (1988) Bone scan flare predicts successful systemic therapy for bone metastases. *J. Nucl. Med.*, **29**, 1354–59.
33. Stokkel, M.P.M., Vale's Olmos, R.A., Hoefnagel, C.A. *et al.* (1993) Tumor and therapy associated abnormal changes in bone scintigraphy: old and new phenomena. *Clin. Nucl. Med.*, **18**, 821–28.
34. Hortobagyi, G.N., Libshitz, H.I. and Seabold, J.E. (1984) Osseous metastases of breast cancer. Clinical, biochemical, radiographic and scintigraphic evaluation of response to therapy. *Cancer*, **55**, 577–82.
35. Rossleigh, M.A., Lovegrove, F.T.A., Reynolds, P.M. *et al.* (1984) The assessment of response to therapy of bone metastases in breast cancer. *Aust. NZ J. Med.*, **14**, 19–22.
36. Langhammer, H.R., Sintermann, G.H. and Pabst, H.W. (1978) Serial bone scintigraphy for assessing the effectiveness of treatment of osseous metastases from prostatic cancer. *Nucl. Med.*, **17**, 87–91.
37. Citrin, D.L., Tuohy, J.B., Bessent, R.G. *et al.* (1974) Quantitative bone scanning. A method for assessing response of bone metastases to treatment. *Lancet*, **ii**, 1132–36.
38. Shearer, R.J., Constable, A.R., Girling, M. *et al.* (1974) Radioisotopic bone scintigraphy with gamma camera in the investigation of prostatic cancer. *BMJ*, **346**, 362–65.
39. Takahashi, H., Yamaguchi, K., Wakui, A. *et al.* (1986) New approach to clinical evaluation of cancer chemotherapy using positron emission tomography with ^{18}FDG (2-deoxy-2-[^{18}F] fluoro-D-glucose). *Sci. Rep. Inst. Tohoku Univ.* (Med.), **33**, 38–43.
40. Strauss, L.G. and Conti, P.S. (1991) The applications of PET in clinical oncology. *J. Nucl. Med.*, **32**, 623–48.
41. Minn, H. and Paul, R. (1992) Cancer treatment monitoring with fluorine-18 2-fluoro-2-deoxy-D-glucose and positron emission tomography: frustration or future? (editorial). *Eur. J. Nucl. Med.*, **19**, 921–24.
42. Tsan, M-F. and Scheffel, U. (1986) Mechanism of gallium-67 accumulation in tumours. *J. Nucl., Med.*, **27**, 1215–19.
43. Edward, C.L. and Hayes, R.L. (1969) Tumor scanning with gallium-67 citrate. *J. Nucl. Med.*, **10**, 103–5.
44. Fletcher, J.W., Herbig, F.K. and Donati, R.M. (1975) Gallium-67 citrate distribution following whole body irradiation or chemotherapy. *Radiology*, **117**, 709–12.
45. Goolden, A.W.G. and Fraser, T.R. (1969) Effect of pretreatment with carbimazole in patients with thyrotoxicosis subsequently treated with radioiodine. *BMJ*, **3**, 443–44.
46. Velkeniers, B., Vanhaelst, L., Cytryn, R. and Jonckheer, M.H. (1988) Treatment of hyperthyroidism with radioiodine: adjunctive therapy with antithyroid drugs reconsidered. *Lancet*, **i**, 1127–29.
47. Clerc, J., Izembart, M., Dagousset, F. *et al.* (1993) Influence of dose selection on absorbed dose profiles in radioiodine treatment of diffuse

toxic goiters in patients receiving or not receiving carbimazole. *J. Nucl. Med.*, **34**, 387–93.
48. Espinasse, D., Mathieu, L., Alexandre, C. *et al.* (1981) The kinetics of ^{99m}Tc labelled EHDP in Paget's disease before and after dichloromethylene diphosphonate treatment. *Metab. Bone Dis. Res.*, **2**, 321–24.
49. Vellenga, C., Pauwels, E.K.J., Bijvoet, O.L. *et al.* (1976) Evaluation of scintigraphic and roentgenologies studies in Paget's disease under treatment. *Radiologia Clin.*, **45**, 293–301.
50. Kao, C-H., Hsieh, K-S., Wang, Y-L. *et al.* (1992) ^{99m}Tc HMPAO WBC imaging to detect myocarditis and to evaluate the results of high dose gamma globulin treatment in Kawasaki disease. *Clin. Nucl. Med.*, **17**, 623–26.
51. Jhingran, S.G., Mukhopadhyay, A.K., Ajmani, S.K. *et al.* (1977) Hepatic adenomas and focal nodular hyperplasia of the liver in young women on oral contraceptives. Case report. *J. Nucl. Med.*, **18**, 263–66.
52. Siemsen, J.K., Grebe, S.F. and Waxman, A.D. (1978) The use of Gallium-67 in pulmonary disorders. *Semin. Nucl. Med.*, **8**, 235–49.
53. Morais, J., LeMarec, H., Peltier, P. *et al.* (1992) MIBG scintigraphy of a patient with pheochromocytoma on labetalol therapy. *Clin. Nucl. Med.*, **17**, 308–11.
54. Domstad, P.A., Kim, E.E., Coupal, J.J. *et al.* (1980) Biologic gastric emptying time in diabetic patients using Tc-99m labeled resin oatmeal with and without metoclopramide. *J. Nucl. Med.*, **21**, 1098–100.
55. Wackers, F.J.T., Gibbons, R.J., Verani, M.S. *et al.* (1989) Serial quantitative planar technetium-99m isonitrile imaging in acute myocardial infarction. Efficacy for noninvasive assessment of thrombolytic therapy. *J. Am. Coll. Cardiol.*, **14**, 861–73.
56. Santoro, G.M., Bisi, G., Seigra, R. *et al.* (1990) Single photon emission computed tomography with technetium-99m hexakis 2-methoxy isobutylisonitrile in acute myocardial infarction before and after thrombolytic treatment: assessment of salvaged myocardium and prediction of late functional recovery. *J. Am. Coll. Cardiol.*, **15**, 301–14.
57. Heller, G.V., Parker, J.N., Silverman, K.J. *et al.* (1987) Intra coronary thallium-201 scintigraphy after thrombolytic therapy for acute myocardial infarction compared with 10 and 100 day intravenous thallium-201 scintigraphy. *J. Am. Coll. Cardiol.*, **9**, 300–7.
58. Hoefnagel, C.A. (1991) Radionuclide therapy revisited. *Eur. J. Nucl. Med.*, **18**, 408–31.
59. Beierwaltes, W.H., Rabbani, R., Dmuchowski, C. *et al.* (1984) An analysis of 'ablation of thyroid remnants' with I-131 in 511 patients from 1947–1984: experience at University of Michigan. *J. Nucl. Med.*, **25**, 1287–93.
60. Leeper, R.D. and Shimaoka, K. (1980) Treatment of metastic thyroid cancer. *Clin. Endocrinol. Metab.*, **9**, 383–404.
61. Mehdi, F., Holmes, R.A., Volkert, W.A. *et al.* (1992) Samarium-153-EDTMP: pharmacokinetic, toxicity and pain response using an escalating dose schedule in treatment of metastatic bone cancer. *J. Nucl. Med.*, **33**, 1451–58.
62. Ketring, A.R. (1987) ^{153}Sm-EDTMP and ^{186}Re-HEDP as bone therapeutic radiopharmaceuticals. *Nucl. Med. Biol.*, **14**, 223–32.
63. Maxon, H.R., Deutsch, E.A., Thomas, S.R., *et al.* (1988) Re-186 (Sn) HEDP for treatment of multiple metastic foci in bone: human distribution and dosimetric studies. *Radiology*, **166**, 501–7.
64. Jakubowski, W., Feltyowski, T., Januszewicz, W. *et al.* (1985) ^{131}I-meta-iodobenzylguanidine in localization and treatment of pheochromocytoma. *Nucl. Med. Commun.*, **6**, 586.
65. Ohita, H., Komibuchi, T., Nishino, I. *et al.* (1992) Brain perfusion abnormalities in a thinner and amphetamine abuser detected by I-123 IMP scintigraphy. *Ann. Nucl. Med.*, **6**, 273–75.
66. Kao, C-H., Liao, S-P., Wang, S-J. and Yeh, S-H. (1992) ^{99m}Tc PYP imaging in amphetamine intoxication associated with non traumatic rhabdomyolysis. *Clin. Nucl. Med.*, **17**, 101–2.
67. Khako, A.K., Gordon, D.H., Bennett, J.M. *et al.* (1977) Myocardial imaging with Tc-99m pyrophosphate in patients on adriamycin treatment of neoplasia. *J. Nucl. Med.*, **18**, 680–83.
68. Carrid, I., Estorch, M., Berna, L. *et al.* (1991) Assessment of anthracyline-induced myocardial damage by quantitative indium-111 myosin specific monoclonal antibody studies. *Eur. J. Nucl. Med.*, **18**, 806–12.
69. Lekakis, J., Vassilopoulos, N., Psichoyiou, H. *et al.* (1991) Doxorubicin cardiotoxicity detected by indium-111 myosin specific imaging. *Eur. J. Nucl. Med.*, **18**, 225–26.

70. Estorch, M., Carrio, I., Berna, L. *et al.* (1990) Indium-111 antimyosin scintigraphy after doxorubicin therapy in patients with advanced breast cancer. *J. Nucl. Med.*, **31**, 1965–69.
71. Hatfield, M.K., Martin, W.B., Ryan, J.W. *et al.* (1986) Increased uptake of 67-gallium citrate activity in a patient with adriamycin-damaged myocardium. *Clin. Nucl. Med.*, **11**, 756–57.
72. Piwnica-Worms, D., Chiu, M.L. and Kronauge, J.F. (1992) Detection of acute adriamycin cardiotoxicity in cultured chick heart with Tc-99m-sestamibi (abstract). *J. Nucl. Med.*, **33**, 864.
73. Ballinger, J.R., Gerson, B., Gulenchyn, K.Y. *et al.* (1988) Technetium-99m red blood cell labelling in patients treated with doxorubicin. *Clin. Nucl. Med.*, **13**, 169–70.
74. Valde's Olmos, R.A., ten Bokkel Huinink, W.W., Greve, J.C. and Hoefnagel, C.A. (1992) I-123 MIBG and serial radionuclide angiocardiography in doxorubicin related cardiotoxicity. *Clin. Nucl. Med.*, **17**, 163–67.
75. Wakasugi, S., Wada, A., Hasegawa, Y. *et al.* (1992) Detection of abnormal cardiac adrenergic neuron activity in adriamycin-induced cardiomyopathy with iodine-125-metaiodobenzylguanidine. *J. Nucl. Med.*, **33**, 208–14.
76. Frost, D., Sorensen, S., O'Rourke, R. *et al.* (1979) Reversibility of adriamycin induced reduction in myocardial thallium-201 uptake by intravenous digoxin (abstract). *Clin. Res.*, **27**, 727A.
77. Sorkin, S.J., Horii, S.C., Passalaqua, A. *et al.* (1977) Augmented activity on bone scan following local chemoperfusion. *Clin. Nucl. Med.*, **2**, 451.
78. Richman, S.D., Levenson, S.M., Bunn, P.A. *et al.* (1975) ^{67}Ga accumulation in pulmonary lesions associated with bleomycin toxicity. *Cancer*, **36**, 1966–72.
79. MacMohan, H. and Bekerman, C. (1978) The diagnostic significance of gallium uptake in patients with normal chest radiographs. *Radiol.*, **127**, 189–93.
80. Ugur, O., Caner, B., Balbay, M.D. *et al.* (1993) Bleomycin lung toxicity detected by technetium-99m diethylenetriamine penta-acetic acid aerosol scintigraphy. *Eur. J. Nucl. Med.*, **20**, 114–18.
81. Lutrin, C.L., McDougall, I.R. and Goris, M.L. (1978) Intense concentration of ^{99m}Tc pyrophosphate in the kidneys of children treated with chemotherapeutic drugs for malignant disease. *Radiology*, **128**, 165–67.
82. Anninga, J.K., DeKraker, J., Hoefnagel, C.A. *et al.* (1990) Ifosfamide induced nephrotoxicity evaluated by ^{99m}Tc-DMSA renal scintigraphy (abstract). *Med. Pediatr. Oncol.*, **18**, 406.
83. Van Luijk, W.H.J., Ensing, G.J., Meijer, S. *et al.* (1984) Is the relative ^{99m}Tc-DMSA clearance a useful marker of proximal tubular dysfunction? *Eur. J. Nucl. Med.*, **9**, 439–42.
84. Perry, M.C. (1982) Hepatotoxicity of chemotherapeutic agents. *Semin. Oncol.* **9**, 65–74.
85. Podoloff, D.A., Kim, E.E. and Haynie, T.P. (1992) SPECT in the evaluation of cancer patients: not quo vadis; rather, ibi fere summus. *Radiology*, **183**, 305–17.
86. Erbas, B., Bekdik, C., Erbengi, G. *et al.* (1992) Regional cerebral blood flow changes in chronic alcoholism using Tc-99m HMPAO SPECT. Comparison with CT parameters. *Clin. Nucl. Med.*, **17**, 123–27.
87. Berger, P.E., Culham, J.A.G., Fritz, C.R. *et al.* (1976) Slowing of hepatic blood flow by halothane: Angiographic manifestations. *Radiology*, **118**, 303–6.
88. Lee, H-B., Wexler, J.P. Scharf, S.C. and Blaufox, M.D. (1983) Pharmacologic alterations in Tc-99m binding by red blood cells: concise communication. *J. Nucl. Med.*, **24**, 397–401.
89. Havens, P.L., Sty, J.R. and Wells, R.G. (1989) Gallium-67 imaging. Chloroquine overdose. *Clin. Nucl. Med.*, **145**, 135.
90. Owunwanne, A., Shihab-Eldeen, A., Sadek, S. *et al.* (1990) The study of the effect of cyclosporin-A on bile flow in experimental animal using technetium-99m EHIDA. *Am. J. Physiol. Imag.*, **5**, 30–5.
91. Owunwanne, A., Shihab-Eldeen, A., Sadek, S. *et al.* (1993) Is cyclosporine-A toxic to the heart? *J. Heart Lung Transplant.*, **12**, 199–204.
92. Klintmalm, G.B.G., Klingensmith, W.C., Iwatsuki, S. *et al.* (1982) ^{99m}Tc DTPA and ^{131}I-hippuran findings in liver transplant recipients treated with cyclosporin-A. *Radiology*, **142**, 199–202.
93. Thomsen, H.S. and Munck, O. (1987) Use of ^{99m}Tc radionuclides to show nephrotoxicity to cyclosporin-A in transplanted kidneys. *Acta Radiol.*, **28**, 59–61.

94. McAfee, J.G., Thomas, F.D., Subramanian, G. *et al.* (1988) Evaluation of cyclosporine nephrotoxicity in rats with various renal radioactive agents. *J. Nucl. Med.*, **29**, 1577–81.
95. Owunwanne, A., Shihab-Eldeen, A., Sadek, S. *et al.* (1990) The use of ^{125}I-HIPDM for studying tissue response due to toxic effects of cyclosporin-A in rats. *Nucl. Med. Biol.*, **17**, 507–9.
96. Nahman, N.S., Cosio, F.G., Kolkin, S. *et al.* (1987) Cyclosporine nephrotoxicity without major organ transplantation. *Ann. Int. Med.*, **106**, 400–2.
97. McCrea, M.S., Rust, R.J., Cook, D.L. and Stepens, B.A. (1991) Cocaine-induced rhabdomyolysis findings on bone scintigraphy. *Clin. Nucl. Med.*, **16**, 292–93.
98. Weber, D.A., Francheschi, D., Ivanovic, M. *et al.* (1993) SPECT and planar brain imaging in crack abuse: iodine-123 iodoamphetamine uptake and localization. *J. Nucl. Med.*, **6**, 899–907.
99. Tumeh, S.S., Nagel, J.S., English, R.J. *et al.* (1990) Cerebral abnormalities in cocaine abusers: demonstration by SPECT perfusion brain (^{123}IMP) scintigraphy. *Radiology*, **176**, 821–24.
100. Ramsingh, P.S., Pujara, S. and Logic, J.R. (1977) ^{99m}Tc pyrophosphate uptake in drug induced gynecomastia. *Clin. Nucl. Med.*, **2**, 206.
101. Kim, Y.C., Brown, M.L. and Thrall, J.H. (1977) Scintigraphic patterns of gallium-67 uptake in the breast. *Radiology*, **124**, 169–75.
102. Grayson, R.R. (1960) Factors which influence the radioactive iodine thyroid uptake test. *Am. J. Med.*, **28**, 397–415.
103. Clark, R.E. and Shipley, R.A. (1957) Thyroidal uptake of ^{131}I after iopanoic acid (Telepaque) in 74 subjects. *J. Clin. Endocrinol.*, **17**, 1008–10.
104. Gross, M.D., Valk, T.W., Swanson, D.P. *et al.* (1981) The role of pharmacologic manipulation in adrenal cortical scintigraphy. *Semin. Nucl. Med*, **11**, 128–48.
105. Carr, E.A., Carroll, M. and Montes, M. (1981) Effect of vitamin D_3, other drugs altering serum calcium or phosphorus concentrations and desoxycorticosterone on the distribution of Tc-99m pyrophosphate between target and non target tissues. *J. Nucl. Med.*, **22**, 526–34.
106. Bobinet, D.J., Sevrin, R., Zurbriggen, M.T. *et al.* (1974) Lung uptake of ^{99m}Tc sulfur colloid in patient exhibiting presence of Al^{+3} in plasma. *J. Nucl. Med.*, **15**, 1220–22.
107. Van Antwerp, J.D., Hall, J.N., O'Mara, R.E. *et al.* (1975) Bone scan abnormally produced by interaction of Tc-99m diphosphonate with iron dextran (Imferon) (abstract). *J. Nucl. Med.*, **16**, 577.
108. Mazzola, A.L., Barker, M.H. and Belliveau, R.E. (1976) Accumulation of ^{99m}Tc - diphosphonate at sites of intramuscular iron therapy. Case report. *J. Nucl. Med. Technol.*, **4**, 133–35.
109. Eshima, M., Shiozaki, H., Ishino, Y. and Nakata, H. (1993) Diffuse liver uptake of Tc-99m phosphate compound associated with intravenous injection of iron colloid solution. *Clin. Nucl. Med.*, **18**, 348–49.
110. Hegge, F.N., Hamilton, G.W., Larson, S.M. *et al.* (1978) Cardiac chamber imaging: a comparison of red blood cells labelled with Tc-99m *in vitro* and *in vivo*. *J. Nucl. Med.*, **19**, 129–34.

Part Two

Basic Aspects of Radiopharmaceuticals

In this section, we describe and discuss the chemistry, in-house preparation, quality control tests, biologic behavior, uses and dosimetry of each radiopharmaceutical. The information on biologic behavior is derived mainly from human data.

The grouping of the diagnostic-imaging radiopharmaceuticals is based on the radionuclide. However, the grouping of antibodies, receptor and positron emission tomographic radiopharmaceuticals is based on their biologic and/or nuclear characteristics. The grouping of non-imaging and therapeutic radiopharmaceuticals is based on their uses.

7

Technetium-99m radiopharmaceuticals

INTRODUCTION

Technetium is a group VIIB transition element which has seven electrons beyond the noble gas electronic configuration. The other members of the group are manganese (Mn) and rhenium (Re); together they form a triad (Mn, Tc, Re). All three elements easily lose the seven electrons to yield the +7 oxidation state of permetallate anions (MnO_4^-, TcO_4^-, ReO_4^-) similar to the perhalate anions of group VIIA (ClO_4^-, BrO_4^-, IO_4^-).

Technetium exhibits multiple oxidation states from –1 to +7 and variable coordination numbers and geometries. In aqueous solution, the most stable oxidation states are +7 (TcO_4^-) and +4 (TcO_2).

The other oxidation states are stabilized by different ligands. Both Tc(V) and Tc(VI) undergo disproportionation reactions, as shown below:

$$3Tc(VI) \rightarrow Tc(IV) + 2Tc(VII)$$

$$3Tc(V) \rightarrow 2Tc(IV) + Tc(VII)$$

Technetium-99m is the most widely used radionuclide in clinical nuclear medicine. Although serendipity played a significant role in its choice, ^{99m}Tc does possess both chemical and physical characteristics which make it the workhorse of radionuclide imaging.

DESIRABLE CHEMICAL CHARACTERISTICS

- Its variable oxidation states and coordination numbers have led to the preparation of a wide variety of ^{99m}Tc radiopharmaceuticals.
- Its ease of formation of complexes and chelates makes it suitable for the 'in-hospital' preparation of many ^{99m}Tc radiopharmaceuticals.
- Its separation from its parent radionuclide (^{99}Mo) is easily accomplished in an enclosed and sterile generator system.
- Its generator eluate ($^{99m}TcO_4^-$) does not need further processing or purification and can either be directly administered or used for the preparation of other ^{99m}Tc radiopharmaceuticals.

DESIRABLE PHYSICAL CHARACTERISTICS

- Its monoenergetic gamma ray of 140 keV is easily collimated and yields a sufficient number of photons.
- Its half-life of 6.0 h is long enough to obtain the desired diagnostic information in many studies and is short enough to cause minimal radiation exposure to the patient and personnel.
- Its lack of beta emissions lowers the radiation dose to both patients and personnel.

- Its daughter radionuclide (^{99}Tc) has a long half-life of 2.12×10^5 years and hence it does not cause additional radiation burden to the patient.

TECHNETIUM-99m PERTECHNETATE ($^{99m}TCO_4^-$)

PREPARATION

Technetium-99m pertechnetate is most often eluted from ^{99}Mo–^{99m}Tc column-type generators with 0.9% sodium chloride solution (saline). The volume of saline used for elution depends upon the activity size of the generator and/or the concentration of $^{99m}TcO_4^-$ required for subsequent use.

The first eluate after a few days' 'standing' of the generator should be discarded because it may contain excess $^{99}TcO_4^-$.

QUALITY CONTROL

The following quality control tests are performed: radionuclidic, radiochemical and chemical.

Radionuclidic test

The major radionuclidic impurity that is commonly tested in a radiopharmacy is ^{99}Mo, and it is quantitatively estimated using a specially designed lead canister. A vial containing the eluate ($^{99m}TcO_4^-$) is put in the canister, which is placed in a dose calibrator, and the radioactivity due to ^{99}Mo is measured. The ^{99}Mo activity is multiplied by a factor appropriate to the thickness of the lead canister, such as 3.5 for 6 mm and 2 for 4 mm thickness.

Note that gamma radiation due to ^{99m}Tc is almost 100% attenuated, while high-energy ^{99}Mo is partially attenuated.

Radiochemical test

Using a 6-cm Whatman 3MM paper/ITLC strip, place a drop of $^{99m}TcO_4^-$ eluate 1 cm from the lower end, develop in acetone or saline (Table 7.1) for up to 5 cm, air dry and cut 2 cm from the origin. Assay each portion separately in a dose calibrator and calculate the radiochemical purity as follows:

$$\text{Radiochemical purity (\%)} = \frac{\text{Activity at solvent front}}{\text{Activity at (origin + solvent front)}} \times 100$$

Chemical test

The major chemical impurity in $^{99m}TcO_4^-$ eluate is Al^{3+} ions. The presence of Al^{3+} is detected by performing a spot test on a filter paper strip presaturated with aurintricarboxylic acid solution. A drop of the eluate and a drop of standard solution of Al^{3+} ion (10 μg/ml) are

Table 7.1 Chromatographic analysis of $^{99m}TcO_4^-$

Chromatographic system		*^{99m}Tc species at*	
Support	*Solvent*	*Origin*	*Solvent front*
ITLC/Whatman 3MM paper	Acetone	$^{99m}TcO_2$	$^{99m}TcO_4^-$
ITLC/Whatman 3MM paper	Saline	$^{99m}TcO_2$	$^{99m}TcO_4^-$

placed side by side on the strip and allowed to air dry. The intensity of the color generated by the two spots is compared. Less intensity or no color formation on the test sample indicates that the eluate contains less than 10 μg/ml Al^{3+} ion.

DOSES

Thyroid imaging	74–185 MBq (2–5 mCi)
In vivo RBC labeling	555–925 MBq (15–25 mCi)
Meckel's diverticulum	74–185 MBq (2–5 mCi)
Dacryocystography	3.7 MBq (100 μCi)
Parathyroid imaging	74 MBq (2 mCi)
Testicular imaging	37–370 MBq (1–10 mCi)
Salivary gland	370–555 MBq (10–15 mCi)

INJECTION TO IMAGING TIME

Meckel's diverticulum and testicular imaging	Immediately
Thyroid, parathyroid and blood pool	15–20 min

BIOLOGIC BEHAVIOR

Following intravenous injection, 70–80% of $^{99m}TcO_4^-$ is weakly bound to serum proteins. Unbound $^{99m}TcO_4^-$ diffuses slowly through the capillary membranes to the interstitial fluids, from where it is cleared by various organs such as stomach wall, intestines, salivary glands, thyroid, choroid plexus, sweat glands, kidneys and mucous membrane. The thyroid uptake of $^{99m}TcO_4^-$ is by active transport, as shown in an *in vitro* experiment using a metabolic inhibitor such as mercaptoimidazole or propylthiouracil [1], and its uptake is 2–4% [2].

In the kidneys $^{99m}TcO_4^-$ is filtered in the glomeruli, but 86% of it is reabsorbed in proximal tubules [2]. Only 30% of the injected dose is excreted in urine in 24 h. Lactating women secrete 10% of $^{99m}TcO_4^-$ in milk [3].

$^{99m}TcO_4^-$ is easily absorbed by the digestive system after oral administration or after intramuscular injection by simple diffusion [4].

USES

- Labeling of various ^{99m}Tc radiopharmaceuticals.
- Imaging and morphologic evaluation of the thyroid.
- Imaging of gastric mucosa to diagnose Meckel's diverticulum.
- *In vivo* labeling of red blood cells for blood pool imaging and first-pass cardiac angiography.
- Evaluation of the nasolacrimal drainage.
- Diagnosis of parathyroid adenoma in conjunction with $^{201}Tl^+$.
- Diagnosis of testicular torsion and infection.
- Imaging of the salivary gland.

DOSIMETRY

The data are modified from [5] and listed in Table 7.2.

Table 7.2 Estimated radiation absorbed dose of $^{99m}TcO_4^-$

Organ	*mGy/MBq*	*rad/mCi*
Thyroid	0.035	0.13
GI tract		
Stomach (wall)	0.068	0.25
Upper large intestine	0.018	0.068
Lower large intestine	0.016	0.061
Testes	0.035	0.13
Bladder wall	0.014	0.053
Ovaries	0.006	0.022
Red bone marrow	0.005	0.019
Total body	0.004	0.014

TECHNETIUM-99m *d,l*-HEXAMETHYL-PROPYLENEAMINE OXIME (^{99m}Tc-*d,l*-HMPAO)

CHEMISTRY

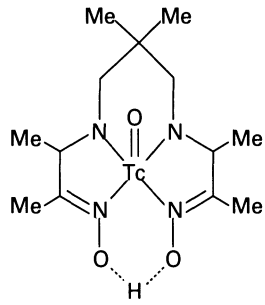

d,l-Hexamethylpropyleneamine oxime (*d,l*-HMPAO) is an N_4 ligand system which forms a neutral, lipophilic complex with technetium. *d,l*-HMPAO is synthesized by condensing butanedione monoxime with 2, 2-dimethyl-1, 3-propanediamine, and the resultant bisimine is reduced with borohydride [6]. The ^{99m}Tc-*d,l*-HMPAO complex is formed by mixing a freeze-dried formulation of the ligand containing stannous chloride with $^{99m}TcO_4^-$. The ^{99m}Tc-HMPAO is optically active and exists in two diastereoisomeric forms (*d,l* and meso). It is the *d,l* form that accumulates in the brain [6,7].

PREPARATION

Add 1.1–2.96 GBq (30–80 mCi) of $^{99m}TcO_4^-$ in 5 ml of saline to a freeze-dried *d,l*-HMPAO (Exametazime) kit and gently mix. The preparation should be used within 30 min because it is converted to a less lipophilic (secondary) form that does not cross blood–brain barrier [7,8].

QUALITY CONTROL

Place a drop of the ^{99m}Tc-*d,l*-HMPAO preparation on a 6-cm Whatman 3MM paper/ITLC strip, 1 cm from the lower end, develop in MEK or saline (Table 7.3) up to 5 cm, air dry and cut 2 cm from the origin. Assay each portion separately in a dose calibrator and calculate the percentage labeling efficiency as follows:

$$\text{Labeling efficiency (\%)} = 100 - \%\ ^{99m}TcO_4^- - \%\ ^{99m}TcO_2 - \%\ \text{secondary}\ ^{99m}\text{Tc-}d,l\text{-HMPAO}$$

Table 7.3 Chromatographic analysis of ^{99m}Tc-*d, l*-HMPAO

Chromatographic system		*^{99m}Tc species at*	
Support	*Solvent*	*Origin*	*Solvent front*
ITLC-SG/ Whatman 3MM	MEK	$^{99m}TcO_2$ and secondary ^{99m}Tc-*d, l*-HMPAO	Lipophilic ^{99m}Tc-*d,l*-HMPAO and $^{99m}TcO_4^-$
ITLC-SG/ Whatman 3MM	Saline	Lipophilic and secondary ^{99m}Tc-*d, l*-HMPAO and $^{99m}TcO_2$	$^{99m}TcO_4^-$
Whatman 1MM	50% acetonitrile	$^{99m}TcO_2$	^{99m}Tc-*d, l*-HMPAO and secondary ^{99m}Tc-*d, l*-HMPAO and $^{99m}TcO_4^-$

DOSE

555–740 MBq (15–20 mCi).

INJECTION TO IMAGING TIME

Dynamic cerebral blood flow	Immediately
Planar or tomographic imaging	At least 5 min (preferably more than 1 h)

BIOLOGIC BEHAVIOR

^{99m}Tc-*d,l*-HMPAO is a neutral lipophilic complex which crosses the blood–brain barrier (BBB), hence it is used as a brain perfusion agent.

Following intravenous injection, 30–50% of the ^{99m}Tc-*d,l*-HMPAO in the internal carotid artery is efficiently extracted into the brain in proportion to regional blood flow, resulting in a ratio of 1.6:1 in gray and white matter respectively. Brain uptake after 2 min reaches a maximum of 3.5–7% of administered dose and has a long biologic half-life of approximately 71 h [9]. The brain retention is thought to be due to the conversion of the ^{99m}Tc-*d,l*-HMPAO in the brain by reaction with glutathione to a secondary hydrophilic form that does not recross the BBB [8]. However, other studies indicate that the concentration of ^{99m}Tc-*d,l*-HMPAO in the brain is independent of the tissue concentration of glutathione [10,11]. In spite of these conflicting reports, it is known that in plasma and *in vitro*, ^{99m}Tc-*d,l*-HMPAO is converted to a secondary hydrophilic form that does not cross the blood–brain barrier [7,8].

A relatively high concentration of activity is observed in the lacrimal gland of normal volunteers [12,13]. It has been shown that ^{99m}Tc-*d,l*-HMPAO crosses the placental barrier in pregnant woman [14]. Approximately 10% of activity remains in blood after 30 min. Of the total activity in the blood, 40–60% is found in the red blood cells [14]. Over 4 h, 29% of the activity is excreted by kidneys, while 23% is excreted by the gastrointestinal system [6].

USES

- Diagnosis of acute cerebral infarction when computed tomography (CT) is negative.
- Detection of intracerebral inflammatory conditions such as suspected herpes simplex encephalitis, lupus cerebritis and abscess with negative CT scan.
- Localization of an abnormal focal area in the brain of patients with epilepsy and monitoring of therapy.
- Detection of an abnormal focus in patients with head trauma and cerebrovascular accidents.
- Differentiation of Alzheimer's disease from multi-infarct dementia.
- Diagnosis of brain death.
- Labeling of leukocytes for detection of inflammation.
- Differentiation of postoperative residual or recurrent brain tumor from fibrosis.

DOSIMETRY

The data are modified from [12] and listed in Table 7.4.

Note:
- The major disadvantage of ^{99m}Tc-*d, l*-HMPAO is that it is not stable *in vitro*. To overcome this problem, stabilizing agents (such as gentisic acid, sodium pyrophosphate) have been added to the reconstituted kit [15].
- Structural modifications have been made on the ligand backbone by introducing a cyclobutyl ring to form ^{99m}Tc-cyclobutylpropyleneamine oxime, which has been reported to be stable for up to 6 h after preparation and has 4.1% brain uptake of the injected dose [16, 17].

Table 7.4 Estimated radiation absorbed dose of ^{99m}Tc-*d, l*-HMPAO

Organ	*mGy/MBq*	*rad/mCi*
Brain	0.0076	0.028
Lacrimal glands	0.0694	0.256
Gallbladder wall	0.0546	0.201
Kidneys	0.0370	0.137
Upper and large intestinal walls	0.0274	0.101
Liver	0.0178	0.066
Urinary bladder wall	0.0156	0.058
Ovaries	0.0064	0.0024
Testes	0.0012	0.004

TECHNETIUM-99m *l, l*-ETHYLCYSTEINATE DIMER (^{99m}*Tc-l,l-ECD)*

CHEMISTRY

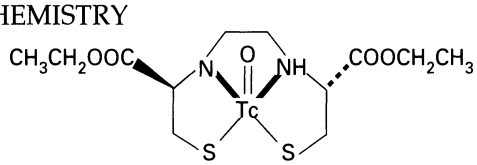

The *l, l*-ethylcysteinate dimer (*l,l*-ECD) is a N_2S_2 ligand system which forms a neutral complex with technetium (TcO^{3+}) at the center. *l,l*-ECD is synthesized by reaction of *l*-thiazolidine-4-carboxylic acid with sodium metal in liquid ammonia to form *N,N'*-ethylene-di-*l*-cysteine (EC). EC is esterified in ethanol and HCl to form ECD as the hydrochloride salt. It is purified by recrystallization with 80% yield [18].

PREPARATION

The commercial kit for preparation of ^{99m}Tc-*l,l*-ECD consists of two vials. Vial A contains *l,l*-ECD, $SnCl_2 \cdot 2H_2O$, $Na_2EDTA \cdot 2H_2O$ and mannitol in lyophilized form, while vial B contains phosphate buffer at pH 7.5. The contents of vial A are dissolved in 1.2 ml of saline, and 1 ml of this mixture is added to vial B, followed by addition of 0.930–3.70 GBq (25–100 mCi) of $^{99m}TcO_4^-$, mixed and allowed to react for 15 min. The preparation is stable for up to 6 h at room temperature [19].

QUALITY CONTROL

Place a drop of the ^{99m}Tc-*l,l*-ECD preparation on a 9-cm-long ITLC Whatman MKC-18 strip at 1 cm from the lower end, develop in a mixture of acetone and ammonium acetate (6:4) (Table 7.5) up to 8 cm and air dry. Cut at 3 cm and 5 cm from the lower end to obtain three pieces; assay each piece in an isotope calibrator. Calculate the labeling efficiency as follows:

$$\text{Labeling efficiency (\%)} = 100 - \%\ ^{99m}TcO_2 - \%\ ^{99m}TcO_4^-$$

DOSE

370–740 MBq (10–20 mCi).

INJECTION TO IMAGING TIME

Dynamic cerebral blood flow	Immediately
Planar or tomographic acquisition	At least 5 min (preferably more than 1 h)

Table 7.5 Chromatographic analysis of ^{99m}Tc-*l, l*-ECD

Chromatographic system		*^{99m}Tc species at*		
Support	*Solvent*	*Origin*	*Middle*	*Solvent front*
ITLC-Whatman MKC-18	Acetone and ammonium acetate	$^{99m}TcO_2$	^{99m}Tc-*l, l*-ECD	$^{99m}TcO_4^-$

PATIENT PREPARATION

Patients are properly hydrated in order to reduce blood background radioactivity.

BIOLOGIC BEHAVIOR

^{99m}Tc-*l,l*-ECD, being a neutral and lipophilic radiopharmaceutical, crosses the blood–brain barrier and accumulates in the brain in proportion to regional blood flow, resulting in a ratio of 4.5:1 in gray and white matter respectively. The brain uptake at 5 min is 6.5% of the injected dose. The clearance of the activity from brain is biexponential with half-lives of 1.3 (40%) and 42.3 h (60%) [20]. The brain retention of ^{99m}Tc-*l,l*-ECD is due to the intracellular hydrolysis of the ester groups to an acidic form [21], and is depicted in Figure 7.1.

It is rapidly cleared from blood with a half-life of approximately 0.8 min. At 5 min less than 10% of activity is found in the blood, while at 1 h 90% of the activity present in the blood is in non-lipophilic form [20].

The major pathway of elimination of ^{99m}Tc-*l,l*-ECD is through the kidneys. Within 2 and 4 h, 50% and 65% of the activity, respectively, is excreted in urine. Approximately 11.2 ± 6.2% of activity is excreted in feces over 48 h. It is also secreted in human milk [20].

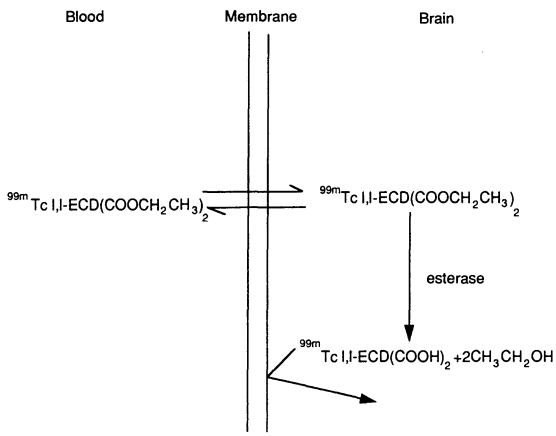

Figure 7.1 Intracellular hydrolysis of ^{99m}Tc-*l,l*-ECD $(COOCH_2CH_3)_2$ to ^{99m}Tc-*l,l*-ECD $(COOH)_2$, which is retained in the brain tissue.

USES

- Diagnosis of acute cerebral infarction when CT is negative.
- Detection of intracerebral inflammatory conditions such as suspected herpes simplex encephalitis, lupus cerebritis and abscess with negative CT scan.
- Localization of an abnormal focal area in the brain of patients with epilepsy and monitoring of therapy.
- Detection of an abnormal focus in patients with head trauma and cerebrovascular accidents.
- Differentiation of Alzheimer's disease from multi-infarct dementia.
- Diagnosis of brain death.

DOSIMETRY

The data are modified from [20] and listed in Table 7.6.

Table 7.6 Estimated radiation absorbed dose of ^{99m}Tc-*l,l*- ECD

Organ	*mGy/MBq*	*rad/mCi*
Brain	0.0055	0.02
Urinary bladder wall	0.073	0.27
Gallbladder wall	0.025	0.092
GI tract		
Upper large intestinal wall	0.017	0.063
Lower large intestinal wall	0.015	0.055
Small intestine	0.010	0.038
Ovaries	0.0080	0.030
Kidneys	0.0074	0.027
Liver	0.0054	0.020
Testes	0.0036	0.013
Total body	0.0029	0.011

TECHNETIUM-99m [*N*-(2(1H-PYROLYMETHYL))-*N'*-(-4-PENTENE-3-ONE-2) ETHANE-1,2-DIAMINE] (^{99m}Tc-MRP 20)

CHEMISTRY

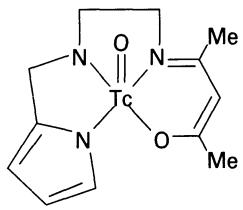

Technetium-99m MRP 20 is a neutral and lipophilic agent which incorporates pyrrole and azomethine moieties containing three atoms of nitrogen and one atom of oxygen in the ligand backbone [22]. The ligand is complexed to TcO^{3+} with technetium in the +5 oxidation state.

PREPARATION

Add 5 ml of 0.930–3.70 GBq (25–100 mCi) of $^{99m}TcO_4^-$ to a vial containing 2 mg of MRP 20, 10 μg of stannous chloride dihydrate and 0.3 mg of $NaHCO_3$, mix gently and allow to stand for 10 min.

DOSE

555–925 MBq (15–25 mCi).

INJECTION TO IMAGING TIME

Dynamic cerebral blood flow	Immediately
Planar or tomographic images	At least 1:5 min (preferably more than 1 h)

BIOLOGIC BEHAVIOR

The brain uptake of ^{99m}Tc-MRP 20 reaches its maximum of 5.2 ± 1.6% within 1 min after injection. This is followed by a slight decrease in radioactivity, which plateaus at approximately 5 min. There is no apparent redistribution or washout of the brain uptake up to 24 h. Brain uptake is due to passive diffusion, while retention is due to *in vivo* decomposition into polar metabolites, probably by hydrolysis at the azomethine moiety [23]. After 3 h, the uptake in other organs is as follows: skeletal muscle, 17.8 ± 3.2%; lung, 12.0 ± 2.4%; liver, 11.7 ± 3.1%; and kidneys, 6.7 ± 0.8%.

The blood clearance is very slow, with 25% of the dose in circulation at 1 h after injection. Of the circulating activity, 20% is bound to plasma protein, while 80% is bound to blood cells. ^{99m}Tc-MRP 20 is excreted through both renal and hepatobiliary systems. At 24 h post injection cumulative urinary and hepatobiliary excretions are 28.5 ± 3.5% and 25.4 ± 4% respectively [23].

USE

This compound is under investigation as a potential brain perfusion agent.

DOSIMETRY

The data are modified from [23] and listed in Table 7.7.

Table 7.7 Estimated radiation absorbed dose of ^{99m}Tc-MRP 20

Organ	*mGy/MBq*	*rad/mCi*
Brain	0.006	0.022
Intestines	0.046	0.170
Kidneys	0.031	0.115
Spleen	0.018	0.068
Lungs	0.016	0.059
Liver	0.014	0.051
Ovaries	0.004	0.014
Red bone marrow	0.003	0.010
Muscles	0.002	0.008
Bladder	0.002	0.008
Thyroid	0.001	0.003
Testes	0.001	0.003

TECHNETIUM-99m MACROAGGREGATED ALBUMIN (^{99m}Tc-MAA)

PREPARATION

Human serum albumin at concentration of 2 mg/ml in acetate buffer (0.15 M, pH 5.6) is mixed with 100 μg/ml $SnCl_2$ and heated at 80°C with constant stirring for macroaggregation to occur. The precipitated albumin so prepared has a particle size of 10–90 μm, with a mean size of 26 μm. The MAA suspension in buffer stored at 4°C is stable for up to 3 months, however freeze drying after adding surfactants such as Tween 80 or PVP-40 increase the shelf life to 1 year. Each milliliter of this suspension contains 1–4 × 10^6 particles per mg [24].

Add 740–1480 MBq (20–40 mCi) of TcO_4^- in 1–4 ml of saline to a freeze-dried kit containing 1 mg of MAA particles and gently mix. Allow the preparation to stand at room temperature for 10 min. The ^{99m}Tc-labeled MAA preparation is stable for up to 8 h at room temperature.

QUALITY CONTROL

Radiochemical test

Place a drop of the ^{99m}Tc-MAA preparation on a 6-cm Whatman/ITLC strip, at 1 cm from the lower end, and develop in saline or acetone (Table 7.8) up to 5 cm and air dry. Cut at 2 cm from the origin, assay each piece in a dose calibrator and calculate the labeling efficiency as follows:

$$\text{Labeling efficiency (\%)} = 100 - \%\ ^{99m}TcO_4^-$$

Particle size

Before injection the particle size of each preparation is checked under a microscope using a hemocytometer. The normal particle size is 10–90 μm. Preparations containing particles larger than 150 μm should not be used.

DOSE

55.5–111 MBq (1.5–3 mCi).

Note

- Gently shake the vial before dispensing.
- Gently invert the syringe repeatedly before injection.
- For lung perfusion imaging, the injection is given with the patient in the supine position, without drawing blood into the syringe.

INJECTION TO IMAGING TIME

Immediately.

BIOLOGIC BEHAVIOR

Following intravenous injection, approximately 90% of ^{99m}Tc-MAA is trapped by the capillary network (diameter less than 8 μm) of the lungs. Most of the particles are cleared from the blood during a first pass through the

Table 7.8 Chromatographic analysis of ^{99m}Tc-MAA

Chromatographic system		*^{99m}Tc species at*	
Support	*Solvent*	*Origin*	*Solvent front*
ITLC/Whatman 3MM paper	Saline or acetone	^{99m}Tc-MAA and $^{99m}TcO_2$	$^{99m}TcO_4^-$

Note: ^{99m}Tc-MAA cannot be separated from $^{99m}TcO_2$ using ITLC or a paper chromatographic system.

Table 7.9 Estimated radiation absorbed dose of ^{99m}Tc-MAA

Organ	*mGy/MBq*	*rad/mCi*
Lungs	0.06	0.226
Bladder wall	0.015	0.056
Liver	0.0049	0.018
Spleen	0.0046	0.017
Whole body	0.004	0.015
Kidneys	0.003	0.011
Ovaries	0.0022	0.008
Testes	0.0017	0.006

lungs. The trapped macroaggregates are broken down to form smaller particles, which are cleared by the reticuloendothelial system with an effective half-life of 3.9–5 h [25]. A diagnostic dose of 2–7 × 10^5 particles in a single injection does not cause hemodynamic effects [26].

Approximately 50–60% of the activity is excreted by kidneys in 48 h, and 1.5–3% is secreted in human breast milk [2].

USES

- Diagnosis of pulmonary embolism.
- Diagnosis of deep venous thrombosis of the lower extremities.

DOSIMETRY

The data are modified from [27] and listed in Table 7.9.

TECHNETIUM-99m HUMAN ALBUMIN MICROSPHERES (^{99m}Tc-HAMs)

PREPARATION

A solution of human serum albumin is agitated vigorously in vegetable oil to form fine droplets. The droplets are coagulated in heated oil to form microspheres. The microspheres are washed free of oil, dried, sieved, impregnated with $SnCl_2$ and lyophilized [28].

Add 0.74–1.85 GBq (20–50 mCi) of $^{99m}TcO_4^-$ in 1–3 ml of saline to a lyophilized kit containing 3 mg of HAMs and 0.15 mg of $SnCl_2$. Mix thoroughly and allow the vial to stand for 15 min before use. The ^{99m}Tc-HAMs preparation is stable for up to 2 h at room temperature.

QUALITY CONTROL

Radiochemical test

Place a drop of the ^{99m}Tc-HAMs preparation on a 6-cm Whatman/ITLC strip at 1 cm from the lower end and develop in saline or acetone (Table 7.10) for up to 5 cm and air dry. Cut at 2 cm from the origin, assay each piece in a dose calibrator and calculate the labeling efficiency as follows:

$$\text{Labeling efficiency (\%)} = 100 - \%\ ^{99m}TcO_4^-$$

Particle size

Before injection the particle size of each preparation is checked under a microscope

Table 7.10 Chromatographic analysis of ^{99m}Tc-HAMs

Chromatographic system		*^{99m}Tc species at*	
Support	*Solvent*	*Origin*	*Solvent front*
ITLC/Whatman 3MM paper	Saline or acetone	^{99m}Tc-HAM and $^{99m}TcO_2$	$^{99m}TcO_4^-$

Note: ^{99m}Tc-HAMs cannot be separated from $^{99m}TcO_2$ using ITLC or a paper chromatographic system.

using a hemocytometer. The normal particle size is 20–40 μm. Preparations containing particles larger than 100 μm should not be used.

DOSE

74–111 MBq (2–3 mCi).

Notes

- Gently shake the vial before dispensing.
- Gently invert the syringe repeatedly before injection.
- For lung perfusion imaging, the injection is given with the patient in the supine position without drawing blood into the syringe.

INJECTION TO IMAGING TIME

Immediately.

BIOLOGIC BEHAVIOR

Following intravenous injection, most of ^{99m}Tc-HAMs is trapped by the capillaries in the lungs. The lung clearance is biexponential, with biological half-lives of 1.8 h (60%) and 36 h (40%) [29]. The mechanism of uptake is the trapping of particles in the pulmonary capillaries with an average diameter of 8 μm. The radioactivity seems to leave the lung as $^{99m}TcO_4^-$, principally by leaching off the microspheres rather than by their break-up [30].

The maximum recommended number of particles for an adult is 5×10^5 (2.8 mg of albumin), however it should not be fewer than 6×10^4 particles.

Approximately 8% of the activity is found in the stomach at 12 h, and 20% is excreted in urine 24 h later. No radioactivity is reported in the liver and spleen [24].

Table 7.11 Estimated radiation absorbed dose of ^{99m}Tc-HAMs

Organ	*mGy/MBq*	*rad/mCi*
Lungs	0.062	0.23
Kidneys	0.038	0.014
Thyroid	0.019	0.072
GI tract		
Stomach	0.019	0.072
Large intestine	0.0094	0.035
Bladder wall	0.011	0.040
Red marrow	0.0054	0.020
Ovaries	0.0035	0.013
Testes	0.0014	0.005

USES

- Diagnosis of pulmonary embolism.
- Diagnosis of deep venous thrombosis of the lower extremities.

DOSIMETRY

The data are modified from [30] and listed in Table 7.11.

TECHNETIUM-99m AEROSOLS

The ^{99m}Tc aerosols are submicronic particles which are produced with jet nebulizers. The aerosol particles are inhaled through the mouth, with the patient preferably in a sitting position, for 3–5 min. Various ^{99m}Tc radiopharmaceuticals ($^{99m}TcO_4^-$, ^{99m}Tc-sulfur colloid, ^{99m}Tc-pyrophosphate, ^{99m}Tc-DTPA, ^{99m}Tc-IDA derivatives and most recently ^{99m}Tc-*d,l*-HMPAO) have been evaluated as radioactive aerosols [31–35]. The most widely used one is ^{99m}Tc-DTPA aerosol, which is described below.

PREPARATION

Add 4–5 ml of $^{99m}TcO_4^-$ containing 2.96–3.70 GBq (80–100 mCi) to a vial of DTPA. After 10–15 min, transfer 2–3 ml containing

1.48–2.22 GBq (40–60 mCi) to a nebulizer reservoir which is driven by oxygen at a flow rate of 8–10 l/min to prepare the submicronic ^{99m}Tc-DTPA aerosols (0.8 μm).

QUALITY CONTROL

Radiochemical quality control of ^{99m}Tc-DTPA is performed to ensure the absence of both $^{99m}TcO_4^-$ and $^{99m}TcO_2$ as described on p. 91.

The aerosol particle size is not checked prior to inhalation because it is not practical to do so. However, care should be exercised when choosing a nebulizer to assure that it produces the correct particle size. The jet-type nebulizer is recommended by some investigators [36, 37].

DOSE

74–111 MBq (2–3 mCi).

INHALATION TO IMAGING TIME

Dynamic studies	Immediately
Static studies	3–5 min

BIOLOGIC BEHAVIOR

The inhaled submicronic aerosol particles diffuse through the alveolar epithelia into the lymphatic (1–2%) and vascular circulation, from where they are excreted in the urine [38]. The rate of diffusion seems to depend on both the molecular weight and the solubility (lipophilicity) of the radioaerosol [31, 35, 39]. In addition to lipophilicity, the clearance rate from the lungs also depends on the site of deposition of the aerosols. The aerosols deposited peripherally seem to clear faster than larger aerosols deposited centrally [31]. In normal subjects, the reported half-life clearance rates of $^{99m}TcO_4^-$, ^{99m}Tc-DTPA and ^{99m}Tc-HMPAO aerosols are 11.4 ± 4.25, 79.2 ± 8.89 and 17.4 ± 3.97 mins respectively [31, 34].

Table 7.12 Estimated absorbed radiation dose of ^{99m}Tc-DTPA aerosol

Organ	*mGy/MBq*	*rad/mCi*
Trachea	0.081	0.30
Bladder wall	0.050	0.180
Lungs	0.022	0.080
Kidneys	0.0026	0.0096
Ovaries	0.0027	0.01
Red marrow	0.0013	0.0048
Testes	0.0019	0.0069
Thyroid	0.00078	0.0029
Total body	0.0016	0.0061

USES

- Diagnosis of pulmonary embolism.
- Evaluation of alveolar epithelial permeability in various disorders such as exposure to toxic inhalants, the adult respiratory distress syndrome and hyaline membrane disease.

DOSIMETRY

The data are modified from [40] and listed in Table 7.12.

TECHNETIUM-99m RED BLOOD CELLS (^{99m}Tc-RBCs)

CHEMISTRY

The labeling of RBCs with ^{99m}Tc is based on the intracellular reaction between reduced ^{99m}Tc and the beta chain of hemoglobin (Hb). The $^{99m}TcO_4^-$ freely diffuses in and out of the RBCs, but in the presence of stannous ion it is reduced intracellularly, where it reacts with Hb approximately 75.8 ± 2.3% to the globin part and 19 ± 1.5% to the heme part [41]. ^{99m}Tc-Hb does not diffuse out of the RBCs, as shown in Figure 7.2.

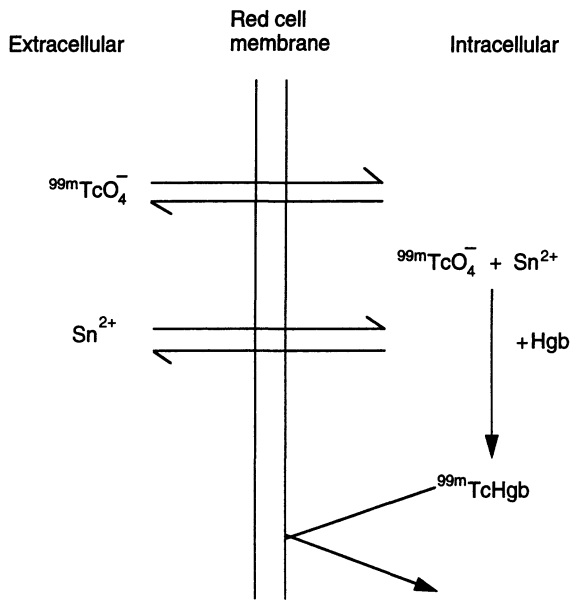

Figure 7.2 Intracellular reaction between reduced ^{99m}Tc and Hb to form ^{99m}Tc-Hb, which is retained within the cell.

PREPARATION

There are three methods of labeling RBCs: *in vivo*, combined *in vivo* and *in vitro*, and *in vitro* techniques.

In vivo labeling method

Add 2 ml of sterile saline to a freeze-dried vial of stannous pyrophosphate, citrate or sodium medronate (for labeling RBCs). Inject the patient intravenously with up to 1 ml of the stannous ion solution (10–20 μg per kg body weight). Wait for at least 20 mins and intravenously inject 0.555–0.925 GBq (15–25 mCi) of $^{99m}TcO_4^-$.

Combined *in vivo* and *in vitro* method

Intravenously inject the patient with 1 ml of the stannous ion solution (10–20 μg per kg body weight). Wait for at least 20 min and withdraw 5 ml of blood into a sterile and heparinized syringe containing 0.555–0.925 GBq (15–25 mCi) of $^{99m}TcO_4^-$. Incubate for 5–10 mins at room temperature and reinject into the patient.

In vitro method

Add up to 2 ml of sterile saline into a freeze-dried vial of stannous pyrophosphate, citrate or sodium medronate (for labeling RBCs). Withdraw 0.5 ml and dilute up to 5 ml using sterile saline. Transfer 0.1 ml of the stannous ion solution into a sterile and evacuated test tube and withdraw 4–6 ml of blood into the tube. Incubate for 5–10 mins, invert the tube and centrifuge. Aspirate the plasma and add 1 ml of $^{99m}TcO_4^-$ containing 0.555–0.925 GBq (15–25 mCi) to the red cells. Gently mix, incubate for 5 mins and reinject into the patient.

Notes

- The *in vivo* labeling technique does not require any manipulation of the blood.
- The *in vitro* technique gives the highest labeling efficiency, but it requires manipulation, is time-consuming and is subject to the potential problem of confusing blood samples if many patients are scheduled at the same time. The *in vitro* labeling technique should be used when the patient is on heparin therapy.
- The combined *in vivo* and *in vitro* technique is a good compromise and is recommended as the method of choice for labeling red blood cells, particularly for gastrointestinal bleeding studies.

QUALITY CONTROL

Centrifuge an aliquot of the labeled RBCs. Decant the plasma/supernatant. Assay radioactivity separately in a dose calibrator. Calculate the labeling efficiency as follows:

$$\text{Labeling efficiency (\%)} = \frac{\text{Radioactivity in RBCs}}{\text{Radioactivity in (RBCs + plasma)}} \times 100$$

DOSE

555–925 MBq (15–25 mCi).

INJECTION TO IMAGING TIME

In vitro and combined *in vivo* and *in vitro* labeling techniques	5 min
In vivo labeling technique	30 min

BIOLOGIC BEHAVIOR

The radioactivity from ^{99m}Tc-RBCs clearly outlines the heart, organs that are very well perfused with blood (liver and spleen) and the major blood vessels. With the *in vitro* and *in vivo* labeling techniques the maximum activity in the RBCs is reached within 5 and 30 mins respectively, and blood radioactivity is generally higher with the *in vitro* than with the *in vivo* labeling technique for up to to 8 h, after which time it becomes less [42].

Blood clearance is biexponential. The $t_{1/2}$ values are 2.5 ± 0.7 h and 176.6 ± 163.6 h for the *in vivo* technique and 2.7 ± 1.5 h and 75.6 ± 25.3 h for the *in vitro* technique. Whole-body retention at 24 hs is therefore higher with the *in vivo* technique (78.7 ± 7.9%) than with the *in vitro* technique (66.3 ± 9.0%) [42].

The radioactivity from ^{99m}Tc-RBCs is eventually excreted in urine and estimated at 24 h to be approximately 21.3 and 33.7% for the *in vivo* and *in vitro* labeling techniques respectively [42].

USES

- Determination of left ventricular ejection fractions and volumes.
- Diagnosis of deep venous thrombosis.
- Detection and localization of site of gastrointestinal bleeding.
- Detection of hemangiomas.

DOSIMETRY

The data modified from [43] were calculated at 48 h voiding schedule and are listed in Table 7.13.

Table 7.13 Estimated radiation absorbed dose of ^{99m}Tc-RBCs

	In vivo		*In vitro*	
Organ	*mGy/MBq*	*rad/mCi*	*mGy/MBq*	*rad/mCi*
Heart wall	0.015	0.057	0.014	0.054
Bladder wall	0.017	0.061	0.024	0.087
Spleen	0.012	0.043	0.011	0.041
Lungs	0.012	0.043	0.011	0.041
Blood	0.010	0.038	0.026	0.097
Liver	0.0076	0.028	0.0070	0.026
Kidneys	0.0073	0.027	0.0068	0.025
Red marrow	0.0054	0.020	0.0051	0.019
Thyroid	0.0051	0.019	0.0049	0.018
Ovaries	0.0051	0.019	0.0049	0.018
Testes	0.0022	0.0082	0.0022	0.0081
Total body	0.0043	0.016	0.0041	0.015

TECHNETIUM-99m HEAT-DENATURED RED BLOOD CELLS (^{99m}Tc-HD-RBCs)

Various methods exist for denaturing ^{99m}Tc-RBCs, and these include the use of excess acid citrate dextrose, excess stannous ion, sulfhydryl inhibitors (*N*-ethylmaleimide or *p*-hydroxy mercury benzoate) and heat [44–46]. Of these, the heat-denaturing technique is the method of choice used routinely in clinical nuclear medicine and is described below.

PREPARATION

Add up to 2 ml of sterile saline into a freeze-dried vial of stannous pyrophosphate, citrate or sodium medronate (for labeling RBCs). Withdraw 0.5 ml and dilute up to 5 ml using sterile saline. Transfer 0.1 ml of the stannous solution into an evacuated tube. Using a heparinized syringe, withdraw 5–10 ml of blood into the tube containing the stannous ion. After 5–10 mins incubation, invert the vial several times and centrifuge. Remove the plasma and discard. Resuspend the packed RBCs in 1–2 ml of sterile saline. Add 1 ml of $^{99m}TcO_4^-$ containing 74.0–185 MBq (2–5 mCi), mix gently and incubate for 5 mins. Heat the tube in a thermostat-controlled water bath preheated to 49°C for 15 mins with occasional gentle agitation to mix the cells.

Note that heat denaturing in plasma is not recommended: the RBCs will not be sufficiently denatured [47].

QUALITY CONTROL

Centrifuge an aliquot of the labeled and heat-denatured ^{99m}Tc-RBCs. Decant the supernatant. Assay radioactivity separately in a dose calibrator. Calculate the labeling efficiency as follows:

$$\text{Labeling efficiency (\%)} = \frac{\text{Radioactivity in RBCs}}{\text{Radioactivity in (RBCs + supernatant)}} \times 100$$

DOSE

37–74 MBq (1–2 mCi).

INJECTION TO IMAGING TIME

60 min.

BIOLOGIC BEHAVIOR

Maximum uptake of heat-denatured ^{99m}Tc-RBCs in the spleen occurs at 1 h after intravenous injection [48]. If the RBCs are not sufficiently damaged there will be radioactivity in the blood pool and the organs that are very well perfused, such as liver and kidney. The half-clearance of the heat-denatured ^{99m}Tc-RBCs is approximately 17 min [49].

USE

Visualization of spleen.

DOSIMETRY

The data are modified from [50] and listed in Table 7.14.

Table 7.14 Estimated radiation absorbed dose of heat-denatured ^{99m}Tc-RBCs

Organ	*mGy/MBq*	*rad/mCi*
Spleen	0.560	2.072
Pancreas	0.036	0.133
GI tract		
Stomach	0.019	0.070
Small intestine	0.004	0.015
Upper large intestinal wall	0.004	0.015
Lower large intestinal wall	0.002	0.007
Liver	0.018	0.067
Kidneys	0.018	0.067
Adrenal	0.013	0.048
Heart	0.006	0.022
Lungs	0.006	0.022
Uterus	0.001	0.004
Ovaries	0.001	0.004
Testes	0.0005	0.002
Thyroid	0.0006	0.002

TECHNETIUM-99m HEXAKIS-2-METHOXY-2-ISOBUTYL ISONITRILE (^{99m}Tc-SESTAMIBI)

CHEMISTRY

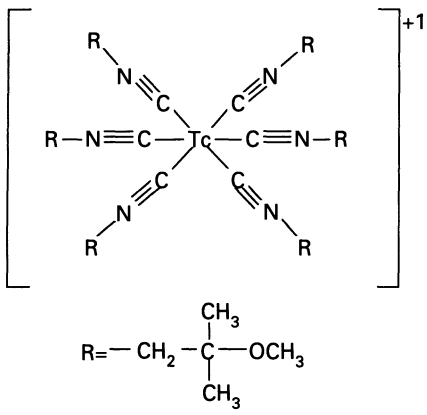

^{99m}Tc-sestamibi is a positively charged lipophilic complex formed with technetium in a +1 oxidation state [Tc(I)]. The ligand tetra (2-methoxyisobutyl isocyanide) copper(I) chloride is synthesized by heating 2-methoxy isobutyl isocyanide with anhydrous cuprous chloride in anhydrous ethanol at 90°C for 1 h. The compound is purified and prepared in a kit form for labeling with $^{99m}TcO_4^-$. After labeling the six monodentate methoxyisobutyl isocyanide (MIBI) ligands are symmetrically attached to the central ^{99m}Tc atom [51].

PREPARATION

Add 1–3 ml of $^{99m}TcO_4^-$ containing 5.5–7.4 GBq (150–200 mCi) to lyophilized tetrakis (2-methoxyisobutylisonitrile)-copper(I)-tetrafluoroborate adduct and stannous chloride dihydrate. Mix thoroughly and heat the vial in an upright position with appropriate shielding in a boiling water bath for 10 min. The preparation is stable for up to 6 h at room temperature.

Note

The manufacturer recommends use of $^{99m}TcO_4^-$ eluted within 2 h.

QUALITY CONTROL

Place a drop of ^{99m}Tc-sestamibi on 6-cm Whatman 3MM paper at 1 cm from the lower end and develop in ethyl acetate (Table 7.15) up to 5 cm, and air dry. Cut at 1 cm from the origin, assay each piece in a dose calibrator and calculate the labeling efficiency as follows [52]:

$$\text{Labeling efficiency (\%)} = 100 - \%\ ^{99m}TcO_4^- + {}^{99m}TcO_2$$

DOSES

Myocardial imaging	370–1110 MBq (10–30 mCi)
Parathyroid imaging	74 MBq (2 mCi)

Table 7.15 Chromatographic analysis of ^{99m}Tc-sestamibi

Chromatographic system		*^{99m}Tc species at*	
Support	*Solvent*	*Origin*	*Solvent front*
Whatman 3MM paper	Ethylacetate	$^{99m}TcO_4^-$ $^{99m}TcO_2$	^{99m}Tc-sestamibi

INJECTION TO IMAGING TIME

Myocardium	1–2 h
Parathyroid	Immediately to 5 mins

PATIENT PREPARATION

Patients should fast for 4 h and refrain from taking beta blockers for 3 days, calcium channel blockers for 2 days and nitrates for 1 day prior to the test.

BIOLOGIC BEHAVIOR

Following intravenous injection, ^{99m}Tc-sestamibi is rapidly cleared from blood with a half-life of 4.3 mins and only 1% binding to plasma proteins [53]. The myocardial uptake is proportional to the regional blood flow in the heart. Its maximum uptake during exercise is 1.5 + 0.04%, while at rest it is approximately 1% [53]. The washout from the myocardium is slow with a $t_{1/2}$ of 7 h and no redistribution. Its uptake mechanism, unlike that of $^{201}Tl^{+}$, is by passive diffusion. Approximately 80% of the activity in the myocyte is bound to negatively charged cytosol [54, 55]. Maublant, Gachon and Moins [55], using cultured myocardial cells in the presence of metabolic inhibitors, namely sodium cyanide (CN), an inhibitor of the respiratory chain [56], sodium iodoacetate (IAA), an inhibitor of glycolysis [57], and ouabain, the inhibitor of Na^{+}–K^{+} ATPase, showed that the uptake of ^{99m}Tc-sestamibi is decreased in the presence of CN and IAA but unaffected by ouabain. They conclude that the transport of ^{99m}Tc-sestamibi is a combination of diffusion and intracellular binding.

^{99m}Tc-sestamibi also accumulates in normal thyroid and parathyroid [57, 58]. The uptake by thyroid gland does not seem to be controlled by TSH [59].

It is eliminated by both hepatobiliary and renal systems. The fecal excretion is 37% over 48 h, and urinary excretion is 27% in 24 h [52].

USES

- Detection of perfusion defects in myocardium at rest and after stress in patients with coronary artery diseases, such as asymptomatic patients with a positive ECG or patients with atypical angina pectoris and a non-diagnostic stress ECG.
- Detection of stenosis of individual coronary arteries.
- Evaluation of thrombolytic therapy in patients with acute myocardial infarction.
- As a potential marker of myocardial viability in patients being considered for bypass surgery.
- Detection of parathyroid adenoma.
- Detection of thyroid metastasis in thyroid cancer patients.

DOSIMETRY

The data are modified from [60] and listed in Table 7.16.

Table 7.16 Estimated radiation absorbed dose of ^{99m}Tc-sestamibi

Organ	*mGy/MBq*	*rad/mCi*
Heart wall	0.0048	0.018
GI tract		
Upper large intestine	0.043	0.159
Lower large intestine	0.030	0.111
Small intestine	0.026	0.096
Gallbladder wall	0.022	0.081
Kidneys	0.018	0.067
Urinary bladder wall	0.017	0.063
Ovaries	0.012	0.044
Thyroid	0.0057	0.021
Liver	0.0053	0.019
Testes	0.0028	0.011
Total body	0.0044	0.016

TECHNETIUM-99m CHLORO-(METHYL-BORON (1-)-TRIS (2,2-CYCLOHEXANE-DIONE DIOXIME) (^{99m}Tc-TEBOROXIME)

CHEMISTRY

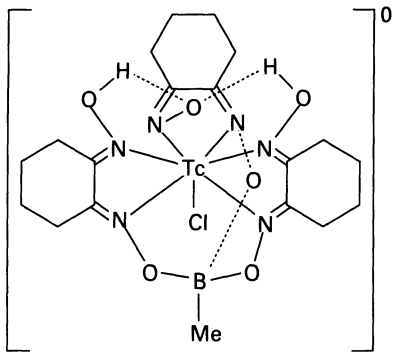

^{99m}Tc-teboroxime is a lipophilic, neutral complex with ^{99m}Tc in the +3 valency state. There are seven coordinate covalent bonds to the ^{99m}Tc central atom, two each from three dioxime molecules and one from the chlorine atom. It belongs to the BATO (boronic adducts of technetium oximes) group of complexes in which the selectivity and chelating portions of the molecule are separate until the final complex is formed [61]. The schematic preparation is shown in Figure 7.3 [62].

PREPARATION

Add 1 ml of $^{99m}TcO_4^-$ containing 3.7 GBq (100 mCi) to a lyophilized cyclohexanedione dioxime, methyl boronic acid, pentetic acid and stannous chloride. Mix properly, heat the vial in an upright position in a boiling water bath for 15 min and cool to room temperature. The preparation is stable for up to 6 h.

QUALITY CONTROL

Place a drop of the ^{99m}Tc-teboroxime preparation on Whatman 31 ET paper at 1 cm from the lower end, develop the strip in a mixture of saline and acetone (50:50) and saline alone (Table 7.17) up to 10 cm and air dry. Cut at 4 cm from the origin, assay each portion separately in a dose calibrator and calculate the percentage labeling efficiency as follows:

$$\text{Labeling efficiency (\%)} = 100 - \%\ ^{99m}TcO_4^- - \%\ ^{99m}TcO_2$$

DOSE

555 MBq (15 mCi).

PATIENT PREPARATION

Patients should fast for 4 h and refrain from taking beta blockers for 3 days, calcium channel blockers for 2 days and nitrates for 1 day prior to the test.

INJECTION TO IMAGING TIME

2 min.

BIOLOGIC BEHAVIOR

Following intravenous injection the maximum myocardial uptake is approximately

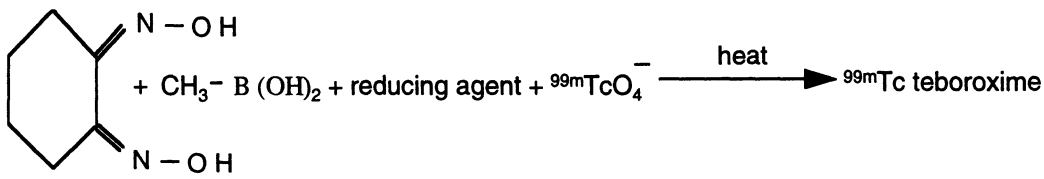

Figure 7.3 The preparation of ^{99m}Tc teboroxime.

Table 7.17 Chromatographic analysis of ^{99m}Tc-teboroxime

Chromatographic system		*^{99m}Tc species at*	
Support	*Solvent*	*Origin*	*Solvent front*
Whatman 31 ET	Saline–acetone	$^{99m}TcO_2$	^{99m}Tc-teboroxime $^{99m}TcO_4^-$
Whatman 31 ET	Saline	^{99m}Tc-teboroxime $^{99m}TcO_2$	$^{99m}TcO_4^-$

2.3 ± 0.8% of the injected dose [63]. It has a rapid washout from myocardium with half-lives of 5.2 min (66%) and 3.8 h (33%). Only 30% of the maximum uptake remains in the myocardium after 1 h. Redistribution of ^{99m}Tc-teboroxime is minimal or does not occur [64]. Its uptake mechanism is passive diffusion and it is unaffected by metabolic inhibitors [65, 66].

^{99m}Tc-teboroxime is cleared rapidly from blood. Its blood level rapidly declines from 39% of the injected dose at 90 s to 9.5% at 15 min [63]. It is predominantly eliminated through the hepatobiliary system.

USES

- Detection of perfusion defects in myocardium at rest, and after stress in patients with coronary artery diseases, such as asymptomatic patients with a positive ECG and patients with atypical angina pectoris and a non-diagnostic stress ECG.
- Detection of individual artery stenosis in the myocardium.
- Evaluation of thrombolytic therapy in patients with acute myocardial infarction.
- As a potential marker of myocardial viability in patients being considered for bypass surgery.

DOSIMETRY

The data are modified from [67] and listed in Table 7.18.

Table 7.18 Estimated radiation absorbed dose of ^{99m}Tc-teboroxime

Organ	*mGy/MBq*	*rad/mCi*
Heart wall	0.0054	0.02
GI tract		
Upper large intestine	0.033	0.123
Lower large intestine	0.023	0.087
Small intestine	0.018	0.068
Gallbladder wall	0.026	0.098
Liver	0.017	0.062
Ovaries	0.0098	0.036
Urinary bladder wall	0.0074	0.027
Kidneys	0.0054	0.02
Testes	0.0028	0.010
Total body	0.0045	0.017

TECHNETIUM-99m 1, 2-BIS [BIS(2-ETHOXYETHYL)PHOSPHINO]ETHANE (^{99m}Tc-TETROFOSMIN)

CHEMISTRY

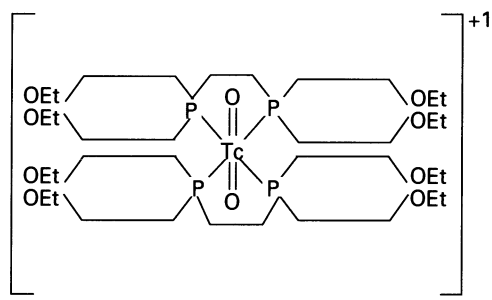

The ligand, 1, 2-bis [bis(2-ethoxyethyl)phosphino]ethane, reacts with technetium in the

+5 oxidation state to form a lipophilic phosphine dioxo cation [^{99m}Tc (tetrofosmin)$_2$ O_2]$^+$ containing eight ethoxy groups [68, 69].

PREPARATION

Add 4–8 ml of $^{99m}TcO_4^-$ containing 4.44–8.88 GBq (120–240 mCi) to a freeze-dried tetrofosmin, stannous chloride, disodium sulfosalicylate and sodium gluconate, gently mix and allow to stand at room temperature for 15 min. The complex is stable for 8 h.

QUALITY CONTROL

Place a drop of the ^{99m}Tc-tetrofosmin preparation on an ITLC/SG strip (2 cm × 20 cm), develop in a mixture of acetone and dichloromethane (35 : 65, v/v) (Table 7.19) and air dry. Cut into three equal pieces and assay each piece separately in a dose calibrator. Calculate the labeling efficiency as follows:

$$\text{Labeling efficiency (\%)} = \frac{\text{Activity at middle portion}}{\text{Activity at (origin + middle portion + solvent front)}} \times 100$$

DOSE

185–250 MBq (5–6.75 mCi) at peak exercise.
500–750 MBq (13.5–20.3 mCi) at rest, 4 h later.

INJECTION TO IMAGING TIME

30 min.

BIOLOGIC BEHAVIOR

Following intravenous injection, ^{99m}Tc-tetrofosmin is rapidly extracted by myocardium from blood. The mean myocardial uptake at 1 h after injection is 1.2 ± 0.3% with no significant change up to 4 h. The myocardial uptake is due to diffusion, while retention is probably due to the ionic reaction between the positively charged ^{99m}Tc-tetrofosmin and negatively charged cytosol [69]. There is a significant uptake in other organs: lungs, liver, gallbladder, kidneys, salivary glands, thyroid, gastrointestinal tract and skeletal muscle. The uptake in the thyroid is not inhibited by perchlorate administration.

Blood clearance is fast, with less than 5% of the injected dose remaining in blood at 10 min. The ^{99m}Tc-tetrofosmin is excreted by both renal and hepatobiliary systems. The cumulative urinary and fecal excretion at 48 h is 39 ± 3.7% and 34.2 ± 4.3% respectively [69].

USES

^{99m}Tc-tetrofosmin is under clinical investigation as a potential myocardial perfusion agent.

Table 7.19 Chromatographic analysis of ^{99m}Tc-tetrofosmin

Chromatographic system		*^{99m}Tc species at*		
Support	*Solvent*	*Origin*	*Middle portion*	*Solvent front*
ITLC/SG	Acetone–dichloromethane (35:65 v/v)	$^{99m}TcO_2$ + other hydrophilic complexes	^{99m}Tc-tetrofosmin	$^{99m}TcO_4^-$

Table 7.20 Estimated radiation absorbed dose of ^{99m}Tc-tetrofosmin

Organ	*mGy/MBq*	*rad/mCi*
Heart wall	0.0039	0.0146
Gallbladder wall	0.0486	0.180
GI tract		
Lower large intestine	0.0221	0.082
Small intestine	0.0170	0.063
Kidneys	0.0125	0.046
Urinary bladder wall	0.0192	0.071
Salivary glands	0.0117	0.043
Ovaries	0.0095	0.035
Thyroid	0.0058	0.022
Liver	0.0041	0.015
Testes	0.0031	0.011
Lungs	0.0020	0.007
Whole body	0.0037	0.013

DOSIMETRY

The data are modified from [69] and listed in Table 7.20.

TECHNETIUM-99m PHOSPHORUS COMPOUNDS

CHEMISTRY

It is well established that phosphorus compounds have affinity for hydroxyapatite crystals. Pyrophosphate contains a P–O–P bond, while the diphosphonates contain a P–C–P bond. The P–C–P bonds of diphosphonates are chemically more stable and resistant to *in vivo* hydrolysis by enzyme phosphatase than the P–O–P bonds of pyrophosphate [70]. The pyrophosphate and diphosphonates form stable complexes with ^{99m}Tc mainly in the oxidation state of +4 [71]. In ^{99m}Tc-diphosphonates the substitution group on the central carbon atom of the P–C–P bond affects the biologic behavior, as observed with ^{99m}Tc-MDP, ^{99m}Tc-HMDP and ^{99m}Tc-HEDP [72]. In ^{99m}Tc-HMDP, substitution of a different alkyl group on the central carbon atom (CH_3 through $C_{10}H_{25}$ results in a decreased skeletal uptake which may be the result of steric hindrance [72].

The ligands pyrophosphate and MDP are available commercially, while HEDP and

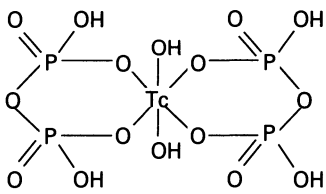

^{99m}Tc-pyrophosphate
(^{99m}Tc-PYP)

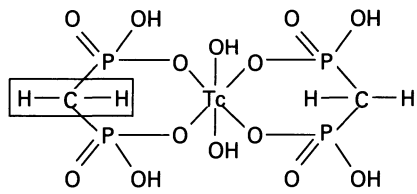

^{99m}Tc-methylene diphosphonate
(^{99m}Tc-MDP)

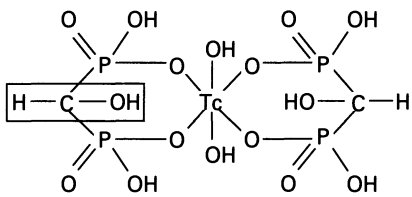

^{99m}Tc-hydroxymethylene diphosphonate
(^{99m}Tc-HMDP)

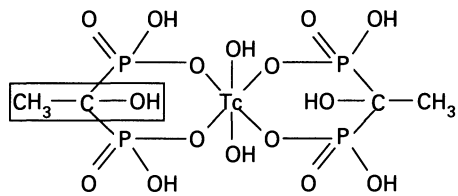

^{99m}Tc-hydroxyethylene diphosphonate
(^{99m}Tc-HEDP)

HMDP may be synthesized in the laboratory. Brief descriptions of the synthesis of HEDP and HMDP are given below.

Synthesis of hydroxyethylene diphosphonate

Phosphorus trichloride is slowly added to a mixture of water and acetic acid while stirring and heating. The reaction mixture is evaporated and the resultant HEDP monohydrate is purified by recrystallization [73].

Synthesis of hydroxymethylene diphosphonate

The tetraisopropyl ester of MDP is chlorinated with hypochlorite to form the tetraisopropyl ester of dichloromethylene diphosphonic acid, which is pyrolized to dichloromethylene diphosphonic acid. This compound is hydrolyzed with sodium hydroxide to yield carbonyl diphosphonate, which is reduced to HMDP with hydrogen and nickel as catalyst. The HMDP is purified by recrystallization [74].

PREPARATION

Add 2–8 ml of $^{99m}TcO_4^-$ containing up to 18.5 GBq (500 mCi) to the appropriate freeze-dried phosphorus ligand, gently mix and allow to stand at room temperature for 10 min. The preparation is stable for up to 8 h.

QUALITY CONTROL

Place a drop of the preparation on a 6-cm Whatman/ITLC strip at 1 cm from the lower end, develop in acetone or saline (Table 7.21) up to 5 cm, air dry, cut in the middle and assay the activity in a dose calibrator. Calculate the labeling efficiency as follows:

$$\text{Labeling efficiency (\%)} = 100 - \%\ ^{99m}TcO_2 - \%\ ^{99m}TcO_4^-$$

DOSE

555–740 MBq (15–20 mCi).

PATIENT PREPARATION

Patients are properly hydrated and encouraged to void frequently without self-contamination.

INJECTION TO IMAGING TIME

Flow studies	Immediately
Blood pool	10 min
Static images	2–4 h

BIOLOGIC BEHAVIOR

Following intravenous injection the ^{99m}Tc-phosphorus radiopharmaceutical (^{99m}Tc-PYP, ^{99m}Tc-MDP, ^{99m}Tc-HEDP or ^{99m}Tc-HMDP) is

Table 7.21 Chromatographic analysis of ^{99m}Tc-phosphorus complexes

Chromatographic system		*^{99m}Tc species at*	
Support	*Solvent*	*Origin*	*Solvent front*
ITLC or Whatman 3MM paper	Acetone	^{99m}Tc compound $^{99m}TcO_2$	$^{99m}TcO_4^-$
ITLC or Whatman 3MM paper	Saline	$^{99m}TcO_2$	^{99m}Tc compound $^{99m}TcO_4^-$

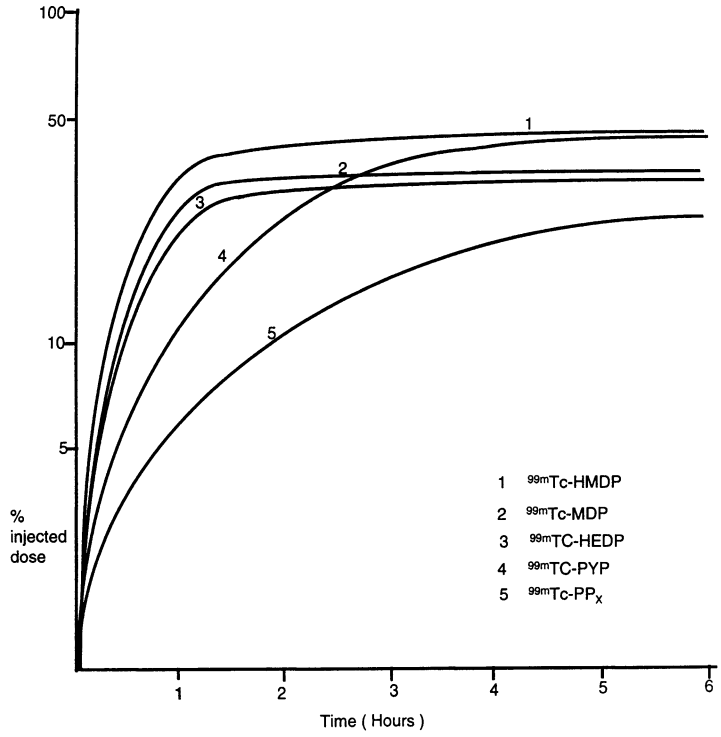

Figure 7.4 Relative percentage bone uptake of ^{99m}Tc phosphorus radiopharmaceuticals.

bound to bone surface probably as a result of adsorption on to the hydroxyapatite crystal [75]. The relative percentage uptake of these radiopharmaceuticals is shown in Figure 7.4 [76]. Owing to the *in vivo* enzymatic hydrolysis of ^{99m}Tc-PYP, several ^{99m}Tc-phosphate compounds are formed and these have different biologic distributions, which is the cause of the poor-quality bone image obtained with administration of ^{99m}Tc-PYP [77].

^{99m}Tc-phosphorus radiopharmaceuticals also accumulate in infarcted myocardium owing to adsorption onto amorphous calcium phosphate [78] or by complexation with denatured native proteins and other macromolecules [79]. ^{99m}Tc-PYP has been shown to have higher uptake in myocardial infarct than the other ^{99m}Tc-phosphorus agents [80, 81].

The comparative blood disappearance of these radiopharmaceuticals is shown in Figure 7.5 [76]. The blood clearance of ^{99m}Tc-PYP is relatively slower than the clearance of ^{99m}Tc-diphosphonates. At 3 h after injection, the total activity in circulating blood due to ^{99m}Tc-PYP, ^{99m}Tc-HEDP, ^{99m}Tc-MDP and ^{99m}Tc-HMDP is 8.58 ± 1.63%, 4.68 ± 0.872%, 3.22 ± 0.269% and 4% respectively [76, 82]. The slow clearance of ^{99m}Tc-PYP is due to higher binding to plasma protein [82].

The major pathway of elimination of ^{99m}Tc-phosphorus radiopharmaceuticals is through the kidneys. At 24 h the percentage cummulative activity excreted in urine for ^{99m}Tc-PYP, ^{99m}Tc-MDP, ^{99m}Tc-HEDP and ^{99m}Tc-HMDP is 58.5 ± 5.86%, 76.5 ± 5.59%, 79.2 ± 7.25% [82] and 75% respectively. Approximately 1.5–3%

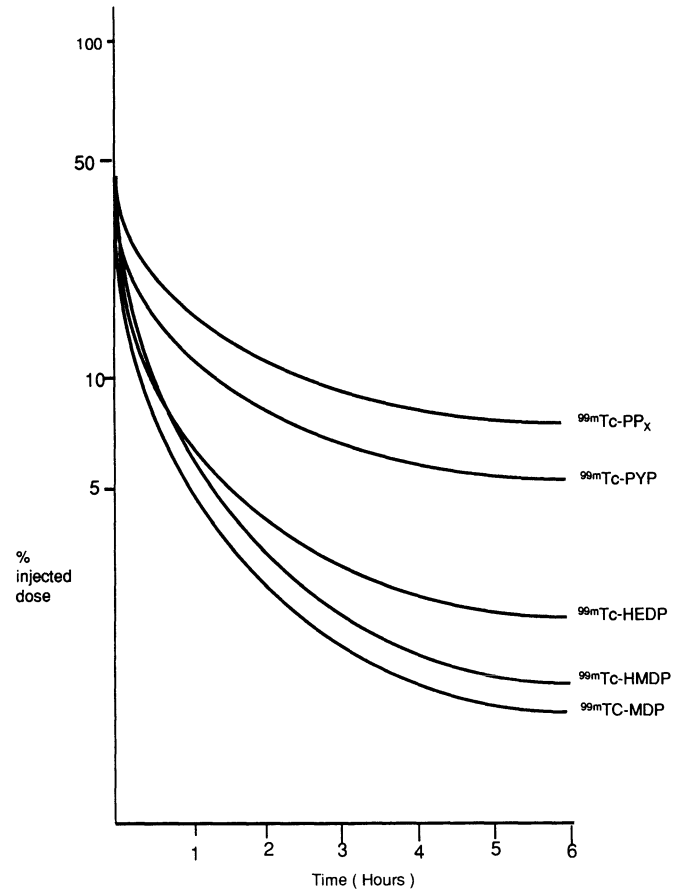

Figure 7.5 Blood clearance of ^{99m}Tc phosphorus radiopharmaceuticals.

of ^{99m}Tc-MDP is reported to be secreted in human breast milk [3].

USES

- Localization of primary bone tumors, metastatic tumors and metabolic bone diseases.
- Diagnosis of osteomyelitis.
- Localization of undetectable fractures on radiographs (stress and hairline fractures, and fractures of the small bones of the hands and feet).
- Evaluation of bone pain in patients with negative radiographs.
- Localization of avascular bone necrosis.
- Evaluation of painful arthroplasty (loosening versus infection).
- Localization of myocardial infarct.

DOSIMETRY

The data modified from [83] were calculated from 4.8 h void time and are listed in Table 7.22.

Table 7.22 Estimated radiation absorbed dose of ^{99m}Tc-phosphorus radiopharmaceuticals

Organ	^{99m}*Tc-PYP*		^{99m}*Tc-MDP*		^{99m}*Tc-HEDP*		^{99m}*Tc-HMDP*	
	mGy/MBq	*rad/mCi*	*mGy/MBq*	*rad/mCi*	*mGy/MBq*	*rad/mCi*	*mGy/MBq*	*rad/mCi*
Bone surface	0.068	0.25	0.061	0.23	0.036	0.13	0.091	0.34
Bladder wall	0.025	0.092	0.034	0.13	0.041	0.15	0.022	0.081
Bone marrow	0.011	0.040	0.0093	0.034	0.0094	0.035	0.013	0.048
Kidneys	0.0063	0.023	0.0084	0.031	0.0066	0.024	0.0059	0.022
Ovaries	0.0037	0.014	0.0032	0.012	0.0037	0.014	0.0032	0.012
Testes	0.0026	0.0096	0.0022	0.0082	0.0025	0.0092	0.0023	0.0085
Whole body	0.0035	0.013	0.0028	0.010	0.0026	0.0094	0.0036	0.013

TECHNETIUM-99m COLLOIDS

CHEMISTRY

Radioactive colloids are particulate materials (up to 2 μm) dispersed in aqueous medium. They are loosely aggregated and have a complex molecular structure. The radioactive colloids are solid–liquid biphasic systems and usually carry a negative charge at their surface (inner compact layer) and are surrounded by a positive ionic cloud from the aqueous medium (diffuse outer layer). The colloidal stability is related to the potential difference between the inner compact layer and the outer diffuse layer, generally referred to as the zeta potential. Colloids with a more negative zeta potential are stable (–30 mV), but strongly agglomerate or precipitate between –5 and +5 mV [24]. Colloidal stability is achieved by adding gelatin, Tween -80, albumin, poloxamer or mannitol so as to decrease the zeta potential. There are three methods of preparing different colloids, namely (a) preformed, (b) *in situ* and (c) *in vivo*.

PREFORMED COLLOIDS

Antimony sulfide (Sb_2S_3) and human serum albumin

Antimony sulfide colloids are prepared by adding water saturated with H_2S gas to antimony potassium tartate solution followed by polyvinylpyrolidone as stabilizer. Excess H_2S is removed by bubbling with nitrogen. The Sb_2S_3 colloid is sterilized by filtration through a 0.22-μm millipore filter. Human serum albumin (HSA) nanocolloids are prepared by heating a mixed solution of human serum albumin, $SnCl_2$ and poloxamer-210 (pH 7.0) at 70°C for 30 min with constant stirring. It is cooled, filtered through a millipore filter and lyophilized [84, 85].

IN SITU COLLOIDS

Sulfur and tin colloids

Both are formed during the reduction of $^{99m}TcO_4^-$ in the presence of sodium thiosulfate or stannous chloride/fluoride [86–88]. The proposed equations for the formation of ^{99m}Tc-sulfur colloid are as follows:

$$Na_2S_2O_3 + 2HCl + \rightarrow S + 2NaCl + H_2O + SO_2$$

$$2S + {}^{99m}TcO_4 \rightarrow TcS_2 \text{ (co-precipitation)}$$

while that for ^{99m}Tc-tin colloid is

$$^{99m}TcO_4 + Sn + 4HCl \rightarrow {}^{99m}Tc(OH)_4 + SnCl_4 \downarrow {}^{99m}TcO_2 \cdot 2H_2O$$

IN VIVO COLLOID

^{99m}Tc-Sn phytate

Upon intravenous injection phytate mini- and microcolloids are formed by chelation with circulating Ca^{2++} *in vivo* [89].

PREPARATION

Add 2–8 ml containing up to 3.7 GBq (100 mCi) of $^{99m}TcO_4$ to a freeze-dried vial of HSA nanocolloid, $SnCl_2/F_2$ or Sn phytate, mix gently and allow to stand for 15 min. The preparation is stable for up to 6 h.

For ^{99m}Tc-sulfur colloid preparation, add the sodium thiosulfate reaction mixture containing stabilizer to hydrochloric acid, followed by up to 3.7 GBq (100 mCi) of $^{99m}TcO_4$ in 2–4 ml and heat in a boiling water bath for 5–10 min. Cool and add buffer to raise the pH to 6–6.5. For ^{99m}Tc-antimony sulfide colloid add up to 3.7 GBq (100 mCi) of $^{99m}TcO_4$ in 2–4 ml to preformed colloid in a vial and heat in a boiling water bath for 30 mins. Cool and add buffer to raise the pH to 6.0–6.5.

QUALITY CONTROL

This involves checking the particle size and labelling efficiency. Normally particle size is checked by the manufacturer, but it can be checked by using an ultramicroscope. Table 7.23 lists the particle sizes of various colloids.

RADIOCHEMICAL TEST

Place a drop of the ^{99m}Tc colloidal preparation on a 7-cm ITLC/Whatman 3MM strip at 1 cm away from the lower end, develop in acetone or saline (Table 7.24) up to 5 cm, air dry, cut in the middle and assay the activity in a dose calibrator. Calculate the labeling efficiency as follows:

$$\text{Labeling efficiency (\%)} = 100 - \%\ ^{99m}TcO_4^-$$

DOSES

Liver and spleen	185 MBq (5 mCi)
Bone marrow	370–555 MBq (10–15 mCi)

Table 7.23 Particle size of various ^{99m}Tc colloids

Type of colloid	*Mean particle size (%)*	*Range*	*Reference*
^{99m}Tc-Sb_2S_3	9 nm	3–30 nm	84, 90
^{99m}Tc-HSA	< 80 nm (95%)	–	91
^{99m}Tc-sulfur	0.3 μm (80%)	0.2 μm	24, 92
^{99m}Tc-Sn		0.03–1 μm	24, 92
^{99m}Tc-Sn-phytate	8 nm (90%)	–	84, 92

Table 7.24 Chromatographic analysis of ^{99m}Tc colloid

Chromatographic system		*^{99m}Tc species of*	
Support	*Solvent*	*Origin*	*Solvent front*
ITLC or Whatman 3MM paper	Acetone or saline	^{99m}Tc-colloid	$^{99m}TcO_4^-$

Note: For ^{99m}Tc-Sn phytate both acetone and saline chromatographic systems are used to determine the amount of $^{99m}TcO_4^-$ and $^{99m}TcO_2$ prior to injection.

GI bleeding	370–740 MBq (10–20 mCi)
Cystogram	37 MBq (1 mCi)
Esophageal reflux	11.1–18.5 MBq (0.3–0.5 mCi)
Lymphoscintigraphy	37–74 MBq (1–2 mCi)
Inflammation	185–340 MBq (5–10 mCi)

INJECTION TO IMAGING TIME

Dynamic liver blood flow	Immediately
Liver and spleen static imaging	10 min
Bone marrow	30 min
Inflammation	45 min
GI bleeding, cystogram, esophageal reflux and lymphoscintigraphy	Immediately and at various time intervals

BIOLOGIC BEHAVIOR

In normal humans approximately 85% of the administered ^{99m}Tc colloids are taken up by the liver, while spleen and bone marrow accumulate 7% and 5% respectively [93]. The mechanism of localization is sequestration by the reticuloendothelial cells in these organs. However, the extent of accumulation of colloids in these organs seems to depend on size of the colloids. ^{99m}Tc-sulfur colloid and ^{99m}Tc-Sn colloid (0.5–1 μm) concentrate more in spleen than ^{99m}Tc-phytate (8 nm). Bigger particles formed by agglomeration accumulate in the lungs [84]. Smaller particles tend to localize in bone marrow, e.g. ^{99m}Tc-antimony sulfide colloid and ^{99m}Tc-HSA nanocolloid. In patients with hepatic insufficiency liver uptakes are reduced while spleen and bone marrow uptake are increased [93].

The ^{99m}Tc colloids are cleared from the circulation with a half-life of less than 5 mins. ^{99m}Tc-Sb_2S_3 colloids and ^{99m}Tc-HSA nanocolloids have a slower blood clearance rate than ^{99m}Tc-S colloids. In normal humans the blood clearance is directly related to hepatic blood flow, but diseases such as cirrhosis affect the extraction efficiency, thereby slowing the rate of blood clearance with a subsequent shift of radioactivity to spleen and marrow [87].

Smaller particles in the range of 1–13 nm (^{99m}Tc-HSA nanocolloid/Sb_2S_3), when injected interstitially, migrate through the lymphatic channels, accumulate in the regional lymph nodes and eventually diffuse into the vascular system, from where they are eliminated by the excretory organs.

^{99m}Tc-sulfur colloid and ^{99m}Tc-Sb_2S_3 colloids are not metabolized and have a long residence time in the body, while it is proposed that ^{99m}Tc-Sn colloids are oxidized in the liver and clear slowly with a half-life of 55 h [84]. ^{99m}Tc-HSA nanocolloids are biodegradable; they are metabolized and excreted via the kidneys and the GI tract.

USES

- Visualization of liver, spleen and bone marrow.
- Assessment of portal hypertension and Budd–Chiari syndrome.
- Detection of disseminated skeletal metastasis in combination with a bone scan.
- Detection of gastroesophageal reflux and aspiration to the lung in children.
- Detection, grading and follow-up of vesicoureteric reflux.
- Localization of the site of bleeding in the GI tract.
- Visualization of regional lymphatic channels and lymph nodes (^{99m}Tc-Sb_2S_3 and ^{99m}Tc-HSA nanocolloids).
- Detection of areas of inflammation (^{99m}Tc-HSA nanocolloid).

DOSIMETRY

The data are compiled from [90], [91], [94] and [95] and listed in Table 7.25.

Table 7.25 Estimated radiation absorbed dose of ^{99m}Tc colloids

Organ	^{99m}*Tc-S colloid*		^{99m}*Tc-Sn colloid*		^{99m}*Tc-phytate*		^{99m}*Tc-Sb_2S_3*		^{99m}*Tc-albumin nanocolloid*	
	mGy/MBq	*rad/mCi*	*mGy/MBq*	*rad/mCi*	*mGy/MBq*	*rad/mCi*	*mGy/MBq*	*rad/mCi*	*mGy/MBq*	*rad/mCi*
Liver	0.0918	0.34	0.074	0.274	0.092	0.34	0.065	0.240	0.078	0.29
Spleen	0.0567	0.21	0.077	0.285	0.025	0.094	0.054	0.200	0.018	0.066
Bone marrow	0.0073	0.027			0.005	0.02	0.006	0.024	0.014	0.053
Ovaries	0.0015	0.0056	0.0022	0.0081	0.002	0.008	0.004	0.016	0.0032	0.012
Testes	0.0003	0.011	0.00062	0.0029	0.0008	0.003	0.004	0.016	0.0011	0.004
Whole body	0.0051	0.019			0.005	0.0019			0.0051	0.019

TECHNETIUM-99m COLLOID SOLID MEALS

Radiopharmaceutical tests of gastric emptying represent an optimal technique for noninvasively and quantitatively characterizing gastric emptying patterns. Simultaneous determination of the rates of solid and liquid gastric emptying can be done by the dual radionuclide technique. If one radionuclide is used, it is preferable to attach it to the solid food because a solid meal is more sensitive for detecting abnormalities in gastric emptying. However, there is some degree of dissociation of the radionuclide from the solid meal. Thus, the rate of gastric emptying may be overestimated using a radiolabeled solid meal as the tracer leaves the stomach with the liquid rather than with the solid food. This problem of weak binding between the radiotracer and solid food can be solved by using egg white or chicken liver labeled *in vivo* or *in vitro* with ^{99m}Tc colloid [96]. Chicken liver labeled *in vivo* is more stable than *in vitro*-labeled chicken liver or egg white. However, it is cumbersome to label chicken liver *in vivo* in a nuclear medicine department. Therefore, in practice, it is preferable to use either chicken liver labeled *in vitro* or egg white. It has been shown that chicken liver labeled *in vitro* is more stable than labeled egg white [97]. *In vitro*-labeled chicken liver is described in detail.

PREPARATION

Inject 37 MBq (1 mCi) of ^{99m}Tc colloid into several cubes (1 cm each) of raw chicken liver, incubate for 15 mins, fry and place on absorbent paper towels to remove any excess ^{99m}Tc colloid and oil. Mix the labeled chicken liver containing 22.2 MBq (600 μCi) with 300 g of beef stew and serve with two pieces of toasted bread. The meal must be consumed within 5–10 mins.

When using frozen chicken liver, thaw at room temperature. If the frozen chicken liver is thawed in hot water, ^{99m}Tc colloid binds poorly to it.

PATIENT PREPARATION

Patients should fast for 6 h prior to the study and should not smoke during the period of the study.

ADMINISTRATION TO IMAGING TIME

Immediately.

DOSE

22.2 MBq (600 μCi).

USES

Determination of the rate and pattern of gastric emptying.

DOSIMETRY

The data are modified from [98] and listed in Table 7.26.

Table 7.26 Estimated radiation absorbed dose of ^{99m}Tc solid meal

Organ	*mGy/MBq*	*rad/mCi*
GI tract		
Stomach wall	0.0378	0.140
Small intestine	0.0683	0.253
Proximal large bowel wall	0.1081	0.400
Distal large bowel wall	0.1027	0.380
Testes	0.0013	0.005
Ovaries	0.0248	0.092
Whole body	0.0459	0.017

TECHNETIUM-99m IMINODIACETATE DERIVATIVES (^{99m}Tc-IDAs)

CHEMISTRY

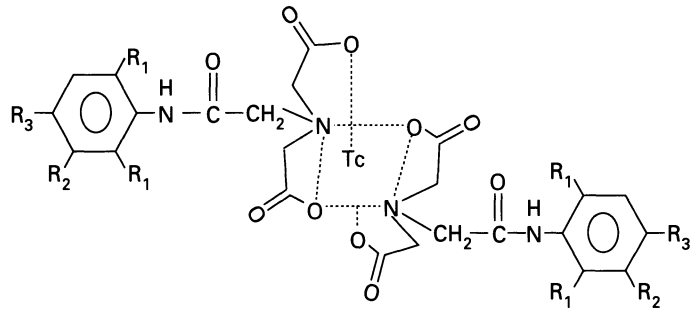

R_1=R_3=CH_3 and R_2=Br	N-(3-bromo-2,4,6-trimethylacetanilide)-iminodiacetate (mebrofenin)
R_1=CH_3–CH_2; R_2=R_3=H	N-(2,6-diethylacetanilide)-iminodiacetate (EHIDA)
R_1=$CH(CH_3)_2$; R_2=R_3=H	N-(2,6-diisopropylacetanilide)-iminodiacetate (disofenin)

Acetanilide iminodiacetate derivatives react with ^{99m}Tc in the +3 oxidation state to form negatively charged ^{99m}Tc complexes generally referred to as^{99m}Tc-IDA derivatives (^{99m}Tc-IDAs) [99]. The acetanilide iminodiacetates are synthesized by the reaction between the appropriate aniline derivative and the anhydride of nitrilotriacetic acid prepared *in situ*. The product is recrystallized and characterized using both chemical and physical methods [100]. Using structure–distribution relationship approach on ^{99m}Tc-IDAs, various investigators [100–106] have established that:

- increased lipophilicity of the substituents on the phenyl rings leads to increased hepatic extraction and decreased urinary excretion;
- substitution on the para position increases lipophilicity and protein binding [e.g. *p*-butyl-IDA(BIDA)];
- substitution on the ortho position decreases lipophilicity and protein binding [e.g. diethyl-IDA (EHIDA) and diisopropyl-IDA (DISIDA or disofenin)];
- when the substitution is concentrated in a single position to achieve the required lipophilicity and low renal excretion, hepatocellular transit time is extensively prolonged [e.g. *p*-butyl-IDA (BIDA)];
- substitution of a small alkyl group (e.g. CH_3, CH_3CH_2) in the ortho position(s) increases hepatocellular transit time;
- substitution of a halogen (preferably a bromo) at the meta position increases hepatic extraction;
- substitution of three methyl groups at the ortho and para positions and bromo at the meta position increases hepatic extraction, decreases hepatocellular transit time, and imparts a high degree of resistance to the competitive effects of bilirubin and low urinary excretion [e.g. trimethylbromo-IDA (mebrofenin)].

Various ^{99m}Tc-IDAs have been prepared. Those that are commercially available include ^{99m}Tc-diethyl-IDA (^{99m}Tc-EHIDA), ^{99m}Tc-DISIDA (^{99m}Tc-disofenin) and ^{99m}Tc-trimethylbromo-IDA (^{99m}Tc-mebrofenin).

PREPARATION

Add 1–6 ml of $^{99m}TcO_4^-$ containing up to 3.7 GBq (100 mCi) to the appropriate freeze-dried IDA, mix gently until the powder is completely dissolved and allow to stand for 10–15 mins before use. The preparation is stable for up to 6 h.

QUALITY CONTROL

Place a drop of the appropriate ^{99m}Tc-IDA 1 cm from lower end of ITLC strip, develop in 20% NaCl or water (Table 7.27) up to 5 cm, air dry and cut in the middle. Assay each portion separately in a dose calibrator and calculate the percentage labeling efficiency as follows:

$$\text{Labeling efficiency (\%)} = 100 - \%\ ^{99m}TcO_4^- - \%\ ^{99m}TcO_2$$

DOSE

150–185 MBq (4–5 mCi).

INJECTION TO IMAGING TIME

Immediately and at various time intervals.

PATIENT PREPARATION

Patients should fast for 4–6 h prior to the study. Note that excessive fasting may lead to non-visualization of the gallbladder.

BIOLOGIC BEHAVIOR

Upon injection, ^{99m}Tc-IDAs are quickly cleared from the blood by the hepatocytes and excreted into the gallbladder and intestine with minimal or negligible uptake by the other organs. Using BSP and bilirubin in dogs and rabbits, it has been shown that the ^{99m}Tc-IDA derivatives are transported to the hepatocytes through the organic anion pathway of the liver [103, 105, 106]. The data for hepatic uptake, urinary excretion, percentage dose in blood and half-life of hepatic clearance of ^{99m}Tc-EHIDA, ^{99m}Tc-disofenin, ^{99m}Tc-mebrofenin and ^{99m}Tc–*p*-*n*-butyl-IDA (^{99m}Tc-BIDA)

Table 7.27 Chromatographic analysis of ^{99m}Tc-IDAs

Chromatographic system		*^{99m}Tc species at*	
Support	*Solvent*	*Origin*	*Solvent front*
ITLC/SA	20% NaCl	^{99m}Tc-IDA $^{99m}TcO_2$	$^{99m}TcO_4^-$
ITLC/SA	Water	$^{99m}TcO_2$	^{99m}Tc-IDA $^{99m}TcO_4^-$

Table 7.28 Uptake and excretion parameters of some ^{99m}Tc-IDAs

^{99m}Tc-IDA	*Hepatic uptake (%)*	*Urinary excretion at 24 h (%)*	*Dose in blood at 24 h (%)*	*$t_{1/2}$ of hepatic clearance (min)*
^{99m}Tc-EHIDA	82.3	17.1±3.2	0.6±0.1	37.3±11.8
^{99m}Tc-disofenin	88.0	11.1±1.5	0.9±0.2	19.0±2.5
^{99m}Tc-mebrofenin	98.1	1.5±0.3	0.4±0.09	17.0±1.3
^{99m}Tc-BIDA	93.7	5.6±1.1	0.7±0.2	107±14.1

Table 7.29 Estimated radiation absorbed dose of ^{99m}Tc-IDAs

Organ	*^{99m}Tc-EHIDA*		*^{99m}Tc-disofenin*		*^{99m}Tc-mebrofenin*		*^{99m}Tc-BIDA*	
	mGy/MBq	*rad/mCi*	*mGy/MBq*	*rad/mCi*	*mGy/MBq*	*rad/mCi*	*mGy/MBq*	*rad/mCi*
Gallbladder	0.045	0.170	0.032	0.12	0.870	0.137	0.187	0.690
GI tract								
Upper large intestine	0.144	0.540	0.104	0.387	0.128	0.474	0.086	0.320
Lower large intestine	0.059	0.220	0.0743	0.275	0.098	0.364		
Small intestine	0.072	0.270	0.059	0.212	0.081	0.299	0.046	0.170
Ovaries	0.025	0.092	0.022	0.081	0.027	0.101		
Urinary bladder wall	0.019	0.082	0.025	0.092	0.008	0.029		
Liver	0.011	0.040	0.010	0.038	0.013	0.070	0.035	0.130
Kidneys	0.005	0.020			0.006	0.022		
Testes	0.001	0.005	0.0016	0.006	0.001	0.005		
Whole body	0.005	0.018	0.005	0.020	0.005	0.020		

are summarized in Table 7.28. The data are taken from [107].

^{99m}Tc-mebrofenin has the highest hepatic uptake (98%). The percentage dose in blood is approximately the same for all the ^{99m}Tc-IDAs. Both ^{99m}Tc-disofenin and ^{99m}Tc-mebrofenin have approximately the same $t_{1/2}$ of hepatic clearance. However, ^{99m}Tc-mebrofenin has a lower percentage urinary excretion than ^{99m}Tc-disofenin. ^{99m}Tc-EHIDA has the highest percentage urinary excretion (17%) and ^{99m}Tc-BIDA has the longest $t_{1/2}$ of hepatic clearance (107 min).

Hence ^{99m}Tc-mebrofenin combines the best characteristics of high hepatic uptake, low urinary excretion, fast blood clearance and hepatocellular transit. ^{99m}Tc-mebrofenin also has the highest degree of resistance to the competitive effects of bilirubin as measured in isolated hepatocytes [100, 107].

USES

^{99m}Tc-IDAs is used to evaluate various hepatobiliary diseases: acute and chronic cholecystitis, biliary dyskinesia, common bile duct obstruction, intrahepatic cholestasis, choledochal cyst, bile leak and primary biliary cirrhosis.

DOSIMETRY

The data are modified from [107]–[110] and listed in Table 7.29.

TECHNETIUM-99m DIETHYLENETRIAMINEPENTAACETIC ACID (^{99m}Tc-DTPA)

CHEMISTRY

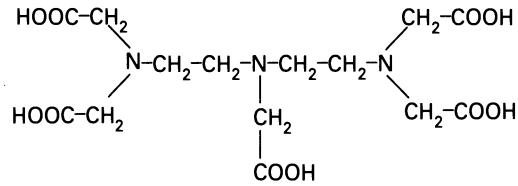

DTPA

DTPA interacts with reduced ^{99m}Tc to form a complex with a net negative charge in neutral or weakly acidic solutions [111]. The oxidation state of ^{99m}Tc in the complex is not known, but it has been reported to be III, IV, V or a combination of these [112].

PREPARATION

Add 2–6 ml of $^{99m}TcO_4^-$ containing up to 11.1 GBq (300 mCi) to freeze-dried DTPA and carefully invert the vial a few times until the powder is completely dissolved. The preparation may be used after 20–30 mins and is stable for up to 8 h.

QUALITY CONTROL

Use a 6-cm Whatman/ITLC strip. Place a drop of ^{99m}Tc-DTPA preparation 1 cm from the lower end and develop in acetone or saline (Table 7.30) up to 5 cm and air dry. Cut

Table 7.30 Chromatographic analysis of ^{99m}Tc-DTPA

Chromatographic system		*99mTc species at*	
Support	*Solvent*	*Origin*	*Solvent front*
3MM Whatman/ITLC	Acetone	^{99m}Tc-DTPA $^{99m}TcO_2$	$^{99m}TcO_4^-$
3MM Whatman/ITLC	Saline	$^{99m}TcO_2$	^{99m}Tc-DTPA $^{99m}TcO_4^-$

at the center, assay each piece in a dose calibrator and calculate the labeling efficiency as follows:

$$\text{Labeling efficiency (\%)} = 100 - \%\ ^{99m}TcO_2 - \%\ ^{99m}TcO_4^-$$

DOSES

Renal imaging	185–370 MBq (5–10 mCi)
Brain imaging	555–740 MBq (15–20 mCi)
Angiography and gastrointestinal bleeding	740 MBq (20 mCi)

INJECTION TO IMAGING TIME

Renal imaging and angiography	Immediately
Brain imaging	1–2 h
Gastrointestinal bleeding	Immediately and various times up to 24 h

BIOLOGIC BEHAVIOR

Following intravenous injection, ^{99m}Tc-DTPA is rapidly cleared from the blood by glomerular filtration [113, 114]. Renal retention is 7% of the injected dose at 1 h and 95% is excreted within 24 h [115]. It is neither secreted nor reabsorbed by the tubules and has negligible biliary excretion and elimination in feces.

The images of the kidneys obtained in the first few minutes after injection represent the vascular pool, while subsequent images represent radioactivity which is in the urine of both the collecting system and the renal pelvis.

In the plasma, 2–6% is bound to protein. The half-life of plasma clearance is 25 min. In humans, about 4–5% of the administered dose is widely distributed in various tissues at 24 h [116].

When the blood–brain barrier is compromized, ^{99m}Tc-DTPA accumulates in the brain lesion(s). It does not accumulate in the choroid plexus [117]. It also accumulates in inflammatory lesions of the gastrointestinal tract [118].

USES

- Assessment of split renal function.
- Measurement of glomerular filtration rate.
- Evaluation of obstructive uropathy.
- Visualization of brain lesions.
- Detection and localization of gastrointestinal bleeding site(s).
- Evaluation of renal transplant complications.
- Preparation of aerosols for lung ventilation studies.

DOSIMETRY

The data are modified from [119] and listed in Table 7.31.

Table 7.31 Estimate radiation absorbed dose of ^{99m}Tc-DTPA

Organ	*mGy/MBq*	*rad/mCi*
Kidneys	0.017	0.069
Bladder wall	0.019	0.07
Spleen	0.013	0.048
Adrenals	0.013	0.048
Liver	0.01	0.037
Pancreas	0.009	0.033
Red marrow	0.006	0.022
GI tract		
Stomach wall	0.005	0.018
Small intestine	0.005	0.018
Uterus	0.005	0.018
Ovaries	0.004	0.015
Bone surfaces	0.003	0.011
Lungs	0.002	0.007
Testes	0.002	0.007

TECHNETIUM-99m DIMERCAPTOSUCCINIC ACID (^{99m}Tc-DMSA)

CHEMISTRY

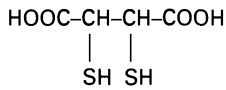

DMSA

Dimercaptosuccinic acid reacts with reduced ^{99m}Tc in various oxidation states to form different complexes which have different biodistributions. The complex suitable as a renal agent is formed at pH 2.5, in two steps: an intermediate is converted to a stable complex within 10 min [120]. The oxidation state of technetium in the renal imaging complex has been reported to be +3 or +4, while that for imaging the medullary carcinoma of the thyroid is +5. The latter complex is formed at pH 7.5–8 [121–122].

PREPARATION

Add 1–6 ml of $^{99m}TcO_4^-$ containing up to 1.48 GBq (40 mCi) to freeze-dried DMSA and carefully invert the vial a few times until the powder is completely dissolved. Incubate for at least 10 min at room temperature and use within 4 h. For pentavalent ^{99m}Tc-DMSA, add sterile 3.5% sodium bicarbonate solution to raise the pH to 7.5–8.

QUALITY CONTROL

Use a 6-cm Whatman/ITLC strip. Place a drop of ^{99m}Tc-DMSA preparation 1 cm from the lower end and develop in acetone (Table 7.32) up to 5 cm and air dry. Cut at the center, assay each piece in a dose calibrator and calculate the percentage labeling efficiency as follows:

$$\text{Labeling efficiency (\%)} = 100 - \%\ ^{99m}TcO_4^-$$

DOSES

Renal imaging	37–185 MBq (1–5mCi)
Imaging of medullary carcinoma of the thyroid	370 MBq (10 mCi)

INJECTION TO IMAGING TIME

Kidneys	30–120 min
Thyroid	2–4 h

BIOLOGIC BEHAVIOR

Renal uptake of ^{99m}Tc(III)-DMSA is 24% of the injected dose at 1 h [123]. Using an autoradiographic technique in rats, it has been shown that at 1 h ^{99m}Tc-DMSA accumulates mostly in the proximal and distal tubular sites of the cortex and to a lesser extent in the renal medulla, glomeruli, collecting tubules and blood vessels [124]. The ratio of radioactivity in the cortex to medulla is 22:1, while that of tubules to glomeruli is approximately 27:1 [125]. The kidney accumulation of Tc(V)-DMSA in rats is 3.7% at 2 h, while that of Tc(III)-DMSA is 19.2% [126]. The accumulation of ^{99m}Tc-DMSA in the kidney is probably due to its binding to metallothionein, a heavy metal-binding protein which has approximately 50 mercapto groups per mole [127].

Table 7.32 Chromatographic analysis of ^{99m}Tc-DMSA

Chromatographic system		*99mTc species at*	
Support	*Solvent*	*Origin*	*Solvent front*
3MM Whatman/ITLC	Acetone	^{99m}Tc-DMSA	$^{99m}TcO_4^-$

Note: ^{99m}Tc-DMSA cannot be distinctly separated from $^{99m}TcO_2$ in saline.

Table 7.33 Estimated radiation absorbed dose of ^{99m}Tc-DMSA

Organ	*mGy/MBq*	*rad/mCi*
Kidneys	0.17	0.63
Bladder wall	0.019	0.07
Adrenals	0.013	0.05
Spleen	0.013	0.05
Ovaries	0.0037	0.014
Testes	0.0018	0.007
Uterus	0.0046	0.017

Since ^{99m}Tc-DMSA is bound to plasma proteins to a large extent (75–90%), glomerular filtration is insignificant compared with tubular secretion [128]. ^{99m}Tc-DMSA has a slow renal clearance with 37% of the injected dose excreted within 24 h [116].

USES

- Evaluation of the anatomy of the renal cortex
- Detection of space-occupying lesions such as tumors, cysts, infarcts, hematomas and abscesses.
- Detection of medullary carcinoma of the thyroid using pentavalent ^{99m}Tc-DMSA.

DOSIMETRY

The data are modified from [129] and listed in Table 7.33.

TECHNETIUM-99m GLUCOHEPTONATE (^{99m}Tc-GHA)

CHEMISTRY

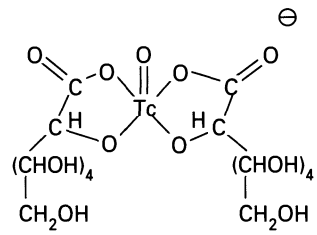

Two molecules of glucoheptonate react with one atom of reduced technetium (+5 oxidation state) in alkaline medium to form a complex with a net negative charge. The ^{99m}Tc (+5) binds to two oxygen atoms of the carboxylic and the adjacent hydroxyl groups with ^{99m}Tc= 0 as the core of the complex [130].

PREPARATION

Add 3–6 ml of $^{99m}TcO_4^-$ containing up to 3.7 GBq (100 mCi) to freeze-dried calcium glucoheptonate and stannous chloride. Shake the vial for 20s to assure complete dissolution of the powder. The preparation is stable for up to 6 h.

QUALITY CONTROL

Use a 6-cm Whatman/ITLC strip. Place a drop of ^{99m}Tc-GHA preparation 1 cm from the lower end and develop in acetone or saline (Table 7.34) up to 5 cm and air dry. Cut at the

Table 7.34 Chromatographic analysis of ^{99m}Tc-GHA

Chromatographic system		*^{99m}Tc species at*	
Support	*Solvent*	*Origin*	*Solvent front*
3MM Whatman/ITLC	Acetone	^{99m}Tc-GHA $^{99m}TcO_2$	$^{99m}TcO_4^-$
3MM Whatman/ITLC	Saline	$^{99m}TcO_2$	^{99m}Tc-GHA $^{99m}TcO_4^-$

center, assay each piece in a dose calibrator and calculate the labeling efficiency as follows:

$$\text{Labeling efficiency (\%)} = 100 - \%\ ^{99m}TcO_4^- - \%\ ^{99m}TcO_2$$

DOSES

Renal imaging	370–555 MBq (10–15 mCi)
Brain imaging	740–925 MBq (20–25 mCi)

INJECTION TO IMAGING TIME

Renal imaging	Immediately
Brain imaging	1–2 h

BIOLOGIC BEHAVIOR

^{99m}Tc-GHA is excreted mainly by the kidneys through glomerular filtration and tubular secretion. Protein-bound ^{99m}Tc-GHA is excreted by tubular secretion, while the unbound component is excreted by glomerular filtration. The retention in renal cortex is 10% of the injected dose at 1 h, and urinary excretion is 70% within 24 h [116].

The half-time plasma clearance is less than 10 min. ^{99m}Tc-GHA is partly excreted through the hepatobiliary system [131]. When the blood–brain barrier is disrupted, ^{99m}Tc-GHA, like $^{99m}TcO_4^-$ and ^{99m}Tc-DTPA, extravasates into the brain lesion. Because ^{99m}Tc-GHA has faster blood clearance than either $^{99m}TcO_4^-$ or ^{99m}Tc-DTPA it can be used for brain imaging 1 h after injection [118].

USES

- Visualization of the kidneys.
- Investigation of renal perfusion and morphology.
- Evaluation of renal transplants.
- Imaging of brain tumors and other brain lesions.

Table 7.35 Estimated absorbed radiation dose of ^{99m}Tc-GHA

Organ	*mGy/MBq*	*rad/mCi*
Kidneys	0.049	0.181
Bladder wall	0.056	0.207
Uterus	0.008	0.030
Ovaries	0.005	0.018
Spleen	0.005	0.018
Adrenals	0.004	0.015
Red marrow	0.004	0.015
Pancreas	0.004	0.015
GI tract		
Stomach wall	0.003	0.011
Small intestine	0.004	0.015
Liver	0.003	0.011
Bone surfaces	0.003	0.011
Testes	0.003	0.011
Lungs	0.002	0.007

Note: ^{99m}Tc-gluconate has renal uptake similar to ^{99m}Tc-GHA and is available commercially in a kit form.

DOSIMETRY

The data are modified from [132] and listed in Table 7.35.

TECHNETIUM-99m MERCAPTOACETYLTRIGLYCINE (^{99m}Tc-MAG_3)

CHEMISTRY

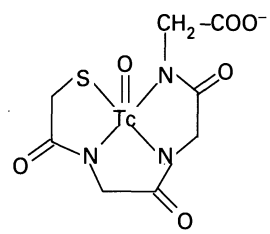

One molecule of MAG_3 reacts with reduced ^{99m}Tc in the oxidation state of +5 to form a negatively charged ^{99m}Tc-MAG_3 complex. A bis ligand complex may also be formed,

which upon heating converts to the single ligand complex. The heating process also increases the rate of hydrolysis of the benzoyl group.

The ligand, benzoylmercaptoacetyl triglycine, is synthesized by reacting glycylglycylglycine with chloroacetyl chloride to form chloroacetylglycylglycylglycine (78% yield), which reacts with sodium thiobenzoate to form the final product (90% yield) [133].

PREPARATION

Add 3 ml of $^{99m}TcO_4$ containing up to 2.6 GBq (70 mCi) to a lyophilized kit containing benzoyl MAG_3, sodium tartrate and stannous chloride. Heat the vial in a boiling water bath for 10 min and cool in water to room temperature. The preparation is stable for up to 6 h.

It has been reported that the boiling step may be omitted by adding $^{99m}TcO_4^-$ to deprotected MAG_3 at alkaline pH followed by neutralization [134].

QUALITY CONTROL

Place a drop of the preparation on a 12-cm Whatman No. 1 strip at 1 cm from the lower end. Develop up to 11 cm in 60% acetonitrile in saline (Table 7.36) and air dry. Cut at 3 cm and 9 cm, and assay the activity of each piece in a dose calibrator. Calculate the labeling efficiency as follows:

$$\text{Labeling efficiency (\%)} = 100 - \%\ ^{99m}TcO_4^- - \%\ ^{99m}TcO_2$$

DOSE

37–370 MBq (1–10 mCi).

INJECTION TO IMAGING TIME

Immediately.

BIOLOGIC BEHAVIOR

After intravenous injection, ^{99m}Tc-MAG_3 is rapidly cleared from the blood by the kidneys and the urinary radioactivity excreted in 30 min is 64.4 ± 3.6% of the administered dose. The plasma half-life is 22.1 ± 3.2 mins [135].

^{99m}Tc-MAG_3 is secreted in the tubules; a negligible amount is filtered in the glomerulus owing to high plasma protein binding (90%) [136]. Approximately 2.6% and 0.5% of the injected dose is found in the liver and gallbladder, respectively, of normal subjects by 30–60 min post injection, and this value does not change for up to 180 min and no gallbladder activity is seen at 24 h. By 3 h post injection, 94.4% of the dose is in the urinary bladder [135]. In patients with renal failure there is little change in gallbladder activity for up to 3 h, however the gut activity is increased during this period from 0.5% to 5% of the injected dose.

USES

- Evaluation of kidney transplant.
- Diagnosis of tubular necrosis.
- Studying tubular function
- Evaluation of renal artery stenosis and obstructive uropathy.

Table 7.36 Chromatographic analysis of ^{99m}Tc-MAG_3

Chromatographic system		*^{99m}Tc species at*		
Support	*Solvent*	*Origin*	*Middle*	*Solvent front*
Whatman No. 1 paper	60% acetonitrile in saline	$^{99m}TcO_2$	^{99m}Tc-MAG_3	$^{99m}TcO_4^-$

Table 7.37 Estimated radiation absorbed dose of ^{99m}Tc-MAG_3

Organ	*mGy/MBq*	*rad/mCi*
Bladder wall	0.047	0.175
GI tract		
Lower large intestine	0.005	0.019
Upper large intestine	0.005	0.019
Small intestine	0.003	0.013
Kidneys	0.005	0.019
Gallbladder	0.004	0.015
Ovaries	0.003	0.012
Testes	0.002	0.006
Red marrow	0.001	0.005
Liver	0.001	0.005
Total body	0.001	0.005

DOSIMETRY

The data obtained from [136], in which it was assumed that the patient voided 30 mins after administration and thereafter at 4-h intervals, are listed in Table 7.37.

NOTE

^{99m}Tc-*l*, *l*-ethylenedicysteine (^{99m}Tc-*l*, *l*-EC) has been developed recently and it is undergoing clinical trials. ^{99m}Tc-*l*, *l*-EC has biologic characteristics very similar to those of ^{99m}Tc-MAG_3. It can be easily prepared from a kit without boiling to yield a highly pure complex (98%) that is stable for more than 8 h. ^{99m}Tc-*l*, *l*-EC shows a similar urinary excretion to ^{99m}Tc-MAG_3 with a 25% higher plasma clearance and lower protein binding. It does not show uptake in the hepatobiliary system [15].

TECHNETIUM-99m HUMAN SERUM ALBUMIN (^{99m}Tc-HSA)

Albumin constitutes approximately 50% of plasma protein and has molecular weight of 69 000 daltons. Serum albumin reacts with reduced ^{99m}Tc in the +5 oxidation state to form ^{99m}Tc-HSA. The reducing agent may be $SnCl_2$, an iron–ascorbic acid mixture or a electrolytic process using tin or zirconium electrodes [137].

PREPARATION

Add aseptically 2–10 ml of $^{99m}TcO_4^-$ up to 3. 7 GBq (100 mCi), to a vial containing HSA, $SnCl_2$ and potassium hydrogen phthalate and mix until the contents are dissolved. Allow to react for 15 min at ambient temperature. The preparation is stable for up to 8 h.

QUALITY CONTROL

Use a 6-cm Whatman No. 3 MM strip. Place a drop of ^{99m}Tc-HSA preparation 1 cm from the lower end and develop in acetone or saline (Table 7. 38) up to 5 cm and air dry. Cut at 3 cm from the origin, assay each piece in a dose calibrator and calculate the labeling efficiency as follows:

$$\text{Labeling efficiency } (\%) = 100 - \%\ ^{99m}TcO_4^-$$

DOSES

Blood flow studies	18. 5–185 MBq (0. 5–5 mCi)

Table 7.38 Chromatographic analysis of ^{99m}Tc-HSA

Chromatagraphic system		*^{99m}Tc species at*	
Support	*Solvent*	*Origin*	*Solvent front*
Whatman 3MM paper	Acetone or saline	^{99m}Tc-HSA, $^{99m}TcO_2$	$^{99m}TcO_4^-$

Cardiac blood pool studies	185–925 MBq (5–25 mCi)
Placental and lymphatic channels visualization	37 MBq (1 mCi)

INJECTION TO IMAGING TIME

Immediately.

BIOLOGIC BEHAVIOR

After intravenous injection ^{99m}Tc-HSA is uniformly distributed throughout the vascular compartment. The blood clearance is slow with 46% of the administered dose remaining in circulation at 1 h [138]. The urine and feces usually contain less than 0. 5% of the injected dose at 24 h [139].

USES

- Blood flow studies.
- Cardiac blood pool studies.
- Visualization of placenta.
- Visualization of lymphatic channels.

DOSIMETRY

The data are modified from [140] and are listed in Table 7. 39.

Table 7.39 Estimated radiation absorbed dose of ^{99m}Tc-HSA

Organ	*mGy/MBq*	*rad/mCi*
Heart	0.02	0.074
Spleen	0.014	0.052
Lungs	0.013	0.048
Bone surfaces	0.009	0.033
Adrenals	0.008	0.030
Kidneys	0.008	0.030
Red marrow	0.007	0.026
Pancreas	0.006	0.022
GI tract		
Stomach wall	0.005	0.018
Small intestine	0.005	0.018
Upper large intestinal wall	0.005	0.018
Lower large intestinal wall	0.004	0.015
Thyroid	0.005	0.018
Uterus	0.005	0.018
Breast	0.005	0.018
Ovaries	0.004	0.015
Bladder wall	0.004	0.015
Testes	0.003	0.011

TECHNETIUM-99m TECHNEGAS

Technegas consists of agglomerated ultrafine graphite particles labeled with ^{99m}Tc. Primary particles measure 7–23 nm in size, have a hexagonal shape and agglomerate into bigger particles of 60–160 nm [141]. The particles are relatively stable, inert, hydrophobic and smaller than the conventional radioactive aerosols. Approximately 2–5 breaths of ^{99m}Tc technegas are inhaled through the mouth, preferably with the patient in a supine position.

PREPARATION

Generators that produce ^{99m}Tc technegas with an efficient delivery system for inhalation are commercially available. Briefly, 0.1 ml of $^{99m}TcO_4^-$ containing 370 MBq (10 mCi) is evaporated to dryness in a graphite crucible. The crucible is heated to 2500°C for 15 s in argon [142] or a mixture of argon (97%) and oxygen (3%) [143]. Approximately 86% of the activity loaded on generator is converted into technegas. It is estimated that 70% and 30% of the loaded activity is available for patient inhalation immediately and 10 min after generation respectively [144].

QUALITY CONTROL

Measurement of the particle size of ^{99m}Tc technegas in a radiopharmacy is not practical. However, the particle size can be checked either by electron microscopy [141] or with a

screen diffusion battery [145]. The average size of agglomerated ^{99m}Tc technegas particles is 97 nm [141].

DOSE

74–111 MBq (2–3 mCi).

INHALATION TO IMAGING TIME

Immediately.

BIOLOGIC BEHAVIOR

Upon inhalation the submicronic ^{99m}Tc technegas particles are distributed uniformly in the lungs. For ^{99m}Tc technegas prepared in a mixture of argon and oxygen in normal subjects the activity is cleared from the lungs with a half-time of 10.1 ± 2. 4 min, while in cigarette smokers and patients with pneumonitis it is cleared with a half-time of 7.0 ± 1.1 and 2.5 ± 0.7 mins respectively. Since technegas particles are hydrophobic in nature they do not induce condensation of water and therefore have a stable size distribution and are not deposited in the central airways [141].

USES

- Evaluation of obstructive airway diseases.
- Evaluation of alveolar epithelial permeability in various disorders such as exposure to toxic inhalants, the adult respiratory distress syndrome and hyaline membrane disease.

REFERENCES

1. Wolff, J. and Maurey, J.R. (1962) Thyroid iodide transport III. Comparison with anions of periodic group VII A. *Biochim. Biophys. Acta*, **57**, 422–26.
2. Harper, P.V., Lathrop, K.A., Gottschalk, A. *et al.* (1966) Pharmacodynamics of technetium-99m, in *Radioactive Pharmaceuticals* (eds G.A. Andrews, R.M. Kinseley and H.N. Wagner Jr), US Atomic Energy Commission, Oak Ridge, pp. 335–58.
3. Ahlgren, L., Ivarsson, S., Johansson, L. *et al.* (1985) Excretion of radionuclides in human breast milk after administration of radiopharmaceuticals. *J. Nucl. Med.*, **26**, 1085–90.
4. Dayton, D.A., Maher, F.T. and Elveback, L.R. (1969) Renal clearance of technetium (^{99m}Tc) as pertechnetate. *Mayo Clin. Proc.*, **44**, 549–51.
5. MIRD dose estimate report No. 8 (1976) Summary of current radiation dose estimate to normal humans from ^{99m}Tc as sodium pertechnetate. *J. Nucl. Med.*, **17**, 74–7.
6. Nowotnik, D.P., Canning, C.R., Cumming, S.A. *et al.* (1985) Development of a ^{99m}Tc labeled radiopharmaceutical for cerebral blood flow imaging. *Nucl. Med. Commun.*, **6**, 499–506.
7. Neirinckx, R.D., Canning, L.R., Piper, I.M. *et al.* (1987) ^{99m}Tc-d, l-HMPAO: a new radiopharmaceutical for SPECT imaging of regional cerebral blood perfusion. *J. Nucl. Med.*, **28**, 191–202.
8. Nakamura, K., Tukatani, Y., Kubo, A. *et al.* (1989) The behaviour of ^{99m}Tc HMPAO in blood and brain. *Eur. J. Nucl. Med.*, **15**, 100–7.
9. Ell, P.J., Hocknell, J.M.L., Jarritt, P.H. *et al.* (1985) A Tc-99m labelled radiotracer for the investigation of cerebral vascular disease. *Nucl. Med. Commun.*, **6**, 437–41.
10. El-Shirbiny, A.M., Sadek, S., Owunwanne, A. *et al.* (1989) Is ^{99m}Tc-hexamethylene propyleneamine oxime uptake in the tissues related to glutathione cellular content? *Nucl. Med. Commun.*, **10**, 905–11.
11. Rowell, N.P., McCready, V.R., Cromin, B. *et al.* (1989) ^{99m}Tc-labeled meso-HMPAO and glutathione content of human lung tumours. *Nucl. Med. Commun.*, **10**, 503–8.
12. Product Information (1992) Kit for the preparation of technetium-99m-exametazime injection, Amersham International, U K.
13. Meyer, J.Y., Thomson, D., Mena, I. and Marcus, C.S. (1990) Lacrimal gland dosimetry for the brain imaging agent ^{99m}Tc-HMPAO. *J. Nucl. Med.* **31**, 1237–39.
14. Maguire, C., Florence, S., Powe, J.E. *et al.* (1990) Hepatic uptake of ^{99m}Tc-HMPAO in a fetus. *J. Nucl. Med.*, **31**, 237–39.

15. Verbruggen, A.M. (1990) Radiopharmaceuticals: state of the art. *Eur. J. Nucl. Med.*, **17**, 346–64.
16. Colombo, F., Lunghi, F., Deleide, G. *et al.* (1989) A new ^{99m}Tc-PAO cerebral perfusion agent with in vitro stability (abstract). *J. Nucl. Med.*, **30**, 742.
17. Messa, C., Zito, F., Rossetti, C. *et al.* (1989) Evaluation of a new tracer for cerebral perfusion studies: ^{99m}Tc d, l-CB-PAO. Preliminary results in humans (abstract). *J. Nucl. Med.*, **30**, 831.
18. Walovitch, R.C., Hill, T.C., Garrity, S.T. *et al.* (1989) Characterisation of ^{99m}Tc-L, L-ECD for brain perfusion imaging. 1. pharmacology of ^{99m}Tc-ECD in non-human primates. *J. Nucl. Med.*, **30**, 1892–901.
19. Leveille, J., Demonceau, G., Roo, M.D. *et al.* (1989) Characterisation of technetium-99m-l, l-ECD for brain perfusion imaging. 2. Biodistribution and brain imaging in humans. *J. Nucl. Med.*, **30**, 1902–10.
20. Vallabhajosula, S., Zimmerman, R.E., Picard, M. *et al.* (1989) Technetium-99m ECD: a new brain imaging agent: in vivo kinetics and biodistribution studies in normal human subjects. *J. Nucl. Med.*, **30**, 599–604.
21. Walovitch, R.C., Makuch, J., Krapik, A.D. *et al.* (1988) Brain retention of ^{99m}Tc-ECD is related to in vivo metabolism (abstract). *J. Nucl. Med.*, **29**, 747.
22. Morgan, G.F., Deblaton, M., Clemens, P. *et al.* (1991) Technetium-99m-MRP20, a potential brain perfusion agent: in vivo biodistribution and SPECT studies in non-primate animals. *J. Nucl. Med.*, **32**, 500–5.
23. Bossuyt, A., Morgan, G.F., Deblaton, M. *et al.* (1991) Technetium-99m-MRP20, a potential perfusion agent: in vivo biodistribution and SPECT studies in normal male volunteers. *J. Nucl. Med.*, **32**, 399–403.
24. McAfee, J.G. and Subramanian, G. (1984) Radionuclide agents for imaging, in *Clinical Scintillation Imaging* (eds L.M. Freeman and P.M. Johnson), Grune & Stratton, New York, pp. 55–177.
25. Subramanian, G., Arnold, R.W., Thomas, F.D. *et al.* (1972) Evaluation of an instant ^{99m}Tc-labeled lung scanning agent. *J. Nucl. Med.*, **13**, 790.
26. Allen, D.R., Nelp, W.B., Chesey, F.W. *et al.* (1973) Clinical assessment of changes in the pulmonary circulation following injection of lung scanning agent (MAA) (abstract). *J. Nucl. Med.*, **14**, 375.
27. Product Information (1991) Kit for the preparation of technetium Tc-99m albumin aggregated, Dupont Merck Pharmaceuticals, MA.
28. Rhodes, B.A., Zolle, I., Buchaman, J.W. *et al.* (1969) Radioactive albumin microspheres for studies of pulmonary circulation. *Radiology*, **92**, 1453–60.
29. Wicks, R., Rosenspire, K., Ackerhalt, R. *et al.* (1981) Distribution of Tc-99m administered as labeled microspheres for lung imaging, in *Third International Radiopharmaceutical Dosimetry Symposium* (eds E.E. Watson, A.T. Schlafke-Stelson, J.I. Coffey, and R.J. Cloutier), US Public Health Service, Rockville, MD, pp. 454–63.
30. Blau, M., Wicks, R., Thomas, S.R., Lathrop, K.A. (1982) MIRD Report No. 10. Albumin microspheres labeled with technetium-99m. *J. Nucl. Med.*, **23**, 915–17.
31. Coates, G. and O'Brodovich, H. (1986) Measurement of pulmonary epithelial permeability with Tc-99m DTPA aerosol. *Semin. Nucl. Med.*, **16**, 275–84.
32. Waldman, D.L. and Weber, D.A. (1984) A pharmacokinetic approach to evaluation of aerosol solutes for lung permeability studies (abstract). *J. Nucl. Med.*, **25**, 18.
33. Chamberlin, M.J., Morgan, W.K.C. and Vinitski, S. (1983) Factors influencing the regional deposition of inhaled particles in man. *Clin. Sci.*, **64**, 69–78.
34. Kawakani, K. and Takagi, H. (1989) Pulmonary clearance of Tc-99m HMPAO aerosols: a new application of a lipophilic substance (abstract). *J. Nucl. Med.*, **30**, 743.
35. Chopra, S.K., Taplin, G.V., Toshkin, D.P. *et al.* (1979) Lung clearance of soluble radioaerosols of different molecular weights in systemic sclerosis. *Thorax*, **34**, 63–7.
36. Dolovich, M.B., Coates, G., Hargreave, F. and Newhouse, M.T. (1985) Aerosols in diagnosis: ventilation, airway penetrance, airway reactivity, epithelial permeability and mucociliary transport, in *Aerosols in Medicine* (eds F. Moren, M.T. Newhouse, M.D. Dolovich), Elsevier, Amsterdam, pp. 225–61.

37. Waldman, D.L., Weber, D.A., Oberdorster, G. *et al.* (1987) Chemical breakdown of technetium-99m DTPA nebulization. *J. Nucl. Med.*, **28**, 378–82.
38. Coates, G. and O'Brodovich, H.M. (1965) The contribution of lymphatic drainage to the clearance of solutes from lungs of sheep (abstract). *Physiologist*, **8**, 279.
39. Huchon, G.J., Mentgomery, A.B., Lipavsky, A. *et al.* (1987) Respiratory clearance of aerosolized radioactive solutes of varying molecular weight. *J. Nucl. Med.*, **28**, 894–902.
40. Atkins, H.L., Weber, D.A., Susskind, H., and Thomas, S.R. (1992) MIRD dose estimate report No. 16: radiation absorbed dose from technetium-99m-diethylenetriamine-pentaacetic acid aerosol. *J. Nucl. Med.*, **33**, 1717–19.
41. Srivastava, S.C. and Chervu, L.R. (1984) Radionuclide-labeled red blood cells: current status and future prospects. *Semin. Nucl. Med.*, **14**, 68–82.
42. Atkins, H.L., Srivastava, S.C., Meinken, G.E. and Richards, P. (1985) Biological behaviour of erythrocytes labeled in vivo and in vitro with technetium-99m. *J. Nucl. Med. Tech.*, **13**, 136–39.
43. Atkins, H.L., Thomas, S.R., Buddemeyer, U., and Chervu, L.R. (1990) MIRD dose estimate report No 14: Radiation absorbed dose from technetium-99m-labeled red blood cells. *J. Nucl. Med.*, **31**, 378–80.
44. Atkins, H.L., Eckelman, W.C., Hauser, W. *et al.* (1972) Splenic sequestration of ^{99m}Tc-labeled red blood cells. *J. Nucl. Med.*, **13**, 811–14.
45. Jacob, H.S. and Jandl, J.H. (1962) Effects of sulfahydryl inhibition on red blood cells. I. Mechanism of hemolysis. *J. Clin. Invest.*, **41**, 779–92.
46. Hamilton, R.G., Alderson, R.G., Harwig, J.F. and Siegel, B.A. (1976) Splenic imaging with ^{99m}Tc-labeled erythrocytes: a comparative study of cell-damaging methods. *J. Nucl. Med.*, **17**, 1038–43.
47. Vaik, P.E. and Guille, J. (1984) Measurement of splenic function with heat damaged RBCs: effect of heating conditions: concise communication. *J. Nucl. Med.*, **25**, 965–68.
48. Gutkoski, R.F. and Dworkin, H.J. (1974) Kit-produced ^{99m}Tc-labeled red cells for spleen imaging. *J. Nucl. Med.*, **15**, 1187–91.
49. Atkins, H.L., Goldman, A.G., Fairchild, R.G. *et al.* (1980) Splenic sequestration of ^{99m}Tc-labeled heat treated red blood cells. *Radiology*, **136**, 501–3.
50. ICRP Publication 53 (1990) *Radiation dose to patients from radiopharmaceuticals*, Pergamon Press, Oxford, pp. 211–12.
51. Jones, A.G., Dionauge, G.F., Davison, A. *et al.* (1985) Biological distribution and structure function relationship of hexakis isonitrile Tc (I) complexes (abstract). *J. Nucl. Med. All. Sci.*, **29**, 200.
52. Patel, M., Jahan, S. and Owunwanne, A. (1993) Miniaturised and rapid paper chromatographic technique for radiochemical quality control of ^{99m}Tc-Hexakis-2-methoxy isobutylisonitrile (99m Tc-Sestamibi) (abstract). *J. Nucl. Med.*, **34**, 234.
53. Wackers, F.J.T., Berman, D.S., Maddahi, J. *et al.* (1989) Technetium-99m hexakis-2-methoxyisobutylisonitrile human biodistribution, dosimetry, safety and preliminary comparison to thallium-201 for myocardial perfusion imaging. *J. Nucl. Med.*, **30**, 301–11.
54. Mousa, S.A. and Williams, S.J. (1986) Myocardial uptake and retention of ^{99m}Tc-hexakis aliphatic isonitriles: evidence for specificity (abstract). *J. Nucl. Med.*, **27**, 995.
55. Maublant, J.C., Gachon, P. and Moins, N. (1988) Hexakis (2-methoxy isobutrylisonitrile) technetium-99m and thallium-201 chloride: uptake and release in cultured myocardial cells. *J. Nucl. Med.* **29**, 48–54.
56. Buja, L.M., Hagler, H.K., Parsons, D. *et al.* (1985) Attractions of ultrastructure and elemental composition in cultured neonatal rat cardiac myocytes after metabolic inhibition with iodoacetic acid. *Lab. Invest.*, **53**, 397–412.
57. McCall, D. (1979) Cation exchange and glycoside binding in cultured rat heart cells. *Am. J. Physiol.*, **236**, C-87–C-95.
58. Taillefer, R., Boucher, Y., Potvin, C. and Lambert, R. (1992) Detection and localization of parathyroid adenomas in patients with hyperparathyroidism using a single radionuclide imaging procedure with technetium-99m-sestamibi (double-phase study). *J. Nucl. Med.*, **33**, 1801–7.
59. Muller, S.T., Guth-Tougelides, B. and Creutzig, H. (1987) Imaging of malignant tumours with

^{99m}Tc-MIBI SPECT, (abstract). *J. Nucl. Med.*, **28**, 562.

60. Product Information (1992) Cardiolite, kit for preparation of technetium-99m sestamibi, Dupont Merck Pharmaceuticals, MA.
61. Treher, E.N., Francesconi, L.C., Gougoutas, J.Z. *et al.* (1989) Mono-capped tris dioxime complexes of technetium (III): synthesis and structural characterization of TCX (dioxime)$_3$ B-R (X=Cl, Br; dioximedimethylglyoxime cyclolexanedioxime; R=CH_3, C_4H_9). *Inorg. Chem.*, **28**, 3411–16.
62. Wang, T.S.T. (1988) ^{99m}Tc-Radiopharmaceuticals: recent advances and clinical prospectives, in *Nuclear Medicine Update* (eds S.D.J. Yeh and D.C.P. Chen), Taipei, Taiwan, The Society of Nuclear Medicine, Republic of China, pp. 77–85.
63. Squibb Diagnostics (1986) Clinical evaluation of SQ 30217 as a myocardial imaging agent, Clinical Report 26742, Squibb Diagnostics New Brunswick, NJ.
64. Johnson, L.L. and Seldin, D.W. (1990) Clinical experience with technetium-99m teboroxime, a neutral, lipophilic myocardial perfusion imaging agent. *Am. J. Cardiol.*, **66**, 63E–67E.
65. Maublant, J.C., Moins, N., Gachon, P. *et al.* (1993) Uptake of technetium-99m-teboroxime in cultured myocardial cells: comparison with thallium-201 and technetium-99m sestamibi. *J. Nucl. Med.*, **34**, 255–59.
66. Rumsey, W.L., Rosenspire, K.C. and Nunn, A.D. (1992) Myocardial extraction of toboroxime: Effects of teboroxime interaction with blood. *J. Nucl. Med.*, **33**, 94–101.
67. Product Information (1992) Cardiotec kit: for the preparation of technetium Tc-99m teboroxime. Squibb Diagnostic, New Brunswick, NJ.
68. Kelly, J.D., Forster, A.M., Higley, B. *et al.* (1993) Technetium-99m tetrofosmin as a new radiopharmaceutical for myocardial perfusion imaging. *J. Nucl. Med.*, **34**, 222–27.
69. Higley, B., Smith, F.W., Smith, T. *et al.* (1993) Technetium-99m-1,2-bis [bis (2-ethoxyethyl) phosphino] ethane: human biodistribution, dosimetry and safety of a new myocardial perfusion imaging agent. *J. Nucl. Med.*, **34**, 30–8.
70. Russell, R.G.G., Muhlbauer, R.C., Bisaz, S. *et al.* (1970) The influence of pyrophosphate, condensed phosphates, phosphonates and other phosphate compounds on the dissolution of hydroxyapatite in vitro and on bone resorption induced by parathyroid hormone in tissue culture and in thyroparathyroidectomized rats. *Calcif. Tissue Res.*, **6**, 183–96.
71. Russell, C.D. and Cash, A.G. (1979) Complexes of technetium with pyrophosphate, etidronate and medronate. *J. Nucl. Med.*, **20**, 532–37.
72. Bevan, J.A., Tofe, J.A., Benedict, J.J. *et al.* (1980) ^{99m}Tc-HMDP (hydroxymethylene diphosphonate): a radiopharmaceutical for skeletal and acute myocardial infarct imaging. I. Synthesis and distribution in animals. *J. Nucl. Med.*, **21**, 961–66.
73. Castronovo, F.P. (1974) Method for the synthesis of 1-hydroxyethylidene-1, 1-disodium phosphonate (HEDSPA): a skeletal seeking radiopharmaceutical after labeling with ^{99m}Tc. *J. Nucl. Med.*, **15**, 127–30.
74. Quimby, O.T., Prentice, J.B. and Nickolson, D.A. (1967) Tetrasodium carbomyldiphosphate, synthesis, reactions and spectral properties. *J. Org. Chem.*, **32**, 4111–14.
75. Francis, M.D., Russell, R.G.G. and Fleish, H. (1969) Diphosphonates inhibit formation of calcium phosphate crystals invitro and pathological calcification invivo. *Science*, **165**, 1264–66.
76. Owunwanne, A., O'mara, R.E. and Wilson, G.A. (1979) Factors influencing blood clearance of bone scanning radiopharmaceuticals. A review. Teaching exhibit presented at the 26th annual meeting of the Society of Nuclear Medicine, Atlanta, GA, June, pp. 26–9.
77. Eckelman, W.C. and Volkert, W.A. (1982) In vivo chemistry of ^{99m}Tc-chelates. *Int. J. Appl. Radiat.*, **33**, 945–51.
78. Buja, L.M., Tofe, A.J., Kulkarni, P.V. *et al.* (1977) Sites and mechanisms of localisation of technetium-99m phosphorus radiopharmaceuticals in acute myocardial infarcts and other tissues. *J. Clin. Invest.*, **60**, 724–40.
79. Dewanjee, M.K. and Kahn, P.C. (1976) Mechanism of localisation of ^{99m}Tc-labeled pyrophosphate and tetracycline in infarcted myocardium. *J. Nucl. Med.*, **17**, 639–46.
80. Kelly, R.J., Chitton, H.M., Hackshaw, B.T. *et al.* (1979) Comparison of Tc-99m pyrophosphate and Tc-99m methylene diphosphonate in acute myocardial infarction: concise communication. *J. Nucl. Med.*, **20**, 402–6.

81. Wakat, M.A., Chitton, H.M., Hackshaw, B.T. *et al.* (1980) Comparison of Tc-99m pyrophosphate and Tc-99m hydroxymethylene disphosphonate in acute myocardial infarction: concise communication. *J. Nucl. Med.*, **21**, 203–6.
82. Subramaniam, G., McAfee, J.G., Blair, R.J. *et al.* (1975) An evaluation of ^{99m}Tc-labeled phosphate compounds as bone imaging agents, in *Radiopharmaceuticals* (eds G. Subramanian, B.A. Rhodes and J.F. Cooper), The Society of Nuclear Medicine, New York, pp. 319–28.
83. Weber, D.A., Makler, P.T., Watson, E.E. *et al.* (1989) Radiation absorbed dose from technetium labeled bone imaging agents: MIRD dose estimate report No. 13. *J. Nucl. Med.*, **30**, 1117–22.
84. Ege, G.N. and Warbick, A. (1979) Lymphoscintigraphy: A comparison of ^{99m}Tc-antimony sulphide colloid and ^{99m}Tc-stannous phytate. *Br. J. Radiol.*, **52**, 124–29.
85. McAfee, J.G., Subramanian, G., Aburano, T. *et al.* (1982) A new formulation of ^{99m}Tc-minimicroaggregated albumin for marrow imaging: comparison with other colloids, In-111 and Fe-59. *J. Nucl. Med.*, **23**, 21–8.
86. Stern, H.S., McAfee, J.G., Subramanian, G. (1966) Preparation, distribution and utilisation of ^{99m}Tc-sulfur colloid. *J. Nucl. Med.*, **7**, 665–75.
87. Subramanian, G., McAfee, J.G. (1970) Stannous oxide colloid labeled with ^{99m}Tc or ^{113m}In for bone marrow imaging, (abstract). *J. Nucl. Med.*, **11**, 365.
88. Hirsh, J.I., Tatum, J.L., Fratkin, M.J., *et al.* (1989) Preparation and evaluation of a ^{99m}Tc-SnF_2 colloid kit for leucocyte labeling. *J. Nucl. Med.*, **30**, 1257–63.
89. Subramanian, G., McAfee, J.G., Mehter, A. *et al.* (1973) ^{99m}Tc-Stannous phytate: a new in-vivo colloid for imaging the reticuloendothelial system (abstract). *J. Nucl. Med.*, **14**, 459.
90. Product Information (1990) Technescan Sb_2S_3, Mallinckrodt Diagnostica, Holland.
91. Product Information (1992) Solco nanocolloid, Sorin Biomedica SPA, Italy.
92. Strand, S-E., Persson, B.R.R. (1979) Quantitative lymphoscintigraphy. II. basic concepts for optimal uptake of radiocolloids in the parasternal lymph nodes of rabbits. *J. Nucl. Med.*, **20**, 1038–46.
93. Atkins, H.L., Cloutier, R.J., Lathrop, K.A. *et al.* (1975) Technetium-99m sulphur colloid in various liver conditions. *J. Nucl. Med.*, **16**, 108A–108B.
94. Product Information (1992) Amerscan hepatate II technetium agent for liver/spleen scintigraphy, Amersham International, UK.
95. Product Information (1993) Frostimage phytate. Mallinkrodt Radiopharmaceuticals, St. Louis.
96. Malmud, L.S., Fisher, R.S., Knight, L.C. and Rock, E. (1982) Scintigraphic evaluation of gastric emptying. *Semin. Nucl. Med.*, **12**, 116–25.
97. Sadek, S., Owunwanne, A., Yacoub, T. and Abdel-Dayem, H.M. (1988) Comparative study of labeled chicken liver and egg-white as solid markers for gastric emptying studies (abstract). *J. Nucl. Med.*, **29**, 752.
98. Wright, R.A., Thomson, D., Syed, I. (1981) Simultaneous markers for fluid and solid gastric emptying: new variations on an old theme: concise communication. *J. Nucl. Med.*, **22**, 772–76.
99. Loberg, M.D. and Fields, A.T. (1978) Chemical structure of technetium-99m labeled N-(dimethyl phenyl carbamoyl methyl)-imminodiacetic acid (^{99m}Tc-HIDA). *Int. J. Appl. Radiat. Isot.* **79**, 167–73.
100. Nunn, A.D., Loberg, M.D. and Conley, R.A. (1983) A structure distribution relationship approach leading to the development of Tc-99m mebrofenin: an improved cholescintigraphic agent. *J. Nucl. Med.*, **24**, 423–30.
101. Subramanian, G., McAfee, J.G., Henderson, R.W. *et al.* (1978) The influence of structural changes on biodistribution of Tc-99m labeled and N-substituted IDA derivatives. *Nuklearmedizin*, **16**, 136–39.
102. Motter, M. and Kloss, G. (1981) Properties of various IDA derivatives. *J. Label. Compounds Radiopharm.*, **18**, 56–8.
103. Janshott, A.L., Scheibe, P.O., Vera, D.R. *et al.* (1982) Use of quantitative structure activity analysis in radiopharmaceutical design, in *Proceedings of the Third World Congress of Nuclear Medicine and Biology, Vol:1* (ed. C. Raynaud), Pergamon Press, Oxford, pp. 261–64.

104. Chiotellis, E. and Varvarigou, A. (1980) ^{99m}Tc-labeled N-substituted carbonyl iminodiacetates: relationship between structure and biodistribution. *Int. J. Nucl. Med. Biol.*, **7**, 1–7.
105. Harvey, E., Loberg, M., Ryan, J. *et al.* (1979) Hepatic clearance mechanism of ^{99m}Tc-HIDA and its effect on quantitation of hepatobiliary function. *J. Nucl. Med.*, **20**, 310–13
106. Loberg, M.D. and Porter, D.W. (1979) Review and current status of hepatobiliary imaging agents, in *Radiopharmaceuticals*, Vol. II (eds G. Subramanian, B.A. Rhodes, I.F. Cooper and V. Sodd), The Society of Nuclear Medicine, New York, pp. 519–43.
107. Krishnamurthy, G.T. and Turner, F.E. (1990) Pharmacokinetics and clinical application of technetium-99m labeled hepatobiliary agents. *Semin. Nucl. Med.*, **22**, 130–49.
108. Product Information (1992) Technetium EHIDA (Etifenin) agent for hepatobiliary scintigraphy, Amersham International, UK.
109. Product Information (1992) Hepatolite (Technetium-99m disofenin), Dupont Merck Pharmaceuticals, North Bilerica, MA.
110. Product Information (1992) Choletec (technetium-99m mebrofenin), Squibb Diagnostics, Princeton, NJ.
111. Russel, C.D., Crittenden, R.C. and Cash, A.G. (1980) Ionic charge on ^{99m}Tc-DTPA and ^{99m}Tc-EDTA by column ion-exchange. *J. Nucl. Med.*, **21**, 354–60.
112. Russel, C.D. and Speiser, A.G. (1982) Iminodiacetate complexes of technetium: an electrochemical study. *Int. J. Appl. Radiat. Isot.*, **33**, 903–6.
113. Kloppen, J.F., Hauser, W., Atkins, H.L. *et al.* (1972) Evaluation of ^{99m}Tc-DTPA for the measurement of glomerular filtration rate. *J. Nucl. Med.*, **13**, 107–10.
114. Duffy, G.J., Casey, M., and Baker, F. (1982) A comparison of individual kidney GFR measured by ^{99m}Tc-DTPA gamma camera renography and by direct collection of creatinine from each kidney, in *Radionuclides in Nephrology. Proceedings of the 5th International Symposium held at the Royal Society, London* (eds Joeckes, Constable, Brown and Tauxe), Academic Press, London, p. 101.
115. Arnold, R.W., Subramanian, G., McAfee, J.G. *et al.* (1975) Comparison of ^{99m}Tc-complexes for renal imaging. *J. Nucl. Med.*, **16**, 357–67.
116. McAfee, J.G., Gangne, G., Atkins, H.I. *et al.* (1979) Biological distribution and excretion of DTPA labeled with ^{99m}Tc and ^{111}In. *J. Nucl. Med.*, **20**, 1273–78.
117. Rollo, F.D., Cavalier, R.R., Barn, M. *et al.* (1977) Comparative evaluation of ^{99m}Tc-GH, $^{99m}TcO_4^-$ and ^{99m}Tc-DTPA as brain imaging agents. *Radiology*, **123**, 379–83.
118. Kadir, S. and Strauss, W.H. (1979) Evaluation of inflammatory bowel disease with ^{99m}Tc-DTPA. *Radiology*, **130**, 443–46.
119. ICRP Publication 53 (1990) *Radiation Dose to Patients from Radiopharmaceuticals*, Pergamon Press, Oxford, pp. 187–88.
120. Ikeda, I., Inone, O. and Kurata, K. (1977) Preparation of various ^{99m}Tc-DMSA complexes and their evaluation as radiotracers. *J. Nucl. Med.*, **18**, 1222–29.
121. Ohta, H., Yamamoto, K., Endo, K. *et al.* (1984) A new agent for medullary carcinoma of the thyroid. *J. Nucl. Med.*, **25**, 323–25.
122. Patel, M.C., Patel, R.B., Ramnathan, P. *et al.* (1988) Clinical evaluation of ^{99m}Tc(V)-dimercapto succinic acid (DMSA) for medullary carcinoma of thyroid and its metastasis. *Eur. J. Nucl. Med.*, **13**, 507–10.
123. Lin, T.H., Khentigam, A. and Winchell, H.S. (1974) A ^{99m}Tc-Chelate substitute for organoradiomercurial renal agents. *J. Nucl. Med.*, **15**, 34–5.
124. Wills, K.W., Martinex, D.A., Hedley-Whyte, E.T. *et al.* (1977) Renal localization of ^{99m}Tc-(Sn) glucoheptonate and ^{99m}Tc-(Sn) dimercaptosuccinate in the rat by frozen section autoradiography. *Radiat. Res.*, **69**, 475–88.
125. Hosokava, S., Kawamura, J. and Yoshida, O. (1978) Basic studies on intrarenal localisation of renal scanning agent ^{99m}Tc-DMSA. *INIS Atom Index*, **9**, 4177–89.
126. Ramamoorthy, N., Shetye, S.V., Pandey, P.M. *et al.* (1987) Preparation and evaluation of ^{99m}Tc (V)-DMSA complex: studies in medullary carcinoma of thyroid. *Eur. J. Nucl. Med.*, **12**, 623–28.
127. Kagi, J.H.R., Himmelhoch, S.R., Whagner, P.D. *et al.* (1974) Equine hepatic and renal metalothineins. *J. Biol. Chem.*, **249**, 3937–40.

128. Yee, C.A., Lee, H.B. and Blaufox, H.D. (1981) ^{99m}Tc-DMSA renal uptake: influence of biochemical and physiologic factors. *J. Nucl. Med.*, **22**, 1054–58.
129. ICRP Publication 53 (1990) *Radiation Dose to Patients from Radiopharmaceuticals*, Pergamon Press, Oxford, pp. 185–86.
130. de Kieviet, W. (1981) Technetium radiopharmaceuticals: chemical characterization and tissue distribution of Tc-glucoheptonate using Tc-99m and carrier Tc-99. *J. Nucl. Med.*, **22**, 703–9.
131. Noronha, O.P.D. (1986) Biliary propensities of technetium-99m glucoheptonate. *J. Nucl. Med.*, **27**, 1646–48.
132. ICRP Publication 53. (1990) *Radiation Dose to Patients from Radiopharmaceuticals*, Pergamon Press, Oxford, pp. 193–94.
133. Fritzberg, A.R., Kasina, S., Eshima, D. and Johnson, D.L. (1986) Synthesis and biological evaluation of ^{99m}Tc-MAG3 as a Hippuran replacement. *J. Nucl. Med.*, **27**, 111–16.
134. Bormans, G., Cleynhens, B., Van Nerom, C. *et al.* (1990) Preparation of ^{99m}Tc-MAG_3 at room temperature (abstract). *Eur. J. Nucl. Med.*, **16**, 538.
135. Bubeck, B., Eisenhut, M., Brandan, W. *et al.* (1988) Pharmacokinetic and metabolism of ^{99m}Tc-MAG_3 (abstract). *J. Nucl. Med.*, **92**, 906.
136. Taylor, A., Eshima, D., Christian, P.E., Wooten, W.W. *et al.* (1988) Technetium-99m MAG_3 kit formulation: preliminary results in normal volunteers and patients with renal failure. *J. Nucl. Med.*, **29**, 616–22.
137. Benjamin, P.P. (1969) A rapid and efficient method of preparing ^{99m}Tc human serum albumin: its clinical application. *Int. J. Appl. Radiat. Isot.* **20**, 187–94.
138. Callahan, R.J., McKusick, K.A., Lamson III, M. *et al.* (1976) Technetium-99m-human serum albumin: evaluation of a commercially produced kit. *J. Nucl. Med.*, **17**, 47–9.
139. Stern, H.S., McAfee, J.G. and Zolle, I. (1972) Technetium-99m-albumin, in *Radioactive Pharmaceuticals*, (eds G.A. Andrews, R.M. Kniseley and H.N. Wagner), USAEC Technical Information Center, Oak Ridge, TN, pp. 359–82.
140. ICRP Publication 53 (1990) *Radiation Dose to Patients from Radiopharmaceuticals*, Pergamon Press, Oxford, p. 173.
141. Lemb, M., Oei, T.H., Eifert, H. and Gunther, B. (1993) Technegas: a study of particle structure, size and distribution. *Eur. J. Nucl. Med.*, **20**, 576–79.
142. Burch, W.M., Sullivan, P.J. and McLaren, C.J. (1986) Technegas: a new ventilation agent for lung scanning. *Nucl. Med. Commun.*, **7**, 865–71.
143. Monaghan, P., Provan, I., Murray, C. *et al.* (1991) An improved radionuclide technique for the detection of altered pulmonary permeability. *J. Nucl. Med.*, **32**, 1945–49.
144. Fawdry, R., Bush, V., King, T. and Grunewald, S. (1988) Initial experience with technegas. A new ventilation agent (abstract). *J. Nucl. Med.*, **29**, 765.
145. Strong, J.C. and Agnew, J.E. (1989) The particle size distribution of technegas and its influence on regional lung deposition. *Nucl. Med. Commun.*, **10**, 425–30.

8

Iodine radiopharmaceuticals

INTRODUCTION

Iodine radiopharmacheuticals are labeled mostly with ^{123}I, ^{125}I or ^{131}I. The physical half-lives, decay modes and gamma energies are listed in Table 8.1. The ^{125}I tracers will be discussed under non-imaging radiopharmaceuticals.

IODINE-123

This is used mainly for imaging and has the following desirable characteristics.

- Its monoenergetic gamma ray of 159 keV is easily collimated and yields sufficient photons (83%).
- Its half-life of 13.2 h is long enough to obtain the desired diagnostic information and is short enough to cause minimal radiation damage to the patient and personnel.
- Its lack of beta emissions lowers the radiation dose to both patients and personnel.

IODINE-125

This is used in *in vitro* tests and in the development of iodine radiopharmaceuticals (chemical synthesis and biologic distribution). Its desirable characteristics include the following:

- Its gamma ray of 35 keV is easily detected by a gamma counter and effectively shielded, thereby lowering radiation dose to personnel.
- Its half-life of 60 days allows enough time for development of a synthetic procedure and provides the labeled compound with long shelf life.

IODINE-131

This is used in therapy and thyroid uptake studies and rarely in imaging procedures. Its desirable characteristics include the following:

- Its β^- particles of 610 keV deliver a high radiation dose to tumor or toxic thyroid.
- Its gamma ray of 364 keV can be used for imaging studies to monitor therapy.
- Its half-life of 8.04 days is long enough to allow delivery of enough radiation to the target.

Table 8.1 Physical properties of iodine radionuclides useful in nuclear medicine

Radionuclide	*Half-life*	*Decay mode*	*Gamma energy (keV)*
^{123}I	13.2 h	EC	159 (83%)
^{125}I	60.14 days	EC	27 (138%), 35 (7%)
^{131}I	8.04 days	β^-	284 (6%), 364 (83%), 637 (7%)

IODINE-123/131 SODIUM IODIDE ($Na^{123/131}I$)

Iodine ($I^{\delta+}I^{\delta-}$) exhibits metal-like properties in its subsititution reactions with organic compounds. This is exemplified in the I^+ for H^+ substitution in the formation of *o*-iodo hippurate. In aqueous solution, it exists in ionized form (I^-), and this form is used for thyroid uptake or imaging studies. There are 23 radioisotopes of iodine, but only two ($^{123/131}I$) are important for imaging and one (^{131}I) for therapy.

PHYSICAL PROPERTIES

Iodine-123 decays by electron capture with a photon energy of 159 keV and a half-life of 13 h.

Iodine-131 decays by beta emission with gamma rays to xenon-131 and has a physical half-life of 8.08 days. The radiation energy of its beta particle is 610 keV, while those of its gamma rays are 284 (6%), 364 (83%) and 637 keV (7%).

PREPARATION

Iodine-123 is produced either directly from enriched tellurium in a medium-energy cyclotron by the ^{124}Te (p, 2n) ^{123}I reaction [1] or indirectly from the decay of xenon-123 produced in a high-energy cyclotron by the ^{127}I (p, 5n) ^{123}Xe reaction [2]. After bombardment, the ^{124}Te target is dissolved in a hot acid solution containing hydrogen peroxide. The solution is distilled and ^{123}I is trapped in sodium hydroxide. It contains the following radioactive contaminants: ^{124}I (< 5%), ^{24}Na (< 0.5%), ^{126}I (< 0.1%) ^{125}I (< 0.5%).

For the ^{127}I (p,5n) ^{123}Xe reaction, molten NaI target is irradiated in a 67.5-MeV proton beam. Helium is pumped through the target to carry the radioactive xenon to a trap. After sufficient ^{123}Xe is trapped, it is vacuum distilled into a decay vessel and allowed to decay for 6 h. The ^{123}Xe is purged out of the decay vessel and the ^{123}I rinsed out with sodium hydroxide [3]. The advantage of this method is that the final product has less than 0.1% ^{125}I as its only contaminant.

Iodine-131 is obtained from uranium fission or by the neutron bombardment of tellurium. To separate ^{131}I from the other radionuclides and chemicals, the tellerium target is dissolved in strong acid or base and filtered. The solution is acidified with sulfuric acid (if required), distilled and the iodine collected in sodium hydroxide solution.

DOSE

Thyroid uptake test	0.37–0.925 MBq (10–25 μCi) ^{131}I
Thyroid imaging	7.4–11.1 MBq (200–300 μCi) ^{123}I
Whole-body imaging for thyroid metastases	296–370 MBq (8–10 mCi) ^{131}I
Treatment of hyperthyroidism	74–110 MBq (2–30 mCi) ^{131}I
Treatment of thyroid carcinoma and its metastases	1110–7400 MBq (30–200 mCi) ^{131}I

INJECTION TO IMAGING TIME

Thyroid uptake and imaging	24 h
Whole-body imaging for thyroid metastases	72 h

PATIENT PREPARATION

Patients should not have undergone a radiologic procedure using an iodine-based contrast agent within at least 30 days. Patients should refrain from ingestion of iodine-containing drugs and compounds and from antithyroid drugs for 1 week, and from the topical application of iodine compounds for 2 weeks.

BIOLOGIC BEHAVIOR

$^{123/131}I$ is administered orally or intravenously. When administered orally, it is effectively absorbed from the gastrointestinal tract into the blood circulation within a few minutes. The $^{123/131}I^-$ ion is concentrated in the thyroid by an active transport system, as shown in an *in vitro* experiment using a metabolic inhibitor such as 1-methyl-1-mercaptoimidazole or propylthiouracil [4,5]. In the thyroid gland it is oxidized to iodine and bound to tyrosine, which is transformed to thyroid hormones: 3, 5, 3'-triiodothyronine (T_3) and thyroxine (T_4). Approximately 2% of the circulating radioactive iodide is concentrated by the thyroid each hour in normal subjects. The iodide tracers are also concentrated to a lesser degree in the salivary glands and gastric mucosa [6]. It is known that iodine crosses the placenta and accumulates in the fetal thyroid [7].

Radioactive iodide is excreted primarily in the urine, but a small amount of radioactivity can be detected in sweat and feces. In normal subjects approximately 65–90% of the administered dose is excreted in urine within 24 h. Radioiodide is secreted in human breast milk [8].

USES

- Study of thyroid functions
- Treatment of hyperthyroidism or thyroid carcinoma.
- Detection of thyroid metastases

DOSIMETRY

The data (assuming 25% uptake) are modified from [9] and listed in Table 8.2.

IODINE 123/131 SODIUM *o*-IODOHIPPURATE ($^{123/131}I$-*o*-IH)

CHEMISTRY

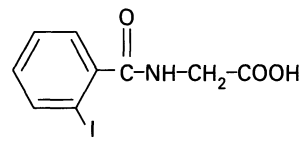

Ortho-iodohippuric acid is a physiologic analog of *p*-aminohippuric acid (PAH) that can be labeled with $^{123/131}I^-$ ion. The clearance value of [$^{123/131}I$]*o*-IH is reported to be less than that of PAH by about 15% [10].

PREPARATION

$^{123/131}I$-*o*-IH is available commercially, however, it can be prepared as follows. To a sterile multidose vial, add 1 ml of acetate buffer, pH 4 (0.2 ml of 0.2 M sodium acetate and 0.8 ml of 0.2 M acetic acid), 5.0 mg of *o*-iodohippuric acid in 0.2 ml of 50% ethanol, 1.0 mg of $CuSo_4 \cdot 5H_2O$ in 0.2 ml of water and $^{123/131}I$ (5–15 mCi) in 0.02 M NaOH (up to 7 ml). Autoclave for 15 min at 121°C and cool to room temperature.

Table 8.2 Estimated radiation absorbed dose of $^{123/131}I^-$ ion

Organ	^{123}I		^{131}I	
	mGy/MBq	*rad/mCi*	*mGy/MBq*	*rad/mCi*
Thyroid	3.51	13.00	351.00	1300.0
Stomach wall	0.06	0.21	0.38	1.4
Ovaries	0.01	0.031	0.04	0.14
Red marrow	0.01	0.031	0.07	0.26
Liver	0.007	0.027	0.013	0.048
Testes	0.003	0.012	0.02	0.08
Total body	0.008	0.029	0.19	0.71

QUALITY CONTROL

Place one drop of the preparation on the lower end of a Merck 5716 plate, develop up to 15 cm in a benzene–glacial acetic acid–distilled water (5:5:2.5) mixture and air dry. Scan the TLC using a TLC scanner. $^{123/131}$I-*o*-IH is detected at an R_f range of 0.5–0.6, $^{123/131}$I ion at 0–0.1 and *o*-iodobenzoic acid at 0.9–1.0. The labeling efficiency i s determined as follows:

$$\text{Labeling efficiency (\%)} = \frac{\text{Radioactivity at } R_{(f)}0.5-0.6}{\text{Radioactivity at } [(R_{(f)}0-0.1+R_{(f)}0.5-0.6+R_{(f)}0.9-1.0)]} \times 100$$

DOSES

^{123}I-*o*-IH 185 Mbq (5 mCi)
^{131}I-*o*-IH 11.1 Mbq (300 μCi)

INJECTION TO IMAGING TIME

Immediately.

PATIENT PREPARATION

Patients are given Lugol's solution, three drops twice daily, 1 day before and 2 days after administration of $^{123/131}$I-*o*-IH.

BIOLOGIC BEHAVIOR

After intravenous injection, $^{123/131}$I-*o*-IH is rapidly cleared from the blood by renal tubular secretion (80%) and glomerular filtration (20%). The total extraction efficiency by the normal kidney is 70–90% [11–13]. The urinary radioactivity excreted in 30 min is 66.8 ± 6.1% [14]. Approximately 3% of radioactivity from $^{123/131}$I-*o*-IH is secreted in human breast milk [15].

DOSIMETRY

The data are modified from [16] and listed in Table 8.3.

Table 8.3 Estimated radiation absorbed dose of $^{123/131}$I-*o*-IH

	^{123}-*I-o-IH*		^{131}*I-o-IH*	
Organ	*mGy/MBq*	*rad/mCi*	*mGy/MBq*	*rad/mCi*
Kidneys	0.0064	0.024	0.03	0.11
Bladder wall	0.200	0.74	0.96	3.55
Uterus	0.017	0.063	0.035	0.13
Ovaries	0.0073	0.027	0.017	0.063
GI tract				
Stomach wall	0.0008	0.003	0.0025	0.009
Small intestine	0.0032	0.012	0.0078	0.029
Upper large intestine	0.0025	0.009	0.0069	0.025
Lower large intestine	0.0075	0.028	0.017	0.063
Testes	0.0046	0.017	0.012	0.044
Red marrow	0.0025	0.009	0.0049	0.018
Bone surfaces	0.0013	0.005	0.003	0.011
Adrenals	0.0009	0.003	0.0028	0.010
Pancreas	0.0009	0.003	0.0026	0.010
Spleen	0.0008	0.003	0.0024	0.009
Liver	0.0007	0.003	0.0023	0.008
Breast	0.0004	0.001	0.0017	0.006
Thyroid	0.0004	0.001	0.0014	0.005

IODINE-123 *N*-ISOPROPYL-*p*-IODOAMPHETAMINE (^{123}IMP)

CHEMISTRY

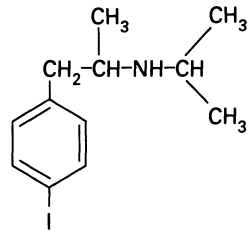

N-isopropyl-*p*-iodoamphetamine is a neutral and lipophilic monoamine that crosses the blood–brain barrier. It is labeled with ^{123}I.

PREPARATION

^{123}IMP is available commercially, however it can prepared as follows. To a sterile multidose vial containing 1–2 mg of IMP, and 130 μg of $CuSO_4 \cdot 5H_2O$, 0.5 mg of $SnSO_4$ and 500 μl of sterile ^{123}I solution containing the required activity. Boil for 30 min and cool to room temperature and adjust pH to 4.0 [17].

QUALITY CONTROL

Place one drop of the ^{123}IMP preparation on the lower end of a Merck silica gel plate 60 F_{254}, develop up to 15 cm in ethylacetate–ethanol (1:1) mixture and air dry. Scan the plate using a TLC scanner. ^{123}IMP is detected at an R_f of 0.1 and iodide at R_f0.8. Calculate the percentage labeling efficiency as follows:

$$\text{Labeling efficiency (\%)} = \frac{\text{Radioactivity at } R_{(f)}0.1}{\text{Radioactivity at } R_{(f)}(0.1+0.8)} \times 100$$

DOSE

185 MBq (5 mCi).

INJECTION TO IMAGING TIME

20–60 min.

PATIENT PREPARATION

Patients are given Lugol's solution, three drops twice daily, 1 day before and 2 days after administration of ^{123}IMP.

BIOLOGIC BEHAVIOR

After intravenous injection, 7–8% of injected ^{123}IMP is extracted into the cerebral parenchyma [18]. Its initial distribution is proportional to cerebral blood flow with a gray to white matter ratio of 2.4 at 15 min and 2.2 at 1 h [19]. However, it redistributes within the brain [20]. The mechanism of its brain retention is unclear, but it has been suggested that it binds to specific or non-specific receptor sites [21]. The ^{123}IMP also accumulates in other organs (lungs, kidneys, spleen, pancreas, adrenal glands and heart), with the lungs and liver having highest accumulation of 11.2% (15 min) and 16% (1 h) respectively [18]. Minimal *in vivo* deiodination occurs, as seen by a slight increase in radioactivity in the thyroid gland of approximately 0.2% of the injected dose at 24 h. It is excreted by both the liver and kidneys.

Baldwin and Wu [20] and Rapin *et al.* [22] have identified the biotransformation of IMP from animal experiments to be dealkylation, deamination and oxidative degradation to iodobenzoic acid, followed by conjugation with glycine to form *p*-iodohippuric acid as the major metabolite.

USES

- Diagnosis of acute cerebral infarction when CT is negative.

- Detection of intracerebral inflammatory conditions such as suspected herpes simplex encephalitis and lupus cerebritis and abscess with negative CT scan.
- Localization of an abnormal focal area in brain of patients with epilepsy.
- Detection of an abnormal focus in patients with head trauma and cerebrovascular accidents.
- Differentiation of Alzheimer's disease from multi-infarct dementia and depression.
- Diagnosis of brain death.

DOSIMETRY

The data are modified from [23] and listed in Table 8.4.

Table 8.4 Estimated radiation absorbed dose of isopropyl ^{123}IMP

Organ	*mGy/MBq*	*rad/mCi*
Brain	0.029	0.143
Lungs	0.12	0.444
Liver	0.11	0.407
Bladder wall	0.029	0.107
Pancreas	0.017	0.063
Adrenals	0.017	0.063
Kidneys	0.014	0.052
Red marrow	0.014	0.052
Breast	0.012	0.044
GI tract		
Stomach	0.012	0.044
Small intestine	0.0087	0.032
Upper large intestinal wall	0.01	0.037
Lower large intestinal wall	0.0064	0.024
Bone surfaces	0.011	0.041
Spleen	0.011	0.041
Uterus	0.008	0.030
Ovaries	0.007	0.026
Thyroid	0.006	0.022
Testes	0.004	0.015

IODINE-123 *N, N, N'* -TRIMETHL-*N'*-[2-HYDROXY-3-METHYL-5-IODOBENZYL]-1, 3- PROPANEDIAMINE (^{123}I-HIPDM)

CHEMISTRY

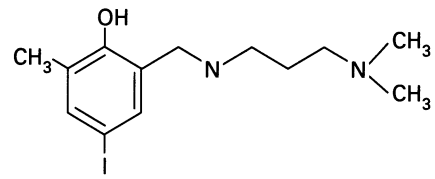

HIPDM is a neutral and lipophilic diamine that is iodinated at the aromatic ring [24]. It is synthesized from 5-iodo-3-methyl salicyl-aldehyde. The latter is prepared by reaction of 3-methylsalicylaldehyde with iodine monochloride (ICl) in glacial acetic acid at 60°C. The non-radioactive HIPDM is prepared by refluxing a solution of iodinated aldehyde and *N, N, N*-trimethyl propane-1, 3-diamine in benzene for 30 min, and the product is reduced with $NaBH_4$ [24].

PREPARATION

Add 1 ml of HIPDM solution (1.5 mg/ml, 0.1 N HCl) to 100 µl of an aqueous solution of $Na^{123}I$ (10–40 mCi , pH 5–7) in a 6-ml rubber-sealed glass vial, and heat the mixture in a boiling water bath for 40 min. Allow the solution to cool to room temperature and adjust the pH to 5–6 by dropwise addition of 0.1 N NaOH [25].

QUALITY CONTROL

Place one drop of the ^{123}I-HIPDM preparation on the lower end of a Merck silica gel plate 60 F_{254}, develop up to 15 cm in a $CHCl_3$–32% NH_4OH–ethyl alcohol (80:15:5) mixture and air dry. Scan the plate using a TLC scanner. ^{123}I-HIPDM is detected at an R_f range of 0.65–0.75 and iodide at R_f 0.1. The labeling efficiency is calculated as follows:

$$\text{Labeling efficiency (\%)} = \frac{\text{Radioactivity at } R_{(f)}\,0.65-0.75}{\text{Radioactivity at } R_{(f)}\,(0.1+0.65-0.75)} \times 100$$

DOSE

185–370 MBq (5–10 mCi).

INJECTION TO IMAGING TIME

30 min.

PATIENT PREPARATION

Patients are given Lugol's solution, three drops twice daily, 1 day before and 2 days after administration of ^{123}-HIPDM.

BIOLOGIC BEHAVIOR

The ^{123}I-HIPDM is a neutral and lipophilic compound which crosses the blood–brain barrier, hence it is used as a brain perfusion agent. Following intravenous injection, brain uptake of ^{123}I-HIPDM is rapid, reaching a peak value of 8.5% within 3–6 mins. The average brain uptake is 6.7% (4.6–8.5%) of the injected dose, and the distribution is proportional to regional blood flow, resulting in more uptake in gray than white matter [26].

The brain retention is thought to be due to the difference between the pH of blood (pH 7.4) and intracellular brain (pH 7.0). At blood pH, ^{123}I-HIPDM exists as a neutral compound that is lipid soluble and can diffuse freely into cells, but at lower intracellular brain pH it becomes protonated and can no longer diffuse out [20], as shown in Figure 8.1. It is doubtful that this is the only mechanism responsible for the brain retention of ^{123}I-HIPDM. In a review article, Kung [27] points out that the concentration ratio of brain to blood is always higher than the predicted value, therefore mechanism(s) other than pH shift may also play an important role in the brain retention of HIPDM.

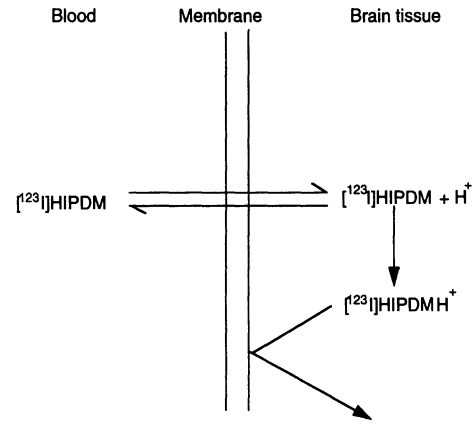

Figure 8.1 Suggested protonation of ^{123}I-HIPDM.

Significant uptake is found in lung and liver. The initial lung uptake is high (57%), and the disappearance is multiphasic, showing a slow component with long half-life (9 h). Using isolated perfused rat lungs in Krebs-Ringer bicarbonate buffer containing 4.5% bovine albumin, Slosman *et al.* [28] studied the transport of HIPDM in the lung and reported that it did not appear to occur by simple diffusion. The addition of chloropromazine, propranolol or imipramine to the perfusate decreased the ^{125}I-HIPDM lung uptake, but the addition of ouabain or the use of sodium-free medium had no effect on the uptake. Thus they concluded that the pulmonary accumulation of ^{125}I-HIPDM does not appear to occur by sodium-dependent active transport. The ^{125}I-HIPDM lung uptake seems to be similar to the uptake of other basic amines such as imipramine and propranolol, which are known to bind by physicochemical interactions to pulmonary endothelial cell membranes. Liver uptake is 23% with prolonged retention. No uptake is found in the eyes of humans, as reported for monkeys. Approximately 1–2% of the dose is found in pancreas [26].

Blood clearance is rapid, but total body retention is high. Cumulative urinary excretion

is only 19% at 24 h and 33% at 48 h, mainly in the form of iodide [26].

USES

- Diagnosis of acute cerebral infarction when CT is negative.
- Detection of intracerebral inflammatory conditions such as suspected herpes simplex encephalitis and lupus cerebritis and abscess with negative CT scan.
- Localization of an abnormal focal area in the brain of patients with epilepsy.
- Monitoring of anticonvulsant therapy.
- Differentiation of Alzheimer's disease from multi-infarct dementia and depression.
- Detection of an abnormal focus in patients with head trauma.
- Diagnosis of brain death.

DOSIMETRY

The data are obtained from [26] and listed in Table 8.5.

Table 8.5 Estimated radiation absorbed dose of ^{123}I-HIPDM

Organ	*mGy/MBq*	*rad/mCi*
Brain	0.038	0.14
Lung	0.154	0.57
Liver	0.100	0.37
Bladder wall	0.027	0.10
Red marrow	0.011	0.04
Ovaries	0.005	0.017
Eye	0.004	0.013
Testes	0.002	0.008
Total body	0.013	0.05

IODINE-123/131 *m*-IODOBENZYLGUANIDINE ($^{123/131}$I-mIBG)

CHEMISTRY

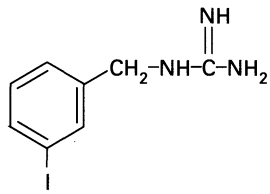

$^{123/131}$I-mIBG is a physiologic analog of norepinephrine and guanethidine. *m*-Iodobenzylguanidine is synthesized by reacting *m*-iodobenzylguanidine hydrochloride with cyanamide. The resulting glassy solid is dissolved in potassium bicarbonate solution to precipitate *m*-iodobenzylguanidine bicarbonate. Reaction with sulfuric acid and purification by crystallization yields *m*-iodobenzylguanidine sulfate [29].

PREPARATION

$^{123/131}$I-mIBG is available commercially, however it can be prepared as follows. Add 500 µl of sterile $^{123/131}$I solution containing the required activity to 1–2 mg of freeze-dried mIBG, an excess of ascorbic acid, 130 µg of $CuSO_4 \cdot 5H_2O$ and 0.5 mg of $SnSO_4$. Boil for 30 min, cool to room temperature and adjust the pH to 4.0 [17].

QUALITY CONTROL

Dilute the sample with water. Place one drop of the aliquot on the lower end of a Merck silica gel plate 60 F_{254}, develop up to 15 cm in an ethylacetate–ethyl alcohol (1:1) mixture and air dry. Scan the plate using a TLC scanner. $^{123/131}$I-mIBG is detected at the origin (R_f0) and iodide at an R_f range of 0.65–0.75. Calculate the labeling efficiency as follows:

$$\text{Labeling efficiency (\%)} = \frac{\text{Radioactivity at } R_{(f)}0}{\text{Radioactivity at } R_{(f)}(0+0.65-0.75)} \times 100$$

DOSES

^{123}I-mIBG 370 MBq (10 mCi)
^{131}I-mIBG 18.5–37 MBq (0.5–1 mCi)

INJECTION TO IMAGING TIME

24, 48 and 72 h.

PATIENT PREPARATION

Patients are given Lugol's solution, three drops twice daily, 1 day before and 2 or 4 days after administration of ^{123}I-mIBG or ^{131}I-mIBG respectively.

BIOLOGIC BEHAVIOR

$^{123/131}$I-mIBG has high affinity for the adrenal medulla and it is sequestered mainly in chromaffin storage granules [30]. It is retained in the myocardium by sequestration within the norepinephrine storage vesicles of the adrenergic nerves of the heart [31]. It has similar percentage uptake (4%) in the heart as ^{201}Tl^{+}[32]. The accumulation of $^{123/131}$I-mIBG in the salivary gland may be related to sympathetic innervation, since this organ is richly supplied by sympathetic nerves [33]. Its uptake in the liver usually reaches a maximum at 24 h, and it is substantially cleared by 72 h.

Splenic uptake is observed, consistent with possible neuronal uptake by the rich sympathetic innervation, and its clearance occurs over 72 h. ^{131}I-mIBG is excreted by the kidneys: 60% within the first 24 h and up to 90% by 4 days [34].

USES

- Localization and treatment of pheochromocytoma, neuroblastoma, non-functioning paraganglioma and carcinoid tumor.
- Diagnosis of cardiomyopathy and cardiac transplant rejection.

DOSIMETRY

The data are obtained from [35] and listed in Table 8.6.

IODINE-123 FATTY ACIDS

Long-chain free fatty acids are the principal source of energy for the normal myocardium [36]. The pathway of fatty acid oxidation in the heart muscle starts with the liberation of free fatty acids from albumin-bound fatty acids or from triglycerides through lipolysis at the endothelial surface of the myocytes [37]. After crossing the plasma membrane, free fatty acids are activated by esterification

Table 8.6 Estimated radiation absorbed dose of $^{123/131}$I-mIBG

Organ	*^{123}I-mIBG*		*^{131}I-mIBG*	
	mGy/MBq	*rad/mCi*	*mGy/MBq*	*rad/mCi*
Adrenal medulla	0.22	0.8	27.03	100
Thyroid	0.59	2.2	9.46	35
Spleen	0.04	0.14	0.43	1.6
Ovaries	0.02	0.06	0.27	1.0
Heart wall	0.01	0.03	0.19	0.7
Liver	0.01	0.05	0.11	0.4
Total body	0.005	0.02	0.03	0.1

with coenzyme A to form acetyl CoA. In mitochondria acyl CoA undergoes beta oxidation, in which two carbon fragments are split off the long-chain free fatty acid and enter the citric acid cycle (Krebs' cycle) after being converted to acetyl CoA (Figure 8.2). The beta oxidation pathway depends on the amount of oxygen present in the heart [38]. Therefore, in myocardial ischemia the rate of beta oxidation of free fatty acid decreases. Hence, fatty acids labeled with gamma-emitting radionuclides might by excellent agents for external detection of myocardial ischemia.

Both iodine and the methyl groups have approximately the same radius of 2 Å, therefore iodine for methyl group substitution has been used for development of ^{123}I long-chain fatty acids, as exemplified by 16-^{123}I-iodohexadecanoic acid (16-^{123}IHA) [39] and 17-^{123}I-iodoheptadecanoic acid (17-^{123}IHA) [40]. There is significant *in vivo* deiodination of the tracer to iodide ion by direct enzymatic cleavage of the alipahtic carbon–iodine bond, which results in a rapid clearance of radioactivity from the heart [41,42]. This rapid increase of radioactive iodide in the blood complicates imaging and renders quantitation of cardiac metabolism of free fatty acid difficult to perform. For example, 20 min after injection of 17–^{123}IHA, approximately 70% of the blood radioactivity is due to $^{123}I^-$ ion.

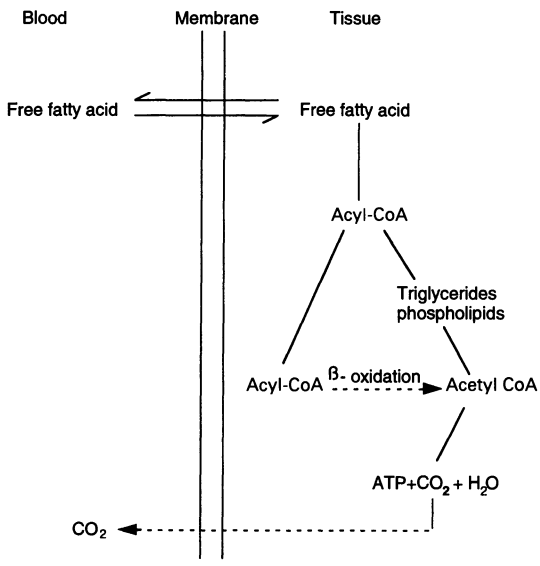

Figure 8.2 Biotransformation of free fatty acids.

To overcome the problem of *in vivo* deiodination, a radioiodinated phenyl group is attached to the fatty acid, as exemplified by *p*-^{123}I-iodophenylpentadecanoic acid [43]. Studies in mice with *p*-^{123}I-iodophenylpentadecanoic acid have shown that this tracer is stable *in vivo*. However, it undergoes rapid beta oxidation, which leads to fast clearance of the tracer from the myocardium. A fast imaging decive such as a multihead gamma camera can be used to record the metabolism of the *p*-^{123}I-iodophenylpentadecanoic acid tracer. Alternatively, the rapid beta oxidation can be slowed by adding a methyl group at the beta position of the fatty acid [44] or a hetero atom in the chain [45].

The ^{123}I fatty acids are not commonly used for myocardial imaging owing to the limited availability of iodine-123.

IODINE-131 6β-IODOMETHYL-10-NORCHOLEST-5(10)-EN-3β-OL (^{131}I-IODOMETHYL NORCHOLESTEROL)

CHEMISTRY

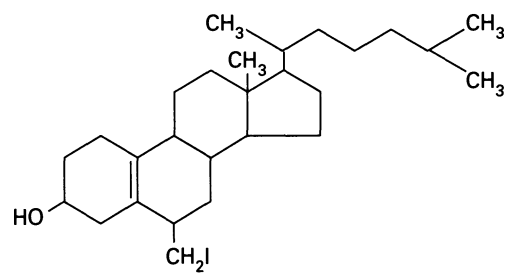

Iodine-131 iodomethyl norcholesterol is a derivative of norcholesterol, which is different from cholesterol by not having a methyl

group at the C-10 position. Non-radioactive iodomethyl norcholesterol is synthesized from cholest-5-en-3β, 19-diol-19-toluene-*P*-sulphonate by refluxing with potassium iodide for 4 h in ethyl alcohol [46].

PREPARATION

^{131}I-iodomethyl norcholesterol is prepared by exchange reaction between the non-radioactive compound and Na^{131}I in ethanol. For intravenous administration, ^{131}I-iodomethyl norcholesterol is formulated in 6.6% ethyl alcohol–1.6% Tween 80 in saline. The compound is stable at –20°C to 4°C for 2 weeks.

QUALITY CONTROL

Place a drop of ^{131}I-iodomethyl norcholesterol preparation 1 cm from the lower end of a 12-cm Whatman 3MM paper strip, develop up to 9 cm in a mixture of $CHCl_3$–acetic acid (9:1, v/v) and air dry. Scan the paper using a TLC scanner. ^{131}I-iodomethyl norcholesterol is detected at the solvent front and iodide at the origin. The radiochemical purity is calculated as follows:

$$\text{Radiochemical purity (\%)} = \frac{\text{Activity at solvent front}}{\text{Activity at origin} + \text{solvent front}}$$

DOSE

18.5–37 MBq (0.5–1 mCi).

INJECTION TO IMAGING TIME

2–3 days and if necessary repeat at 6–7 days.

PATIENT PREPARATION

Patients are given Lugol's solution, three drops twice daily, 1 day before and 7 days after administration of ^{131}I-iodomethyl norcholesterol. Patients may be injected with 2–4 mg/day dexamethasone from 2 days prior to administration of ^{131}I-iodomethyl norcholesterol until the termination of the study.

BIOLOGIC BEHAVIOR

After intravenous injection of ^{131}I-iodomethyl norcholesterol, the highest concentrations are found in the adrenal, liver and intestine [47]. The mean percentage uptake in the adrenals of a normal subject is 0.3%. However, increased uptake of the order of 0.6–0.8% is observed in patients with Cushing's disease [47, 48]. The elimination of activity from the adrenal is bioexponential with half-lives of 25 h and 13 days [48].

Liver uptake of the order of 18% is observed with elimination half-lives of 1.4 day (75%) and 13 days (25%) [49]. In spite of blocking the thyroid gland with non-radioactive iodine, 4–8% of the activity is observed in the thyroid, probably as a result of *in vivo* deiodination of ^{131}I-iodomethyl norcholesterol [50].

Table 8.7 Estimated radiation absorbed dose for ^{131}I-iodomethyl norcholesterol

Organ	*mGy/MBq*	*rad/mCi*
Adrenal	4.0	14.8
Thyroid	3.0	11.1
Liver	1.2	4.44
Pancreas	0.43	1.59
Kidneys	0.41	1.52
GI tract		
Stomach wall	0.40	1.48
Small intestine	0.41	1.52
Upper large intestine	0.41	1.52
Lower large intestine	0.39	1.44
Uterus	0.40	1.48
Bladder wall	0.39	1.44
Red marrow	0.39	1.44
Spleen	0.39	1.44
Lungs	0.38	1.40
Testes	0.36	1.33

Total body elimination has two components with half-lives of 1.4 (20%) and 13 days (80%). The major pathway of clearance is through the hepatobiliary system [49].

USE

^{131}I-iodomethyl norcholesterol is used for the diagnosis of adrenocortical malfunction such as aldosteronism, adrenal hyperplasia and Cushing's syndrome.

DOSIMETRY

The data are modified from [51] and listed in Table 8.7.

REFERENCES

1. Kondo, K., Lambrecht, R.M. and Wolf, A.P. (1977) Iodine-123 production for radiopharmaceuticals. *Int. J. Appl. Radiat. Isot.*, **28**, 395.
2. Lambrecht, R.M., Mantescu, C, Redvanly C. *et al.* (1972) Preparation of high-purity carrier-free ^{123}I-Iodine monochloride as iodination reagent for synthesis of radiopharmaceuticals. IV. *J. Nucl. Med.*, **13**, 224–26.
3. Lagnunas-Solar, M.C. (1982) Cycloton production of high-purity iodine-123 for medical application via the ^{127}I (p, 5n) ^{123}Xe-^{123}I nuclear reaction. Presented at the International Symposium on the developing role of short-lived radionuclides in Nuclear Medicine Practice, Washington DC.
4. Wolf, J., and Maurey, J.R. (1962) Thyroid iodide transport (III). Comparison with anions of periodic group VII A. *Biochim. Biophys. Acta*, **57**, 422–26.
5. Wolf, J. (1964). Transport of iodide and other anions into the thyroid gland. *Physiol. Rev.*, **44**, 45–90.
6. Atkins, H.L. (1975) The thyroid, in *Clinical Scintillation Imaging*, 2nd edn (eds L.M. Freeman and P.M. Johnson), Grune & Stratton, New York, pp. 671–708.
7. Hodges, R.E., Evans, T.C., Bradbury, J.T. and Keettel, W.C. (1955) The accumulation of radioactive iodine by human fetal thyroids. *J. Clin. Endocrinol. Metab.*, **15**, 661–67.
8. Coakley, J.L., and Mountford, P.J., (1985) Nuclear medicine and nursing mother. *BMJ*, **291**, 159–60.
9. Mird/dose estimate report No. 5. (1975) Summary of current radiation dose estimates to human from ^{123}I, ^{124}I, ^{125}I, ^{126}I, ^{130}I and ^{132}I as sodium iodide. *J. Nucl. Med.*, **16**, 857–60.
10. Mailoux, L. and Gagnon, J.A. (1972) Measurement of effective renal plasma flow, in *Progress in Nuclear Medicine*, Vol. 2., *Evaluation of Renal Function and Disease with Radionuclides*, Karger, (Baltimore University Park Press), Basle, pp. 54–70.
11. Taylor, A.T. (1980) Quantitative renal function scanning: a historical and current status report on renal radiopharmaceuticals, in *Nuclear Medicine Annual*, (eds L.M. Freeman and H.S. Weissman), Raven Press, New York, pp. 303–40.
12. McAfee, J.G., Grossman, Z.D., Gagne, G.R., *et al.* (1981) Comparison of renal extraction efficiencies for radioactive agents in the normal dog. *J. Nucl. Med.*, **22**, 333–38.
13. Stadalnik, R.C., Vogel, J.M., Jansholt, A.L., *et al.* (1980) Renal clearance and extraction parameters of ortho-iodohippurate (I-123) compared with OIH (I-131) and PAH. *J. Nucl. Med.* **21**, 168–70.
14. Taylor, A.T., Eshima, D., Fritzberg, A.R., *et al.* (1986) Comparison of iodine-131 OIH and technetium MAG_3 renal imaging in volunteers. *J. Nucl. Med.* **27**, 795–803.
15. Ahlgreen, L., Ivarsson, S., Johansson, L., *et al.* (1985) Excretion of radionuclides in human breast milk after the administration of radiopharmaceuticals. *J. Nucl. Med.* **26**, 1085–90.
16. ICRP Publication 53 (1990) *Radiation Dose to Patients from Radiopharmaceuticals*, Pergaman Press, Oxford, pp. 306–11.
17. Mertens, J., Vanryckeghem, W., Gysemans, M. *et al.* (1987) New fast preparation of ^{123}I labelled radiopharmaceuticals. *Eur. J. Nucl. Med.* **13**, 380–81.
18. Holman, B.L., Hill, T.C., and Magistretti, P.L. (1982) Brain imaging with emission computed tomography and radiolabeled amines. *Invest. Radiol.*, **17**, 206–15.
19. Kuhl, D.E., Barrio, J.R., Huang, S.C., *et al.* (1982) Quantifying local cerebral blood flow by N-isopropyl-P-[^{123}I] iodoamphetamine (IMP) tomography. *J. Nucl. Med.*, **23**, 196–203.

20. Baldwin, R.M., and Wu, J.L. (1988) In vivo chemistry of iofetamine HCI[123]I (IMP) *J. Nucl. Med.* **29**, 122–24.
21. Winchell, H.S., Horst, W.D., Braun, L. *et al.* (1980) N-Isopropyl [[123]I]-P-iodoamphetamine: Single pass brain uptake and washout; binding to brain synaptosomes; and localization in dog and monkey brain. *J. Nucl. Med.* **21**, 947–52.
22. Rapin, J.R., Le Poncin-Lafitte, M., Duterte, D. *et al.* (1983) Radiopharmacologic studies of isopropyliodoamphetomorine, in *Functional Radionuclide Imaging of the Brain*, (ed. P.L. Magistretti), Raven Press, New York, pp. 209–16.
23. ICRP Publication 53 (1990) *Radiation Dose to Patients from Radiopharmaceuticals*. Pergamon Press, Oxford, pp. 279–80.
24. Kung, H.F., Tramposch, K.M., and Blau, M. (1983) A new brain perfusion imaging agent: [I-123] HIPDM: N, N, N'-trimethyl-N' [2-hydroxy-3-methyl-5-iodobenzyl]-1, 3-propane diamine. *J. Nucl. Med.*, **24**, 66–72.
25. Lui, B., Chang, J., Sun, J.S. *et al.* (1987) Radioactive iodine exchange reaction of HIPDM: Kinetics and mechanism. *J. Nucl. Med.*, **28**, 360–65.
26. Fazio, F., Lenzi, G.L., Gerundini, P. *et al.* (1984) Tomographic assessment of regional cerebral perfusion using intravenous I-123-HIPDM and a rotating gamma camera. *J. Comput. Assist. Tumogr.*, **8**, 911–21.
27. Kung, H.F. (1988) Iodine labelled brain perfusion imaging agents, in *Nuclear Medicine Update* (eds S.D.J. Yeh and D.C.P. Chem), The Society of Nuclear Medicine, Taipei, Taiwan, pp. 87–103.
28. Slosman, D.O., Brill, A.B., Polla, B.S., and Alderson, P.O. (1987) Evaluation of [iodine-125] N, N, N'-trimethyl-N'-(2-hydroxy-3-methyl-5-iodobenzyl)-1, 3-propanediamine lung uptake using an isolated-perfused lung model. *J. Nucl. Med.*, **28**, 203–8.
29. Wieland, D.M., Wu, J.L., Brown, L.E. *et al.* (1980) Radiolabeled adrenergic neuron-blocking agents: adrenomedulary imaging with [[131]I] iodobenzylguanidine. *J. Nucl. Med.* **21**, 349–53.
30. Wieland, D.M., Brown, L.E., Tobes, M.C. *et al.* (1981) Imaging the primate adrenal medulla with [[123]I] and [[131]I] metaiodobenzylguanidine: concise communication. *J. Nucl. Med.*, **22**, 358–64.
31. Wieland, D.M., Brown, L.E., Rogers, W.L. *et al.* (1981) Myocardial imaging with a radioiodinated norepinephrine storage analog. *J. Nucl. Med.*, **22**, 22–31.
32. Kline, R.C., Swanson, D.P., Wieland, D.M. *et al.* (1981). Myocardial imaging in man with [123]I-meta-iodobenzylguanidine. *J. Nucl. Med.*, **22**, 129–32.
33. Nakajo, M., Shapiro, B., Sisson, J.C. *et al.* (1984) Salivary gland accumulation of meta-[[131]I] iodobenzylguanidine. *J. Nucl. Med.*, **25**, 2–6.
34. Mangner, T.J., Tobes, M.C., Wieland, D.M. and Sisson, J.C. (1984) Metabolism of [131]I-meta-iodobenzylguanidine in humans (abstract). *J. Nucl. Med.*, **25**, 123.
35. McEwan, A.J., Shapiro, B., Sisson, J.C. *et al.* (1985) Radioiodobenzylguanidine for the scintigraphic location and therapy of adrenergic tumors. *Semin. Nucl. Med.*, **15**, 132–53.
36. Evans, J.R., Gunton, R.W., Baker, R.G. *et al.* (1965) Use of radioiodinated fatty acids for photoscans of the heart. *Circ. Res.*, **16**, 1–10.
37. Opie, L.H. (1984) Carbohydrate and lipids, in *The Heart: Physiology, Metabolism Pharmacology and Therapy* (ed. L.H. Opie) , Grune & Stralton, Orlando, FL, pp. 118–35.
38. Morgan, H.E. and Neely, J.R. (1990) Metabolic regulation and myocardial function, in *The Heart, Arteries and Veins*, 7th edn (eds J.W. Hurst, R.B. Logue and C.E. Rackley), McGraw-Hill, New York, pp. 91–105.
39. Poe, N.D., Robinson, G.D., Zidinski, F.W. *et al.* (1977) Myocardial imaging with [123]I-Hexadecenoic acid. *Radiology*, **124**, 419–24.
40. Vyska, K., Hock, A., Profant, M., *et al.* (1979) Myocardial imaging and measurement of myocardial fatty acid metabolism using *w*-I-123 heptadecanoic acid (abstract). *J. Nucl. Med.*, **20**, 650.
41. Machulla, H.J., Stocklin, G., Kupfernagel, C.H. *et al.* (1978) Comparative evaluation of fatty acids labeled with C-11, CI-34m, Br-77 and I-123 for metabolic studies of the myocardium: concise communication. *J. Nucl. Med.*, **19**, 298–302.
42. Poe, N.D., Robinson, Jr, G.D., Gram, L.S. *et al.* (1976) Experimental basis for myocardial

imaging with ^{123}I-labeled hexadecanoic acid. *J. Nucl. Med.*, **17**, 1077–82.

43. Machulla, H.J., Marsmann, M. and Dutchka, K. (1980) Biochemical concept and synthesis of a radioiodinated phenyl fatty acid for *in vivo* metabolic studies of the myocardium. *Eur. J. Nucl. Med.*, **5**, 171–73.
44. Elmaleh, D.R., Livini, E., Levy, S. *et al.* (1983) Comparison of C-11 and C-14 labeled fatty acids and their β-methyl analogs. *Int. J. Nucl. Med. Biol.*, **10**, 181–87.
45. Knapp, E.F., Ambrose, K.R., Callahan, A.P. *et al.* (1981) Effects of chain length and tellurium position on the myocardial uptake of Te-123m fatty acids. *J. Nucl. Med.*, **22**, 988.
46. Sarkar, S.D., Beierwates, W.H., Rodney, D. *et al.* (1975) A new and superior adrenal scanning agent NP-59. *J. Nucl. Med.*, **16**, 1038–42.
47. Ryo, U.Y., Johnston, A.S., Kim, I. and Pinsky, S.M. (1978) Adrenal scanning and uptake with [^{131}I]-iodomethylnorcholesterol. *Radiology*, **128**, 157–61.
48. Carey, J.E., Thrall, J.H., Freitas, J.E., and Beierwaltes, W.H. (1979) Absorbed dose to the human adrenals from [^{131}I]–iodomethyl nor cholesterol 'NP-59': concise communication. *J. Nucl. Med.*, **20**, 60–2.
49. Kletter, K., Herkner, K., Kallinger, W. and Nowotny, R. (1978) Strahlenbelastung bei Nebennierenszintigraphie mit dem neuen Radiopharmakon I-131-NP-59, in *Nuklearmedizin and Biokybernetik* (eds K. Oeff and H.A.E. Schmidt), Medico-Informationsdienste, Berlin, pp. 225–230.
50. O'Connor, M.K., Cullen, M.J. and Malone, J.F. (1979) High thyroid radiation dose associated with ^{131}I-iodo cholesterol NP-59 adrenal scanning. *Br. J. Radiol.*, **52**, 130–33.
51. CRP Publication 53 (1990) *Radiation dose to patients from radiopharmaceuticals*, Pergamon Press, Oxford, pp. 317–18.

9

Group IIIA radiopharmaceuticals

The elements of group IIIA which have useful radionuclides for imaging are gallium, indium and thallium. Being group III elements, they have three electrons in their outermost shells. Hence, in aqueous solution, they can exist in the +1, +2 or +3 oxidation state. However, at neutral or plasma pH their common salts, particularly those of gallium and indium, are insoluble, and if the ionic form (Ga^{3+} or In^{3+}) is added to water it hydrolyzes very easily. To stabilize them, they are complexed to ligands such as citrate and oxine. Thallium in the +1 oxidation state is stable in aqueous medium and is administered intravenously as thallous chloride. The radiopharmaceuticals of gallium-67, indium-111 and thallium-201 are described in this chapter.

GALLIUM-67 CITRATE (^{67}Ga CITRATE)

CHEMISTRY

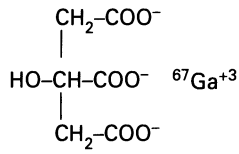

Gallium is a metallic element of group IIIA. In aqueous medium, gallium salts of halides, sulfates, nitrates, phosphates and sulfides undergo a hydrolysis reaction and precipitate at physiologic pH. However, it forms a positively charged complex at pH 6.8 [1] with the possibility of polymerization [1–3]. In acidic medium it exists as the +3 ion.

PHYSICAL PROPERTIES

^{67}Ga decays by electron capture (100%) with a half-life of 78.3 h. It emits several gamma rays: 93 keV (40%), 184 keV (24%), 296 keV (22%) and 388 keV (7%). For imaging, it is the 93-, 184- and 296-keV gamma rays that are used.

PREPARATION

Gallium-67 is produced in a cyclotron by bombarding enriched ^{68}Zn oxide with 20-MeV protons according to the following reaction: ^{68}Zn (p, 2n) ^{67}Ga. The irradiated zinc oxide is dissolved in 7 M HCl. ^{67}Ga is extracted with isopropyl ether, evaporated to dryness and dilute HCl is added. The complex is formed with the addition of sodium citrate and benzyl alcohol as preservative. The pH is adjusted to 5–8 with either sodium hydroxide or hydrochloric acid [4]. It is supplied as an isotonic, sterile and pyrogen-free solution for intravenous administration.

QUALITY CONTROL

The manufacturer performs the necessary quality control tests for ^{67}Ga citrate prior to distribution. However the following tests may be performed if required.

Radionuclidic test

This is performed using a multichannel analyzer. The ^{67}Ga citrate should contain not more than 0.01% ^{66}Ga and 0.1% of other radionuclidic impurities on the reference date.

Radiochemical test

Using a 6-cm ITLC-SG strip, place a drop of the ^{67}Ga citrate preparation 1 cm from the lower end, develop in a methanol–acetic acid (9:1) mixture for up to 5 cm, air dry and cut at 3 cm from the origin. Assay each piece in a dose calibrator. The ^{67}Ga citrate is at the origin while other ^{67}Ga impurities are at the solvent front [5]. Calculate the labeling efficiency as follows.

$$\text{Labeling efficiency (\%)} = \frac{\text{Radioactivity at origin}}{\text{Radioactivity at (origin + solvent front)}} \times 100$$

DOSE

74–370 MBq (2–10 mCi).

PATIENT PREPARATION

Patients may be given laxatives during the first week after injection.

INJECTION TO IMAGING TIME

24–72 h.

BIOLOGIC BEHAVIOR

^{67}Ga citrate, after injection, accumulates in viable primary and metastatic tumors and at focal sites of infection. The tumor uptake of ^{67}Ga citrate is thought to be mediated through transferrin [6–8]. Its mechanism of uptake in abscesses is not known, however it has been reported that it is not *in vivo* labeling of leukocytes [9].

At 24–72 h after injection, the highest accumulation of ^{67}Ga citrate is in the bone, including marrow (24%), liver (5%), kidney (2%) and spleen (1%). Other organs with relatively high accumulation include adrenals, bowels and lung. Muscle, skin, fat and brain retention is low [10]. Autoradiographic studies indicate that in the kidney ^{67}Ga citrate is concentrated in the cortex, primarily in the proximal convoluted tubules, in the spleen in the phagocytic cells and in the liver in both the recticuloendothelial cells and hepatocytes [10, 11]. ^{67}Ga citrate crosses the placenta to the fetal circulation [12].

The blood clearance of ^{67}Ga citrate is very slow. It binds to the plasma proteins transferrin and haptoglobin and loosely to albumin [13]. At 24 h after injection, 10% of the dose is in plasma; 25% is excreted in urine and 10% in feces over 1 week [14]. Gallium-67 citrate is secreted in human breast milk but it is not absorbed through the gastrointestinal tract of an infant [15].

USES

- Demonstration of the presence of primary tumor and metastases of lung cancer, lymphomas and Hodgkin's disease, malignant melanoma and hepatocellular carcinoma.
- Detection of focal sites of infection.
- Assessment of extent and activity of sarcoidosis.
- Assessment of the activity of iodiopathic pulmonary fibrosis.

DOSIMETRY

The data are modified from [16] and listed in Table 9.1.

Table 9.1 Estimated radiation absorbed dose of ^{67}Ga citrate

Organ	*mGy/MBq*	*rad/mCi*
GI tract		
Lower large intestine	0.24	0.90
Upper large intestine	0.15	0.56
Small intestine	0.097	0.36
Stomach	0.059	0.22
Bone marrow	0.156	0.58
Spleen	0.143	0.53
Liver	0.124	0.46
Skeleton and marrow	0.119	0.44
Kidneys	0.111	0.41
Ovaries	0.075	0.28
Testes	0.065	0.24
Total body	0.070	0.26

INDIUM-111 RADIOPHARMACEUTICALS

Indium exists in ionic form (In^{+3}) at low pH and as hydroxide [$In(OH)_3$] at high pH and forms labile complexes with weak complexing agents such as acetate and citrate. However, it forms stable complexes with strong chelating agents such as oxine, tropolone, DTPA and EDTA.

Indium-111 decays by electron capture (100%) with a half-life of 67.2 h. It emits gamma radiations of 173 keV (89%) and 247 keV (94%), which are used for imaging.

Indium-111 is produced in a cyclotron by irradiating either ^{111}Cd with 15-MeV protons according to the ^{111}Cd(p,n)^{111}In reaction or ^{109}Ag with 30-MeV alpha particles according to the ^{109}Ag (α,2n) ^{111}In reaction. After irradiation, the cadmium or silver target is dissolved in hydrochloric acid and indium-111 is separated by passing the solution through an anion-exchange resin or by solvent extraction [4].

It is recommended that $^{111}InCl_3$ is not directly injected into a patient, probably because of high radiation dose [17]. However, it is used in the preparation of ligands which may be used directly or for labeling blood components and antibodies.

INDIUM-111 DIETHYLENETRIAMINEPENTAACETIC ACID (^{111}IN-DTPA)

CHEMISTRY

Diethylenetriaminepentaacetic acid forms a water-soluble complex with $^{111}In^{3+}$, which has a stability constant of 28.4. When ^{111}In-DTPA is prepared at low pH and adjusted to pH 7.0, it does not precipitate; however, if $^{111}InCl_3$ is added to DTPA solution at high pH, it precipitates as $^{111}In(OH)_3$.

PREPARATION

^{111}In-DTPA is available commercially, however it can be prepared in the radiopharmacy as follows. Add 37 MBq (1 mCi) of $^{111}InCl_3$ in 0.1–1.0 ml of 0.05 N HCl to 0.4 ml (2 mg) of DTPA solution and mix. Add 0.5 ml (0.2 mg) of calcium chloride solution to the reaction mixture. Adjust the final pH of the preparation to 7.0 by adding 0.2 ml of phosphate buffer [18]. The preparation is sterilized by filtration through a 0.22-μm millipore filter.

QUALITY CONTROL

Place a drop of the ^{111}In-DTPA preparation on to an 11-cm silica gel ITLC strip at 2 cm from the lower end, develop up to 8 cm in a mixture of 10% ammonium acetate and methanol, and air dry. Cut at 2 cm from the origin and assay the activity of each piece in a dose calibrator. ^{111}In-DTPA is at the solvent front, while $^{111}InCl_3$ is at the origin. Calculate the labeling efficiency as follows:

$$\text{Labeling efficiency (\%)} = \frac{\text{Activity at solvent front}}{\text{Activity at origin + solvent front}} \times 100$$

DOSE

18.5 MBq (500 μCi).

INJECTION TO IMAGING TIME

4–6, 24 and 72 h.

BIOLOGIC BEHAVIOR

Upon intrathecal injection in the lumbar spine, ^{111}In-DTPA flows in the cerebrospinal fluid (CSF) to the vertex region. ^{111}In-DTPA is absorbed from the subarachnoid space into the blood circulation, from where it is excreted in urine. The plasma level is highest at 2–6 h. Intrathecally injected ^{111}In-DTPA has a biological $t_{1/2}$ of approximately 12 h in the CSF [18].

Approximately 65% of the injected activity is excreted through urine in 24 h and 85% in 72 h.

Table 9.2 Estimated radiation absorbed dose of ^{111}In-DTPA

Organ	*mGy/MBq*	*rad/mCi*
Spinal cord	0.95	3.515
Red marrow	0.24	0.888
Bladder wall	0.20	0.740
Uterus	0.044	0.163
Ovaries	0.039	0.144
Testes	0.011	0.040

USES

^{111}In-DTPA is used in the determination of normal-pressure hydrocephalus, CSF leaks and shunts.

DOSIMETRY

The data are obtained from [19] and listed in Table 9.2.

INDIUM-111 OXINE- OR TROPOLONE-LABELED LEUKOCYTES AND PLATELETS

Chemistry

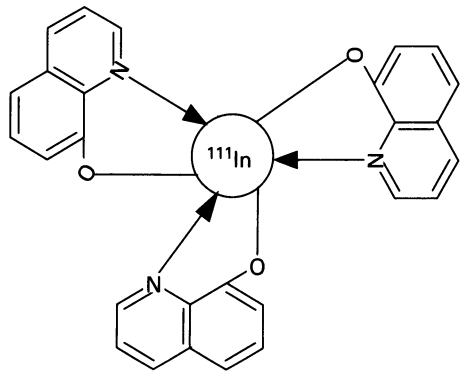

Indium-111 oxine

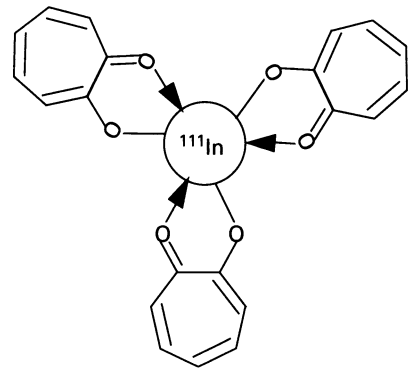

Indium-111 tropolone

8-Hydroxyquinoline (oxine) and 2-hydroxy-2, 4, 6-cycloheptatrien-1-one (tropolone) forms a 3:1 complex with the trivalent $^{111}In^{3+}$ ion [20, 21]. The complex is neutral and lipophilic and therefore penetrates through the cell membrane into the cells. It dissociates intracellularly and the ^{111}In binds to nuclear and cytoplasmic proteins [20, 22]. Aqueous solutions of both ^{111}In-oxine and ^{111}In-tropolone are available commercially, however they can be prepared in the radiopharmacy.

Preparation of ^{111}In-oxine

Dissolve 1 mg of oxine sulfate in 10 ml of distilled water. Pass 0.5 ml through a millipore filter (0.22 μm) into an empty syringe and cap the syringe. Add 0.5 ml of 0.03 M HCl containing 37 MBq (1 mCi) of $^{111}InCl_3$ to the oxine solution in the syringe.

Preparation of ^{111}In-tropolone

Dissolve 1 mg of tropolone in 1 ml of sterile isotonic HEPES saline buffer [20 mM HEPES in 0.8% (w/v) saline, adjust to pH 7.4 with 1 M NaOH]. Add 50–100 μl of 0.03 N HCl containing 18.5–37 MBq (0.5–1 mCi) of $^{111}InCl_3$ to 50 μl of tropolone solution in a sterile Vacutainer tube, mix and add to the cell suspension. Note the following:

- Do not use a metallic needle to transfer $^{111}InCl_3$ because the metal ion might form complex(es) with oxine.
- ^{111}In complex(es) adhere to glass materials, therefore avoid the use of glassware.

Separation and labeling of leukocytes and platelets with ^{111}In-oxine or ^{111}In-tropolone

None of the procedures in current use for labeling white blood cells or platelets is carried out either *in vivo* or in whole blood. As yet no radiopharmaceutical can selectively label a particular cell type in whole blood. Hence, separation is required prior to labeling. It is important that the separation technique does not change the morphology and viability of the cells. The separation procedure must be carried out in a clean room and in a laminar flow hood.

Leukocytes

Mix 35–40 ml of blood, 5 ml of acid citrate dextrose (ACD) and 7 ml of 6% hydroxyethylstarch in a syringe.

With the needle pointing up and 1–2 ml of air space above the blood level allow the red blood cells to settle for 45 min.

Expel leukocyte-rich plasma (LRP) into a sterile centrifuge tube.

Centrifuge the LRP at 450 *g* for 5 min. Aspirate leukocyte-poor plasma (LPP) and preserve

^{111}In-oxine labeling	^{111}In-tropolone labeling
Gently suspend the cell button in 10 ml of preservative-free saline and centrifuge for 4 mins at 180 *g*	Centrifuge the LPP (650 *g*, 10 min) and add 1 ml of cell-free supernatant to the leukocyte button and gently mix until no clumps are seen
Aspirate the supernatant and resuspend the cells gently in 5 ml of saline until no clumps are seen	Add ^{111}In-tropolone containing 37 MBq (1 mCi) to the cells, mix and incubate at 37°C for 15 min
Add ^{111}In-oxine containing 37 MBq (1 mCi) dropwise to the cells, mix and incubate at 37°C for 15 min	Add 5 ml of cell free ACD plasma

Note that with ^{111}In tropolone, cells are labeled in plasma.

Platelets

Mix 20–25 ml of blood and 5.0 ml of ACD in a conical tube. Centrifuge at 200 *g* for 10 min. Aspirate platelet-rich plasma into a 15-ml tube (avoid red blood cell contamination)

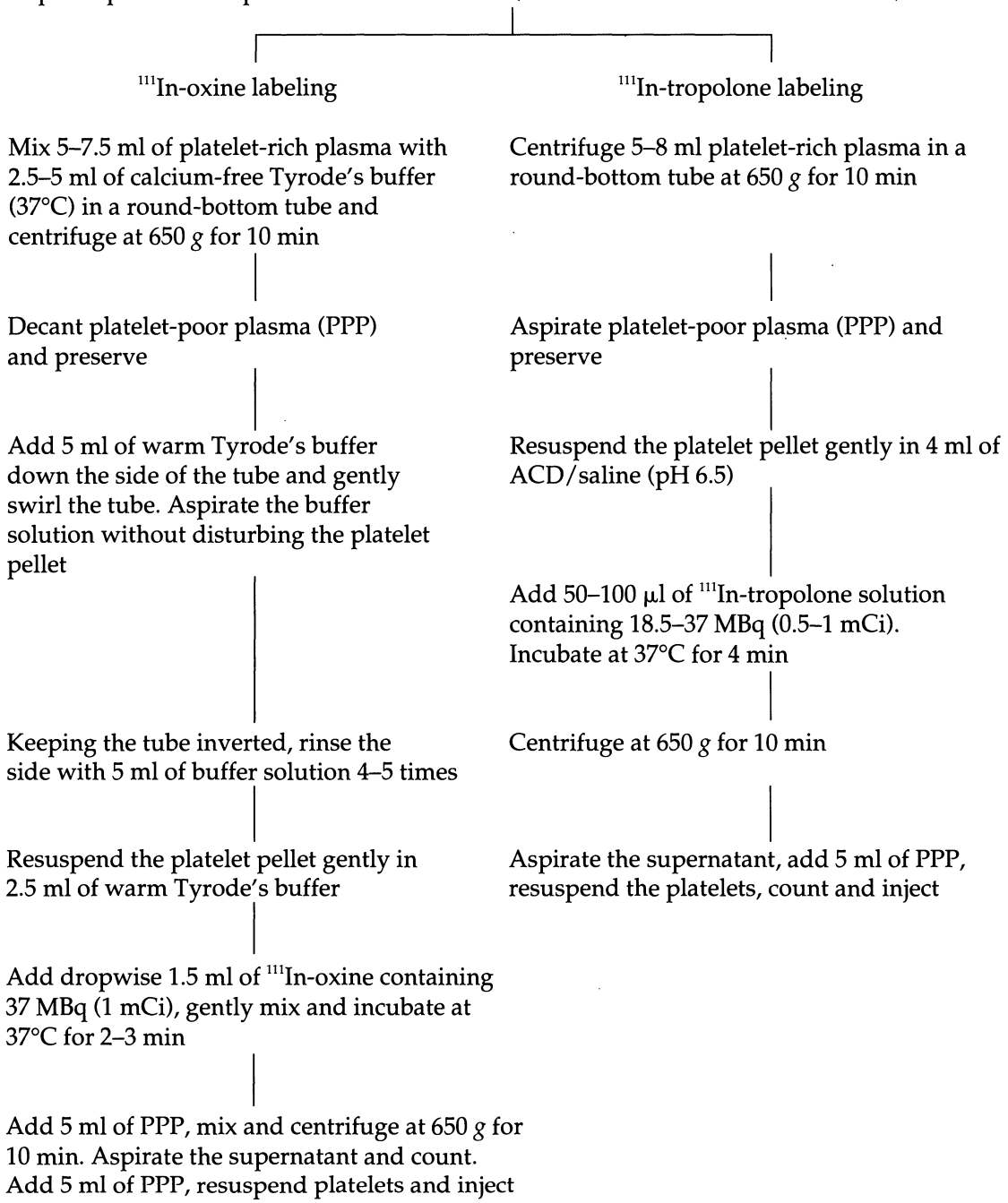

Note that with ^{111}I tropolone platelets are also labeled in plasma.

QUALITY CONTROL

Leukocytes

It is important to determine the labeling efficiency prior to injection.

- Remove 0.2 ml of labeled leukocytes into a tube, add 0.8 ml of saline and centrifuge at 150 *g* for 4 min.
- Aspirate supernatant and separately assay the activity in the cell pellet and supernatant. Calculate the labeling efficiency as follows:

$$\text{Labeling efficiency (\%)} = \frac{\text{Activity in the cell pellet}}{\text{Activity (cell pellet + supernatant)}} \times 100$$

- If the labeling efficiency is higher than 90%, inject. If it is lower than 90%, centrifuge at 150 *g* for 4 min, remove the supernatant, resuspend the pellet in 5 ml of cell-poor plasma and inject.

Platelets

Separately assay the radioactivity in supernatant and platelet suspension. Calculate the percentage labeling efficiency as follows:

$$\text{Labeling efficiency (\%)} = \frac{\text{Activity in cell suspension}}{\text{Activity (cells + supernatant)}}$$

DOSES

Leukocytes

Infection	18.5–37 MBq (0.5–1 mCi)
Leukocyte survival	3.7 MBq (100 μCi)

Platelets

Thrombus and renal transplant	11.1–18.5 MBq (300–500 μCi)
Platelet survival	1.85–3.7 MBq (50–100 μCi)

INJECTION TO IMAGING TIME

Infection	3–24 h
Thrombus	2–6, 24 h
Renal transplant	5–7 days

BIOLOGIC BEHAVIOR

Leukocytes

After intravenous injection, ^{111}In-oxine or ^{111}In-tropolone leukocytes accumulate in area(s) of inflammation depending on the extent of the inflammatory activity. Visualization of the inflammation may be seen within 40 min and 4 h with ^{111}In-tropolone and ^{111}In-oxine leukocytes respectively [23, 24].

Initially the injected ^{111}In-oxine leukocytes accumulate in the lungs. Approximately 25–50% of the radioactivity is cleared within 15 min and is distributed in the liver, spleen and bone marrow [23]. However, with ^{111}In-tropolone leukocytes only circulating activity is seen in the lungs, and this is cleared within 5 min. The ^{111}In-tropolone leukocytes show lower accumulation of radioactivity in liver and spleen [24].

^{111}In-oxine leukocytes (free from red blood cells) and ^{111}In-tropolone leukocytes are cleared from blood circulation with half-lives of 7.5 and 9 ± 2.5 h respectively [23]. The clearance of radioactivity is influenced by the cell viability and red cell contamination. Leukocytes labeled with ^{111}In-oxine or ^{111}In-tropolone are very stable *in vivo* and show more than 90% of the activity associated with leukocytes for up to 22 h [21, 24, 25].

Less than 0.05% of the activity is excreted in urine within 24 h [23]. Radioactivity from

^{111}In leukocytes is secreted in human breast milk [26].

Platelets

^{111}I-oxine or ^{111}In-tropolone platelets accumulate in area(s) of thromboemboli, reaction to prosthetic devices, occluded blood vessel grafts, bacterial endocarditis and renal transplant rejection. The mechanism of accumulation is thought to be platelet adherence to the site of injured blood vessels and thrombi.

The accumulation of ^{111}In-oxine or ^{111}In-tropolone platelets in the spleen and liver is exponential, and the percentage uptake at 90 min is 30 ± 6.3 for spleen and 9.6 ± 1.2 for the liver [27]. At the end of their lifespan, the maximum accumulation of ^{111}In-oxine platelets in the spleen and liver is 35.6 ± 9.7% and 28.7 ± 8.3% respectively [28], while that of ^{111}In-tropolone platelets is 45.3 ± 6.9% and 31.3 ± 6.4% respectively [27, 29]. The disappearance of ^{111}In-oxine or ^{111}In-tropolone platelets from the circulation is linear, with a mean survival time of 230 ± 29 h and 226 ± 13 h respectively. At equilibrium *in vivo* recovery of ^{111}In-oxine and ^{111}In-tropolone platelets is approximately equal to 61 ± 12% and 58 ± 11% respectively [27].

USES

Leukocytes

- Detection of sites of infection and inflammation.
- Leukocytes survival studies.

Platelets

- Detection of thromboemboli, occluded blood vessel grafts, the reaction to various prosthetic devices and renal transplant rejection.
- Platelet survival studies.

DOSIMETRY

The data are modified from [30] and [31] and listed in Tables 9.3 and 9.4.

Table 9.3 Estimated radiation absorbed dose of ^{111}In-oxine leukocytes

Organ	*mGy/MBq*	*rad/mCi*
Spleen	5.5	20.35
Liver	0.71	2.63
Red marrow	0.69	2.55
Pancreas	0.52	1.92
Kidneys	0.33	1.22
Adrenals	0.31	1.15
GI tract		
Stomach wall	0.28	1.04
Small intestine	0.16	0.59
Upper large intestinal wall	0.16	0.59
Lower large intestinal wall	0.13	0.48
Heart	0.17	0.63
Ovaries	0.12	0.44
Uterus	0.12	0.44
Testes	0.045	0.17

Table 9.4 Estimated radiation absorbed dose of ^{111}In-oxine platelets

Organ	*mGy/MBq*	*rad/mCi*
Spleen	7.50	27.75
Liver	0.73	2.70
Pancreas	0.66	2.44
Kidneys	0.41	1.52
Heart	0.39	1.44
Adrenals	0.37	1.37
Red marrow	0.36	1.33
GI tract		
Stomach wall	0.35	1.29
Small intestine	0.14	0.52
Upper large intestinal wall	0.14	0.52
Lower large intestinal wall	0.097	0.36
Lungs	0.28	1.04
Ovaries	0.098	0.36
Uterus	0.095	0.35
Testes	0.043	0.16

THALLIUM-201 THALLOUS CHLORIDE ($^{201}TlCl$)

CHEMISTRY

Thallium is a metalic element of group IIIA. In aqueous solution it is stable and exists as a monovalent cation (Tl^+). Its ionic radius is close to that of potassium (K^+) and hence it exhibits similar biologic behavior.

PHYSICAL PROPERTIES

^{201}Tl decays by electron capture (100%) with a half-life of 73.1 h. It emits two gamma radiations, 135 keV (2%) and 167 keV (10%), and mercury X-rays, 69–83 keV (95%). The mercury X-rays are used for imaging.

PREPARATION

Thallium-201 is produced in a cyclotron by irradiating the natural thallium-203 target (29.6% isotopic abundance) with a 19–31 MeV proton beam according to the ^{203}Tl (p, 3n) ^{201}Pb reaction. The ^{201}Pb ($t_{1/2}$ 9.4 h) is purified from the ^{203}Tl target by repeated ion-exchange column chromatography and allowed to decay for 32 h to $^{201}Tl^{3+}$. $^{201}Tl^{3+}$ is passed through an ion-exchange column to remove ^{201}Pb. $^{201}Tl^{3+}$ is reduced to $^{201}Tl^+$, evaporated to dryness, reconstituted with a physiologic solution of sodium chloride and sterilized [32]. It is commercially available as an isotonic, sterile and pyrogen-free solution for intravenous administration.

QUALITY CONTROL

Normally, the manufacturer performs all the quality control tests for $^{201}Tl^+$ before shipping, however, the following tests may be performed if necessary.

Radionuclidic test

This is performed using a multichannel analyzer. The product should contain not more than 1% ^{200}Tl ($t_{1/2}$ 26.1 h), 1.9% ^{202}Tl ($t_{1/2}$ 12 days) and 0.25% ^{203}Pb ($t_{1/2}$ 52.1 hr) on the reference date.

Radiochemical test

Place a drop of the $^{201}TlCl$ preparation on a 6-cm Whatman 3MM strip at 1 cm from the lower end, develop in mixture of $Na_2HPO_4 \cdot 5H_2O$ and acetone (1:9) for up to 5 cm and air dry. Cut in the middle and assay the activity in a dose calibrator. The $^{201}Tl^+$ is at the origin while $^{203}Tl^{+3}$ migrates to the solvent front [32].

Calculate the radiochemical purity as follows :

$$\text{Radiochemical purity (\%)} = \frac{\text{Activity at origin}}{\text{Activity at (origin + solvent front)}} \times 100$$

DOSES

Myocardial perfusion imaging (exercise)	74–111 MBq (2–3 mCi)
Rest reinjection imaging	Additional 37 MBq (1 mCi)
Parathyroid imaging	74 MBq (2 mCi)
Tumor imaging	111–148 MBq (3–4 mCi)

PATIENT PREPARATION

Patients should refrain from taking long-acting beta blockers (atenalal) for 3 days, short-acting beta blockers (Inderal and Lopresser) and calcium channel blockers (Procardia) for 2 days and/or nitrates (isordil, nitropaste) for 1 day prior to the test. Fix an

intravenous line or cannula prior to exercising and inject $^{201}Tl^{+}$ 60 s before the end of exercise.

INJECTION TO IMAGING TIME

Stress (myocardium)	5 min
Delayed myocardial redistribution and/or rest myocardial reinjection	3–4 h
Parathyroid imaging	Immediately
Tumor imaging	30–60 min

BIOLOGIC BEHAVIOR

Following intravenous injection, ^{201}Tl chloride is eliminated from the blood circulation with a half-life of 2.9 min [33]. The maximum myocardial uptake of approximately 4% occurs within 10–20 mins with a myocardial clearance half-life of 4 h [34]. The myocardial uptake of $^{201}Tl^{+}$ depends on the coronary blood flow, extent of myocardial extraction and viability. $^{201}Tl^{+}$ is redistributed in ischemic but viable areas of myocardium as a result of continuous exchange between intracellular and interstitial compartments.

The mechanism of the transfer of $^{201}Tl^{+}$ from blood to myocardium is based on the Na^{+}–K^{+}-ATPase transport system. The energy required is derived from the conversion of ATP to ADP by the activation of membrane-bound, Na^{+}–K^{+}-ATPase and $^{201}Tl^{+}$, being a biologic analog of K^{+}, is transferred into the myocardial cell. Inside the cell, the concentration of $^{201}Tl^{+}$ is relatively lower than that of K^{+}, and during muscular contractions efflux of $^{201}Tl^{+}$ ion is therefore predominated by K^{+} ion. The active transport system for the transfer of $^{201}Tl^{+}$ ion is therefore a mechanism that allows the maintenance of a higher intracellular concentration of $^{201}Tl^{+}$ without biotransformation.

$^{201}Tl^{+}$ accumulates in skeletal muscles and splanchnic viscera in proportion to the regional perfusion. Normal thyroid and parathyroid adenomas also accumulate $^{201}Tl^{+}$ [35]. It has also been reported that the uptake of $^{201}Tl^{+}$ in tumors is not proportional to vascularization [36].

Approximately 20% of $^{201}Tl^{+}$ is excreted in urine within 24 h [37, 38]. Thallium-201 is secreted in human milk [39].

USES

- Detection of perfusion defects in the myocardium at rest and after stress in patients with coronary artery diseases, such as asymptomatic patients with a positive ECG or patients with atypical angina pectoris and a non-diagnostic stress ECG.
- Detection of individual artery stenosis in the myocardium.
- Evaluation of thrombolytic therapy in patients with acute myocardial perfusion defects.

Table 9.5 Estimated radiation absorbed dose of $^{201}Tl^{+}$

Organ	*mGy/MBq*	*rad/mCi*
Heart wall	0.226	0.835
Testes	0.562	2.080
Kidneys	0.537	1.99
GI tract		
Lower large intestine	0.362	1.34
Upper large intestine	0.188	0.675
Small intestine	0.162	0.60
Stomach	0.120	0.445
Bone surface	0.338	1.25
Thyroid	0.250	0.925
Liver	0.176	0.65
Red marrow	0.176	0.65
Spleen	0.138	0.51
Ovaries	0.120	0.445
Lungs	0.120	0.445
Pancreas	0.054	0.20
Adrenals	0.051	0.19
Uterus	0.050	0.185
Bladder wall	0.036	0.135
Breasts	0.027	0.100

- As a potential marker of myocardial viability in candidates for bypass surgery or coronary angioplasty.
- Localization of parathyroid adenoma.
- Detection of solitary tumors.

DOSIMETRY

The data are taken from [40] and listed in Table 9.5.

REFERENCES

1. Owunwanne, A., O'Mara, R.E., Blau, M. *et al.* (1979) Ion exchange methods for the determination of the net charge on some radiopharmaceuticals, in *Radiopharmaceuticals*, Vol. II (ed. J.A. Sorensen), The Society of Nuclear Medicine, New York, pp. 163–72.
2. Harris, W.R. and Martell, A.E. (1976) Aqueous complexes of gallium (III). *Inorg. Chem.*, **15**, 713–20.
3. Glickson, J.D., Pitner, T.P., Webb, J. *et al.* (1975) Hydrogen-1 and gallium-71 nuclear magnetic resonance study of gallium citrate in aqueous solution. *J. Am. Chem. Soc.*, **97**, 1679–83.
4. Dahl, J.R. and Tilbury, R.S. (1972) The use of compact, multi-particle cyclotron for the production of ^{52}Fe, ^{67}Ga, ^{111}In and ^{123}I for medical purposes. *Int. J. Appl. Radiat. Iso.*, **23**, 431–37.
5. Frier, M. and Hesslewood, S.R. (1980) Quality assurance of radiopharmaceuticals. A guide to hospital practice. *Nucl. Med. Commun.*, **1**, 29–.
6. Stephton, R.G. and Harris, W. (1974) Gallium-67 uptake by cultured tumor cells, stimulated by transferrin. *J. Natl Cancer Inst.*, **54**, 1263–66.
7. Harris, A.W. and Stephton, R.G. (1977) Transferrin promotion of ^{67}Ga and ^{59}Fe uptake by cultured mouse myeloma cells. *Cancer Res.*, **37**, 3634–38.
8. Hoffer, P.B., Huberty, J.P. and Khayam Bashi, H. (1977) The association of ^{67}Ga and lactoferrin, *J. Nucl. Med.*, **18**, 713–17.
9. Terner, U.K., Wong, H., Noujaim, A. *et al.* (1979) Differential uptake of ^{67}Ga in cannine tumors and abscesses, in *Radiopharmaceuticals* Vol. II (ed. J.A. Sorensen), The Society of Nuclear Medicine, New York, pp. 309–19.
10. Nelson, B., Hayes, R.L., Edwards, C.L. *et al.* (1972) Distribution of gallium in human tissues after intravenous administration. *J. Nucl. Med.*, **13**, 92–100.
11. Cloutier, R.J, Watson, E.E., Hayes, R.L. *et al.* (1971) Radiation doses from isotopes of gallium (abstract). *J. Nucl. Med.*, **12**, 348.
12. Watson, E.E. (1992) Radiation dose estimates for the fetus from intakes of gallium citrate by the mother. *Radiat. Prot. Dos.*, **41**, 123–26.
13. Hartman, R.E. and Hayes, R.L. (1969) The binding of gallium by blood serum. *J. Pharmacol. Exp. Ther.*, **168**, 193–98.
14. Edwards, C.L., Hayes, R.L., Nelson, B.M. *et al.* (1970) Clinical investigation of ^{67}Ga for tumor scanning. *J. Nucl. Med.*, **11**, 316–17.
15. Rubon, S.M., Klopper, J. and Scholtz, P. (1991) Excretion of gallium-67 in human breast and its inadvertent ingestion by a 9 month old child. *Eur. J. Nucl. Med.*, **18**, 829–33.
16. Cloutier, R.J., Watson, E.E., Hayes, R.L. *et al.* (1973) Summary of current radiation dose estimates to humans from ^{66}Ga, ^{67}Ga, ^{68}Ga and ^{72}Ga-citrate. MIRD dose estimate report no. 2. *J. Nucl. Med.*, **14**, 755–56.
17. Product Information (1992) Indium [^{111}In] chloride. Amersham International, UK.
18. Goodwin, D.A., Song, C.H., Finston, R. and Matin, P. (1973) Preparation, physiology and dosimetry of ^{111}In-labeled radiopharmaceuticals for cisternography. *Radiology*, **108**, 91–8.
19. ICRP Publication 53 (1990) *Radiation Dose to Patients from Radiopharmaceuticals*, Pergamon Press, Oxford, pp. 237–38.
20. Thakur, M.L., Coleman, R.E. and Welch, M.J. (1977) Indium-111-labeled leukocytes for the localization of abscesses: preparation, analysis, tissue distribution, and comparison with gallium-67 citrate in dogs. *J. Lab. Clin. Med.*, **89**, 217–28.
21. Dewanjee, M.K., Rao, S.A. and Didisheim, P. (1981) Indium-111-tropolone, a new high affinity label. Preparation and evaluation of labeling parameters. *J. Nucl. Med.*, **22**, 981–87.
22. Thakur, M.L., Segal, A.W., Louis, L. *et al.* (1977) Indium-111 labeled cellular blood components: mechanism of labeling and intracellular location in human neutrophils. *J. Nucl. Med.*, **18**, 1020–24.

23. Thakur, M.L., Lavender, J.P., Rosemary, N. *et al.* (1977) Indium-111 labeled autologus leukocytes in man. *J. Nucl. Med.*, **18**, 1014–19.
24. Peters, A.M., Sethna, H.S., Reavy, H.J. *et al.* (1983) Imaging of inflammation with ^{111}In-tropolone labeled leukocytes. *J. Nucl. Med.*, **24**, 29–44.
25. Danpure, H.J. and Osman, S. (1988) Optimum conditions for radiolabeling human granulocytes and mixed leucocytes with ^{111}In-tropolonate. *Eur. J. Nucl. Med.*, **13**, 537–42.
26. Mountford, P.J. and Coakley, A.J. (1985) Excretion of radioactivity in breast milk after an In-111 leucocyte scan (letter). *J. Nucl. Med.*, **26**, 1096–97.
27. Kotze, H., Heys, A.P., Lotter, M.G. *et al.* (1991) Comparison of oxine and tropolone methods for labeling human platelets with Indium-111. *J. Nucl. Med.*, **32**, 62–6.
28. Wessels, P., Heyns, A., Pieters, H. *et al.* (1985) An improved method of the in vivo kinetics of a representative population of ^{111}In-labeled platelets. *Eur. J. Nucl. Med.*, **10**, 522–27.
29. International Committee for Standardisation in Hematology (1988) Panel report on diagnostic applications of radionuclides. Recommended method for In-111-platelet survival studies. *J. Nucl. Med.*, **29**, 564–66.
30. ICRP Publication 53 (1990) *Radiation dose to patients from radiopharmaceuticals*, Pergamon Press, Oxford, pp. 255–56.
31. IRCP Publication 53 (1990) *Radiation dose to patients from radiopharmaceuticals*, Pergamon Press, Oxford, pp. 253–54.
32. Lebowitz, E., Greene, M.W., Fairchild, R. *et al.* (1975) Thallium-201 for medical use. Part 1. *J. Nucl. Med.*, **16**, 151–55.
33. Grunwald, A.M., Watson, D.D., Holzgrefe, H.H. *et al.* (1981) Myocardial thallium-201 kinetics in normal and ischemic myocardium. *Circulation*, **64**, 610–18.
34. Bradley-Moore, P.R., Lebowitz, E., Greene, M.W. *et al.* (1975) Thallium-201 for medical use. II. Biological behaviour. *J. Nucl. Med.*, **16**, 156–60.
35. Miller, D.L., Doppman, J.L., Shawker, T.H. *et al.* (1987) Localisation of parathyroid adenomas in patients who have undergone surgery. I. Non-invasive imaging methods. *Radiology*, **162**, 133–37.
36. Sahweil, A.M., McKillop, J.M., Milroy, R., Abdel-Dayem, H.M. (1988) Mechanism of Tl-201 uptake in tumours (abstract). *J. Nucl. Med.*, **29**, 750.
37. Atkins, H.L., Budinger, T.F., Lebowitz, E. *et al.* (1977) Thallium-201 for medical use. Part 3: Human distribution and physical imaging properties. *J. Nucl. Med.*, **18**, 133–40.
38. Bartlet, R.D., Lathrop, K.A., Faulhaber, P.F. and Harper, P.V. (1984) Transfer of thallous ion to and from gastrointestinal sections. (abstract) *J. Nucl. Med.*, **25**, P92.
39. Murphy, P.H., Beasley, C.W., Moore, W.H. and Stabin, M.G. (1988) Tl-201 in human milk (abstract). *J. Nucl. Med.*, **29**, 278.
40. Brian, H., Smith, F.W., Smith, T. *et al.* (1993) ^{99m}Tc-1, 2-bis [bis (2-ethoxyethyl) phosphino] ethane: human biodistribution, dosimetry and safety of a new myocardial perfusion imaging agent. *J. Nucl. Med.*, **34**, 30–8.

10

Group VIA radiopharmaceuticals

The elements of group VIA which have useful radionuclides for nuclear medicine studies are oxygen, selenium and tellurium. They have two electrons in their outermost shells and in general form covalent bonds. The useful radionuclides are oxygen-15, selenium-75 and tellurium-123m. The radiopharmaceuticals of oxygen-15 are described in Chapter 14 (positron emitters); selenium-75 taura-23-selena-25-homocholic acid (^{75}Se-HCAT) is described in Chapter 15 (non-imaging). There are no available radiopharmaceuticals containing tellurium-123m. Selenium-75 *l*-selenomethionine was evaluated for pancreas imaging but because of high background radioactivity it is seldom used. Only selenium-75 selenomethyl norcholesterol is described in this chapter.

SELENIUM-75 6-METHYL-SELENOMETHYL-19-NORCHOLEST-5-(10)-EN-3β-OL (^{75}Se-SELENOMETHYL NORCHOLESTEROL)

CHEMISTRY

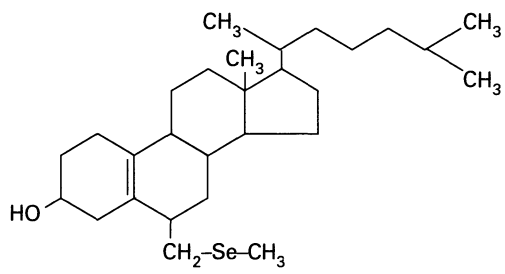

Selenomethyl norcholesterol is a derivative of norcholesterol which differs from cholesterol in not having a methyl group at the C-10 position. Cholesterol is an unsaturated alcohol containing a steroid nucleus with four condensed rings and an eight-carbon side-chain. There are eight asymmetric centers, and therefore it has 256 possible stereoisomers, but only one of these occurs naturally. Cholesterol, either free or in the form of esters, is synthesized in the body and stored for energy requirements later.

PHYSICAL PROPERTIES OF ^{75}Se

Selenium-75 decays by 100% electron capture to stable arsenic with a half-life of 120.4 days. It has several gamma emissions, of which 121 (17%), 136 (57%), 265 (60%) and 280 keV (25%) are important for imaging.

PREPARATION

^{75}Se-selenomethyl norcholesterol is commercially available. Briefly, ^{75}Se-selenomethyl norcholesterol is synthesized by the displacement of the halide of 6-halomethyl-19-norcholest-5 (10)-en-β-ol with the methyl selenide anion. The methyl selenide anion is produced by a series of reactions involving reduction of selenium-75 metal with sodium borohydride to form sodium hydrogen selenide, which upon addition of one equivalent of ^{75}Se metal produces sodium diselenide; the latter is alkylated with methyliodide followed by reduction with sodium borohydride[1].

QUALITY CONTROL

Quality control tests are performed by the manufacturer prior to shipping.

DOSE

0.74–1.11 MBq (200–300 μCi).

INJECTION TO IMAGING TIME

2–4 days and if necessary repeat at 6–10 days.

PATIENT PREPARATION

Patients may be injected with 2–4 mg/day dexamethasone 2 days prior to administration of ^{75}Se-selenomethyl norcholesterol and continued until the termination of the study.

BIOLOGIC BEHAVIOR

Two days after intravenous injection of ^{75}Se-selenomethyl norcholesterol, the highest concentration is in the adrenal cortex, liver, intestines and blood [2]. The highest adrenal uptake in normal subjects is 0.19–0.3% of the administered dose. Increased uptake of the order of 0.3–8.5% is observed in patients with cortisol- and aldosterone-secreting adenomas or adrenal hyperplasia [2, 3]. The estimated effective half-life in the adrenals is within the range of 25–105 days [3].

At 24 h after injection, approximately 70% of the injected activity is cleared from the circulation. The clearance of the remaining 30% has three components with half-lives of 1.8 (18%), 6.3 (11%) and 72 days (1%) [3]. The radioactivity in blood is evenly distributed between the red blood cells and plasma [3].

Total body elimination has two components with half-lives of 13.7 (57%) and 153 days (43%) [3]. The major pathway of clearance is through the hepatobiliary system.

USES

^{75}Se-selenomethyl norcholesterol is used in the diagnosis of adrenocortical malfunction, such as aldosteronism, adrenal hyperplasia and Cushing's syndrome.

Table 10.1 Estimated radiation absorbed dose of ^{75}Se-selenomethyl norcholesterol

Organ	*mGy/MBq*	*rad/mCi*
Adrenals	5.1	18.87
Liver	2.0	7.40
Pancreas	1.8	6.66
GI tract		
Small intestine	1.8	6.66
Upper large intestine	1.7	6.29
Lower large intestine	1.6	5.92
Stomach	1.6	5.92
Red marrow	1.8	6.66
Uterus	1.8	6.66
Kidneys	1.6	5.92
Bladder wall	1.6	5.92
Ovaries	1.6	5.92
Bone surfaces	1.6	5.92
Lungs	1.4	5.18
Testes	1.2	4.44
Thyroid	1.1	4.07

DOSIMETRY

The data are taken from [4] and listed in Table 10.1

REFERENCES

1. Riley, A.L.M. (1978) The development of selenium-75 cholesterol analogues. *J. Labelled Compounds Radiopharm.*, **16**, 28–30.
2. Shapiro, B., Britton, K.E., Hawkins, L.A. and Edwards, C.R.W. (1981) Clinical experience with ^{75}Se-selenomethylcholeserol adrenal imaging. *Clin. Endocrinol.*, **15**, 19–27.
3. Hawkins, L.A., Britton, K.E. and Shapiro, B. (1980) Selenium 75 selenomethyl cholesterol: a new agent for quantitative functional scintigraphy of the adrenals: physical aspects. *Br. J. Radiol.*, **53**, 883–89.
4. ICRP Publication 53 (1990) *Radiation Dose to Patients from Radiopharmaceuticals*, Pergamon Press, Oxford, pp. 151–52.

11

Antibodies

INTRODUCTION

Antibodies (Abs) are immunoglobulin (Ig) molecules that are formed in response to the presence of foreign substances (antigen, Ag) in the blood. The antibodies have binding sites that recognize the Ag(s) and bind specifically with them. There are five classes of immunoglobulins: gamma, IgG; mu, IgM; alpha, IgA; delta, IgD; and epsilon, IgE [1]. The antibodies have 'variable' and 'constant' regions of light and heavy chains. The variable region (Fab) contains amino-terminal portions responsible for the antibody's specificity (the specific binding sites for the antigens). The constant region (Fc) controls the binding of complement, the transport of the antibody molecule across membranes and the binding of antibody to membranes (non-specific binding). The Fab and Fc fragments of an IgG molecule are obtained by enzymatic cleavage using papain, while the Fab' fragment is obtained using pepsin, as shown in Figure 11.1.

The intact IgG and the fragments [Fab, $F(ab)_2$ and Fab'] have been labeled with radionuclides and evaluated for either imaging or therapy [2–11]. Various factors influence the efficacious use of the radioactive antibodies, and these include the reactivity of the antibody, the radionuclide, the radiochemical labeling process and the integrity of the radioactive antibody.

THE REACTIVITY OF THE ANTIBODY

- The antibody should be of high purity and have high binding affinity for the antigen [12–14]. However, it has been shown that some antibodies with lower binding affinity may penetrate the tumor bed better, because of reduced binding to circulating or extracellular antigen [15, 16].
- The presence and amount of cellular antigen on the lesions influence the extent of the binding of the antibody to the antigen. Lesions with large quantities of antigens, such as myocardial infarcts and rejection [17], thrombus [18, 19] and focal sites of infarction [20–22], are easier to image than tumors, which have low quantities of surface antigens [23].
- The shed antigens in circulation may react with antibodies, thereby making less antibody available to react with surface antigens. A second antibody (known as the anti-antibody technique) has been used to enhance clearance of non-tumor-bound antibody [24].
- The nature and size of the antibody influences its pharmacokinetics and distribution. Polyclonal antibody is less specific than monoclonal antibody, while the fragments [Fab, monovalent; $F(ab)_2$, divalent] have been shown to penetrate further into the tumor than the intact antibody. The

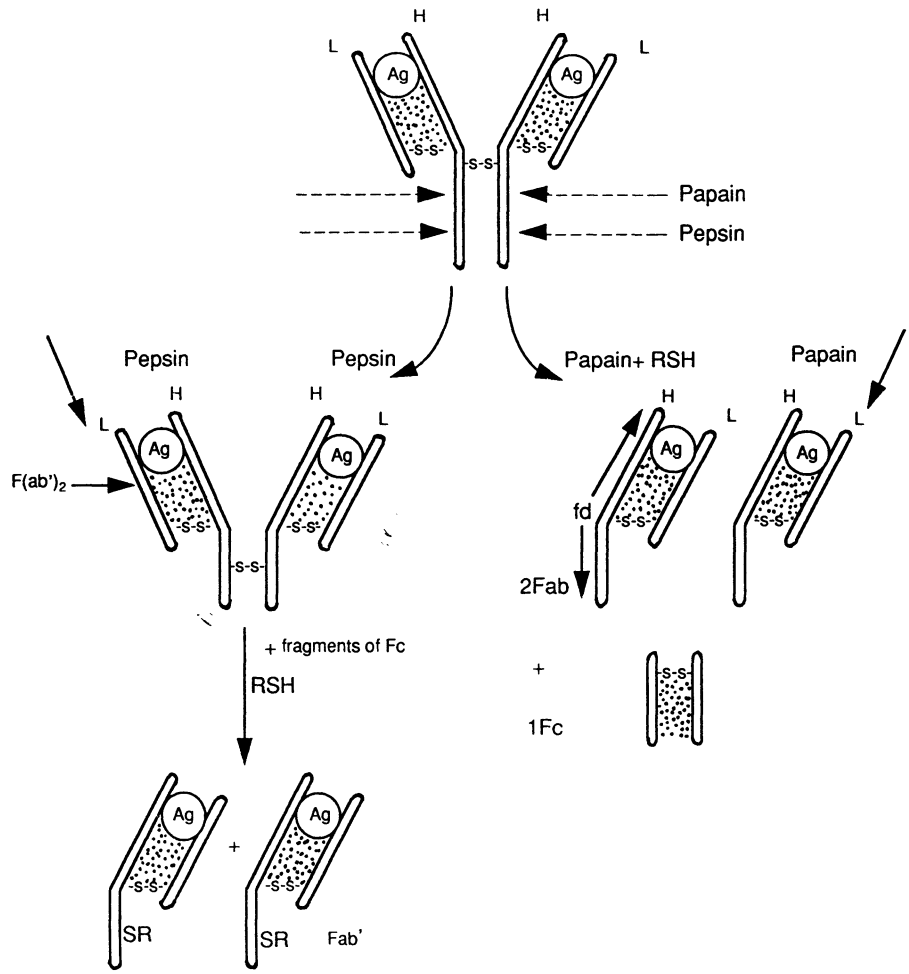

Figure 11.1 Enzymatic cleavage of IgG molecule using pepsin and papain. H and L are heavy and light chains respectively and RSH is alkylthiol.

fragments also have much faster blood clearance and greater specific tumor uptake than the corresponding intact antibody [8, 25–30].

- Even monoclonal antibodies are not as specific as they were once thought to be because of cross-reaction with antigens. Normal tissues have been shown to sometimes bind tumor-specific antibodies [31]. Anticarcinoembryonic antigen (CEA) has been used to detect not only colorectal cancer but also other types of tumor [14]. Apparently cross-reactivity of antibody–antigen can be gainfully used to detect or image cancer.

THE RADIONUCLIDE SELECTION

The radionuclide to be used for labeling the antibody, in addition to possessing the appropriate radionuclide properties (for imaging or therapy) as previously described, should also

match the pharmacokinetics of the antibody [8]. Thus, radionuclides (^{99m}Tc and ^{123}I) with short half-lives are best suited for labeling antibody fragments with faster blood clearance, while ^{111}In and ^{131}I, with comparatively longer half-lives may be better for labeling intact antibodies. Technetium-99m with a half-life of 6 h is better for Fab and Fab', while ^{123}I with a half-life of 13 h is better for F(ab)$_2$ [8, 32–34]. The combination of short physical half-life and faster blood clearance allows imaging to be done as early as 4–6 h (^{99m}Tc) and 24 h (^{123}I) after injection using ^{99m}Tc-Fab' and ^{123}I-F(ab)$_2$ of the same antibody. The short half-life also allows the administration of a high dose of radioactivity [740–1110 MBq (20–30 mCi)] at a reduced radiation dose to the patient. It has been estimated that the radiation dose from ^{99m}Tc-F(ab)$_2$ is 0.033 of that from ^{111}In-F(ab)$_2$ of the same monoclonal antibody [8].

THE RADIOCHEMICAL LABELING PROCESS

- The labeling procedure should not alter the immunoreactivity of the antibody [12, 35–37]. A low-immunoreactive antibody preparation decreases both blood and nontumor clearance, but increases the clearance of the labeled antibody from the tumor, thereby lowering the target to nontarget ratio [12].
- The final step of the labeling process should be simple enough that it can be performed in the hospital, and the preparation should not need any purification prior to administration. The radioactive antibody should be of high specific activity to minimize the quantity of the nonradioactive components to be injected.
- There are two basic techniques for attaching radionuclide to antibodies: radioiodination and coupling of radioactive metal either directly or indirectly through a ligand popularly known as a bifunctional chelate.

THE INTEGRITY OF THE RADIOACTIVE ANTIBODY

The radiolabeled antibody should maintain its immunogenicity and be stable both *in vitro* and *in vivo*. Unstable radioactive antibody leads to a poor-quality image or diminished radiotherapeutic value. It can also increase or decrease the radiation exposure to the patient depending on whether or not the breakdown component carrying the radionuclide binds to plasma/cellular protein or is excreted in urine through the kidneys.

TYPES OF RADIOACTIVE ANTIBODIES

There are four major radionuclides used for labeling antibodies: iodine-123/131, indium-111 and technetium-99m.

IODINE-123/131 ANTIBODIES

Iodine-123/131 antibodies can be used for imaging, while ^{131}I can also be used for therapy. There are two procedures for incorporating radioactive iodine into antibodies.

1. Direct substitution of radioactive iodine into an activated ortho position of the aromatic ring, mostly tyrosine.
2. Conjugation of a radioiodinated organic molecule to the side-chain functional group of the antibody.

Direct substitution

This method involves the use of mild oxidizing agents in order to maintain the immunoreactivity of the antibody. Chloramine-T [38, 39], tetrachlorodiphenylglycouril (iodogen) [40–42] and hydrogen peroxidases (lactoperoxidase) [43–44] have been used as mild oxidizing agents to radioiodinate antibodies. The major problems associated with the use of the direct substitution technique are as follows:

- The inaccessibility of the tyrosyl residue may require 'unfolding' of the protein. This unfolding process could damage the structural integrity of the protein to the reaction medium [45].
- The *in vivo* deiodination of the antibody might result in a release of iodide ion, which accumulates in the thyroid and stomach or remains in circulation [46–48].

Radioiodinated antibodies are not used commonly for imaging. Upon intravenous injection, they may dehalogenate, releasing radioactive iodide into the circulation, which increases the radioactivity in thyroid, stomach and urinary bladder. However, research activity into the possibility of labeling antibodies with ^{131}I for therapy is increasing.

Conjugation method

In this method, two steps are involved: a small organic molecule is radioiodinated using the direct substitution method and conjugated to the antibody. Radioiodinated *N*-hydroxysuccinimide ester [49], the *N*-hydroxysuccinimide ester derivative of orthoiodohippurates [50] and succinimidyl para-iodobenzoate [51] have been developed and evaluated for covalent bonding with antibodies. This conjugation technique is amenable to kit formulation. The limitations of the conjugation method include the following:

- The probable *in vivo* breakdown of the conjugated antibody with the radionuclide attached to the organic molecule. Depending on the biologic behavior of the radioiodinated organic molecule, it might stay in circulation, be bound intracellularly or excreted in urine through the kidneys. It is because of this metabolic problem that ortho-iodohippurate is preferred as the conjugate because it is rapidly excreted in urine.
- The synthesis and purification of the radioactive conjugate might be cumbersome.
- The radiochemical yield is generally low compared with the direct radioiodination method.

INDIUM-111 ANTIBODIES (^{111}In–AB)

Indium-111 antibodies can be formed by either directly or indirectly reacting In^{3+} ion with the appropriate antibody (poly- or monoclonal). In the direct reaction, a weak In–Ab complex is formed. When injected it dissociates *in vivo*, releasing the radioactive ^{111}In, which binds to plasma proteins such as transferrin. In the indirect method, the antibody is conjugated to ^{111}In through a ligand. Such a ligand is generally referred to as a bifunctional chelate in which there is a strong metal-binding group at one end and a reactive functional group that can bind to protein at the other end. Several bifunctional chelates have been synthesized and evaluated [45, 52–58], but the most commonly used ones include aminopolycarboxylates of DTPA [the mixed anhydrides (MAs) or the cyclic anhydrides (CAs)] and the isothiocyanates [45, 52, 58]. The synthesis of DTPA carboxycarbonic mixed anhydrides requires several steps; in addition, the yield is low and the DTPA–MA conjugate is unstable and therefore cannot be isolated in sufficient amount for molecular characterization [45]. On the other hand, the CAs are simple to synthesize [59] and can be isolated, purified and characterized. The coupling of the bifunctional chelating agent is presumed to occur through the amino groups of the lysine residues of the antibody. With both the MAs and CAs, one carboxyl group of DTPA binds covalently to the antibody, while the other four groups are 'reserved' for binding to In^{+3} [45]. This bond has been shown to be weak, and radioactive ^{111}In dissociates relatively faster than ^{111}In bound to DTPA alone. To overcome this problem, the isothiocyanates were developed; in these the five carboxyl groups are free for binding to $^{111}In^{3+}$ ion, while the thiocarbamoyl group

binds to amino groups of the antibody [45, 52–56]. In this way, ^{111}In is strongly bound to the DTPA and consequently to the derivatized protein, thereby making the ^{111}In-DTPA-thiocyanate-Ab more stable *in vivo* [57]. The derivatized antibody is purified by dialysis or column chromatography to remove unreacted DTPA [45, 58]. This antibody derivatization procedure is amenable to kit formulation and requires only the addition of $^{111}In^{3+}$ ion (in acidic solution) as the final step.

The following parameters are important for the optimization of the radiochemical conjugation of the $^{111}In^{3+}$ ion to DTPA-derivatized antibody:

- the mole ratio of the DTPA linker to the antibody;
- the metabolism of the indium chelates with the possibility of *in vivo* transchelation and cross-linkage;
- the blood clearance rate of the ^{111}In-linker–Ab complex;
- the immunoreactivity of the ^{111}In-linker–Ab complex;

The major disadvantage of the ^{111}In-linker–Ab complexes is the high concentration of radioactivity in the liver, spleen, bone marrow and intestine, while the major advantages include the possibility of kit formulation and reasonably long physical half-life of ^{111}In.

The following indium-111-labeled antibodies are described in detail: antimyosin, anticarcinoembryonic antigen and antitumor-associated glycoprotein.

INDIUM-111 ANTIMYOSIN (^{111}In-AM)

^{111}In-AM is one of the few radioactive antibodies approved for routine clinical practice. It binds to extracellularly exposed myosin. Myosin is a globulin protein that is most abundant in the muscle and occurs mostly in the A band. It is soluble in salt solution, but on standing for a long time coagulates into an insoluble protein called myosin fibrin. With actin, it is responsible for the contraction and relaxation of muscle. It exhibits enzymatic properties and acts as a hydrolyzing ATPase. It is the main constituent of the thick filaments of muscle fibers.

Several bifunctional chelates have been evaluated for labeling intact and or fragmented antimyosin with ^{111}In [56, 60]. Commercially available AM contains mixed anhydride of DTPA and mouse monoclonal antibody [60].

PREPARATION

Non-radioactive reagents for the preparation of ^{111}In-AM are supplied in two vials as follows:

- vial 1: 0.5 mg of R11D10-Fab-DTPA in 1 ml of 10 mM phosphate buffer, 145 mM sodium chloride, 10% maltose (pH 6.5);
- vial 2: 1.0 ml of 0.2 M citrate (pH 5.0).

Add 1 ml of vial 1 content to vial 2, invert and mix several times; add a solution of $^{111}InCl_3$ (pH 2.5) containing 74 MBq (2 mCi) and mix several times. Allow to stand for 10 min before use. The preparation is stable for up to 8 h [61].

DOSE

55.5–74 MBq (1.5–2 mCi).

INJECTION TO IMAGING TIME

8–48 h.

BIOLOGIC BEHAVIOR

^{111}In-antimyosin accumulates in regions of infarcted myocardium [60, 62], damaged skeletal muscle [63, 64], rejected heart transplants [17, 65] and acute myocarditis [66]. The uptake is due to the binding of ^{111}In-antimyosin to intracellular myosin that is exposed to extracellularfluid as a result of the loss of the cell

Table 11.1 Estimated radiation absorbed dose of ^{111}In-AM

Organ	*mGy/Bq*	*rad/mCi*
Heart	0.086	0.320
Kidney	0.196	0.724
Liver	0.045	0.167
Ovaries	0.044	0.165
Spleen	0.008	0.031
Lung	0.006	0.022
Intestine	0.004	0.016
Muscle	0.0003	0.001
Total body	0.037	0.137

membrane integrity. In infarcted myocardium the extent of binding is inversely exponentially related to regional myocardial bloodflow as determined by the microsphere technique [62] and early ^{201}Tl distribution [67]. ^{111}In-antimyosin binds maximally to freshly infarcted myocardium [68] or damaged skeletal muscle [63] but binding decreases in intensity with healing or age. ^{111}In-AM blood clearance is very slow, hence imaging is done 8–48 h after injection. It is excreted through the liver and kidney.

USES

^{111}In-AM is used in the diagnosis of acute myocardial infarction, heart transplant rejection, acute myocarditis and adriamycin toxicity.

DOSIMETRY

The data are modified from [61] and listed in Table 11.1.

INDIUM-111 ANTICARCINOEMBRYONIC ANTIGEN (^{111}In-ANTI-CEA)

Indium-111 anti-CEA is being evaluated for imaging patients with various types of tumors, including tumors of colon, rectum, breast, ovary and lung. ^{111}In-anti-CEA binds to CEA, an oncofetal antigen. CEA is a glycoprotein with a high molecular weight (180 000) and is probably the most studied tumor antigen found in many neoplasms of epithelial origin [69]. Using various bifunctional chelates of DTPA, ^{111}In has been linked to intact anti-CEA, the Fab and F(ab)$_2$ fragments [70, 71]. Many different preparations of anti-CEA have been produced: anti-CEA 17-1A, 19-9, 791T/36, PR1A3, NR-LU-10 and BW431/31 [8, 72–74]. None of these preparations has yet been approved for routine clinical use. The cyclic dianhydride-DTPA-derivatized murine F(ab)$_2$ has been developed commercially into a freeze-dried kit.

PREPARATION

For anti-CEA F(ab)$_2$BW431/31, add $^{111}InCl_3$ in acidic solution containing up to 148 MBq (4 mCi) to the freeze-dried antibody conjugate and incubate for 45 min. Add 0.1 ml of sterile EDTA (0.01 M) to scavenge any unbound ^{111}In.

DOSE

37–74 MBq (1–2 mCi) by either bolus injection or slow infusion.

INJECTION TO IMAGING TIME

48–72 h.

BIOLOGIC BEHAVIOR

Irrespective of the preparation used, ^{111}In-anti-CEA accumulates in malignant tissues of colon, rectum, breast, ovary and lung. In normal tissues, most accumulation occurs in the liver and kidney, followed by the other well-perfused organs such as spleen, marrow and lungs. The liver and kidney uptakes are rapid and persistent. For ^{111}In-anti-CEA F(ab)$_2$ BW431/31, the accumulation in the liver, marrow and muscle is 11.6, 8 and 7.4% respectively, while blood activity is 5.8% and persistent. The liver uptake in males is in the range 7.0–12% at 2–3 days while in females it

is 1.6–47.8% at 4 days. In males, the uptake in marrow is 8.0–19.9% at 2–3 days, while in female muscle it is 3.5–5.9% at 4 days [75]. The above percentages were from a limited study of six patients (three males and three females). It would appear that ^{111}In-anti-CEA F(ab)$_2$ BW431/31 shows a sex difference in its accumulation in these organs. For ^{111}In-anti-CEA F(ab)$_2$ 19.9, the maximum accumulations in liver, kidneys and spleen are 20 ± 8%, 10% and 2% respectively, at 24 h for liver and 20 h for kidneys and spleen [77]. The blood clearance of anti-CEA 19.9 has two components with $t_{1/2}$ values of 1.9 and 19.3 h. It is also metabolically stable *in vivo*. Both anti-CEA-BW431/31 and 19.9 are excreted by the liver and kidneys [75–77].

Table 11.2 Estimated radiation absorbed dose of ^{111}In-anti-CEA F(ab)$_2$ BW431.31

Organ	*mGy/MBq*	*rad/mCi*
Kidneys	2.27	8.40
Testes	0.80	2.96
Spleen	0.51	1.85
Bone marrow	0.37	1.37
Liver	0.29	1.07
Adrenals	0.24	0.88
GI tract		
Upper large intestine	0.21	0.78
Small intestine	0.18	0.67
Stomach wall	0.12	0.44
Pancreas	0.20	0.77
Bone surfaces	0.19	0.74
Gallbladder wall	0.19	0.74
Ovaries	0.11	0.41
Uterus	0.10	0.37
Heart	0.096	0.35
Bladder wall	0.091	0.34
Lungs	0.07	0.26
Thyroid	0.038	0.14
Total body	0.092	0.34

USES

- Evaluation of therapeutic treatment (chemotherapy, radiotherapy or surgery) in patients with breast, ovarian, lung or colorectal cancer.
- Clinical investigation for initial diagnosis of cancer and staging of tumor.

DOSIMETRY

The data for ^{111}In-anti-CEA F(ab)$_2$ BW431/31 are taken from [75] and listed in Table 11.2. The studies were done in rats and the rat data were modified for humans.

INDIUM-111 ANTITUMOR-ASSOCIATED GLYCOPROTEIN (^{111}In-ANTI-TAG/B72.3)

The monoclonal antibody B72.3 is murine IgG prepared by using a membrane-enriched extract of human breast carcinoma metastasis to the liver [78]. It binds to a high molecular weight mucin (10^6 daltons) referred to as tumor-associated glycoprotein (TAG). Using immunohistochemical techniques, TAG has been shown to be present in 85% of colonic adenocarcinomas and in 70% of breast, 95% of ovarian and 50% of non-small-cell lung cancers, and also in pancreatic, gastric and esophageal cancers. It has minimal or no expression in normal adult tissues [78, 79].

It has been labeled with $^{125/131}$I and ^{111}In. However, for imaging purposes, it is ^{111}In linked through glycyl-tyrosyl-(*N*, *E*-diethylenetriamine pentaacetic acid)-lysine hydrochloride that is used. This particular antibody is commercially available and is referred to as Oncoscint CR/OV [80].

PREPARATION

The non-radioactive reagents for the preparation of Oncoscint CR/OV (^{111}In-anti-TAG/B72.3) are supplied commercially in two vials. Vial 1 contains 1 mg of B72.3 (Satumomab Pendetide) in 2 ml of sodium phosphate-buffered saline. Vial 2 contains sodium acetate buffer (136 mg of sodium acetate trihydrate dissolved in 2 ml of sterile water).

Using aseptic technique, add 0.5 ml of the buffer (vial 2) to a solution of ^{111}In chloride containing 185–222 MBq (5–6 mCi) and mix. Add the buffered ^{111}In chloride to the antibody (vial 1) and gently mix. Allow to react at room temperature for 30 min and pass through a 0.22-μm millipore filter before use. The preparation is stable for up to 8.0 h.

DOSE

185 MBq (5 mCi) infused over 5 min.

INJECTION TO IMAGING TIME

48–72 h.

BIOLOGIC BEHAVIOR

Upon injection, ^{111}In-anti-TAG/B72.3 remains in organs that are well perfused: heart, liver and spleen. With time it slowly accumulates in primary and metastatic tumor sites of colon, breast, ovary, non-small-cell lung, pancreatic, gastric and esophageal cancers [81].

It has prolonged whole-body retention, high liver uptake and is excreted into the bowel. A small amount is excreted slowly in urine. Its blood clearance and whole-body elimination half-lives are 63 ± 5 h and 11.8 days respectively [81].

USES

^{111}In-anti-TAG/B72.3 is used for the detection of colorectal and ovarian cancer.

DOSIMETRY

The data are modified from [80] and listed in Table 11.3.

Table 11.3 Estimated radiation absorbed dose of ^{111}In-anti-TAG/B72.3

Organs	*mGy/MBq*	*rad/mCi*
Spleen	0.865	3.2
Liver	0.811	3.0
Bone marrow	0.649	2.6
Kidney	0.524	1.94
Lungs	0.265	0.98
Adrenal	0.243	0.90
Pancreas	0.200	0.74
Bone	0.178	0.66
Heart wall	0.173	0.64
GI tract		
Stomach wall	0.173	0.64
Small intestine	0.173	0.64
Upper large intestine	0.168	0.50
Lower large intestine	0.168	0.50
Ovaries	0.157	0.58
Uterus	0.146	0.52
Skin	0.086	0.32
Thyroid	0.081	0.30
Testes	0.076	0.20
Total body	0.146	0.54

TECHNETIUM-99m ANTIBODIES

Technetium-99m can be incorporated into antibodies either directly or indirectly [82].

DIRECT METHOD

The direct method involves the reduction of a disulfide bond to a thiol group (–SH), which binds to technetium in a reduced state, probably the +4 oxidation state. Reduction of the disulfide bond is achieved either by treating the antibody with stannous ion [83, 84] or by using weak reducing agents such as dithiothreitol [85], 2-mercaptoethanol [86] or ascorbic acid [87].

Stannous ion is incubated with $F(ab)_2$ antibody fragment for 21 h. This procedure is referred to as the pretinning process and reduces the $F(ab)_2$ to a mixture of $F(ab)_2$, Fab'; and peptides [84]. The mixture can be labeled immediately with ^{99m}Tc by adding $^{99m}TcO_4^-$, or preserved by freezing or lyophilizing for subsequent use. The yield is approximately 70–90%. The preparation requires purification prior to administration by passing through a Sephadex G-25 column to remove $^{99m}TcO_4^-$ and $^{99m}TcO_2$.

With the weak reducing agent, the antibody solution is mixed with the appropriate agent and a weak ^{99m}Tc complex such as ^{99m}Tc-gluconate or -pyrophosphate is added to the mixture. Labeling is achieved by ligand exchange, in which ^{99m}Tc binds to the –SH group of the antibody. The yield is generally very high (>90%). The preparation does not need any purification prior to administration. This procedure is amenable to a one-step process in which the reducing agent, antibody, gluconate and stannous ion are mixed in a vial and lyophilized. When needed, the $^{99m}TcO_4^-$ is added to the vial. This technique has been used to make ^{99m}Tc-antifibrin.

INDIRECT METHOD

^{99m}Tc is linked to the antibody through a ligand which binds to the amino groups of the lysine and arginine residues of the antibody [88–92]. Depending on the ligand used, ^{99m}Tc is bound either to the antibody [88] or to the ligand [89–92]. With iminothiolane as the conjugate ligand (which is also the reducing agent), the ^{99m}Tc is bound to the antibody through the –SH group [88]. With N_2S_2 or N_3S tetradentate ligands, ^{99m}Tc is bound to the ligand [89–92]. The ^{99m}Tc-labeled ligand may be preformed and attached to the antibody, as exemplified by ^{99m}Tc-diamide dithiolate (^{99m}Tc-DADS) [90], or the ligand–antibody may first be derivatized, and reduced ^{99m}Tc added to form ^{99m}Tc-ligand–antibody. Examples of this procedure include the production of mercaptotriamide, MAG_3 [91] and bis(aminoethanethiol) [92]. The derivatization procedure lends itself to a one-step final preparation process because the ligand, antibody and stannous ion can be lyophilized and ready for use.

Depending on the ^{99m}Tc antibody preparation, upon injection, radioactivity is seen in gallbladder and intestine; the blood clearance is fast and excretion is through the kidneys. Imaging can be performed 4–6 h post injection. ^{99m}Tc antibodies are not yet available commercially, however many are being investigated for clinical use.

REFERENCES

1. Leder, P. (1982) The genetics of antibody diversity. *Sci. Am.*, **246**, 3–115.
2. Pressman, D. and Korngold, L. (1953) The *in vivo* localization of anti-Wagner-osteogenic-sarcoma antibodies. *Cancer*, **6**, 7619–23.
3. Goldenberg, D.M. (1978) Immunodiagnosis and immunodetection of colorectal cancer. *Cancer Bull.*, **30**, 213–18.
4. Goldenberg, D.M., Kim, E.E. and DeLand F.H. *et al.* (1980) Radioimmunodetection of cancer with radioactive antibodies to carcinoembryonic antigen. *Cancer Res.*, **40**, 2984–92.
5. Goldenberg, D.M., Kim, E.E., DeLand F.H. *et al.* (1980) Clinical studies of the radioimmunodetection of tumors containing alpha-fetoprotein. *Cancer*, **45**, 497–501.
6. Chetanneau, A., Baum, R.P., Lehur, P.A. *et al.* (1990) Multi-centre immunoscintigraphic study using indium-111-labeled CEA-specific and/or 19.9 monoclonal antibody F (ab')2 fragments. *Eur. J. Nud. Med.*, **17**, 223–29.
7. Larson, S.M. (1991) Radioimmunology imaging and therapy. *Cancer*, **67**, 1253–60.
8. Goldenberg, D.M. and Larson, S. (1992) Radioimmunodetection in cancer identification. *J. Nucl. Med.*, **33**, 803–14.
9. Hinkle, G.H., Loesch, J.A., Hill, T.L. *et al.* (1990) Indium-111-monoclonal antibodies in radioimmunoscintigraphy. *J. Nucl. Med. Tech.*, **18**, 16–25.
10. Benz, P., Oberhausen, E. and Berberich, R. (1991) Monoclonal antibody BW431/26 labelled with technetium-99m and indium-111: an investigation of the biodistribution and the dosimetry in patients. *Eur. J. Nucl. Med.*, **18**, 813–16.
11. Khaw, B.A., Yasuda, T., Gold, H.K. *et al.* (1989) Acute myocardial infarct imaging with indium-111-labeled monoclonal antimyosin Fab. *J. Nucl. Med.*, **28**, 1671–78.
12. Yokoyama, K., Reynolds, J.C., Paik, C.H. *et al.* (1980) Immunoreactivity affects the biodistribution and tumour targeting of radiolabeled

anti-P_{97} Fab fragment. *J. Nucl. Med.*, **31**, 220–22.

13. Goldenberg, D.M. (1988) Targeting of cancer with radiolabeled antibodies: prospects for imaging and therapy. *Arch. Pathol. Lab. Med.*, **112**, 580–87.
14. Goldenberg, D.M., DeLand F., Kim, E.E. *et al.* (1978) Use of radiolabeled antibodies to carcinoembryonic antigen for detection and localisation of diverse cancers by external photoscanning. *N. Engl. J. Med.*, **298**, 1384–88.
15. Sharkey, R.M., Goldenberg, D.M., Goldenberg, H. *et al.* (1990) Murine monoclonal antibodies against carcinoembryonic antigen. Immunological, pharmacokinetic, and targeting properties in humans. *Cancer Res.*, **50**, 2823–31.
16. Weinstein, J.N., Eger, R.R., Covell, D.G. *et al.* (1989) The pharmacology of monoclonal antibodies. *Ann. NY Acad. Sci.*, **507**, 199–210.
17. Frist, W., Yasuda, T., Segall, G. *et al.* Noninvasive detection of human cardiac transplant rejection with In-111-labeled monoclonal antimyosin (Fab) imaging. *Circulation*, **76**, 81–5.
18. Oster, Z.H., Srivastava, S.C., Som, P. *et al.* (1983) Thrombus radioimmunoscintigraphy: an approach using monoclonal antiplatelet antibody. *Proc. Natl. Acad. Sci. USA*, **82**, 3465–88.
19. Rosebrough, S.F., Grossman, Z.D., McAfee, J.G. *et al.* (1988) Thrombus localization with indium-111 and iodine-131-labeled fibrin-specific monoclonal antibody and its $(Fab')_2$ and Fab fragments. *J. Nucl. Med.*, **29**, 1212–22.
20. Locher, J.T., Seybold, K., Andres, R.Y. *et al.* (1986) Imaging of inflammatory and infectious lesions after injection of radiolabeled monoclonal antigranulocyte antibodies. *Nucl. Med. Commun.*, **7**, 659–60.
21. Joseph, K., Koffen, H., Bosslet, K. *et al.* (1978) *In vivo* labeling of granulocytes with Tc-99m anti-NCA monoclonal antibodies for imaging inflammation. *Eur. J. Nucl. Med.*, **14**, 367–73.
22. Fischman, A.J., Rubin, R.H., Khaw, B.A. *et al.* (1988) Detection of acute inflammation with In-111-labeled non-specific polyclonal IgG. *Semin. Nucl. Med.*, **18**, 335–44.
23. Fischman, A.J., Khaw, B.A., Strauss, H.W. *et al.* (1989) Quo vadis radioimmune imaging. *J. Nucl. Med.*, **30**, 1911–15.
24. Goldenberg, D.M., Sharkey, R. and Ford, E. (1987) Anti-antibody enhancement of iodine-131 anti CEA radioimmunodetection in experimental and clinical studies. *J. Nucl. Med.*, **28**, 1604–10.
25. Wahl, R.L., Parker, C.W. and Philpott, G.W. (1983) Improved radioimaging with tumour localization with monoclonal F $(ab')_2$. *J. Nucl. Med.*, **24**, 316–25.
26. Bucheggar, F., Haskell, C.M., Schreyer, M. *et al.* (1983) Radiolabeled fragments of monoclonal antibodies against carcinoembroyonic antigens for localization of human colon carcinoma grafted to nude mice. *J. Exp. Med.*, **158**, 413–27.
27. Bucheggar, F., Pfister, C., Fournier, K. *et al.* (1989) Ablation of human colon carcinoma in nude mice by I-131-labeled monoclonal anti-carcino-embryonic antigen antibody F $(ab')_2$ fragments. *J. Clin. Invest.*, **83**, 1449–56.
28. Delaloye, B., Bischof-delaloye, A., Bacheggar, F. *et al.* (1988) Detection of colorectal carcinoma by emission computerized tomography after injection of I-123-labeled Fab or $F(ab')_2$ fragments from monoclonal anti-carcino-embryonic antigen antibodies. *J. Clin. Invest.*, **77**, 301–11.
29. Larson, S.M., Carrasquillo, J.A., Krohn, K.A. *et al.* (1983) Localization of I-131-labeled P97 specific Fab fragments in human melanoma as a basis for radiotherapy. *J. Clin. Invest.*, **72**, 2101–14.
30. Bucheggar, F., Pelegrin, A., Delaloye, B. *et al.* (1990) Iodine-131-labeled MAb F $(ab')_2$ fragments are more efficient and less toxic than intact anti-CEA antibodies in radioimmunotherapy of large human colon carcinoma grafted in nude mice. *J. Nucl. Med.*, **31**, 1035–44.
31. Warren, L., Back, C.A. and Tuszynski, G.P. (1978) Glycopeptide changes and malignant transformation. A possible role for carbohydrate in malignant behaviour. *Biochim. Biophys. Acta*, **516**, 97–127.
32. Goldenberg, D.M., Goldenberg, H., Sharkey, R.M. *et al.* (1990) Clinical studies of cancer radioimmuno detection with carcinoembryonic antigen monoclonal antibody fragments labelled with I-123 or Tc-99m. *Cancer Res.*, **50**, 909–21.
33. Pinsky, C.M., Goldenberg, D.M., Wlodkowski, T.J. *et al.* (1991) Detection of occult metastasis of colorectal cancer by the use of anti-CEA Fab' fragments labelled with Tc-99m (Abstract). *J. Nucl. Med.*, **32**, 1053.

34. Baum, R.P., Hertel, A., Lorenz, M. *et al.* (1989) Tc-99m-labelled anti-CEA monoclonal antibody for tumour immunoscintigraphy: first clinical results. *Nucl. Med. Commun.*, **10**, 345–52.
35. Carney, P.L., Rogers, P.E. and Johnson, D.K. (1989) Dual isotope study of Iodine-125 and Indium-111-labelled antibody in athymic mice. *J. Nucl. Med.*, **30**, 374–84.
36. Hnatowich, D.J. and McGraw, J. (1988) DTPA-coupled proteins procedures and precautions. *Nucl. Med. Biol.*, **14**, 563–68.
37. Fritzberg, H.R. and Beamier, P.L. (1992) Targeted proteins for diagnostic imaging: does chemistry make a difference? (editorial). *J. Nucl. Med.*, **33**, 394–97.
38. Hunter, W.M. and Greenwood, F.C. (1962) Preparation of iodine-131-labelled growth hormone of high specific radioactivity. *Nature*, **194**, 495–96.
39. Matzku, S., Kirchgessner, H., Digold, W.G. *et al.* (1985) Immunoreactivity of monoclonal anti-melanoma antibodies in relation to the amount of radioactive iodine substituted to the antibody molecule. *Eur. J. Med.*, **11**, 260–64.
40. Markwell, A.A.K. (1982) A new solid-state reagent to iodinate proteins. *Ann. Biochem.*, **125**, 427–32.
41. Lee, D.S.C. and Griffiths, J. (1984) Comparative studies of iodobeads and chloramine-T methods for the radioiodination of human alphafetoprotein. *J. Immunol. Methods*, **74**, 181–89.
42. Haisma, H.J., Hilgers, J. and Zurawski, V.R. (1986) Iodination of monoclonal antibodies for diagnosis and radiotherapy using convenient one-vial method. *J. Nucl. Med.*, **27**, 1890–95.
43. Thorell, J.I. and Johanson, B.G. (1972) Enzymatic iodination of polypeptides with I-123 to high specific activity. *Biochem. Biophys. Res. Commun.*, **48**, 464–71.
44. Newman, P.J., Kahn, R.A. and Hines, A.J. (1981) Detection and characterization of monoclonal antibodies to platelet membrane proteins. *J. Cell. Biol.*, **90**, 249–53.
45. Bhargawa, K.K. and Acharya, S.A. (1989) Labelling of monoclonal antibodies with radionuclides. *Semin. Nucl. Med.*, **19**, 187–201.
46. Hodalgo, J.U. and Nadler, S.B. (1962) Stability studies on I-131 labelled albumin. *J. Nucl. Med.*, **3**, 268–72.
47. DeNardo, G.L., Young, W.C., DeNardo, S.J. *et al.* (1986) Urinary metabolities after injection of mono clonal antibodies (MAB) or fibrinogen (F) radioiodinated with a small and large number of iodine atoms (abstract). *J. Nucl. Med.*, **27**, 958.
48. Engler, D. and Burger, A.G. (1984) The deiodination of the iodothryonines and of their derivatives in man. *Endocrine Rev.*, **5**, 151–84.
49. Bolton, A.E. and Hunter, W.M. (1973) The labeling of proteins to high specific radioactivities by conjugation to I-125 containing acylating agent. *Biochem. J.* **33**, 529–37.
50. Bhargava, K.K. and Chervu, L.R. (1987) N-hydroxysuccinimide hippuran ester: application for radiolabelling of macromolecules. *Biochem. Biophys. Res. Commun.*, **144**, 323–28.
51. Wilbur, D.S., Hadley, S.W. and Hylarides, M.D. (1989) Development of a stable radioiodinating reagents to label monoclonal antibodies for radiotherapy of cancer. *J. Nucl. Med.*, **30**, 216–26.
52. Krejcanek, G.E., Tucker, K.L. (1977) Covalent attachment of chelating groups to macromolecules. *Biochem. Biophys. Res. Commun.*, **77**, 581–85.
53. Hnatowich, D.J., Layne, W.W., Childs, R.L. (1982) The preparation and labelling of DTPA-coupled albumin. *Int. J. Appl. Radiat. Isot.*, **33**, 327–32.
54. Paik, C.H., Ebbert, M.A., Murphy, P.R. *et al.* (1983) Factors influencing DTPA conjugation with antibodies by cyclic DTPA anhydride. *J. Nucl. Med.*, **24**, 1158–63.
55. Scheinberg, D.A., Strand, M. and Gansow, O.A. (1982) Tumour imaging with radioactive metal chelates conjugated to monoclonal antibodies. *Science*, **215**, 1511–13.
56. Khaw, B.A., Gansow, O.A., Brechbiel, M.W. *et al.* (1990) Use of isothiocyanato benzyl-DTPA derivatized monoclonal antimyosin Fab for enhanced in-vivo target localization. *J. Nucl. Med.*, **31**, 211–17.
57. Mirzadeh, S.M., Brechbiel, M.W., Atcher, R.A. *et al.* (1990) Radiometal labelling of immunoproteins: covalent linkage of 2-(4-isothiocyanatobenzyl) DTPA ligands to immunoproteins. *Bioconjug. Chem.*, **1**, 59–65.
58. Gansow, O.A. (1991) Newer approaches to the radiolabelling of monoclonal antibodies by use of metal chelates. *Nucl. Med. Biol.*, **18**, 369–81.

59. Eckelman, W.C., Karesh, S.M. and Reba, R.C. (1975) New compounds: fatty acid and long chain hydrocarbon derivatives containing a strong chelating agent. *J. Pharmacol. Sci.*, **64**, 704–6.
60. Khaw, B.A., Strauss, H.W., Moore, R. *et al.* (1987) Myocardial damage delineated by indium-111 antimyosin Fab and technetium-99m, pyrophosphate. *J. Nucl. Med.*, **28**, 76–82.
61. Product Information (1986) Myoscint. Centocor Europe, Leiden, The Netherlands.
62. Khaw, B.A., Beller, G.A., Haber, E. *et al.* (1976) Localisation of cardiac myosin specific antibody in myocardial infarction. *J. Clin, Invest.*, **58**, 439–46.
63. Owunwanne, A., Malki, A., Sadek, S. *et al.* (1989) Investigative study of radiopharmaceuticals useful for imaging skeletal muscle injury in experimental animals. *Am. J. Physiol. Imaging.*, **4**, 62–5
64. Elgazzar, A.M., Malki, A.A., Abdel-Dayem, H.M. *et al.* (1989) Indium-111 monoclonal antimyosin antibody in assessing skeletal muscle damage in trauma. *Nucl. Med. Commun.*, **10**, 477–85.
65. Allen, M.D., Tsubi, H., Togo, T. *et al.* (1989) Detection of cardiac allograft rejection and myocyte necrosis by monoclonal antibody to cardiac myosin. *Transplantation*, **48**, 923–28.
66. Yasuda, T., Palacios, I.F., Dec, G.W. *et al.* (1987) Indium-111 monoclonal antimyosin antibody imaging in the diagnosis of acute myocarditis. *Circulation*, **76**, 306–11.
67. Khaw, B.A., Strauss, H.W., Pohost, G.M. *et al.* (1983) Relation of immediate and delayed thallium-201 distribution to localisation of iodine-125 antimyosin antibody in acute experimental myocardial infarction. *Am. J. Cardiol.*, **51**, 1428–32.
68. Khaw, B.A. and Narula, J. (1991) Of antimyosin imaging and histopathology of myocardial infarction: when, where and why? *J. Nucl. Med.*, **32**, 867–70.
69. Shively, J.E. and Beatty, J.D. (1985) CEA-related antigens: molecular biology and clinical significance: *Crit. Rev. Oncol. Hematol.*, **2**, 355–99.
70. Hnatowich, D.J., Layne, W.W., Childs, R.L. *et al.* (1983) Radioactive labelling of antibody: a simple and efficient method. *Science*, **220**, 613–15.
71. Hnatowich, D.J., Childs, R.L., Lanteigne, D. *et al.* (1983) The preparation of DTPA-coupled antibodies radiolabelled with metallic radionuclides: an improved method. *J. Immunol Methods*, **65**, 145–47.
72. Kuhlmann, L. and Steinstrasser, A. (1988) Effect of DTPA to antibody ratio on chemical, immunological and biological properties of In-111-labelled F(ab')2 fragment of the antibody 431.31. *Nucl. Med. Biol.*, **15**, 617–27.
73. Bosslet, K., Steinstrasser, A., Schwarz, A. *et al.* (1985) Immunohistochemical localisation and molecular characteristics of three monoclonal antibody-defined epitopes detectable on carcinoembryonic antigen (CEA). *Int. J. Cancer.*, **36**, 75–84.
74. Esteban, J.M., Schlom, J., Gansow, O.A. *et al.* (1987) New method for the chelation of indium-111 to monoclonal antibodies: biodistribution and imaging of athymic mice bearing human colon carcinoma xenografts. *J. Nucl. Med.*, **28**, 861–70.
75. Bo-Anders, J., Strand, S.E., Anderson, L. (1992) Radiation dosimetry for indium-111-labelled anti-CEA-F(ab')2 fragments evaluated from tissue distribution in rats. *J. Nucl. Med.*, **33**, 1654–60.
76. Ingvar, C., Wingardh, K., Ljungberg *et al.* (1991) Quantitative biokinetic study of In-111-F(ab')2 in patients with colorectal cancer. *Antibody Immunoconj. Radiopharmacol.*, **4**, 587–93.
77. Hnatowich, D.J., Griffin, T.W., Kosciuczyk, C. *et al.* (1985) Pharmacokinetics of an indium-111-labelled monoclonal antibody in cancer patients. *J. Nucl. Med.*, **26**, 849–58.
78. Nabi, H.A. and Doerr, R.J. (1992) Radiolabeled monoclonal antibody imaging (immunoscintigraphy) of colorectal cancers: current status and future perspectives. *Am. J. Surg.*, **163**, 448–56.
79. Goldenberg, D.M., Goldenberg, H., Sharkey, R.M. *et al.* (1989) Imaging of colorectal carcinoma with radiolabelled antibodies. *Semin, Nucl. Med.*, **19**, 262–81.
80. Product Information (1992) Oncoscint CR/OV, Cytogen, New Jersey.
81. Yokoyama, K., Carrasquillo, J.A., Chang, A.E. *et al.* (1989) Differences in biodistribution of indium-111- and iodine-131-labelled B72.3

monoclonal antibodies in patients with colorectal cancer. *J. Nucl. Med.*, **30**, 320–27.

82. Verbruggen, A.M. (1990) Radiopharmaceuticals: state of the art. *Eur. J. Nucl. Med.*, **17**, 346–60.
83. Rhodes, B.A. and Burchiel, S.W. (1983) Radiolabeling of antibodies with technetium-99m, in *Radioimmunoimaging and Radioimmunotherapy* (eds S.W. Burchiel and B.A. Rhodes), Elsevier, New York, pp. 207–22.
84. Rhodes, B.A., Zamora, P.O., Newell, K.D. *et al.* (1989) Technetium-99m labelling of marine monoclonal antibody fragments. *J. Nucl. Med.*, **27**, 685–93.
85. Pak, K.Y., Nedelmen, M.A., Stewarz, R. *et al.* (1986) A rapid and efficient method for labelling IgG antibodies with Tc-99m and comparison to Tc-99m Fab' antibody fragments (abstract). *J. Nucl. Med.*, **30**, 793.
86. Schwarz, A. and Steinstrasser, A. (1987) A novel approach to Tc-99m-labelled monoclonal antibodies (abstract). *J. Nucl. Med.*, **28**, 721.
87. Thakur, M.L., Defulvio, J. and Park, C.H. (1990) Use of ascorbic acid (AA) for direct Tc-99m labeling of monoclonal antibodies (MAbs) (abstract). *Eur. J. Nucl. Med.*, **16**, 392.
88. Goedemans, W.T., Panek, K.J., Ensing, G.J. *et al.* (1990) A new simple method for labelling of proteins with Tc-99m by derivatization with I-imino-4-mercaptobutyl groups, in *Technetium and Rhenium in Chemistry and Nuclear Medicine*, Vol. 3 (eds M. Nicolini, G. Bandolini and U. Mazzi), Cortina International, Verona and Raven Press, New York, pp. 595–604.
89. Joiris, E., Bastin, B. and Thornback, J.R. (1990) A new method for labelling of monoclonal antibodies, their fragments and other proteins with technetium-99m, in *Technetium and Rhenium in Chemistry and Nuclear Medicine*, Vol. 3 (eds M. Nicolini, G. Bandolini and U. Mazzi), Cortina International, Verona and Raven Press, New York, pp. 609–14.
90. Fritzberg, A.R., Abrams, P.G., Beaunier, P.C. *et al.* (1988) Specific and stable labeling of antibodies with technetium-99m with a diamidedithiolate chelating agent. *Proc. Natl Acad. Sci. USA*, **85**, 4025–29.
91. Dean, R.T., Weber, R., Pak, K. *et al.* (1990) New facile methods for stably labelling antibodies with technetium-99m, in *Technetium and Rhenium in Chemistry and Nuclear Medicine*, Vol. 3 (eds M. Nicolini, G. Bandolini and U. Mazzi), Cortina International, Verona and Raven Press, New York, pp. 605–8.
92. Esienhart, M., Brandan, W., Missfeldt, M. (1989) Synthesis and in-vivo testing of bromobutyl amine substituted 1, 2-dithio-5, 9-diazacycloundecane: a verstile precursor for new Tc-99m-bis (aminoethanethiol) complexes. *Nucl. Med. Biol.*, **16**, 805–11.

12

Receptor radiopharmaceuticals

INTRODUCTION

Receptors are macromolecules with two distinct characteristics:

- the ability to recognize and selectively bind ligands with similar structures;
- the ability to initiate a biologic response when an appropriate ligand is bound to it.

Radiopharmaceuticals do not initiate a biologic response when bound to any biologic molecule because the tracer quantity used does not evoke any pharmacodynamic effect. Therefore, receptor radiopharmaceuticals are used mainly to study and quantitate the change in receptor density. This change can be measured by using as imaging technique and/or by estimating the equilibrium dissociation or association constant and the number of occupied (bound) receptor sites.

THE BINDING OF RADIOPHARMACEUTICAL TO RECEPTOR SITES

The binding of receptor radiopharmaceuticals to receptor sites can be described in terms of the law of mass action:

$$\underset{(RP)}{\text{Radiopharmaceutical}} + \underset{(R)}{\text{Receptor}} \underset{k_{-1}}{\overset{k_1}{\rightleftharpoons}} \text{Radiopharmaceutical–receptor complex (RP–R complex)}$$

- Let the the initial molar concentration of the RP be $[A]$.
- Let the initial (that is total) concentration of receptor be R.
- Let the concentration of the occupied receptors (RP–R complex) be r.
- The concentration of the unoccupied receptors will be $R–r$.

At equilibrium, the rate of the forward reaction equals the rate of the reverse reaction:

$$k_1[A]\,(R-r) = k_{-1}r$$

$$k_{-1}/k_1 = K_D = ([A](R-r)/r$$

where k_1 and k_{-1} are the rate constants of the forward and reverse reactions and K_D is the equilibrium dissociation constant. By measuring the radioactivity due to the bound and unbound radiopharmaceutical at equilibrium, K_D can be calculated. To estimate the number of occupied receptor sites, the above equation is rearranged to

$$r = [A] \times R/(K_D + [A])$$

A receptor radiopharmaceutical therefore offers a potential technique for studying the *in vivo* biochemical interaction between a radioactive ligand and a receptor site using an external monitoring device. Such a study might have a diagnostic utility and could also be used for monitoring the efficacy of therapeutic drugs. Various factors affect the use of receptor radiopharmaceuticals, and these include the receptor system, the choice of radionuclide, ligand and the labeling process, and the optimum time required for biologic distribution.

THE RECEPTOR SYSTEM

Few radiopharmaceuticals have been evaluated for imaging receptor systems, and these are summarized in Table 12.1. The binding of the radiopharmaceutical to the receptor site should be saturable and the distribution of the radioactive tracer within the organ should correspond to known sites of the receptor.

For example, a D_2 dopamine radioactive tracer should concentrate mostly in the basal ganglia [1–3], while a somatostatin tracer should concentrate at a somatostatin tissue-positive site(s) [4].

THE CHOICE OF RADIONUCLIDE

The half-life of the radionuclide should be compatible with the kinetics of the ligand–receptor interaction. If the radioactive ligand can accumulate and is retained at the receptor

Table 12.1 Characteristics of receptor systems and some receptor-based radiopharmaceuticals

Receptor	*Characteristics*	*Radiopharmaceutical*
Cholinergic		
Nicotinic	Mostly in cortical regions of the brain	^{11}C-nicotine
Muscarinic	Distributed throughout the body (brain and periphery)	^{11}C-QNB, ^{123}I-QNB
M_1 subtype	Localized in CNS	
M_2 subtype	Periphery and also in the cerebellum and ponsmedulla	
Dopamine		
D_1	Located on intrinsic neurons within the corpus striatum; stimulates adenylate cyclase and opens potassium channels	^{123}I-SCH 23982
D_2	Located on the basal ganglia (striatum); inhibits adenylate cyclase and closes potassium channels Both D_1 and D_2 play an important role on movement disorders	^{123}I-BZM, ^{11}C-*N*-methyl spiperone, ^{18}F-*N*-fluoroethyl spiperone
GABA/benzodiazepine		
Central type	Mediates all pharmacologic actions of the benzodiazepine group of drugs	^{11}C-diazepan, ^{11}C-flumazenil, ^{123}I-iomazenil
Peripheral type	Role not yet well established Both types found in brain	
Opiate	Found in thalamus, caudate nucleus, temporal, frontal and parietal cortices	^{11}C-carfentanil, ^{11}C-diprenorphine
Serotonin 5-HT_2 or S_2 type	Found in frontal cortex and plays important role in mood disorders	^{11}C-ketanserin ^{11}C- or ^{18}F-methylspiperone
Somatostatin	Neuroregulatory peptide found in neurons and endocrine cells (brain, periphery, pancreas and gastrointestinal tract)	^{111}In-DTPA octreotide

site within a few minutes, the ligand can be labeled with a short half-life radionuclide such as carbon-11 ($t_{1/2}$ = 20.4 min). However, if the radioactive ligand has slow accumulation and clearance kinetics, then a radionuclide with a long half-life should be used. Both ^{123}I and ^{111}In have been used successfully to label receptor ligands.

THE CHOICE OF LIGAND

The ligand to be labeled can be a natural substrate or a biologic analog. For natural substrates, the biochemical behavior is known, but it is important that the labeling process does not alter its biologic behavior. For analogs it is important that the binding characteristics (specificity and affinity) be established using *in vitro* and *in vivo* models. To establish specific binding characteristics, displacement and blocking (presaturation) experiments with agonist and antagonists are done. An agonist forms a drug–receptor complex that initiates an active response from the cell, while an antagonist forms a drug–receptor complex that does not trigger an active response from the cell. The antagonist merely prevents the attachment of an agonist to the receptor.

In the displacement experiment, an agonist or excess non-radioactive ligand is administered intravenously, when the concentration of the radioactive ligand has reached its maximum. As a result of the competitive binding by the agonist, the concentration of the radioactive tracer begins to decrease. In the blocking or presaturation experiment, an antagonist or excess non-radioactive ligand is used to block the receptor site(s), so that when the radioactive ligand is injected the amount bound to the tissue is less than that measured in the absence of the antagonist.

The binding affinity of the ligand to the receptor is very important in determining the extent of background radioactivity. High background radioactivity can be due to high binding affinity to other receptors and non-receptors, low binding affinity to other receptors and non-receptors or low binding affinity to a non-saturable tissue. ^{11}C-methylspiperone binds to both D_2 dopamine receptors and serotonin receptors [5, 6].

^{111}In-octreotide binds to somatostatin tissue-positive sites present in tumors and normal tissues in the brain, peripheral neurons, endocrine pancreas and gastrointestinal tract [4]. *In vitro* binding assay technique is used for determining the affinity or dissociation constants of ligands with similar structures that bind to the same receptor. Using such a technique, Kung *et al.* [7] studied D_2 dopamine receptor-binding ligands and ranked them as follows:

Spiperone > S(–) IBZM> (+) butaclamol >>
R (+) IBZM ≥ S(–) BZM >
dopamine > ketanserin > SCH-23390 >>
propanolol.

LABELING PROCESS

The labeling procedure should not change the biologic behavior of the labeled tracer. The final step in the preparation should be simple enough to be performed in the radiopharmacy, and the labeled tracer can be administered without further purification. The labeled ligand should have very high specific activity so that a nanogram quantity of the non-radioactive ligand will be administered in order to avoid any probable toxic effect from the ligand. Much more importantly, the receptor system has a finite number of binding sites, therefore it is important that these sites are not saturated and that binding to non-specific sites does not increase unduly.

OPTIMUM IMAGING TIME

This time is reached when there is a differential spatial distribution of the radioactive ligand between the known receptor site and

other tissues. Several factors affect the optimum imaging time, and these include the concentration (density) of the receptor, the extent of non-specific binding to proteins and lipids and the dissociation rate of the radiopharmaceutical–receptor complex. These factors have been described previously.

Two receptor radiopharmaceuticals are described in detail in this chapter: ^{123}I-BZM and ^{111}In-DTPA octreotide.

IODINE-123 (*S*)-(–)-3-IODO-2-HYDROXY-6-METHOXY-*N*-[(1-ETHYL-2-PYRROLIDINYL) METHYL] BENZAMIDE (^{123}IBZM)

CHEMISTRY

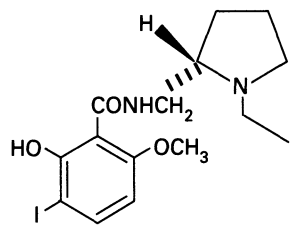

IBZM belongs to a class of structurally related benzamides which are known to display significant antidopaminergic activity. They bind specifically to CNS D_2 dopamine receptors and selectively block apomorphine-induced hyperactivity *in vivo* [8, 9]. Kung *et al.* [1] showed that *S*-(–)-1-^{125}I-IBZM has high specific dopamine D_2 receptor binding in rat striatum (K_D = 0.426 ± 0.082 nM, β_{max} = 480 ± 22 fmol per mg of protein). The relatively high affinity and brain uptake of IBZM is partially attributed to the incorporation of iodine in the molecule, presumably causing increased lipophilicity.

PREPARATION

^{123}IBZM is available commercially and is supplied in a sterile, isotonic solution [10]. IBZM can be radioiodinated in house using the chloramine-T method [11]. This procedure requires the use of HPLC (PRP - 1 column with acetonitrile–buffer mixture) to separate the radioactive IBZM from other materials. The radiochemical yield and specific activity have been reported to be as high as 95% and 600 Ci/mmol respectively [8].

DOSE

185 MBq (5 mCi).

INJECTION TO IMAGING TIME

Blood flow	Immediately
SPET acquisition	1.5 h

PATIENT PREPARATION

Patients are asked to stop taking all neuroleptic medications at least 2 weeks prior to the study. Lugol's solution is given, three drops twice daily, 1 day before and 3 days after administration of ^{123}IBZM.

BIOLOGIC BEHAVIOR

^{123}IBZM is a neutral and lipophilic compound and is presumed to cross the blood–brain barrier by simple diffusion [12]. In the brain, it is concentrated slowly in the basal ganglia (where the D_2 dopamine receptors are located), reaching a plateau 60 min after injection [1–3]. Displacement experiments using *S*(–) and *R*(+) isomers of IBZM have shown that the uptake of ^{123}IBZM in rat brain is highly stereoselective for the *S*(–) isomer. Re-extraction of the radioactivity in the rat striatal tissue has shown that re-extracted ^{123}IBZM has the same retention time in HPLC as the injected parent, thereby indicating minimal or no metabolism in the brain [1]. However, in plasma, metabolism of ^{123}IBZM has been reported to include a polar metabolite and two non-polar metabolites with

shorter retention time than parent IBZM on reversed-phase HPLC [11]. In addition, *in vivo* deiodination of ^{123}IBZM occurs, as evidenced by radioactivity in the thyroid.

^{123}IBZM and its metabolites are taken up in the lung, liver, kidney, stomach and muscle, with the lung showing the highest accumulation. It is cleared quickly from the lungs and excreted in both urine and bile.

USES

^{123}IBZM is under clinical investigation for imaging D_2 dopamine receptor density change in neuropsychiatric conditions such as Parkinson's disease, Huntington's charea tardive dyskinesia and schizophrenia.

INDIUM-111 DTPA-D-PHE-1-OCTREOTIDE (^{111}In-OCTREOTIDE)

CHEMISTRY

^{111}In-DTPA-D-phe-Cys-phe-D-Trp-Lys-Thr-Cys-Thr(ol)

Octreotide is a long-acting (biological $t_{1/2}$ 2–3 h) synthetic analog of somatostatin (biological $t_{1/2}$ 2–3 min) [13, 14]. Somatostatin is a neuroregulatory peptide found in neurons and endocrine cells. It is synthesized in a wide variety of human tissues, with the highest density in the brain, the peripheral neurons, the endocrine pancreas, the gastrointestinal tract and in small quantities in the thyroid, the submandibular glands and placenta [4, 15]. It has been shown that somatostatin receptors are present in most neuroendocrine tumors, including carcinoids, islet cell carcinomas and growth hormone-producing adenomas [15, 16], meningiomas, breast carcinomas, astrocytomas and oat cell carcinomas of the lung [17]. Hence, ^{111}In-octreotide can be used as a somatostatin receptor-positive tumor-seeking radiopharmaceutical [18].

DTPA-D-Phe-1-octreotide is synthesized by conjugating DTPA-dianhydride to the α-NH_2 group of the N-terminal of the D-phenylalanine (Phe) residue [18]. DTPA-D-Phe-1-octreotide is available commercially as Octreoscan [19].

PREPARATION

Add 2 ml of $^{111}InCl_3$ in 0.05 M HCl containing 1000–1500 MBq (47–40.5 mCi) to 60 μg of DTPA-octreotide in 300 ml of 0.01 M acetic acid. Allow to react for up to 10 min at room temperature.

QUALITY CONTROL

Place a drop of ^{111}In-octreotide 1 cm from the lower end of an ITLC-SG strip, develop in 0.1 M sodium citrate (pH 5) (Table 12.2) up to 5 cm [18]. Air dry and cut the strip into two equal pieces. Assay each piece separately in a dose calibrator and calculate the percentage labeling efficiency as follows:

$$\text{Labeling efficiency (\%)} = \frac{\text{Activity at origin}}{\text{Activity at origin + solvent front}} \times 100$$

Table 12.2 Chromatographic analysis of ^{111}In-octreotide

Chromatographic system		*^{111}In species at*	
Support	*Solvent*	*Origin*	*Solvent front*
ITLC-SG	Sodium citrate	^{111}In-octreotide	^{111}In-chloride ^{111}In-citrate

DOSE

185–259 MBq (5–7 mCi).

INJECTION TO IMAGING TIME

24 and 48 h.

PATIENT PREPARATION

Patients are asked to stop taking non-radioactive octreotide (Sandostatin) 1 week prior to intravenous administration of ^{111}In-octreotide. Laxatives may be given on the day of injection to avoid artefacts due to radioactivity in the intestine. If indicated, an enema may be given to cleanse the colon [20].

BIOLOGIC BEHAVIOR

Upon intravenous injection, ^{111}In-octreotide accumulates in somatostatin receptor-positive tumors, liver, kidneys and spleen. Pretreatment of tumor-bearing rats with non-radioactive octreotide showed a significantly lower accumulation of ^{111}In-octreotide on the tumor site, indicating saturation of the somatostatin receptor binding site. The saturation of the receptor site by the agonist is positive proof that ^{111}In-octreotide is bound to somatostatin receptor site(s) in the tumor [20]. Experiments using HPLC have shown that up to at least 4 h after injection ^{111}In-octreotide remains intact in both plasma and urine. However, at 20 h and more non-octreotide-bound ^{111}In, presumably ^{111}In-DTPA, can be detected in both plasma and urine [19, 20].

^{111}In-octreotide is rapidly cleared from blood and excreted mostly by the kidneys. At 3, 6, 24 and 48 h after injection 25%, 50%, 85% and over 90% of the injected dose is excreted in urine respectively [20]. Urinary excretion of ^{111}In-octreotide in somatostatin-positive tumor-bearing rats is slower than in control rats [21].

Table 12.3 Estimated radiation absorbed dose of ^{111}In-octreotide

Organ	*mGy/MBq*	*rad/mCi*
Kidneys	0.45	1.66
Spleen	0.32	1.18
Urinary bladder wall	0.18	0.67
Pituitary	0.11	0.41
Liver	0.07	0.26
Gastrointestinal tract		
Lower large intestinal wall	0.06	0.22
Upper large intestinal wall	0.04	0.15
Small intestinal wall	0.03	0.11
Thyroid	0.04	0.15
Red bone marrow	0.02	0.074

USES

^{111}In-octreotide is under clinical investigation for visualization of neuroendocrine tumors, brain tumors, granulomas, malignant lymphomas and breast cancer.

DOSIMETRY

The data are modified from [20] and listed in Table 12.3.

REFERENCES

1. Kung, H.F., Sangren, P., Kung, M.-P. *et al.* (1989) In vitro and in vivo evaluation of [^{123}I] IBZM: A potential CNS D-2 dopamine receptor imaging agent. *J. Nucl. Med.*, **30**, 88–92.
2. Seibyl, J.P., Woods, S.W., Zoghbi, S.S. *et al.* (1992) Dynamic SPECT imaging of dopamine D_2 receptors in human subjects with iodine-123-IBZM. *J. Nucl. Med.*, **33**, 1964–71.
3. Toyama, H., Ichise, M., Ballinger, J.R. *et al.* (1993) Dopamine D_2 receptor SPECT imaging: Basic in vivo characteristics and clinical applications of ^{123}I-IBZM in humans. *Ann. Nucl. Med.*, **7**, 29–38.
4. Reichlin, S. (1983) Somatostatin. *N. Engl. J. Med.*, **309**, 1495–1501, 1556–63.

5. Maziere, B., Maziere, M. (1990) Where have we got to with neuroreceptor mapping of the human brain? *Eur. J. Nucl. Med.*, **16**, 817–35.
6. Kilbourn, M.R. and Zalutsky, M.R. (1985) Research and clinical potential of receptor based radiopharmaceuticals. *J. Nucl. Med.*, **26**, 655–62.
7. Kung, H.F., Kasliwal, R., Pan, S. *et al.* (1988) Dopamine D-2 receptor imaging radiopharmaceutical: synthesis, radiolabeling, and in vitro binding of (R)-(+)-and (S)-(–)-3-iodo-2-hydroxy-6-methoxy-N-[(1-ethyl-2-pyrrolidinyl) methyl] benzamide. *J. Med. Chem.*, **31**, 1039–43.
8. Kohler, C., Hall, H. and Gawell, L. (1986) Regional in-vivo binding of the substituted benzamide [^{3}H]-eticlopride in the rat brain: evidence for selective labelling of dopamine receptors. *Eur. J. Pharmacol.*, **120**, 217–26.
9. Hall, H. and Wedel, I. (1986) Comparisons between the in-vitro binding of two substituted benzamides and two butyrophenones to dopamine-D-2 receptors in the rat striatum. *Acta Pharmacol. Toxicol.*, **58**, 368–73.
10. Product Information (1993) ^{123}I-IBZM imaging of dopamine D_2 receptors in the brain by SPECT. Cygne, Eindhoven University of Technology, The Netherlands.
11. Kung, H.F., Guo, Y.-Z., Billings, J. *et al.* (1988) Preparation and biodistribution of [^{125}I] IBZM: a potential CNS D-2 dopamine receptor imaging agent. *Nucl. Med. Biol.*, **2**, 195–201.
12. Kung, H.F. (1986) Brain radiopharmaceuticals, in *Advances in Radiopharmaceuticals*, Vol. 1 (ed. A. Fritzberg) CRC Press, Boca Raton, FL, pp. 21–40.
13. Kvols, L.K., O'Dorisio, T., Patel, S. *et al.* (1989) Pharmacokinetic studies of SMS 201-995 (Sandostatin) comparing two subcutaneous injection sites. *J. Natl. Cancer Inst.*, **81**, 1926–29.
14. Bauer, W., Briner, U., Doepfner, W.S. *et al.* (1982) SMS 201-995; a very potent and selective octapeptide analogue of somatostatin with very prolonged action. *Life Sci.*, **31**, 1133–41.
15. Reubi, J.C., Kvols, L.K., Krenning, E. and Lamberts, S.W. (1990) Distribution of somatostatin in normal and tumour tissue. *Metabolism*, **30** (Suppl. 2), 78–81.
16. Reubi, J.C., Hacki, W.H., Lamberts, S.W. (1987) Hormone-producing gastrointestinal tumours contain high density of somatostatin receptors. *J. Clin. Endocrinol. Metab.*, **65**, 1127–34.
17. Reubi, J.C., Kvols, L.K., Nagorney, D.M. *et al.* (1990) Detection of somatostatin receptors in surgical and percutaneous needle biopsy samples of carcinoids and islet cell carcinoma. *Cancer Res.*, **50**, 5969–77.
18. Bakker, W.H., Albert, R., Bruns, C. *et al.* (1991) [^{111}In-DTPA-D-Phe']-octreotide, a potential radiopharmaceutical for imaging of somatostatin receptor-positive tumors: Synthesis, radiolabeling and in vitro validation. *Life Sci.*, **49**, 1583–91.
19. Product Information (1992) Somatostatin receptor imaging using Octreoscan. Mallinckrodt Medical, Petten, The Netherlands.
20. Krenning, E.P., Bakker, W.H., Kooij, P.P.M. *et al.* (1992) Somatostatin receptor scintigraphy with indium-111-DTPA-D-Phe-1-octreotide in man: metabolism, dosimetry and comparison with iodine-123-tyr-3-octreotide. *J. Nucl. Med.*, **33**, 652–58.
21. Bakker, W.H., Krenning, E.P., Reubi, J.C. *et al.* (1991) In vivo application of [^{111}In-DTPA-D-Phe]-octreotide for detection of somatostatin receptor positive tumors in rats. *Life Sci.*, **49**, 1593–601.

13

Radioactive noble gases

CHEMISTRY

Xenon and krypton are noble gases of group O. They are chemically inert at body temperature with limited solubility in aqueous media. The physical half-lives, decay mode and gamma energies of $^{127/133}$Xe and ^{81m}Kr are listed in Table 13.1.

^{127}Xe has better physical properties for imaging than ^{133}Xe, however it is more expensive and availability is limited by the requirement of a high energy linear accelerator for production.

PREPARATION

^{127}Xe is produced by ^{127}I (p,n) ^{127}Xe reaction, while ^{133}Xe is produced by the fission of ^{235}U. ^{81m}Kr is produced from a generator using ^{81}Rb as a parent [1]. ^{81}Rb is produced by the ^{79}Br (α, 2n) ^{81}Rb reaction.

DOSE

296–555 MBq (8–15 mCi).

INHALATION TO IMAGING TIME

Immediately.

BIOLOGIC BEHAVIOR

Following inhalation or injection in aqueous medium, $^{127/133}$Xe or ^{81m}Kr is rapidly eliminated by the lungs with a biologic half-life of about 30 s [2]. Xenon has higher solubility than krypton in fatty and cerebral tissues and therefore clears slowly [3].

USES

$^{127/133}$Xe

- Pulmonary ventilation studies.
- Measurement of regional cerebral blood flow.
- Organ perfusion.

^{81m}Kr

- Pulmonary ventilation studies.
- Determination of right ventricular ejection fraction.

Table 13.1 Physical properties of $^{127/133}$Xe and ^{81m}Kr

Radionuclide	*Half-life*	*Decay mode*	*Gamma energy (keV)*
^{127}Xe	36.4 days	EC	145 (4.2%), 172 (22%), 203 (65%), 375 (20%)
^{133}Xe	5.3 days	β^-	81 (38%), 31 (50%)
^{81m}Kr	13 s	IT	193 (65%)

Table 13.2 Estimated radiation absorbed dose from inhaled ^{127}Xe, ^{133}Xe or ^{81m}Kr gas[a]

	^{127}Xe		^{133}Xe		^{81m}Kr	
Organ	*mGy/MBq*	*rad/mCi*	*mGy/MBq*	*rad/mCi*	*mGy/MBq*	*rad/mCi*
Lungs	0.00034	0.0012	0.00077	0.0028	0.00021	0.00078
Pancreas	0.00014	0.0005	0.00011	0.0004	0.00003	0.00001
Red marrow	0.00014	0.0005	0.00012	0.0004	0.00002	0.00001
Adrenals	0.00013	0.0005	0.0001	0.0004	0.00003	0.00001
Bone surfaces	0.00012	0.0004	0.00012	0.0004	0.000002	0.00001
GI tract						
Stomach wall	0.00012	0.0004	0.0001	0.0004	0.000002	0.00001
Small intestine	0.00012	0.0004	0.00011	0.0004	0.000003	0.00001
Upper large intestinal wall	0.00012	0.0004	0.00011	0.0004	0.000003	0.00001
Liver	0.00012	0.0004	0.00011	0.0004	0.000001	0.0000003
Spleen	0.00012	0.0004	0.00011	0.0004	0.000003	0.00001
Uterus	0.00012	0.0004	0.0001	0.0004	0.0000001	0.0000003
Breast	0.00011	0.0004	0.00012	0.0004	0.000005	0.000018
Bladder wall	0.00011	0.0004	0.0001	0.0004	0.0000007	0.000002
Kidneys	0.00011	0.0004	0.0001	0.0004	0.000001	0.0000037
Ovaries	0.00011	0.0004	0.0001	0.0004	0.0000002	0.0000007
Thyroid	0.0001	0.0004	0.0001	0.0004	0.000001	0.0000037
Testes	0.0001	0.0004	0.0001	0.0004	0.00000002	0.00000007

[a] Assumes single inhalation or i.v. injection, with 30 s breath hold.

DOSIMETRY

The data are modified from [4] and listed in Table 13.2.

REFERENCES

1. Philips, M.S., Ramsy, C.E., Ma, J.M. and Lamb, J.F. (1984) A $^{81}Rb/^{81m}Kr$ perfusion generator, in *Radionuclide Generators. American Chemical Society Symposium Series 241* (eds F.F. Knapp Jr and T.A. Butler), American Chemical Society, Washington DC, pp. 67–73.
2. Mettler, F.A. and Guiberteau, M.J. (1991) *Essentials of Nuclear Medicine Imaging*. 3rd edn, W.B. Saunders, Philadelphia, pp. 141–76.
3. Susskind, H., Atkins, H.L., Cohn, S.H., *et al.* (1977) Whole body retention of radio xenon. *J. Nucl. Med.*, **18**, 462–71.
4. ICRP Publication 53 (1990) *Radiation Dose to Patients from Radiopharmaceuticals*, Pergamon Press, Oxford, 159–60, 341–45.

14

Positron emission tomographic (PET) radiopharmaceuticals

There are two main sources of PET radiopharmaceuticals: cyclotron produced and generator produced.

CYCLOTRON PRODUCED

Positron emitters produced in a cyclotron for labeling PET radiopharmaceuticals are mainly carbon-11 (^{11}C), nitrogen-13 (^{13}N), oxygen-15 (^{15}O) and fluorine-18 (^{18}F). They are often referred to as physiologic radionuclides because they can be labeled to substrates, substrate analogs and drugs without changing their biochemical behavior. They are therefore useful for investigating and measuring biochemical processes that are essential to life. Some of these processes include local rates of blood flow, metabolism, membrane transport (passive or specialized), protein synthesis, change in receptor density and/or binding and regional cerebral blood volume. The physical characteristics and production reactions of the four radionuclides are summarized in Table 14.1.

SUBSTRATE OR SUBSTRATE ANALOG

Several factors influence the choice of a substrate or its analog for measuring biochemical processes. If an analog is used, the relationship between it and the substrate must be established. The proper choice of substrate or analog depends mostly on the physiologic process to be measured, and other factors include availability, ease of synthesis of the tracer and its radiation dosimetry.

The tracer must be related to the process to be measured, and both its physical half-life

Table 14.1 Physical properties and production of some positron emitters

Radionuclide	*Half-life (min)*	*Energy (MeV)*	*Mode of production*
Carbon-11	20	0.970 (100%)	^{10}B (d, n) ^{11}C ^{11}B (p, n) ^{11}C ^{14}N (p, α) ^{11}C
Nitrogen-13	10	1.190 (100%)	^{12}C (d, n) ^{13}N ^{13}C (p, n) ^{13}N
Oxygen-15	2	1.7 (100%)	^{15}N (p, n) ^{15}O ^{14}N (d, n) ^{15}O
Fluorine-18	110	0.630 (97%)	^{20}Ne (d, α) ^{18}F ^{18}O (p, n) ^{18}F

and residence time in the target organ must be within the time frame of acquisition by the PET instrumentation. The tracer should not be related to other processes so that the tracer kinetics will reflect only the process under study. For example, carbon-11-labeled glucose (like the natural glucose substrate) goes through many reaction steps in the glycolytic pathway before it is eliminated as CO_2 or other labeled metabolite(s). Some ^{11}C-labeled metabolic intermediates will probably appear in the blood circulation shortly after intravenous injection of the tracer. Hence, labeled glucose is not a good tracer for measurement of glucose utilization because the kinetic measurement will contain parameters about kinetic processes that are not directly related to utilization of glucose by the tissue.

The type and position of the label in the tracer is very important. Consider the study of protein synthesis using amino acids (leucine labeled with ^{13}N at the amino group or ^{11}C at the carboxylic end; Figure 14.1). The leucine, in addition to being incorporated into proteins, is also metabolized to glutamate and ultimately to carbon dioxide through a series of biochemical reactions shown in Figure 14.2. If the leucine is labeled with ^{13}N, some of the label will be incorporated into the protein, while the rest will end

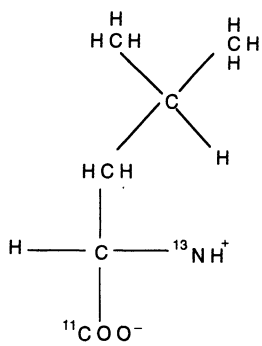

Figure 14.1 Structural formula of leucine showing labeling with ^{13}N at the amino group of ^{11}C at the carboxylic group.

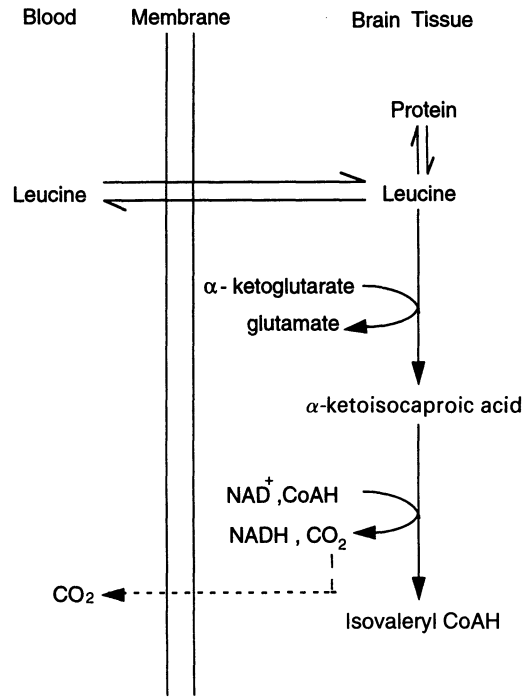

Figure 14.2 The biotransformation of leucine involving several biochemical reactions that lead to the cleavage of carbon dioxide.

up in the glutamate or some other amino acid. If the leucine is labeled with ^{11}C (at the carboxylic group), the label is either incorporated into the protein or cleaved off as $^{11}CO_2$ which is cleared through the venous blood and exhaled from the lungs. The remaining ^{11}C in the tissue is involved in protein synthesis. Thus, when labeling, important consideration should be given not only to the type but also to the position of the radionuclide in the tracer.

The relationship of the analog to the substrate must be established. For example, ^{11}C-2-deoxy-D-glucose (^{11}C-DG) or [^{18}F] 2-fluoro-2 deoxy-D-glucose (^{18}FDG) can be used instead of labeled glucose. ^{11}C has a short $t_{1/2}$ (20 min), but it takes more than 40 min for the blood clearance to reach a low level. Therefore ^{11}C-DG is not suitable for measuring

Table 14.2 Labeled positron compounds produced in automated system

Carbon-11	*Nitrogen-13*	*Oxygen-15*	*Fluorine-18*
Carbon dioxide	Ammonia	Oxygen	Fluorine
Carbon monoxide	Nitrogen	Carbon dioxide	Fluorodeoxyglucose
Hydrogen cyanide	Nitrous oxide	Carbon monoxide	Fluoridic acid
Deoxyglucose		Water	
Methane			
Methyl iodide			
Palmitic acid			

glucose utilization. ^{18}F has a $t_{1/2}$ of 110 min, which is long enough to achieve low level background activity. ^{18}FDG is transported and phosphorylated as glucose, but ^{18}FDG-6-PO_4 does not participate in further glycolytic reactions and does not cross the membrane and leave the tissue. This behavior makes ^{18}FDG a good substrate for measuring glucose utilization in tissue. The relationship between ^{18}FDG and glucose in their membrane transport and phosphorylation is characterized by a parameter called a lump constant, which is based on the principles of competitive enzyme kinetics [1, 2]. The value of the lump constant in cerebral and myocardial tissues under various conditions has been extensively studied so that rate of glucose utilization is predictable from the kinetics of ^{18}FDG [1–4].

Automated systems have been developed for the preparation of precursors and a few radiopharmaceuticals are labeled with ^{11}C, ^{13}N, ^{15}O and ^{18}F. These are summarized in Table 14.2 [5].

Many tracers labeled with these radionuclides have been evaluated for a number of biochemical processes in animals and humans and are summarized in Table 14.3. Most of these tracers have not been developed beyond the animal stage; few have been tried in humans and data on them are very sketchy. Many more receptor tracers are listed in Table 14.3 than in Table 12.1 in order to emphasize the amount of research into the use of cyclotrons to produce PET radiopharmaceuticals, as reviewed nicely by Stocklin [6].

Of these cyclotron-produced positron-emitting radiopharmaceuticals, ^{18}F-fluoro-2-deoxyglucose, ^{15}O-oxygen, ^{15}O-carbon dioxide, ^{15}O-carbon monoxide and ^{13}N-ammonia are described in this chapter.

Table 14.3 Biochemical imaging applications of PET radiopharmaceuticals

Carbon-11	*Nitrogen-13*	*Oxygen-15*	*Fluorine-18*
Blood flow			
^{11}C-acetylene	^{13}N-ammonia	^{15}O-water	^{18}F-ethanol
^{11}C-methane	^{13}N-nitrous oxide	^{15}O-carbon dioxide	^{18}F-methanol
^{11}C-nicotine		^{15}O-ethanol	^{18}F-antipyrine
^{11}C-butanol			
Blood volume			
^{11}C-carbon monoxide		^{15}O-carbon monoxide	

Table 14.3 Continued

Carbon-11	*Nitrogen-13*	*Oxygen-15*	*Fluorine-18*
Myocardial free fatty acid metabolism			
^{11}C-palmitate			^{18}F-fluoro-6-thioheptadecanoic acid
Myocardial metabolism			
^{11}C-pyruvate	^{13}N-glutamine		
^{11}C-lactate	^{13}N-glutamate		
	^{13}N-alanine		
Glucose metabolism			
^{11}C-glucose			^{18}F-fluoro-deoxy-D-glucose
^{11}C-deoxyglucose			
^{11}C-methyl-D-glucose			
Oxygen metabolism			
		^{15}O-carbon dioxide	
		^{15}O-oxygen	
Protein synthesis			
^{11}C-*l*-*l*-leucine			^{18}F-*l*-4-fluorophenylalanine
^{11}C-methylleucine			
^{11}C-*l*-*S*-methionine			
^{11}C-*l*-*l*-tyrosine			
^{11}C-*l*-*l*-tryptophan			
Receptors			
Benzodiazepine			
^{11}C-flunitrazepam			
Opioid			
^{11}C-diprenorphine			
^{11}C-carfentanil			
Dopamine			
^{11}C-*l*-DOPA			^{18}F-fluorodopamine
^{11}C-pimozide			^{18}F-fluorohaloperidol
^{11}C-methylspiperone			^{18}F-spiroperidol
^{11}C-(S)-6-O-methyl eticlopride			^{18}F-ethylspiroperidol
^{11}C-(S)-12-O-methyl eticlopride			^{18}F-methylspiroperidol
Serotonin			
^{11}C-methylspiperone			
^{11}C-ketanserin			
^{11}C-methylketanserin			

Table 14.3 Continued

Carbon-11	*Nitrogen-13*	*Oxygen-15*	*Fluorine-18*
Dopamine (*continued*) ^{11}C-N-methyl benperidol ^{11}C-SCH 239166			
Muscarinic cholinergic ^{11}C-2-α-tropanyl benzylate			
Myocardial presynaptic cholinergic ^{11}C-*m*-hydroxyephedrine ^{11}C-benzovesamical			
Myocardial postsynaptic cholinergic ^{11}C-methylquinuclidinylbenzylate ^{11}C-methyltropanyl benzylate			

GENERATOR PRODUCED

The generator-produced positron radionuclides include copper-62 (^{62}Cu), gallium-68 (^{68}Ga), iodine-122 (^{122}I), manganese-52m (^{52m}Mn) and rubidium-82 (^{82}Rb). Of these, ^{68}Ga and ^{82}Rb seem to be most important. Several radiopharmaceuticals have been made with ^{68}Ga and evaluated clinically. A summary of these radiopharmaceuticals modified from [5] is given in Table 14.4. The ^{68}Ga PET radiopharmaceuticals behave biologically as the corresponding ^{67}Ga tracers.

The clinical utility of the generator-produced positron emitting radionuclides is limited because they cannot be used for labeling substrates, analogs and drugs without changing their biochemical behavior. Once changed, such a tracer may not be useful for studying biochemical processes.

However, ^{82}Rb rubidium chloride has been used for the diagnosis of coronary artery

Table 14.4 Generator-produced PET radiopharmaceuticals and their potential applications

Radiopharmaceutical	*Physical $t_{1/2}$ (min)*	*Energy (MeV)*	*Mode of production*	*Application*
^{52m}Mn-manganese chloride	21	1.63	^{50}Cr (α, 2n) ^{52}Fe $\rightarrow$ ^{52m}Mn	Myocardial perfusion
^{62}Cu-copper microspheres	9.8	2.91	^{63}Cu (p, 2n) ^{62}Zn $\rightarrow$ ^{62}Cu	Myocardial perfusion
^{68}Ga-albumin microspheres	68.3	1.9	^{66}Zn (α, 2n) ^{68}Ge $\rightarrow$ ^{68}Ga	Lung perfusion
^{68}Ga citrate				Soft-tissue tumors
^{68}Ga colloid				Liver
^{68}Ga-EDTA aerosol				Ventilation
^{68}Ga-RBCs				Myocardial blood volume

disease [7, 8], and it has been suggested that it might be useful for monitoring thrombolytic therapy because of its 75 s half-life [9–11]. The transport pathway and distribution of ^{82}Rb are similar to those of potassium [12]. Its myocardial uptake is flow limited; it is linear only up to 2.5 times normal flow rate. Consequently, at higher flow rate, the uptake is significantly underestimated, and at a lower flow rate it might be overestimated [9, 13]. The parent radionuclide (strontium-82) has a half-life of 25.0 days, so ^{82}Rb can easily be used by centers with a PET instrument and no cyclotron.

FLUORINE-18 2-DEOXY-2-FLUORO-D-GLUCOSE (^{18}FDG)

CHEMISTRY

Both FDG and 2-deoxy-D-glucose (DG) are substrate analogs of glucose. In DG a hydrogen atom is substituted for a hydroxyl group on the C-2 of glucose, while in FDG a fluorine atom is substituted for a hydrogen atom on the C-2 of DG. Unlike the carbon–iodine bond, the carbon–fluorine bond is strong, thereby making the label stable both *in vitro* and *in vivo*. Hexokinase activity is insensitive to structural modification at the C-2 position [14] and therefore catalyzes the phosphorylation of FDG as well as DG [15]. The physical characteristics of ^{18}F ($E\gamma = 511$ keV, $t_{1/2} = 110$ min) are suitable for (PET) imaging and chemical synthesis of ^{18}F radiopharmaceuticals. The most widely used ^{18}F radiopharmaceutical is ^{18}FDG.

PREPARATION

Fluorine-18 is produced in a cyclotron using the ^{20}Ne (d, α) ^{18}F reaction with 13.8 MeV deutrons on a target consisting of 0.1% F_2 in neon [16]. ^{18}F–F_2 is reacted with 3,4,6-tri-O-acetyl-D-glucal to yield ^{18}F-3,4,6-tri-O-acetyl-2-deoxy-2-fluoro-D-glucopyranosyl fluoride, which is hydrolyzed to ^{18}FDG [17]. The process of the preparation of ^{18}FDG is now fully automated.

QUALITY CONTROL

Place a drop of the ^{18}FDG preparation 1 cm from the lower end of an 8-cm TLC-SG strip and develop in a chloroform–methanol–water (30:9:1) mixture up to 6 cm and air dry. Cut the strip into two equal pieces and count each piece separately in a dose calibrator.

^{18}FDG is close to the origin (R_f 0.25), while the impurities are towards the solvent front (R_f 0.7) [15]. Calculate the radiochemical purity as follows:

$$\text{Radiochemical purity (\%)} = \frac{\text{Activity at origin}}{\text{Activity at (origin + solvent front)}} \times 100$$

DOSE

74–370 MBq (2–10 mCi).

INJECTION TO IMAGING TIME

45 min.

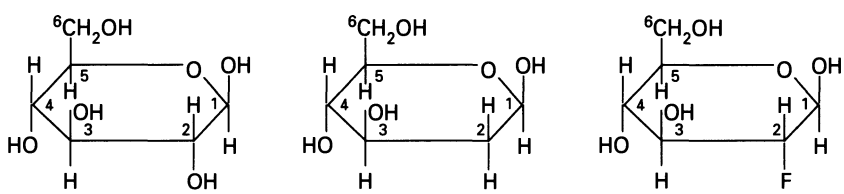

D-glucose | 2-Deoxy-D-glucose | 2-Fluoro-deoxy-D-glucose

BIOLOGIC BEHAVIOR

Following intravenous administration, ^{18}FDG is distributed to the brain, heart, lungs, liver and kidney, but it is retained only in the brain and heart, where the radioactivity is constant for 1–2 h in rats [15] and up to 4 h in human myocardium [18]. The myocardial and brain uptake in humans is 1–4 and 4–8% respectively [18]. The extracted ^{18}FDG is intracellularly converted to ^{18}FDG-6-phosphate by hexokinase activity [15]. ^{18}FDG-6-PO_4 does not significantly cross the cell membrane and is therefore trapped in the tissue (Figure 14.3). ^{18}FDG-6-PO_4 is also not a good substrate for glucose-6-phosphotase activity and is not converted to glycogen. Hence, the intracellular biotransformation of ^{18}FDG to ^{18}FDG-6-PO_4 and its subsequent retention make it a good analog for the *in vivo* study of local glucose metabolism or utilization in the brain and heart using PET for external detection [1,3]. The technique for the quantitation of local glucose utilization was developed by Sokoloff *et al.* [2] using carbon-14 deoxy-D-glucose. ^{18}FDG also accumulates in tumors, particularly central nervous system tumors [19, 20], presumably as a result of high glucose utilization and hexokinase activity in these tumors.

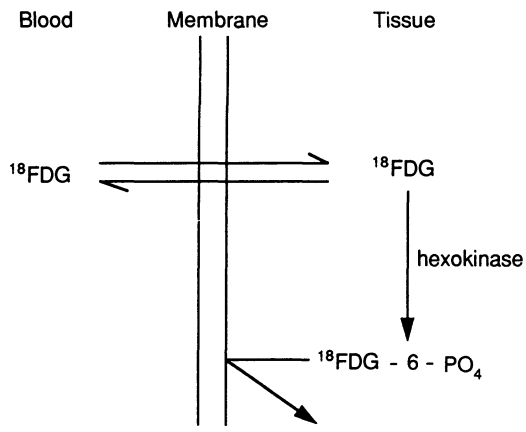

Figure 14.3 Intracellular phosphorylation of ^{18}FDG to ^{18}FDG-6-PO_4

^{18}FDG is cleared rapidly from blood with half-lives of 0.2–0.3 and 11.6 ± 1.1 min, followed by a small component with $t_{1/2}$ of 88 ± 4 min [18]. ^{18}FDG in liver, lungs and kidneys is cleared rapidly and excreted into urine mostly as the parent ^{18}FDG, probably because of low hexokinase and/or glucose-6-phosphatase activity in these organs. ^{18}FDG is not reabsorbed in the renal tubules [15, 21].

USES

^{18}FDG is used for imaging and measuring glucose utilization or metabolism in the brain, heart and CNS tumors.

DOSIMETRY

The data are modified from [22] and listed in Table 14.5.

Table 14.5 Estimated radiation absorbed dose of ^{18}FDG

Organ	*mGy/MBq*	*rad/mCi*
Brain	0.029	0.107
Heart	0.045	0.166
Bladder wall	0.066	0.244
Kidneys	0.030	0.111
Liver	0.023	0.085
Spleen	0.022	0.081
Pancreas	0.020	0.074
Uterus	0.019	0.070
Adrenals	0.018	0.067
GI tract		
Lower large intestine	0.018	0.067
Upper large intestine	0.017	0.063
Small intestine	0.017	0.063
Stomach	0.015	0.056
Testes	0.015	0.056
Bone surface	0.015	0.056
Thyroid	0.013	0.048
Red marrow	0.012	0.044
Lungs	0.011	0.041
Breast	0.010	0.037
Other tissues	0.010	0.037

OXYGEN-15-LABELED OXYGEN, CARBON DIOXIDE AND CARBON MONOXIDE ($^{15}O_2$, ^{15}O-CO_2, ^{15}O-CO)

Oxygen, carbon dioxide and carbon monoxide are molecular gases. Both O_2 and CO_2 are contained in the atmospheric air with respective partial pressures of 159 and 0.2 mmHg or 21% and 0.03% by volume. Inhaled oxygen is transported in arterial blood as oxyhemoglobin to tissues, where it is released and metabolized to CO_2, which is exhaled from the lungs. Both the inhalation of O_2 and exhalation of CO_2 occur by the process of diffusion, as summarized in Figure 14.4.

Oxygen-15 is a pure positron emitter (99.98%) with a mean energy of 0.72 MeV and a half-life of 2 min. $^{15}O_2$, ^{15}O-CO_2 and ^{15}O-CO are prepared by automated processes in a medical cyclotron using either the ^{15}N (p, n)-^{15}O or ^{14}N (d, n)^{15}O reaction [5].

DOSE

37 MBq (1 mCi) per liter of air by either bolus or continuous inhalation.

INHALATION TO IMAGING TIME

Immediately.

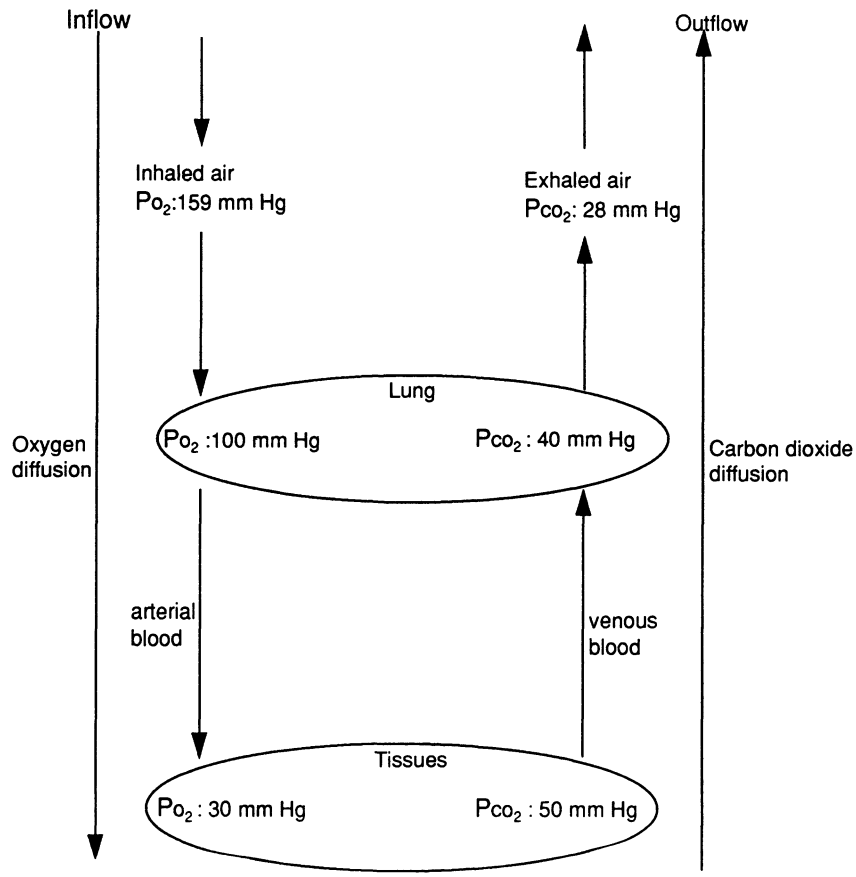

Figure 14.4 Diffusional transport of oxygen and carbon dioxide in the body.

BIOLOGIC BEHAVIOR

Inhaled $^{15}O_2$ is either dissolved or bound to hemoglobin in blood. Dissolved $^{15}O_2$ is metabolized to water, and $^{15}O_2$-bound hemoglobin is transported by diffusion to the tissues, where it is metabolized to ^{15}O-CO_2 and exhaled from the lungs.

Inhaled ^{15}O-CO_2 is rapidly biotransformed to bicarbonate within the lung and to water in the alveolar region [23]. The disappearance of CO_2 from the lung has a $t_{1/2}$ of 1.0 ± 0.1 s [24].

Once the inhaled ^{15}O-CO is absorbed, it is basically bound to hemoglobin and its clearance from the lung has a $t_{1/2}$ of 10.8 s [24].

Within the tissues, exchange of the gases is faster in the brain than in the muscles, as shown by the estimated radiation dose to these organs (Table 14.6).

USES

- Estimation of blood flow (^{15}O-CO_2).
- Measurement of oxygen metabolism ($^{15}O_2$ and ^{15}O-CO_2).
- Measurement of blood volume (^{15}O-CO).

DOSIMETRY

The data are modified from [24] and listed in Table 14.6. It was assumed that the gas was inhaled for 1 h at a concentration of 37 MBq (1 mCi per liter) of air.

NITROGEN-13 AMMONIA ($^{13}NH_3$)

Ammonia in aqueous solution does not exist in the hydroxide from (NH_4OH) but rather as dissolved gas. Its myocardial uptake is by diffusion and not by active transport of NH^+_4 [25]. Biologically, it behaves like an amine, and it is considered to be the simplest member of the group. $^{13}NH_3$ has a physical half-life of 10 min and is produced according to the ^{12}C (d, n) ^{13}N or ^{13}C (p, n) ^{13}N reaction in a cyclotron. Methane gas is bombarded with 7–8 MeV deuterons; $^{13}NH_3$, the main product of the reaction, is purified by distillation in basic solution to remove contaminants such as low molecular weight amines and traces of cyanide. $^{13}NH_3$ is bubbled through sterile, pyrogen-free saline and is sterilized by membrane filtration [25].

DOSE

370–555 MBq (10–15 mCi).

ADMINISTRATION TO IMAGING TIME

Immediately.

Table 14.6 Estimated radiation absorbed doses of $^{15}O_2$, ^{15}O-CO_2 and ^{15}O-CO

	$^{15}O_2$		^{15}O-CO_2		^{15}O-CO	
Organ	*mGy/MBq*	*rad/mCi*	*mGy/MBq*	*rad/mCi*	*mGy/MBq*	*rad/mCi*
Lung	946	3500	276	1020	798	2700
Heart contents	4.86	18	3.5	13.0	10.0	37
Muscle	4.22	15.6	13.5	50.0	3.19	11.8
Liver	1.78	6.6	2.6	9.7	2.05	7.6
Heart wall	0.81	3.0	1.1	4.0	1.1	4.0
Spleen	0.38	1.4	0.24	0.9	0.65	2.4
Kidneys	0.16	0.6	0.19	0.7	0.22	0.8
Brain	0.11	0.4	0.19	0.7	0.03	0.1
Residual body	10.00	37.0	15.0	55.7	11.2	41.7

BIOLOGIC BEHAVIOR

Following administration of $^{13}NH_3$ by inhalation or intravenous or subcutaneous injection, ammonia is taken up by the brain, heart, liver, lungs and kidneys [25–27]. It is extracted by the myocardium largely during the first pass and decreases slightly during the next few minutes but remains virtually constant for up to 30 min. The activity in the lungs is cleared slowly, and it is about 50% of the accumulated activity in the myocardium. The uptake in the liver is about the same as that in the myocardium within 6–8 min after injection. Its excretion into urine is very rapid with a half-life of 10 min. Its blood clearance is also very rapid, and approximately 85% of the radioactivity is eliminated from blood in the first minute [25]. Total body and liver radiation absorbed dose is 1.35 mGy/MBq (5 mrad/mCi) and 6.75 mGy/MBq (25 mrad/mCi) respectively.

USES

- Diagnosis of coronary artery disease.
- Measurement of blood flow.
- Preparation of other ^{13}N-labeled radiopharmaceuticals.

REFERENCES

1. Phelps, M.E., Huang, S.C., Hoffman, E.J. *et al.* (1979) Tomographic measurements of local cerebral glucose metabolic rate in humans with [F-18]-2-fluorodeoxy-D-glucose: validation of method. *Ann. Neurol.*, **6**, 371–88.
2. Sokoloff, L., Reivich, M., Kennedy, C. *et al.* (1977) The [C-14] deoxyglucose method for the measurement of local cerebral glucose utilization: theory, procedure and normal values in the conscious and anesthetized albino rat. *J. Neurochem.*, **28**, 897–916.
3. Reivich, M., Kuhl, D., Wolf, A. *et al.* (1979) The [F-18] fluorodeoxy glucose method for the measurement of local cerebral glucose utilization in man. *Circ. Res.*, **44**, 127–37.
4. Sokoloff, L. (1981) Localization of functional activity in the central nervous system by measurement of glucose utilization with radioactive deoxyglucose. A review. *J. Cereb. Blood Flow Metab.*, **1**, 7–36.
5. Product Information (1986) *Positron Emission Tomography Planning Guide*, Computer Technology and Imaging, TN.
6. Stocklin, G. (1992) Tracers for metabolic imaging of brain and heart. A review. *Eur. J. Nucl. Med.*, **19**, 527–51.
7. Gould, K.L., Goldstein, R.A., Mullani, N.A. *et al.* (1986) Noninvasive assessment of coronary stenoses by myocardial perfusion imaging during pharmacologic vasodilation. VIII. Clinical feasibility of positron cardiac imaging without a cyclotron using rubidium-82. *J. Am. Coll. Cardiol.*, **7**, 775–89.
8. Goldstein, R.A., Mullani, N.A., Wong. W.-H. *et al.* (1986) Positron imaging of myocardial infarction with rubidium-82. *J. Nucl. Med.*, **27**, 1824–29.
9. Goldstein, R.A., Mullani, N.A., Fisher, D.J. *et al.* (1983) Myocardial perfusion with rubidium-82. II. Effects of metabolic and pharmaceutical interventions. *J. Nucl. Med.*, **24**, 907–15.
10. Smalling, R.W., Fuentes, F., Mathews, M.W. *et al.* (1983) Sustained improvement in left ventricular function and mortality by intracoronary streptokinase administration during evolving myocardial infarction. *Circulation*, **68**, 131–38.
11. Kennedy, J.W., Ritchie, J.L., David, K.B. *et al.* (1983) Western Washington randomized trial of intracoronary streptokinase in acute myocardial infarction. *N. Engl. J. Med.*, **309**, 1477–82.
12. Sheehan, R.M. and Renkin, E.M. (1972) Capillary interstitial and cell membrane barriers to blood–tissue transport of potassium and rubidium in mammalian skeletal muscle. *Circ. Res.*, **30**, 588–607.
13. Selwyn, A.P., Allan, R.M., L'abbate, A. *et al.* (1982) Relation between regional myocardial uptake of rubidium-82 and perfusion: absolute reduction of cation uptake in ischemia. *Am. J. Cardiol.*, **50**, 112–21.
14. Coe, E.L. (1972) Inhibition of glycolysis in ascites tumor cells pre-incubated with 2-deoxy-2-fluoro-D-glucose. *Biochim. Biophys. Acta*, **264**, 319–27.

15. Gallagher, B.M., Fowler, J.S., Gutterson, N.I. *et al.* (1978) Metabolic trapping as a principle of radiopharmaceutical design: some factors responsible for the biodistribution of [^{18}F] 2-deoxy-2-fluoro-D-glucose. *J. Nucl. Med.*, **19**, 1154–61.
16. Lambrecht, R.M. and Wolf, A.P. (1973) Cyclotron and short-lived halogen isotopes for radiopharmaceutical applications, in *Radiopharmaceuticals and Labeled Compounds*, IAEA-SM-171/79, Copenhagen, Denmark.
17. Ido, T., Wan, C.N., Fowler, J.S. *et al.* (1977) Fluorination with F_2. A convenient synthesis of 2-deoxy-2-fluoro-D-glucose. *J. Org. Chem.*, **42**, 2341–42.
18. Phelps, M.E., Hoffman, E.J., Selin, C. *et al.* (1978) Investigation of [^{18}F] 2-fluoro-2-deoxyglucose for the measure of myocardial glucose metabolism. *J. Nucl. Med.*, **19**, 1311–19.
19. Di Chiro, G., De Lapaz, R.L., Brooks, R.A. *et al.* (1982) Glucose utilization of cerebral gliomas measured by [^{18}F] fluorodeoxy glucose and positron emission tomography. *Neurology*, **32**, 1323–29.
20. Di Chiro, G. (1987) Positron emission tomography using [^{18}F] fluorodeoxyglucose in brain tumors. *Invest. Radiol.*, **22**, 360–70.
21. Gallaghar, B.M., Ansari, A., Atkins, H. *et al.* (1977) Radiopharmaceuticals XXVII. 18F-labeled 2-deoxy-2-fluoro-D-glucose as a radiopharmaceutical for measuring regional myocardial glucose metabolism in-vivo: tissue distribution and imaging studies in animals. *J. Nucl. Med.*, **18**, 990–96.
22. Mejia, A.A., Nakamura, T., Masatoshi, I. *et al.* (1991) Estimation of absorbed doses in humans due to intravenous administration of fluorine-18-fluorodeoxyglucose in PET studies. *J. Nucl. Med.*, **32**, 699–706.
23. West, J.B. and Dollery, C.T. (1962) Uptake of oxygen-15-labeled CO_2 compared with carbon-11-labeled CO_2 in lung. *J. Appl. Physiol.*, **17**, 14–20.
24. Bigler, R.E. and Sgouros, G. (1983) Biological analysis and dosimetry for ^{15}O-labeled O_2, CO_2 and CO gases administered continuously by inhalation. *J. Nucl. Med.*, **24**, 431–37.
25. Harper, P.V., Lathrop, K.A., Krizek, H. *et al.* (1972) Clinical feasibility of myocardial imaging with $^{13}NH_3$. *J. Nucl. Med.*, **13**, 278–80.
26. Harper, P.V., Lathrop, K.A., Krizek, H. (1975) ^{13}N radiopharmaceuticals, in *Radiopharmaceuticals* (eds G. Subramanian, B.A. Rhodes, J.F. Cooper and V.J. Sodd), The Society of Nuclear Medicine, New York, pp. 180–83.
27. Monahan, W.G., Tilbury, R.S. and Laughlin, J.S. (1972) Uptake of ^{13}N-labeled ammonia. *J. Nucl. Med.*, **13**, 274–77.

15

Non-imaging radiopharmaceuticals

The non-imaging radiopharmaceuticals described in this chapter include ^{51}Cr-RBCs, $^{57/58}$Co-vitamin B_{12}, ^{59}Fe citrate, ^{125}I-HSA and ^{125}I-fibrinogen. Details of procedures and calculations involving the use of these radioactive tracers are included for practical uses.

CHROMIUM-51 RED BLOOD CELLS (^{51}Cr-RBCs)

CHEMISTRY

Sodium chromate ($^{51}CrO_4^{2-}$) diffuses freely into the red cells, where it is reduced to the trivalent cation Cr^{3+}, which binds firmly to the beta chains of hemoglobin [1]. Cationic chromium is not used directly because it binds to plasma proteins and therefore cannot diffuse into cells. Within 20 min of incubation 85–95% of ^{51}Cr binds to RBCs [2].

PHYSICAL PROPERTIES OF ^{51}Cr

Chromium-51 decays by 100% electron capture, emitting monoenergetic 320 keV gamma rays with a photon abundance of approximately 9%. It is produced in a nuclear reactor by the $^{50}Cr\ (n,\gamma)^{51}Cr$ reaction and has a half-life of 27.8 days.

PREPARATION

Withdraw 15–20 ml of blood into a sterile vented vial containing 4 ml of ACD solution. Add 1.85–11.1 MBq (50–300 μCi) of ^{51}Cr-Na_2CrO_4, gently mix and allow to stand at room temperature for 20 min. Add 100 mg (1 ml) of ascorbic acid to reduce unreacted CrO_4^{2-} to Cr^{3+} ion.

To ensure high labeling efficiency and to avoid chromium toxicity to red cells, do not use ^{51}Cr-Na_2CrO_4 that has a specific activity less than 1.85 GBq/mg (50 mCi/mg).

QUALITY CONTROL

Withdraw 0.2 ml of labeled red cells into a test tube, add 1 ml of saline, mix and centrifuge at 1000 g for 5 min. Aspirate the supernatant and count each layer separately in a well counter. Calculate the labelling efficiency as follows:

$$\text{Labeling efficiency (\%)} = \frac{\text{Counts in RCBs}}{\text{Counts in (supernatant + RCBs)}} \times 100$$

Note: If the labeling efficiency is more than 90% inject the preparation. If not, centrifuge, remove supernatant, resuspend the packed cells in saline and inject.

DOSES

Red cell mass estimation	740–1110 KBq (20–30 μCi)
Red cell survival determination	2.96–3.7 MBq (80–100 μCi)

INJECTION TO STUDY TIME

Red cell mass	20 min
Red cell survival	20 min, daily for the first week and on alternate days for another 2–3 weeks

BIOLOGIC BEHAVIOR

Upon intravenous injection ^{51}Cr-RBCs remain in the circulation for a long time and are distributed uniformly throughout the body. The half-life of the blood clearance in normal subjects is 25–33 days [3] but is reduced in patients with various blood disorders, such as hemolytic anemia and liver and spleen functional abnormalities [4]. Approximately 1% of ^{51}Cr is eluted daily from the red cells of normal subjects [5]. The radioactivity eluted from the RBCs is excreted in urine.

USES

- Estimation of red cell mass and blood volume.
- Determination of red cell survival and sequestration.

CALCULATIONS

RBC mass estimation

Make a standard solution by diluting 2 ml of labeled red cells to 100 ml. Withdraw 5 ml of venous blood 20 min (A_{20}) post injection into a tube containing 1–2 mg of EDTA. Count 3 ml of the sample and standard separately into well counter. Calculate blood volume as follows:

$$\text{Blood volume} = \frac{SVD}{A_{20}}$$

where S is the counts/min of 3 ml of standard, V is the volume of blood injected, D is the dilution factor of the standard and A_{20} is the counts/min of 3 ml of blood sample collected at 20 min.

$$\text{Red cell mass} = \text{blood volume} \times \text{hematocrit} \times 0.91$$

The hematocrit is determined by the standard microhematocrit method. The normal range for total blood volume is 60–80 ml per kg body weight [6]. The normal range for red cell mass is 30 ± 5 ml per kg body weight [6].

Red cell survival determination

Withdraw 5 ml of venous blood 20 min post injection into a tube containing 1–2 mg of EDTA. Repeat daily for a week and on alternate days for another 2 weeks. Determine the hematocrit of all the blood samples on the day of collection. On the final day of collection count the radioactivity in 3 ml of each sample and calculate the net counts per minute (c.p.m.) as follows:

$$\text{Net c.p.m. per ml of red blood cells} = \frac{\text{Total c.p.m} - \text{background c.p.m}}{3 \times \text{hematocrit factor}}$$

Apply the necessary corrections for daily elution of ^{51}Cr from red cells using Table 15.1. Normalize all results by dividing each count

Table 15.1 Correction of ^{51}Cr elution from ^{51}Cr-RBCs (data taken from [5])

Day	*Correction factor*	*Day*	*Correction factor*
1	1.03	9	1.13
2	1.05	11	1.16
3	1.06	13	1.18
4	1.07	15	1.20
5	1.08	17	1.22
6	1.10	19	1.26
7	1.11	21	1.29
8	1.12		

Table 15.2 Estimated radiation absorbed of ^{51}Cr-RBCs

Organ	*mGy/MBq*	*rad/mCi*
Spleen	1.6	5.92
Heart	0.51	1.89
Lungs	0.32	1.18
Uterus	0.085	0.314
Ovaries	0.082	0.303
Testes	0.063	0.233

by the 20-min sample count and multiply by 100. Plot a semilogarithmic graph of percentage activity versus time and determine the half-life of ^{51}Cr-labeled RBCs. The normal half-life of ^{51}Cr-labeled RBCs is 25–33 days [4].

SURFACE COUNTING

Count the radioactivity over liver, spleen and heart using a scintillation detector fitted with a 10° flat-field collimator (thyroid uptake unit). Determine the ratio of counts over spleen/heart and liver/heart. If the spleen/heart ratio is greater than 2, abnormal sequestration in the spleen is indicated.

DOSIMETRY

The data are modified from [7] and listed in Table 15.2.

COBALT-57/58 CYANOCOBALAMIN ($^{57/58}$CO-VITAMIN B_{12})

Cynocobalamin (vitamin B_{12}) is a corrinoid complex with cobalt as the central atom. It has two characteristic components: a corrin ring system and a ribonucleotide. The corrin ring system is the larger component and resembles the porphyrin ring system of hemoglobin. It contains four pyrrole rings, but in a pair of these a five-membered ring is joined directly rather than through a methene bridge. Four nitrogen atoms of the corrin ring are coordinated to the cobalt atom. The ribonucleotide is joined to the corrin ring by a coordination bond between the other nitrogen atom of the nucleotide and the cobalt atom, and by an ester linkage between the 3′-phosphate group of the ribonucleotide and a side-chain of the corrin ring. Cyanide occupies one of the coordination positions of the cobalt atom, hence the name cyanocobalamin. Ironically, cyanide is present as an artefact of isolation. In coenzyme B_{12} the cyanide ligand is replaced by a 5-deoxyadenosyl group.

It is difficult to chemically synthesize vitamin B_{12} in the laboratory, hence it is produced by biosynthesis. The bacterium *Streptomyces griseus* is cultured in a medium containing either ^{57}Co or ^{58}Co. After adequate multiplication the bacteria are harvested and the radioactive vitamin B_{12} is isolated [7].

PHYSICAL PROPERTIES OF $^{57/58}$Co

The physical half-life, decay modes and gamma energies are summarized in Table 15.3.

^{57}Co and ^{58}Co are produced in a cyclotron by the following respective nuclear reactions: ^{56}Fe (d,n) ^{57}Co and ^{55}Mn (α,n) ^{58}Co.

DOSES

^{57}Co-vitamin B_{12} (orally)	18.5–37 kBq (0.5–1 μCi)
^{58}Co-vitamin B_{12} (orally)	37 kBq (1 μCi)

Table 15.3 Physical characteristics of $^{57/58}$Co

Radionuclide	*Half-life*	*Decay mode*	*Gamma energy (keV)*
^{57}Co	270 days	EC	122 (87%), 136 (11%)
^{58}Co	72 days	EC, β^+, γ	511 (30%), 810 (99%)

Non-radioactive vitamin B_{12}	1 mg as a flushing dose is injected intramuscularly 1–2 h after oral administration of radioactive vitamin B_{12}.

PATIENT PREPARATION

Patients are asked to fast overnight and to continue fasting for 2 h after oral administration of the radioactive vitamin B_{12}.

BIOLOGIC BEHAVIOR

In normal adults, 70% of the orally administered dose is absorbed in the terminal ileum. Upon intramuscular administration of the flushing dose, 33% of the absorbed radiopharmaceutical is eliminated by glomerular filtration, while 40% accumulates in the liver. The body retention is multiexponential with half-lives of 100 min (34%), 1 day (6%) and 500 days (60%) [8].

USES

- Assessment of vitamin B_{12} malabsorption.
- Diagnosis of pernicious anemia.

ABSORPTION TEST (SCHILLING)

This involves the ingestion of $^{57/58}$Co-vitamin B_{12}, followed by intramuscular injection of a flushing dose, and quantitative estimation of subsequent urinary excretion. If the estimated absorption is low, the test is repeated with administration of exogenous intrinsic factor (IF) for correction of IF deficiency to rule out pernicious anemia. The repetition of the test is inconvenient to the patient, and to overcome this problem a dual isotope Schilling test has been introduced, which involves the simultaneous administration of free ^{58}Co-vitamin B_{12} and ^{57}Co-vitamin B_{12} bound to IF [9, 10]. The dual isotope procedure is also helpful in eliminating errors associated with urine collection.

Procedure and calculations

Single isotope test

One microgram of vitamin B_{12} containing 3.7 kBq (1 μCi) of ^{57}Co in either liquid or capsule form is given orally to the patient. After 1–2 h, 1 mg of non-radioactive cyanocobalamin is adminstered intramuscularly. The patient is asked to collect urine for 24 h. A standard is prepared by diluting an equivalent dose to 100 ml. A 2-ml aliquot is counted. The volume of urine collected is measured, and the 2-ml aliquot is also counted.

Calculations

$$\text{Excretion of } ^{57}\text{Co-vitamin } B_{12}(\%) = \frac{2 \times U \times \text{count/min in urine aliquot}}{\text{Counts/min in standard}}$$

$$\text{where } U = \frac{\text{Total volume of urine (ml)}}{\text{Volume of urine counted}}$$

If the calculated excretion is less than 6% of the administered dose, the test is repeated with ^{57}Co-vitamin B_{12} bound to intrinsic factor.

Dual isotope test

A dose of 0.25 μg of vitamin B_{12} containing 29.6 kBq (0.8 μCi) of ^{58}Co and 18.5 kBq (0.5 μCi) of ^{57}Co bound to intrinsic factor is orally administered simultaneously to the patient. After 1–2 h, 1 mg of non-radioactive vitamin B_{12} is injected intramuscularly as a flushing dose. The patient is also asked to collect urine for 24 h. The total volume of urine collected is

Table 15.4 Procedure of counting $^{57/58}$Co

Aliquot	*^{57}Co setting c.p.m. – background*	*^{58}Co setting c.p.m. – background*	*Scatter factor*	*Net c.p.m. due to ^{57}Co*	*Net c.p.m. due to ^{58}Co*
^{57}Co standard (2%)	*A*	–	–	*A*	–
^{58}Co standard (2%)	*B*	*C*	*B/C=S*	–	*C*
Urine sample	*D*	*E*	–	*D – ES*	*E*

measured and a 2-ml aliquot is pipetted out for counting. Standards of ^{57}Co- and ^{58}Co-vitamin B_{12} are prepared as previously described. An aliquot of 2 ml each is counted separately. The test sample and standards are counted in the integral mode. For ^{57}Co, the baseline is set at 100, while that of ^{58}Co is set at 450. Background radioactivity is also counted for 15 ± 5 min. Record the counts as shown in Table 15.4.

Calculations

Excretion of ^{57}Co-vitamin $B_{12}(\%) = 2U(D-ES)/A$

Excretion of ^{58}Co-vitamin $B_{12}(\%) = 2UE/C$

$$\text{where } U = \frac{\text{Total volume of urine collected (ml)}}{\text{Volume of urine counted}}$$

$$\text{excretion ratio} = \frac{^{57}\text{Co excreted (\%)}}{^{58}\text{Co excreted (\%)}}$$

It is recommended that gross count rates of urine be at least twice the background in the ^{57}Co setting and $1\frac{1}{2}$ times in the ^{58}Co setting.

DOSIMETRY

The data are modified from [8] and listed in Table 15.5.

Table 15.5 Estimated radiation absorbed dose of $^{57/58}$Co-vitamin B_{12}

Organ	*^{57}Co-vitamin B_{12}*		*^{58}Co-vitamin B_{12}*	
	mGy/MBq	*rad/mCi*	*mGy/MBq*	*rad/mCi*
Liver	24.0	88.8	36.0	133.2
Pancreas	2.6	9.6	6.1	22.5
Adrenal	2.5	9.25	6.7	24.79
Kidneys	2.3	8.51	5.3	19.61
GI tract				
Upper large intestinal wall	1.8	6.66	4.4	16.28
Stomach wall	1.4	5.18	3.3	12.21
Small intestine	1.4	5.18	3.2	11.84
Lungs	1.6	5.92	3.6	13.32
Red marrow	1.5	5.55	2.2	8.14
Bone surfaces	1.2	4.44	1.8	6.66
Uterus	0.84	3.10	1.9	7.03
Ovaries	0.83	3.07	1.8	6.66
Bladder wall	0.64	2.37	1.6	5.92
Testes	0.46	1.70	1.4	5.18

FERROUS-59 CITRATE (^{59}Fe CITRATE)

CHEMISTRY

Iron is a transition element of group VIII. In aqueous medium, iron salts of halides, sulfates and nitrates undergo hydrolysis reaction to form ferric hydroxide at high pH. However, it is stabilized by reacting with ligands (such as citrate and acetate) to form weak complexes.

^{59}Fe has a half-life of 44.5 days; it decays by β^- with gamma emissions of 1.095 (56%) and 1.292 MeV (44%). ^{59}Fe citrate is produced in a nuclear reactor by irradiating enriched $^{58}FeCl_2$ according to the $^{58}Fe(n,\gamma)$ ^{59}Fe reaction. The target is dissolved in sodium citrate solution.

QUALITY CONTROL

The manufacturer performs the necessary quality control tests for ^{59}Fe prior to distribution. ^{59}Fe is usually > 99.9% pure with minimal contamination of ^{55}Fe ($t_{1/2}$ 2.6 years).

DOSES

Iron absorption study	74–185 kBq (2–5 μCi)
Ferrokinetic studies	185–370 kBq (5–10 μCi)

ADMINISTRATION TO STUDY TIME

Iron absorption study	5 days
Ferrokinetic studies	5 min to 2 weeks

BIOLOGIC BEHAVIOR

Following intravenous injection, ^{59}Fe citrate binds to transferrin and the complex is transported to the bone marrow or other sites of erythropoiesis with a normal half-life of 60–140 min [11]. Within 24 h, 70–90% of the ^{59}Fe citrate accumulates in bone marrow, where the complex dissociates, releasing the $^{59}Fe^{2+}$ ion at the surface of the erythroblasts. The Fe^{2+} ion is incorporated into hemoglobin. More than 80% of the radioactive iron incorporated into red cells is released into circulation within 7–8 days and remains in the red cells for approximately 120 ± 6 days in a normal subject [3].

Iron absorption in normal adult humans is 15–30% of the administered dose when given orally. This increases to 50–80% in iron defiency anemia and decreases to less than 10% in the malabsorption syndrome (11).

USES

^{59}Fe citrate is used in the determination of iron absorption, plasma clearance rate, plasma iron turnover and red cell utilization.

IRON METABOLISM STUDIES AND CALCULATIONS

Iron absorption test

To a solution containing 15 mg of $FeSO_4 \cdot 7H_2O$ and 18 mg of ascorbic acid in 10 ml of 1×10^{-3}M HCl, add 74 kBq (2 μCi) of $^{59}FeCl_3$, dilute to 25 ml with distilled water and orally administer 24 ml to the patient, who should have fasted overnight. The remaining 1 ml is used as a standard for counting. Collect the patient's feces in a plastic container for 5–7 days. Count each feces sample in a large-volume detector system with the standard diluted to an appropriate volume in a similar container. Calcualte the percentage excreted as follows:

$$\text{Excreted (\%)} = \frac{\text{Count in feces} \times 100}{\text{Count in standard} \times 24}$$

If a whole-body counting facility is available, measure the activity immediately after administration and 7 days later. Calculate the percentage absorption from the measured activity on the seventh day as follows:

$$\text{Absorbed (\%)} = \frac{\text{Activity on day 7}}{\text{Activity on day 1}} \times 100$$

The normal percentage absorption in adults is 15–30%. The value increases to 50–80% in iron deficiency anemia, while it decreases to less than 10% in the malabsorption syndrome.

FERROKINETIC TESTS

Ferrokinetic studies provide information on erythropoiesis, which includes plasma clearance rate, plasma iron turnover, iron incorporation into red cells and turnover by different organs.

PLASMA IRON CLEARANCE

Using an aseptic technique, add approximately 185 kBq (5 μCi) of ^{59}Fe citrate to 5–10 ml of the patient's plasma, and incubate at 37°C for 30 min. Inject 4–8 ml intravenously and save 2–4 ml to be used as a standard for counting. Collect 5-ml blood samples in a test tube containing anticoagulant at 10, 30, 60, 90 and 120 min. Centrifuge each blood sample and count 1 ml of plasma in a well counter. Plot a graph of activity versus time on semilogarithmic paper and determine both half-life and clearance rate from the slope. Slope = $-k/2.303$ and $t_{1/2} = k/0.693$, where k is the plasma clearance rate constant and $t_{1/2}$ is the half-life of plasma clearance.

The normal half-time of plasma clearance is 60–140 min.

Note that if the patient's plasma transferrin and iron-binding capacity is less than 0.6g/l and 20 μmol/l respectively a suitable donor plasma sample is substituted for the test.

PLASMA IRON TURNOVER (PIT)

Plasma iron turnover is determined by multiplying the plasma clearance rate by the plasma iron concentration, which is estimated chemically and expressed in the equation below:

$$\text{Plasma iron turnover} = k \times \text{plasma iron concentration}$$

where k is the plasma clearance rate constant. The normal value of PIT is 4.8 mg/l/day (70–140 μmol/l/day).

IRON UTILIZATION OR RED CELL UTILIZATION (RCU)

Blood samples of 3 ml are collected each day for 2 weeks after administration of ^{59}Fe. An aliquot of 1 ml and the stardard are counted separately in a well counter. The percentage red cell uptake is calculated as follows:

$$\text{RCU (\%)} = \frac{\text{c.p.m in 1 ml of red cells} \times \text{total red cell mass}}{\text{c.p.m in 1 ml of standard} \times \text{volume injected}} \times 100$$

Note that the red cell mass is estimated using ^{51}Cr-RBCs.

The graph of the RCU versus time is plotted on linear paper to determine the maximum iron utilization value. The normal value of RCU is 70–80%.

Table 15.6 compares the normal values of ferrokinetics with those obtained in various hemotological disorders.

DOSIMETRY

The data are modified from [12] and listed in Table 15.7.

SELENIUM-75 TAURA-23-SELENA-25-HOMOCHOLIC ACID (^{75}Se-HCAT)

CHEMISTRY

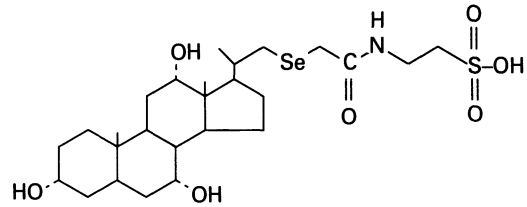

Table 15.6 Ferrokinetics in various hematological disorders

Hematological disorder	*Plasma clearance ($t_{1/2}$)*	*Plasma iron turnover*	*Red cell utilization*
Normal	60–140 min	70–140 μmol/l/day	70–80%
Hemolytic anemia	Lower	Higher	Higher
Aplastic anemia	Higher	Normal	Lower
Iron deficiency anemia	Higher	Normal	Higher
Secondary anemia	Slightly Lower	Normal	Normal
Polycythemia vera	Lower	Higher	Normal
Dyserythropolesis	Slightly Lower	Higher	Lower
Myelofibrosis	Lower	Higher	Lower

Se-HCAT is a ^{75}Se-labeled bile acid analog in which the carbon methylene group in the C-17 side-chain is replaced by selenium-75. Bile acids are 24-carbon steroid compounds. There are primary and secondary bile acids. It is the primary bile acids that are synthesized in the liver from cholestrol. In human bile, about 45% is chenodeoxycholic acid, 31% cholic acid and 24% deoxycholic acid. Bile acids are conjugated with glycine or taurine before

Table 15.7 Estimated radiation absorbed dose of ^{59}Fe citrate

Organs	*^{59}Fe i.v.*		*^{59}Fe oral*	
	mGy/MBq	*rad/mCi*	*mGy/MBq*	*rad/mCi*
Red marrow	13.00	48.1	1.50	5.55
Spleen	26.00	96.2	2.70	9.99
Heart	32.00	118.4	3.20	11.84
Liver	12.00	44.4	1.30	4.81
Lungs	19.00	70.3	2.00	7.40
Adrenal	14.00	51.8	1.50	5.55
Bone surfaces	13.00	48.1	1.40	5.18
Pancreas	8.50	31.5	0.97	3.59
Thyroid	8.30	30.7	0.84	3.11
GI tract				
Stomach wall	7.10	26.3	1.00	3.70
Small intestine	6.70	24.8	1.80	6.66
Upper large intestinal wall	6.40	23.7	3.70	13.69
Lower large intestinal wall	6.40	23.7	8.20	30.34
Uterus	6.60	24.4	1.10	4.07
Bladder wall	6.00	22.2	0.92	3.40
Ovaries	5.80	21.5	1.60	5.92
Testes	5.00	18.5	0.60	2.22

being secreted into bile. Sulfate esters of bile acids are also formed to a small extent. At the alkaline pH of bile and in the presence of alkaline cations (Na^+,K^+), the acids and their conjugates are present as salts. Bile functions include absorption of lipids and the lipid-soluble vitamins A,D,E, and K by the emulsifying action of the bile salts.

PREPARATION

^{75}Se-HCAT is available commercially. Briefly, steriodal halide reacts with disodium diselenide to form disteroidal diselenide, which is reduced with sodium borohydride and is reacted with bromoacetate. The ^{75}Se bile acid is subsequently conjugated with taurine [13].

The nucleophile disodium diselenide is prepared by reacting red selenium with sodium borohydride in ethanol.

QUALITY CONTROL

Quality control tests are performed by the manufacturer prior to shipping.

DOSES

37 kBq (1 μCi) using a whole-body counter.
370 kBq (10 μCi) using a gamma camera for counting.

INGESTION TO COUNTING TIME

5 or 7 days.

PATIENT PREPARATION

Patients should fast overnight.

BIOLOGIC BEHAVIOR

Following oral administration, in normal humans, approximately 95% of the bile acid is absorbed by the terminal ileum during each enterohepatic cycle [14]. ^{75}Se-HCAT is absorbed and excreted at the same rate as ^{14}C-cholic acid [15]. ^{75}Se-HCAT first appears in the gallbladder 73 min after oral administration [16], and it undergoes an enterohepatic circulation roughly five times each day [17]. The distribution of the bile acid pool in the fasting state is 8%, 30% and 62% in liver, gallbladder and small intestine respectively [16]. Using whole-body retention data, 97–100% of ^{75}Se-HCAT is excreted with a half-life of 2.6 days, and a small component of about 3% is slowly eliminated with a mean half-time of 62 days [18]. The urinary excretion is negligible, even in the presence of severe hepatic dysfunction [19, 20].

USE

Study of bile acids malabsorption.

DOSIMETRY

The data are modified from [21] and listed in Table 15.8.

Table 15.8 Estimated radiation absorbed dose of ^{75}Se-HCAT

Organ	*mGy/MBq*	*rad/mCi*
Gallbladder wall	6.4	23.68
GI tract		
Stomach wall	0.45	1.66
Small intestine	2.7	9.99
Upper large intestine	2.2	8.14
Lower large intestine	2.1	7.77
Ovaries	1.0	3.7
Uterus	0.72	2.66
Liver	0.59	2.07
Pancreas	0.43	1.59
Kidneys	0.39	1.44
Urinary bladder wall	0.36	1.33
Adrenals	0.27	1.00

IODINE-125 HUMAN SERUM ALBUMIN (^{125}I-HSA)

Albumin constitutes approximately 50% of the plasma protein and has a molecular weight of 69 000 daltons. The albumin molecule is a zwitterion which binds either positively or negatively charged ions and also binds covalently (particularly iodine) through the tyrosine amino acid. Iodination is accomplished by using mild oxidizing agents such as iodine monochloride, chloromine-T and lactoperoxidase. The iodination reaction is faster at higher pH 8–9 than at lower pH. Denaturation of albumin may occur if more than one atom of iodine binds to each molecule [22].

PREPARATION

Iodine-125-labeled HSA is available commercially, however it can be prepared as follows. HSA is labeled with ^{125}I using chloramine-T (sodium-*N*-monochloro-*p*-toluene sulfonamide) as the oxidizing agent. To 100 μg of HSA in 50 μl of phosphate buffer (0.1 M, pH 7.6), add 10 μl containing 3.7 MBq (100 μCi) ^{125}I-sodium iodide (without reducing agent) and 50 μg of chloramine-T in 20 μI of phosphate buffer and mix. After 30 s, add 100 μg of sodium bisulfite in 20 μl of phosphate buffer to stop further iodination reaction. Unreacted $^{125}I^-$ ion is removed by a Sephadex G-50 gel column previously equilibrated with non-radioactive HSA. The labeled ^{125}I-HSA fraction from column elution is sterilized by 0.22-μm millipore filtration.

Note the following points:

- Freshly prepared solutions are used for the labelling procedure.
- The iodination reaction should be carried out in a fume hood.

QUALITY CONTROL

Use a 10-cm Whatman 3MM paper strip. Place a drop of the ^{125}I-HSA preparation 1 cm from the lower end and develop up to 9 cm in 0.05 M HCl and air dry. Cut the strip at 4 cm from the lower end and assay each piece separately in a well counter. ^{125}I-HSA remains at the origin, while the $^{125}I^-$ ion moves with the solvent front. Calculate the radiochemical purity as follows :

$$\text{Radiochemical purity (\%)} = \frac{\text{Activity at origin}}{\text{Activity at (origin + solvent front)}} \times 100$$

DOSE

Plasma/blood volume determination	185–370 kBq (5–10 μCi)

INJECTION TO STUDY TIME

Collect blood samples at 10, 20 and 30 min.

PATIENT PREPARATION

Patients are given Lugol's solution orally (three drops daily) 1 day before and 2 days after administration of ^{125}I-HSA.

BIOLOGIC BEHAVIOR

^{125}I-HSA, upon intravenous injection, stays in circulation for a very long time unless it is denatured during the iodination procedure. The blood disappearance is multiexponential with half-lives of 6.8 h (40%), 1.29 days (22%) and 19.4 days (38%) [23]. It is slowly deiodinated *in vivo*, releasing radioactive iodide, which is taken up by thyroid gland. If the thyroid is blocked, the released iodide can cross the placenta, resulting in fetal thyroid uptake [24].

USES

^{125}I-HSA is used for the determination of plasma volume and blood volume.

PROCEDURE AND CALCULATIONS

Inject intravenously 0.5 ml of ^{125}I-HSA containing 185–370 kBq (5–10 μCi). At 10, 20 and 30 min post injection withdraw 5 ml of blood into a test tube containing 1–2 mg of EDTA powder (anticoagulant). Prepare a standard solution of ^{125}I-HSA by diluting 0.5 ml containing 185–370 kBq to 100 ml with water.

Remove a 1-ml aliquot of blood to a counting tube and centrifuge the remaining sample to separate plasma. Pipette 1 ml of plasma and 1 ml of diluted standard to counting tubes. Count each tube (containing blood, plasma or standard) in a well counter. Plot a graph of background-subtracted counts against time of plasma and blood on semilogarithmic paper. Extrapolate to obtain 'zero time' counts for calculating plasma and total blood volume.

$$\text{Plasma volume} = \frac{\text{Counts in 1 ml of standard}}{\text{Counts in 1 ml of plasma at zero time}} \times 100$$

$$\text{Total blood volume} = \frac{\text{Counts in 1 ml of standard}}{\text{Counts in 1 ml of blood at zero time}} \times 100$$

$$\text{Red cell volume} = \text{Total blood volume} - \text{plasma volume}$$

DOSIMETRY

The data are modified from [25] and listed in Table 15.9.

Table 15.9 Estimated radiation absorbed dose of ^{125}I-HSA

Organ	*mGy/MBq*	*rad/mCi*
Heart	0.064	0.237
Spleen	0.046	0.170
Lungs	0.044	0.163
Kidneys	0.027	0.099
Adrenals	0.026	0.096
Liver	0.024	0.089
Thyroid	0.017	0.063
GI tract		
Stomach wall	0.016	0.059
Small intestine	0.016	0.059
Upper large intestinal wall	0.015	0.055
Lower large intestinal wall	0.014	0.052
Ovaries	0.015	0.055
Uterus	0.015	0.055
Testes	0.010	0.037

IODINE-125 FIBRINOGEN (^{125}I-FIBRINOGEN)

Fibrinogen is a glycoprotein present in human plasma at concentration of approximately 300 mg/100 ml and has a molecular weight of 340 000 daltons. It is soluble in aqueous medium containing salt. It is a relatively labile protein because it is easily denatured during isolation and labeling procedures. Highly purified fibrinogen should be used since the presence of impurities such as thrombin and plasmin can cause denaturation while in storage [26]. Iodination of fibrinogen with radioactive iodine is done by covalently binding it to the tyrosine amino acid moiety. The iodine monochloride (ICl) or lactoperoxidase method is preferred to the chloramine-T or electrolytic method because fibrinogen tends to aggregate with the latter methods. Denaturation due to iodination is minimized by carefully controlling incorporation of less than one atom of iodine per molecule of fibrinogen [22].

PREPARATION

Iodine-125-labeled fibrinogen is available commercially, however it can be prepared in house.

ISOLATION OF FIBRINOGEN

Owing to recent concern regarding infectious hepatitis B and/or HIV-III antigen, the use of

autologus fibrinogen is recommended [27, 28]. The method described below takes less than 1 h and denaturation is avoided by deactivating prothrombin and plasminogen using aminocaproic acid [27].

Withdraw 10 ml of the patient's blood into a heparinized sterile tube, centrifuge at 190 *g* for 10 min and separate plasma. Add dropwise 2 ml of 3 M ammonium sulfate solution to 4 ml of the plasma to precipitate fibrinogen, centrifuge at 500 *g* for 5 min and discard the supernatant. Dissolve the protein precipitate in 4 ml of phosphate buffer (0.1 M, pH 7.4) containing 0.65% ε-aminocaproic acid and 0.38% trisodium citrate. Reprecipitate with ammonium sulfate solution. Redissolve the protein precipitate in 2 ml of phosphate buffer [27].

IODINATION OF FIBRINOGEN

In a reaction vial maintained at 0–4°C, add 0.35 ml of ICl (3×10^{-4}M) containing 37 MBq (1 mCi) of ^{125}I to 4–12 mg of fibrinogen (in 2 ml of phosphate buffer), mix and allow to react for 3 min. Remove the unreacted ^{125}I by passing the reaction mixture through a Dowex 1 × 8 anion-exchange resin column previously treated with human serum albumin. Sterilize the ^{125}I-fibrinogen eluate by 0.22-μm millipore filtration [27].

Note the following points :

- Use only freshly prepared solutions.
- The iodination reaction should be carried out in a fume hood.

QUALITY CONTROL

Use a 10-cm Whatman 3MM paper strip. Place a drop of the ^{125}I-fibrinogen preparation at the lower end of the Whatman 3MM paper strip, and develop up to 9 cm in 0.05 N HCl. Air dry, cut in the middle and count each piece separately in a well counter. ^{125}I-fibrinogen remains at the origin while the $^{125}I^-$ ion moves with the solvent front. Calculate the radiochemical purity as follows:

$$\text{Radiochemical purity (\%)} = \frac{\text{Radioactivity at origin}}{\text{Radioactivity at (origin + solvent front)}} \times 100$$

DOSE

3.7–5.55 MBq (100–150) μCi).

INJECTION TO STUDY TIME

Once per day for 7 days.

PATIENT PREPARATION

Patients are given Lugol's solution (three drops daily), 1 day before and 2 days after administration of ^{125}I-fibrinogen.

BIOLOGIC BEHAVIOR

^{125}I-fibrinogen, upon intravenous injection, stays in the circulation for a long time and may bind to a clot if present [29, 30]. It is slowly cleared from blood and is uniformly distributed in the extravascular space [31]. The mean plasma half-life is 4.2 ± 0.3 days [27]. It is also metabolized and deiodinated *in-vivo*.

USES

^{125}I-fibrinogen is used in the detection of deep vein thrombosis.

DOSIMETRY

The data are modified from [32] and listed in Table 15.10.

REFERENCES

1. Heisterkamp, D. and Ebaugh, F.G. (1962) Site of attachment of the chromate ion to the haemoglobin molecule. *Nature*, **193**, 1253–55.
2. Sharma, S.M., Patel, M.C., Ramnathan, P. *et al.* (1970) A new technique to denature red cells for spleen scanning. *J. Nucl. Med.*, **11**, 228–32.

Table 15.10 Estimated radiation absorbed dose of ^{125}I-fibrinogen

Organ	*mGy/MBq*	*rad/mCi*
Heart	0.32	1.184
Spleen	0.24	0.888
Lungs	0.23	0.851
Kidneys	0.12	0.444
Bladder wall	0.12	0.444
Red marrow	0.11	0.407
Adrenals	0.10	0.370
Liver	0.099	0.366
Thyroid	0.084	0.311
Uterus	0.055	0.203
Ovaries	0.053	0.196
Testes	0.043	0.159
GI tract		
Stomach wall	0.056	0.207
Small intestine	0.055	0.203
Upper large intestinal wall	0.056	0.207
Lower large intestinal wall	0.055	0.203

3. International Committee for Standardisation in Hematology (1971) Recommended methods for radioisotope red cell survival studies. *Blood*, **38**, 378–86.
4. Najean, Y., Cacchione, R., Dresch, C. and Rain, J.D. (1975) Methods of evaluating the sequestration site of red cells labeled with ^{51}Cr: a review of 96 cases. *Br. J. Haematol.*, **29**, 495–510.
5. ICRP Publication No. 53 (1990) *Radiation Dose to Patients from Radiopharmaceuticals*, Pergamon Press, Oxford, p. 106.
6. International Committee for Standardisation in Haematology (1980) Recommended methods for radioisotope red cell survival studies. *Br. J. Haematol.*, **45**, 659–66.
7. Lehninger, A.L., (1975) Vitamins and coenzymes, in *Biochemistry* (ed. A.L. Lehninger), Worth Publishing, New York, pp. 335–36.
8. ICRP Publication No. 53 (1990) *Radiation Dose to Patients from Radiopharmaceuticals*, Pergamon Press, Oxford, pp. 133–34.
9. Katz, J.H., dMase, J. and Donaldson, R.M. (1963) Simultaneous administration of gastric juice bound and free radioactive cyanocobalamin; rapid procedure for differentiating between intrinsic factor deficiency and other causes of vitamin B_{12} metabolism. *J. Lab. Clin. Med.*, **61**, 266–71.
10. Lionel, S.Z. and Rao, C. (1984) Schilling evaluation of pernicious anemia: current status. *J. Nucl. Med.*, **25**, 1032-39.
11. Peters, A.M. and Lewis, S.M. (1991) Hematology in *Clinical Nuclear Medicine* (eds M.N. Maisey, K.E. Britton and D.L. Gilday), J.B. Lippincott, London, pp. 346–82.
12. ICRP Publication No. 53. (1990) *Radiation Dose to Patients from Radiopharmaceuticals*, Pergamon Press, Oxford, pp. 119–24.
13. Monks, R and Thomas, I.L. (1982) ^{75}Se labelled bile acid analogues. *J. Labelled Compounds Radiopharmacol.*, **20**, 463–86.
14. Heaton, K.W. (1976) Clinical aspects of bile acid metabolism. *Rec. Adv. Gastroenterol.*, **3**, 199–230.
15. Boyd, G.S., Merrick, M.V., Monks, R. and Thomas, I.L. (1981) ^{75}Se-labelled bile acid analogues. New radiopharmaceuticals for investigating the enterohepatic circulation. *J. Nucl. Med.*, **22**, 720–25.
16. Jazrawi, R.P., Lanzini, A., Britten, A. *et al.* (1984) Dynamics of gall bladder function and of the enterohepatic circulation studied γ bile acid. *Clin. Sci.*, **66**, 10P.
17. Merrick, M.V., Eastwood, M.A. and Ford J.J. 1985) Is bile acid malabsorption underdiagnosed? An evaluation of accuracy of diagnosis of measurement of Se HCAT retention. *B.M.J.*, **290**, 665–68.
18. Nyhlin, H., Merrick, M.V., Eastwood, M.A. and Brydan, W.G. (1983) Evaluation of ileal function using 23-selena-25-homo taurocholate, a γ-labeled conjugated bile acid. *Gastroenterology*, **84**, 63–8.
19. Merrick, M.V., Eastwood, M.A., Anderson, J.R. and Ross, H.McL (1982) Enterohepatic circulation in man of a gamma-emitting bile acid conjugate, 23-selena-25-hamotaurocholic acid (SeHCAT). *J. Nucl. Med.*, **23**, 126–30.
20. Delhez, H., van den Berg, J.W.O., Blankenstein, M. and Meerwaldt, J.H. (1982) New method for the determination of bile acid turnover using ^{75}Se homocholic acid taurine. *Eur. J. Nucl. Med.*, **7**, 269–71.

21. ICRP Publication No. 53 (1990) *Radiation dose to patients from radiopharmaceuticals*. Pergamon Press, Oxford, pp. 153–54.
22. Hunter, W.M. (1966) Iodination of protein compounds, in *Radioactive Pharmaceuticals* (eds G.A. Andrews, R.M. Kniseley and H.N. Wagner Jr), US Atomic Energy Commission, Oak Ridge, pp. 245–63.
23. Takeda, Y. and Reeve, E.B. (1963) Studies of the metabolism and distribution of albumin with autologus ^{131}I albumin in healthy man. *J. Lab. Clin. Med.*, **61,** 183–202.
24. Hibbard, B.M. and Herbert, R.J.T. (1960) Foetal radiation dose following administration of radioiodinated albumin. *Clin. Sci.*, **19**, 337–44.
25. ICRP Publication No. 53 (1990) *Radiation Dose to Patients from Radiopharmaceuticals*, Pergamon Press, Oxford, pp. 285–87.
26. Welch, M.J. and Krohn, K.A. (1975) Critical review of radiolabeled fibrinogen, in *Radiopharmaceuticals* (eds G. Subramanian, B.A. Rhodes, J.F. Cooper, and V.J. Sodd), The Society of Nuclear Medicine, New York, pp. 493–502.
27. Loberg, M., Miller, I. and Cooper, M. (1975) Radioiodinated autologus fibrinogen: a rapid method of preparation for clinical use, in *Radiopharmaceuticals* (eds G. Subramanian, B.A. Rhodes, J.F.Cooper and V.J. Sodd), The Society of Nuclear Medicine, New York pp. 503–13.
28. Product Information (1992) Iodinated [^{135}I] human fibrinogen. Amersham International, UK.
29. Kakkar, V.V., Howe, C.T., Nicolaides, A.N. *et al.* (1970) Deep vein thrombosis of the leg. *Am. J. Surg.*, **120**, 527–30.
30. Regoeczi E. (1971) The clottability of iodinated fibrinogen. *J. Nucl. Biol. Med.*, **15**, 37–41.
31. Regoeczi E. (1971) Iodine-labeled fibrinogen. A review. *Br. J. Haemotol.*, **20**, 649–63.
32. ICRP Publication No. 53. (1990) *Radiation Dose to Patients from Radiopharmaceuticals*, Pergamon Press, Oxford, pp. 281–83.

16

Therapeutic radiopharmaceuticals

There are three types of radiation for therapy: external beam, implantation of radioactive sources and orally or parenterally administered radiopharmaceuticals. This chapter is concerned with the third type. Within the last decade, there has been an increasing interest in developing new radiopharmaceuticals for therapy, especially those used for palliation of pain from bone metastases. ^{32}P-chromic phosphate, ^{32}P-sodium phosphate, ^{89}Sr-strontium chloride, ^{153}Sm-ethylenediaminetetramethylene phosphonate (^{153}Sm-EDTMP) and ^{186}Re-1, 1-hydroxyethylidene diphosphonate (^{186}Re-HEDP) are described in this chapter. ^{131}I sodium iodide and ^{131}I-mIBG were covered in Chapter 8.

Side-effects and long-term complications do not constitute a major problem with administered radiopharmaceuticals for therapy. Possible acute side-effects are nausea and vomiting. Possible long-term effects are mild and transient bone marrow suppression, which leads to a transient decline in the white cell and platelet counts. For radiopharmaceuticals used for palliation of bone pain, non-hematologic toxicity is limited to a transient exacerbation of pre-existing pain (flare reaction) beginning 2–3 days after therapy and lasting 3–4 days.

PHOSPHORUS-32 CHROMIC PHOSPHATE (^{32}P-$CrPO_4$) AND SODIUM PHOSPHATE (^{32}P-Na_2HPO_4)

Phosphorus is a non-metallic element of group VB and exists in the +5 oxidation state in phosphate salts. Phosphorus-32 decays by beta emission (E_{max} 1.71 MeV) with a physical half-life of 14.3 days. It is produced by the $^{31}P(n,\gamma)^{32}P$ reaction.

DOSE

330–660 MBq (8.9–17.8 mCi).

BIOLOGIC BEHAVIOR

Following administration, phosphate has an initial high concentration in the liver and skeleton, but eventually about 90% of the residual activity is contained in the skeleton [1].

USES

- Treatment of polycythemia vera (soluble phosphate).
- Treatment of leukemia and bone metastasis (soluble phosphate).
- Intracavitary treatment of malignant effusion (colloidal chromic phosphate).
- Interstitial treatment of cancer (colloidal chromic phosphate).

DOSIMETRY

The data are modified from [2] and listed in Table 16.1.

STRONTIUM-89 CHLORIDE ($^{89}SrCl_2$)

Strontium is an alkaline earth divalent cation of group IIA and behaves biologically like

Table 16.1 Estimated radiation absorbed dose of ^{32}P-phosphate

Organ	*mGy/MBq*	*rad/mCi*
Bone surfaces	11.0	40.70
Red marrow	11.0	40.70
Breast	0.92	3.41
Adrenals	0.74	2.63
Bladder wall	0.74	2.63
GI tract		
Stomach wall	0.74	2.63
Small intestine	0.74	2.63
Upper large intestine	0.74	2.63
Lower large intestine	0.74	2.63
Kidneys	0.74	2.63
Liver	0.74	2.63
Lungs	0.74	2.63
Ovaries	0.74	2.63
Pancreas	0.74	2.63
Spleen	0.74	2.63
Testes	0.74	2.63
Thyroid	0.74	2.63
Uterus	0.74	2.63

Table 16.2 Estimated radiation absorbed dose of $^{89}SrCl_2$

Organ	*mGy/MBq*	*rad/mCi*
Bone surfaces	17	62.9
Red marrow	11	40.7
GI tract		
Stomach wall	0.78	2.89
Small intestine	0.023	0.085
Upper large intestinal wall	1.80	6.66
Lower large intestinal wall	4.70	17.39
Bladder wall	1.30	4.81
Breast	0.96	3.55
Adrenals	0.78	2.89
Kidneys	0.78	2.89
Liver	0.78	2.89
Lungs	0.78	2.89
Ovaries	0.78	2.89
Pancreas	0.78	2.89
Spleen	0.78	2.89
Testes	0.78	2.89
Thyroid	0.78	2.89
Uterus	0.78	2.89

calcium. Strontium-89 is essentially a pure beta emitter (E_{max}1.46 MeV) with a physical half-life of 50.6 days. It gives off Bremsstrahlung radiation, which can be used in imaging for monitoring the efficacy of the therapy. It is produced by the $^{88}Sr(n,\gamma)$ ^{89}Sr reaction.

DOSE

1.5–2.0 MBq (40–60 μCi)/kg.

BIOLOGIC BEHAVIOR

Following intravenous injection, $^{89}SrCl_2$ localizes selectively in bone [3]. Its uptake by bone occurs preferentially in sites of active osteogenesis, giving a high therapeutic ratio of metastasis to normal bone [4–7]. Kinetic studies indicate that uptake of $^{89}SnCl_2$ in osteoblastic lesions is 2–25 times more than that in normal bone [8]. It is excreted mainly by the kidneys [9].

USE

$^{89}SrCl_2$ is used in the palliation of pain resulting from osseous metastases.

DOSIMETRY

The data are modified from [10] and listed in Table 16.2.

SAMARIUM-153 ETHYLENEDIAMINETETRAMETHYLENE PHOSPHONIC ACID (^{153}Sm-EDTMP)

CHEMISTRY

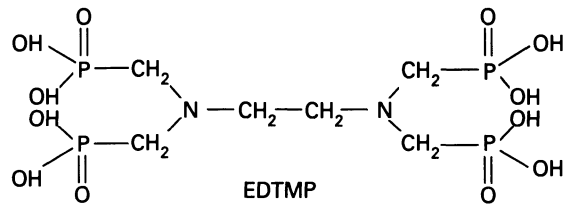

Samarium is an element of group IIIB (lanthanides). It forms a stable complex with ethylenediaminetetramethylene phosphonic acid (EDTMP) with a 1:1 metal to ligand ratio [11, 12]. EDTMP is synthesized by the condensation of ethyleneamine, phosphorous acid and formaldehyde using a modified Mannich reaction in the presence of hydrochloric acid [13]. Recrystallization of the crude product from water yields white crystals of pure ligand.

Samarium-153 has a physical half-life of 46.27 h and emits therapeutically useful beta particles with maximum energies of 640 keV (30%), 710 keV (50%) and 810 keV (20%). ^{153}Sm also emits a gamma ray of 103 keV (28%) that is suitable for imaging.

PREPARATION

Samarium-153 is produced by thermal neutron irradiation of enriched $^{152}Sm_2O_3$ (99.06%) in a nuclear reactor. The oxide target is dissolved in 1.0 N HCl and diluted to 0.1 N with sterile water.

To a vial containing lyophilized EDTMP, add 6 ml of $^{153}SmCl_3$ solution and mix until it dissolves. Adjust the pH of the final product to 7.0–8.5 with sodium hydroxide. The preparation is stable for up to 7 days [14].

QUALITY CONTROL

Place a drop of the preparation on a cellulose TLC plate at 1 cm from the lower end, develop up to 15 cm in pyridine–ethanol–water (1:2:4) and air dry. Scan the plate using a TLC scanner. ^{153}Sm-EDTMP is detected at $R_{(f)}$ 0.85 and uncomplexed ^{153}Sm at the origin [15]. The labeling effiency is determined as follows:

$$\text{Labeling efficiency (\%)} = \frac{\text{Radioactivity at } R_{(f)}0.85}{\text{Radioactivity at (origin + } R_{(f)}0.85)} \times 100$$

DOSE

10–37 MBq (0.27–1 mCi) per kg body weight.

PATIENT PREPARATION

Patients are properly hydrated and encouraged to void frequently.

BIOLOGIC BEHAVIOR

Following intravenous injection, ^{153}Sm-EDTMP is probably adsorbed onto the hydroxyapatite crystals of the bone [16]. Autoradiographic studies using normal dogs and sheep indicate that ^{153}Sm-EDTMP tends to concentrate in trabecula rather than cortical bone [15, 17]. The biologic behavior of ^{153}Sm-EDTMP is similar to that of technetium-99m phosphorus complexes, as shown in the excellent correlation between the lesion to normal bone ratio and lesion to soft tissue ratio [14].

By 2–3 hours, 50–66% of the administered dose is localized in bone with long-term retention [18] and less than 2% is present in non-osseous tissues, mainly liver [19].

^{153}Sm-EDTMP clears rapidly from blood with 5.2 ± 1.1% and 2.1 ± 0.5% remaining in plasma at 2 and 4 h respectively. The major pathway of excretion is through the kidneys. The amount of radioactivity excreted by the kidneys into the bladder at 24 h is 56 ± 10.5%, with most of the excretion (53.4 ± 16.4%) occurring during the first 8 h [20].

USE

^{153}Sm-EDTMP is used in the palliation of pain resulting from osseous metastases.

DOSIMETRY

The data are modified from [21] and are listed in Table 16.3.

Table 16.3 Estimated radiation absorbed dose of ^{153}Sm-EDTMP

Organ	*mGy/MBq*	*rad/mCi*
Bone surfaces	6.757	25.000
Red marrow	1.540	5.700
Urinary bladder	0.973	3.600
Kidney	0.018	0.065
Ovaries	0.009	0.032
Lungs	0.008	0.031
Testes	0.005	0.020
Liver	0.005	0.019

RHENIUM-186 1,1-HYDROXYETHYLIDENE DIPHOSPHONATE (^{186}Re-HEDP)

CHEMISTRY

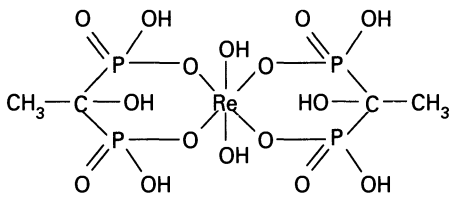

Rhenium and technetium have similar chemistry owing to their positions in the periodic table (group VIIA), as previously described in Chapter 7. Hence, ^{186}Re can form complexes with hydroxyethylidene diphosphonate after reduction of perrhenate by stannous ions to the +4 oxidation state.

HEDP is synthesized by slow addition of phosphorus trichloride to a mixture of water and acetic acid while stirring and heating. The reaction mixture is evaporated to dryness and the resultant HEDP monohydrate is purified by recrystallization [22]. Rhenium-186 has a physical half-life of 89.3 h and emits a therapeutically useful beta particle with a maximum energy of 1.07 MeV. ^{186}Re also emits a gamma ray of 137 keV that is suitable for imaging before therapy to determine the appropriate dose and after therapy to monitor the efficacy of the treatment. The low abundance (9.5%) of gamma emission is sufficient for imaging and also minimizes the radiation exposure to patient, personnel and environment.

PREPARATION

Enriched ^{185}Re metal (1 mg) is irradiated in a nuclear reactor. Excess 30% H_2O_2 is added to oxidize the resulting ^{186}Re metal to perrhenate ion ($^{186}ReO_4^-$). The solution is dried by vacuum distillation to remove the peroxide and yield a pale-yellow to orange residue. The residue is dissolved in normal saline to yield a ^{186}Re perrhenate solution.

To a vial containing HEDP, $SnCl_2 \cdot 2H_2O$ and gentisic acid add the perrhenate solution, under an inert atmosphere. Heat the solution for 10 min to facilitate the reduction of perrhenate and the chelation to HEDP. Cool to room temperature and adjust the pH of the product to 5.0–6.0 with sodium acetate buffer. The preparation is stable for up to 14 days [23].

QUALITY CONTROL

Place a drop of the preparation on a 7-cm Whatman/ITLC strip at 1 cm from the lower end, develop up to 5 cm in acetone or saline (Table 16.4). Air dry and cut the strip in the middle. Assay each piece separately in a dose calibrator and calculate the percentage labeling efficiency as follows:

Labeling efficiency (%) = 100 – % $^{186}ReO_4^-$ – % $^{186}ReO_2$

DOSE

0.9–1.3 GBq (24.3–35.13 mCi).

PATIENT PREPARATION

Patients are properly hydrated and encouraged to void frequently.

Table 16.4 Chromatographic analysis of ^{186}Re-HEDP

Chromatographic system		*^{186}Re species at*	
Support	*Solvent*	*Origin*	*Solvent front*
Whatman 3MM paper/ITLC	Acetone	^{186}Re-HEDP $^{186}ReO_2$	$^{186}ReO_4^-$
Whatman 3MM paper/ITLC	Saline	$^{186}ReO_2$	^{186}Re-HEDP $^{186}ReO_4^-$

BIOLOGIC BEHAVIOR

Following intravenous injection, ^{186}Re-HEDP is probably adsorbed onto the hydroxyapatite crystals of the bone surface [16]. ^{186}Re-HEDP exhibits high bone uptake (21–38% at 3 h) and low soft-tissue accumulation equivalent to ^{99m}Tc-HEDP [23]. ^{186}Re activity is slowly eliminated from the normal bone, with 14% remaining at 96 h [23]. The clearance from blood is rapid, with 14% remaining in the blood 30 min after injection [23]. The percentage binding of ^{186}Re-HEDP and $^{186}ReO_4^-$ to plasma protein is 52 ± 1% and 80 ± 1% respectively [24].

The major pathway of elimination is through the kidneys. The cumulative urinary activity at 5 and 72 h is 45 and 71% respectively [23].

USE

^{186}Re-HEDP is used in the palliative treatment of pain from osseous metastases.

Table 16.5 Estimated radiation absorbed dose of ^{186}Re-HEDP

Organ	*mGy/MBq*	*rad/mCi*
Skeleton	0.864	3.2
Kidney	1.108	4.1
Red marrow	0.757	2.8
Bladder wall[a]	0.486	1.8
Whole body	0.081	0.3

[a] Void interval 2–4 h.

DOSIMETRY

The data are modified from [25] and listed in Table 16.5.

REFERENCES

1. McAfee, J.G. and Subramanian, G. (1975) Radioactive agents for imaging, in *Clinical Scintillation Imaging* (eds M.L. Freeman and P.M. Johnson), Grune & Stratton, New York, p. 28.
2. ICRP Publication No. 53 (1990) *Radiation Dose to Patients from Radiopharmaceuticals*, Pergamon Press, Oxford, p. 84.
3. Volkert, W.A., Goeckeleer, W.F. and Ehrhardt, G.J. (1991) Therapeutic radionuclides, production and decay property considerations. *J. Nucl. Med.*, **32**, 174–85.
4. Robinson, R.G., Blake, G.M., Preston, D.F. *et al.* (1989) Strontium-89: treatment results and kinetics in patients with painful metastatic prostate and breast cancer in bone. *Radiographics*, **9**, 271–81.
5. Blake, G.M., Zivanovic, M.A., Blaquiere, R.M. *et al.* (1988) Strontium-89 therapy: Measurement of absorbed dose to skeletal metastases. *J. Nucl. Med.*, **29**, 549–57.
6. Blake, G.M., Zivanovic, M.A., McEwan, A.J. *et al.* (1986) Sr-89 therapy: strontium kinetics in disseminated carcinoma of the prostate. *Eur. J. Nucl. Med.*, **12**, 447–54.
7. Silberstein, E.B. and Williams, C. (1985) Strontium-89 therapy for the pain of osseous metastases. *J. Nucl. Med.*, **26**, 345–48.
8. Breen, S.L., Powe, J.E. and Ponter, A.T. (1992) Dose estimation in strontium-89 radiotherapy

of metastatic prostatic carcinoma. *J. Nucl. Med.*, **33**, 1316–23.

9. Dickinson, C.Z. and Hendrix, N.S. (1993) Strontium-89 therapy in painful bony metastases. *J. Nucl. Med. Technol.*, **21**, 133–37.
10. ICRP Publication No. 53 (1990) *Radiation Dose to Patients from Radiopharmaceuticals*, Pergamon Press, Oxford, p. 171.
11. Goeckeler, W.F., Edwards. B., Volkert, W.A. *et al.* (1987) Skeletal localization of Sm-153 chelates: potential therapeutic bone agents. *J. Nucl. Med.*, **28**, 495–504.
12. Volkert, W.A., Simar, J., Ketring, A.R. *et al.* (1989) Radiolabeled phosphonic acid chelates: potential therapeutic agents for treatment of skeletal metastases. *Drug Future*, **14**, 799–811.
13. Moedritzer, K. and Irani, R.R. (1966) The direct synthesis of α-amino-methyl phosphonic acids. Mannich-type reactions with orthophosphorous acid. *J. Org. Chem.*, **31**, 1603–07.
14. Singh, A., Holmes, R.A., Farhangi, M. *et al.* (1989) Human pharmacokinetics of samarium-153 EDTMP in metastatic cancer. *J. Nucl. Med.*, **30**, 1814–18.
15. Turner, J.H., Martindale, A.A., Sorby, P. *et al.* (1989) Samarium-153 EDTMP therapy of disseminated skeletal metastasis. *Eur. J. Nucl. Med.*, **15**, 784–95.
16. Francis, M.D., Russel, R.G.G. and Fleish, H. (1969) Diphosphonate inhibits formation of calcium phosphate crystals in vitro and pathological calcification in vivo. *Science*, **165**, 1264–66.
17. Lattimer, J.C., Corwin, L.A., Stapleton, J. *et al.* (1990) Clinical and clinicopathologic effects of samarium-153 EDTMP administered intravenously in normal dogs. *J. Nucl. Med.*, **31**, 586–93.
18. Holmes, R.A. (1992) [^{153}Sm] EDTMP: potential therapy for bone cancer pain. *Semin. Nucl. Med.*, **22**, 41–5.
19. Appelbaum, F.R., Sandmaier, B., Brown, P. *et al.* (1980) Myelosuppression and mechanism of recovery following administration of ^{153}Sm EDTMP. *Antibody Immunoconj. Radiopharmacol.*, **1**, 263–70.
20. Farhangi, M., Holmes, R.A., Volkert, W.A. and Singh, A. (1987) ^{153}Sm EDTMP. A potential radiotherapeutic agent for metastatic bone cancer (abstract). *Am. Soc. Clin. Oncol. Proc.*, **6**, 22.
21. Eary, J.F., Collins, C., Stabin, M. *et al.* (1993) Samarium-153 EDTMP biodistribution and dosimetry estimation. *J. Nucl. Med.*, **34**, 1031–36.
22. Castronovo, F.P. (1974) Method for the synthesis of 1-hydroxyethylidene-1, 1-disodium phosphonate (HEDSPA): a skeletal seeking radiopharmaceutical after labeling with Tc-99m. *J. Nucl. Med.*, **15**, 127–30.
23. Pipes, D.W. and Deutsch, E. (1993) Rhenium Re-186 Etidronate injection. *Drug Future*, **18**, 520–24.
24. deKlerk, J.M.H., Van Dijk, A., Vanhet Schip, A.D. *et al.* (1992) Pharmacokinetics of rhenium-186 after administration of rhenium-186 HEDP to patients with bone metastases. *J. Nucl. Med.*, **33**, 646–51.
25. Maxon, H.R., Deutsch, E.A., Thomas, S.R. *et al.* (1988) Re-186 (Sn) HEDP for treatment of multiple metastatic foci in bone: human biodistribution and dosimetric studies. *Radiology*, **166**, 501–7.

Part Three

Good Radiopharmacy Practice

The primary functions performed in the radiopharmacy are preparing and dispensing high-quality radiopharmaceuticals and monitoring their fate both *in vitro* and *in vivo*. To make available high-quality radiopharmaceuticals, a systematic approach should be established in the preparation methodology. Quality cannot be established by testing alone, but must be built into the product manufacturing and preparation processes, and must be maintained until administered to the patient. This built-in system approach is the basis of good radiopharmacy practice (GRP).

The important elements of GRP are design of a radiopharmacy, quality assurance, record keeping, dispensing, radiation protection and safety and waste disposal of radioactive material according to appropriate national regulatory policies.

17

Design of a radiopharmacy

The design of a radiopharmacy depends upon the nature of the work to be done, which includes the production of cold kits and in-house preparation of radiopharmaceuticals from ready-to-use kits. The basic organization required for making kits include sterility- and pyrogen-testing facilities, raw material quality analyses, stability studies, biodistribution studies in appropriate animal species and qualified personnel. This involves a large capital outlay, which most institutions cannot afford. With commercial production of cold kits very few institutions make their own. Hence the description of the design of a radiopharmacy will be limited to in-house preparation of radiopharmaceuticals from ready-to-use kits. In designing a radiopharmacy, emphasis should be given to a clean environment.

PREMISES

The radiopharmacy should be located near or in the nuclear medicine department to minimize travel with radioactive material. The premises should be designed and constructed of sufficient floor space to suit the local requirements. The first stage in planning is to identify the function and scope of the operation, bearing in mind the need for future expansion.

LAYOUT OF ROOMS

The layout of rooms of a radiopharmacy as shown in Figure 17.1 is basically aimed at protecting personnel and environment from radiation, and protecting the product from

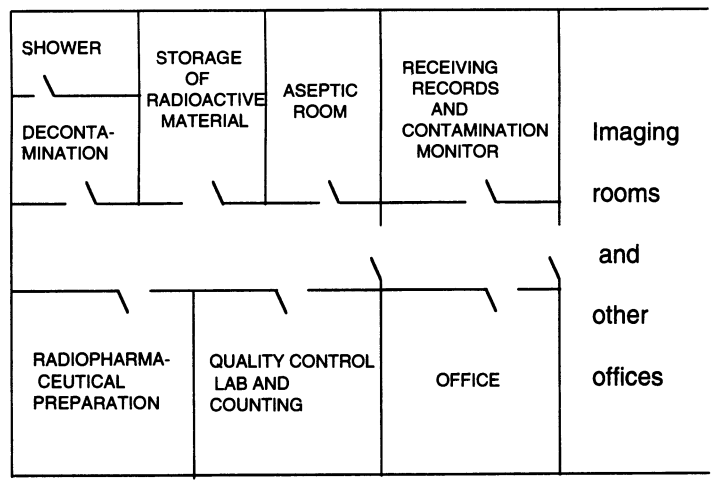

Figure 17.1 Suggested floor plan of a radiopharmacy.

contamination. Essentially, the individual room is designated according to its function. Only relevant personnel should have access to the facility, with minimal entry by the maintenance staff.

Separate rooms should be assigned to receiving and unpacking shipments, preparing radiopharmaceuticals, quality control tests, storage and radioactive waste products. The storage room should have sufficient shielding. Preparation of radiopharmaceuticals which require open procedures such as separation and labeling of biologic samples (blood cells and antibodies) should be done in an aseptic room. Separate rooms should be provided for offices, decontamination and showering.

SURFACES

The floor surface of the radiopharmacy should be smooth and non-porous. It should be made of material of adequate density and texture and which is non-electrostatic to avoid the retention of dust, dirt and moisture, which can create a favorable environment for the proliferation of micro-organisms. The surfacing material should be such that it is not damaged by repeated cleaning with water, detergents and disinfectants. It should not give off particles by flaking, cracking, pulverization, corrosion or mechanical impairment. Polyvinyl chloride (PVC) tiles are frequently used for flooring because they can be joined with minimum joint gaps without nooks and sharp corners; they are evenly fixed and rounded off at the corners; and they are easily cleaned, decontaminated and/or replaced.

VENTILATION

This is achieved by provision of a clean air supply through a proper ventilation system. The contaminated air from the working area should not be recirculated or vented out to the environment without proper filtration. The radiopharmacy is kept under negative pressure relative to the surroundings, however the aseptic room is kept under positive pressure (1.5 mm of water gauge).

FURNITURE

Table or bench tops should be made of post-formed formica or cast-resin with a continuous smooth and impervious surface. Items such as drawers, shelves and hanging lamps should be avoided in the aseptic rooms. A speaker phone which can be operated without lifting the receiver should be installed in the radioactive laboratory.

SINKS

The radiopharmacy should have sinks with a smooth finish (stainless steel) which can be easily decontaminated. It is preferable if taps and the hand dryer can be operated automatically. The aseptic room should not be fitted with a sink in order to avoid possible bacterial contamination.

EQUIPMENT

The most essential pieces of equipment in a radiopharmacy include a dose calibrator, radiation area monitor, survey meter and laminar flow hood. Lists of other equipment, accessories and common chemicals are given in Appendix A. It may not be necessary to have all the material listed. Selection should be made according to requirements.

PERSONNEL

Good radiopharmacy practice largely depends upon the personnel involved in the organization. Well-trained and motivated staff can appreciate the importance of system control, thereby reducing the undesirable radiopharmaceutical defects. During trouble-shooting only trained staff can resolve the

problems of altered biologic behavior or drug–radiopharmaceutical interactions. The desirable qualities in personnel working in a radiopharmacy include respect for but not fear of radiation, a basic understanding of the subject, a liking for cleanliness and a methodical working habit.

The responsibility of routine radiopharmaceutical preparation and dispensing of doses may be entrusted to a trained technologist who will seek advice from a competent radiopharmacist or radiopharmaceutical scientist.

It is necessary that personnel involved in preparing and dispensing of radiopharmaceuticals are familiar with the safe handling of radioactive material, tracer techniques and quality control of drugs prepared for administration to humans.

18

Quality assurance

Quality assurance is the total process of in-house preparation and administration of radiopharmaceutical to the patient. It therefore involves quality control testing of dose calibrators and radiopharmaceuticals, and proper dispensing and record keeping. Details of the quality control testing of each radiopharmaceutical were given in Part Two. In this Chapter, performance checking of the dose calibrator and dispensing and record keeping are described.

PERFORMANCE CHECKING OF THE DOSE CALIBRATOR

It is absolutely necessary to have a reliable, accurate and precisely functioning dose calibrator. The following tests are performed to check the functioning of the dose calibrator: accuracy, precision, linearity and geometry.

ACCURACY TEST

Sealed gamma-emitting radioactive standard sources of low, medium and high energies (Table 18.1) are measured in fixed geometry and appropriate calibration setting.

Express the net activity as '*A*' after subtracting background. Calculate the percentage accuracy as follows:

$$\text{Accuracy (\%)} = (A - S)\ 100/S$$

where A is the measured activity and S is the standard certified activity after decay correction. The percentage accuracy should be within ± 10% of the certified value.

PRECISION TEST

Ten readings are taken for each radionuclide, background is subtracted and mean is calculated. Calculate the percentage precision as follows:

$$\text{Precision (\%)} = (A_i - A)\ \frac{100}{A}$$

where A_i is the individual measured activity and A is the mean activity. The percentage precision of each measurement should be within ± 5% of the mean.

Table 18.1 Physical properties of radionuclides used for dose calibrator checking

Radionuclide	*Principal photon energies (keV)*	*Half-life*	*Activity*	
			MBq	*mCi*
^{57}Co	122	271 days	185	5
^{133}Ba	81, 356	10.7 years	9.3	0.250
^{137}Cs	662	30 years	7.4	0.200
^{60}Co	1173, 1332	5.27 years	1.9	0.050

LINEARITY TEST

Use a radionuclide with a short half-life such as ^{99m}Tc of initial activity equal to or greater than the highest activity to be used in the radiopharmacy. Measure the activity of the ^{99m}Tc source and note the exact time of the measurement. Periodically measure the activity of the same source until it has decayed to less than the lowest activity to be measured in the radiopharmacy.

Plot a graph of activity versus time on semilogarithmic paper. The graph should be a straight line consistent with the physical decay of ^{99m}Tc. The linearity response should be within ± 10% of the value corresponding to the point fitted on the straight line.

This test can be performed by dilution technique, but it requires precise pipetting and handling of a large amount of unsealed activity.

GEOMETRY RESPONSE TEST

Measure approximately 740 MBq (20 mCi) of ^{99m}Tc into a multidose sealed vial and place the vial at the bottom of the well of a dose calibrator. Raise the vial in 1-cm increments and measure the activity each time until the vial is raised to the top of the well. Calculate the percentage variation of activity at each level as follows:

$$\text{Variation (\%)} = \frac{\text{Activity at each level}}{\text{Activity at the bottom}} \times 100$$

The variation of activity at each level should be within ± 5% of the activity at the bottom level.

DISPENSING OF RADIOPHARMACEUTICALS

One of the important elements of a built-in system of quality assurance is dispensing of doses for administration to humans. It is essential that the correct radiopharmaceutical and amount of radioactivity be dispensed and administered to the appropriate patient. Request for a particular radiopharmaceutical to be dispensed should be given in a proper prescription form specifying the dose and the time of injection.

Calculate the activity and volume to be dispensed applying the necessary decay correction (Appendix B). In order to avoid frequent calculations, each radiopharmaceutical may be prepared in standardized concentrations.

A plastic tray lined with absorbent paper which does not give off fibers should be used to confine any probable spillage. Wear gloves and secure the vial containing the radiopharmaceutical in an appropriately colored lead shield. Wipe the rubber stopper with an antiseptic swab. Hold the lead pot upside down and withdraw the required volume in an appropriately labeled and color-coded disposable syringe secured in a lead glass syringe shield.

Dispensing of radiopharmaceuticals should be carried out behind a lead glass-shielded work bench. Precautions should be taken to replace air in the vial if a large volume is to be withdrawn. If the required dose is to be diluted, first withdraw the required amount of diluent in the syringe followed by the radiopharmaceutical. If excess is withdrawn initially, do not squirt the excess into the vial. The needle used for withdrawing the dose should be sharp, because a blunt needle may introduce rubber particles into the preparation.

Prior to injection, all dispensed doses should be measured in a dose calibrator. Relevant information concerning the radiopharmaceutical should be entered in the product dispensing record and on the color-coded syringe label, as shown in Figures 18.1 and 18.2. To avoid misadministration it is recommended that each radiopharmaceutical should have one color code. Dispensed doses should not be kept in the syringe for longer than 1 h because some radiopharmaceuticals may interact with the plastic material and

Lot/Batch No.....Product.....
Activity.....Volume.....
Concentration.....Time.....

Date	Time	Pt's Name	N.M.No.	Dose mCi/MBq	Vol ml	Remark

Q.C. ITLC/Whatman 3MM paper

Solvent

Seg I :.....
Seg II :.....
.....

Solvent

Seg I :.....
Seg II :.....

Figure 18.1 Suggested dispensing record for each radiopharmaceutical.

particulate radiopharmaceuticals (macroaggregated albumin or microspheres) may stick to the syringe.

Dispensing large therapeutic doses of ^{131}I sodium iodide should be done in a fume hood or glove box to avoid the risk of airborne radioactivity.

Occasional misadministration may occur, and this can be minimized by taking following precautions:

- Make sure of the planned study and identify the appropriate radiopharmaceutical.
- Determine the recommended dose according to the established imaging protocol.
- Examine the vial to assure that the appropriate radiopharmaceutical is being dispensed.
- Make sure that the patient is an adult and not a child. If the patient is a child, be sure to dispense appropriate dose (Appendices C and D).
- Handle one radiopharmaceutical at a time.

RECORD KEEPING

Documentation of preparation, dispensing and disposal of unused radiopharmaceuticals is absolutely necessary for an effective quality assurance system. The records provide a trail from the manufacturer to the patient that could be used in the event of undesired biologic behavior of an administered radiopharmaceutical. Well-kept records can be helpful in resolving medicolegal problems.

An inventory record of each incoming radiopharmaceutical must be kept. A separate log entry for each radiopharmaceutical received or prepared will help in calculating

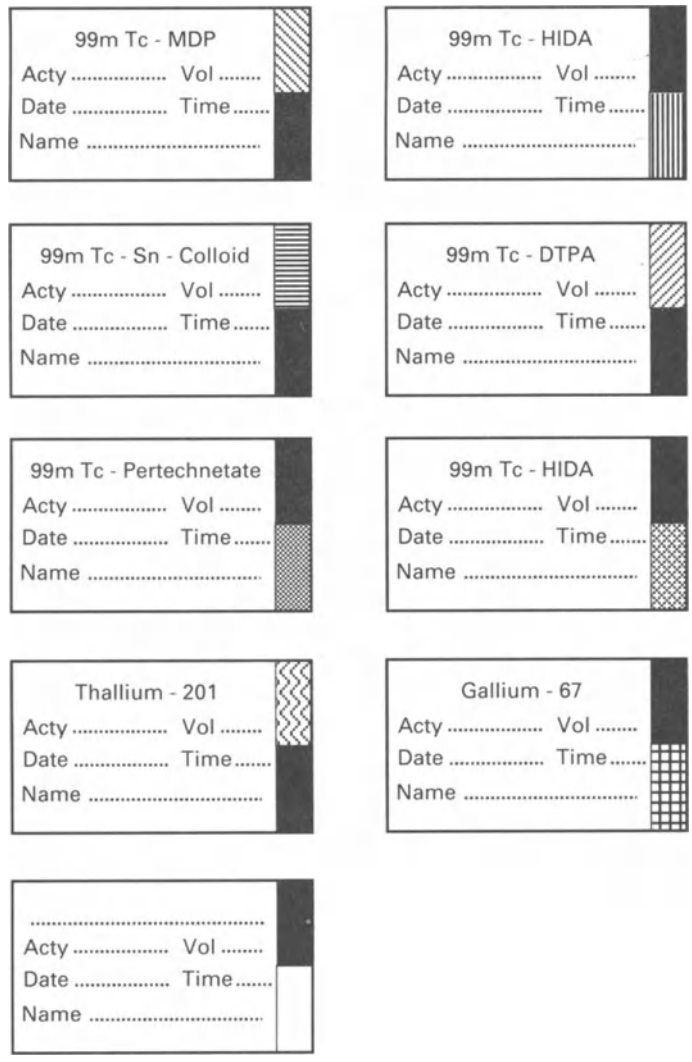

Figure 18.2 Suggested syringe labels. Each label should have a different code (color or shading).

how much is used and future procurement. An inventory format should be designed to include administrative, pharmaceutical and radiation protection aspects. A typical format of inventory record is shown in Figure 18.3.

In addition, the following records should also be kept.

- Records of quality control test of dose calibrator.
- Records of complaints regarding altered behavior, misadministration and/or adverse reactions.
- Records of waste disposal of radioactive materials.

Received											Distributed		Remainder	
Log No.	Date	Order No.	Airway Bill No.	Rec. voucher No.	Pack No.	Lot No.	Activity	Amount	Ref. Date	Exp. Date	Date	Activity	Date	Activity

Figure 18.3 Suggested format for inventory record of radiopharmaceuticals.

- Records of radiation exposure to personnel.
- Records of monitoring radioactivity, microbial and particulate contamination of the facilities.
- Records of service maintenance of all instruments.

All records should be kept for at least 2 years or for as long as national legislation may require.

19

Radiation protection and safety

The degree of risk(s) associated with radiation increases with increasing exposure. It is always good to reduce the radiation exposures to 'as low as reasonably achievable' (ALARA), consistent with provision of benefits to patient, personnel and society in general. The radiation exposure can be minimized by good working habits. Hence radiation protection forms a part of good radiopharmacy practice. The following discussion is a guideline to minimizing radiation exposure to the personnel and patient.

PERSONNEL

The occupational radiation exposure to personnel working with radioactive material(s) is regulated by international and national organizations such as the International Commission for Radiological Protection (ICRP), the International Atomic Energy Agency (IAEA), the World Health Organization (WHO) and the Environmental Protection Agency (EPA).

The maximum permissible doses for radiation workers recommended by ICRP (ICRP Publication No. 60) is summarized in Table 19.1. Frequent monitoring for contamination is encouraged for radiation workers.

No separate provisions are made for women of reproductive capacity working with radioactive materials. However, the abdominal exposure should not be more than 1.3 rem in any calender quarter. Once a woman is known to be pregnant, her abdominal exposure should be less than 1 rem during the first 2 months. She may continue to work with radiation, but her annual exposure rate shall not exceed 1.5 rem.

HANDLING OF RADIOACTIVE MATERIAL

The radiation exposure to the personnel can be reduced to ALARA level by three factors: distance, shielding and time.

Table 19.1 Maximum occupational radiation dose limits recommended by ICRP

Application	*Dose limits*
Effective dose	20 mSv (2 rem) per year averaged over defined 5 years
Annual equivalent dose to	
the lens of the eyes	150 mSv (15 rem)
the skin	500 mSv (50 rem)
the hands and the feet	500 mSv (50 rem)

Distance

Radiation exposure can be considerably reduced by increasing the distance between the source and the personnel. The amount of radiation at a given distance from a source is inversely proportional to the square of the distance. The principle of the inverse square law can be easily put into practice in the radiopharmacy by using long tongs and forceps to handle radioactive material and in the imaging room by staying as far away as possible from the patient.

Shielding

Shielding is a body or material used to prevent or reduce the passage of radiation. Beta emitters are shielded with plastic materials or wooden blocks, while gamma radiation is shielded with lead materials.

Time

Radiation exposure can be reduced by spending the minimum possible time working with radioactive material. This is effectively achieved by proper planning of the work, which includes getting all the materials and accessories ready before starting and, once the work is finalized, by staying away from the radiation area.

SUGGESTED SPECIFIC SAFETY MEASURES FOR A RADIATION WORKER

- Wear laboratory coats, gloves, safety goggles and film badge(s) while working with radioactive materials.
- Work in a ventilated fume hood, particularly when handing gaseous or volatile radioactive materials(s).
- Do not eat, drink, smoke or use cosmetics in the radioactive laboratory.
- Do not pipette any radioactive material by mouth.
- Survey work areas for any contamination as frequently as possible.
- Clean up spills promptly and survey the areas after decontamination.
- Monitor hands and feet after the day's work.
- Cover trays and work benches with absorbent paper.
- Store and transport radioactive materials in appropriate containers.
- Identify all radionuclides and note calibration and expiration dates.
- Do not hang laboratory coats with a film badge in a radiation laboratory.

THE PATIENT

The radiation absorbed dose is based on type of radiopharmaceutical and the amount of radioactivity to be administered. The recommended adult and pediatric doses are listed in Appendices C and D respectively.

Radiopharmaceuticals are not normally administered to pregnant women, however under extraordinary circumstances one may be given. Prior to administering a radiopharmaceutical to a woman of child-bearing age ascertain whether or not she is pregnant. In the event it is later discovered that a woman injected with a radiopharmaceutical is pregnant, it is always a concern whether or not the pregnancy should be terminated because of radiation dose to the fetus. The National Council on Radiation Protection and Measurements (NCRP) has stated that this risk is considered to be negligible at 5 rad or less when compared with the other risks of pregnancy, and the risk of malformations is significantly increased above control levels only at doses above 15 rad. Therefore, the radiation dose from a diagnostic examination seldom justifies the termination of pregnancy [1].

The ICRP recommended actions for women who are breast feeding are modified and summarized in Table 19.2 [2].

Table 19.2 Modified ICRP recommended actions for breast feeding

Group I
Stop breast feeding for at least 3 weeks (all ^{131}I radiopharmaceuticals except hippuran, ^{67}Ga citrate and ^{201}Tl)
Group II
Stop breast feeding for at least 12 h ($^{123/131}I$-hippuran, all ^{99m}Tc radiopharmaceuticals except RBCs, phosphorus complexes and renal agents)
Group III
Stop breast feeding for at least 4 h (^{99m}Tc-RBCs, phosphorus complexes and renal agents)

The radiation absorbed dose of a patient may be reduced either by inducing rapid elimination of the radiopharmaceuticals from the body or by pretreating the patient with drugs. Rapid elimination of most hydrophilic radiopharmaceuticals can be induced by proper hydration of patient or administration of Lasix, while the rapid elimination of the radiopharmaceuticals excreted through the gastrointestinal tract can be induced by administration of a laxative. Uptake of radioactive iodide or $^{99m}TcO_4^-$ by the thyroid can be blocked by prior treatment with Lugol's solution.

REFERENCES

1. National Council on Radiation Protection and Measurements (NCRP) (1977) Report No. 54, Medical Radiation Exposure of Pregnant and Potentially Pregnant Women, Washington DC.
2. Annals of the ICRP Publication No. 52 (1987) Protection of the Patient in Nuclear Medicine, Pergamon Press, Oxford.

20

Disposal of radioactive waste material

The radionuclides used in nuclear medicine have short half-lives, therefore radioactive waste disposal does not pose a serious problem. There are two practical methods of disposing of these radioactive wastes: sewer dilution and decay in storage.

SEWER DILUTION

The amount of radioactive material discarded daily in the sewer system depends upon the half-life and concentration. The quantity of any individual radionuclide that can be disposed of in the sewers is regulated by both local and national agencies.

DECAY IN STORAGE

This is the more practical method of disposing of radioactive materials. The radioactive material is allowed to decay for at least 10 half-lives, when it is presumed to be non-radioactive. However, ^{99}Mo–^{99m}Tc generators should be allowed to decay for 25 half-lives of ^{99}Mo because ^{99}Mo may contain a large amount of activity. Before disposal, the radioactive waste should be monitored and show less than 0.05 mR/h exposure rate at the surface.

21

Regulatory policies and practice

Possession and use of radioactive materials require licenses from local and national regulatory agencies such as the Atomic Energy Agency and Radiation Protection Department. There are two basic types of licenses: individual and institutional. An individual license requires proof of competence in handling radioactive materials as obtained through formal education and workshops. An institutional license may permit the use of specific radionuclides or may be a broad license. Institutions with a broad license have the responsibility for approving use of specific radionuclides. The institution should have a radiation safety officer and committee to ensure safe handling of radioactive materials.

FURTHER READING FOR PART THREE

1. Freeman, L.M. and Blaufox, M.D. (eds) (1986) *Seminars in Nuclear Medicine*, Vol. 16, Nos. 2 and 3, Grune & Stratton, Orlando, FL.
2. ICRP Publication No. 60. (1990) Recommendations of the International Commission on Radiological Protection, Pergamon, Oxford.
3. Kirstensen K. (ed.) (1979) *Preparation and Control of Radiopharmaceuticals in Hospitals*, IAEA technical reports series No. 194, IAEA, Vienna.
4. *Radiation Protection Procedures, Safety* (1973) IAEA technical series No. 38, IAEA Vienna.

Part Four

Appendices

Appendix A

List of equipment, chemicals and consumables required in a radiopharmacy

Equipment

Dose calibrator

pH-meter

Seal cappers and decappers

Vortex shakers

Magnetic stirrer with hot plate

Oven

All-glass distilled water unit

Contamination monitors

Fraction collector

Centrifuge

Electrostatic particle collector

Lead glass shield for syringes

Lead-lined radioactive storage bins

Plastic trays

Tongs and forceps with vial-holding grip.

Refrigerator

Laminar flow work station: vertical flow type.

Analytic precision balance

Propipette bulbs

Electrophoresis apparatus

Autoclave

Well-type gamma counter

Survey meter

Constant-temperature water bath with shaker

Optical microscope – general purpose

Lead glass shielding work bench

Micropipettes

Lead bricks

Equipment, chemicals and consumables

Chemicals

Incubator

Acetic acid

Acetone

Acetonitrile

n-Butanol

Citric acid

Dextrose

Ethylacetate

Ethyl-alcohol

Hydrochloric acid

Methanol

Methyl ethyl ketone

Nitric acid

Saline (0.9% NaCl solution)

Sodium dihydrogen phosphate
Sodium hydroxide

Sodium monohydrogen phosphate

Stannous chloride
Stannous fluoride

Sulfuric acid

Trisodium citrate

Consumables

Absorbent sheets

Aluminium seal: 13 mm diameter

Color-coded labels

Disposable aerosol ventilation system

ITLC plates: silica gel, silicic acid, aluminium oxide

Milliporefilters: pore size 0.22 μ to 25 mm sterile

Serum vials: 10 ml, 30 ml, 50 ml, 100 ml

(13 mm diameter)

Rubber stopper: gray butyl rubber, 13 mm diameter

Whatman No. 1 and 3 paper strips

Appendix B

Decay factors of radionuclides useful for nuclear medicine procedures

^{67}Ga

Hours	Precalibration decay factor	Postcalibration decay factor
3	1.03	0.974
6	1.05	0.948
9	1.08	0.923
12	1.11	0.899
15	1.14	0.876
18	1.17	0.853
21	1.20	0.830
24	1.24	0.809
27	1.27	0.787
30	1.30	0.767
33	1.34	0.747
36	1.38	0.727
39	1.41	0.708
42	1.45	0.689
45	1.49	0.671
48	1.53	0.654
51	1.57	0.637
54	1.61	0.620
57	1.66	0.603
60	1.70	0.588
63	1.75	0.573
66	1.79	0.558
69	1.84	0.542
72	1.89	0.529
75	1.94	0.515
78	1.99	0.501
81	2.05	0.488
84	2.10	0.475
87	2.16	0.463

^{99m}Tc

Hours	Precalibration decay factor	Postcalibration decay factor
1	1.12	0.891
2	1.25	0.794
3	1.41	0.708
4	1.58	0.631
5	1.77	0.562
6		0.501
7		0.447
8		0.398
9		0.355
10		0.316
11		0.282
12		0.251

^{111}In

Days	Precalibration decay factor	Postcalibration decay factor
0.25	1.06	0.941
0.5	1.13	0.885
0.75	1.20	0.832
1	1.28	0.783
1.25	1.36	0.736
1.5	1.44	0.693
1.75	1.54	0.651
2	1.63	0.613
2.25	1.74	0.576
2.5	1.84	0.542
2.75	1.96	0.510

^{111}In *Continued*

Days	Precalibration decay factor	Postcalibration decay factor
3	2.09	0.480
3.25	2.22	0.451
3.5	2.36	0.424
3.75	2.51	0.399
4	2.66	0.375
4.25	2.83	0.353
4.5	3.01	0.332
4.75	3.20	0.312
5	3.40	0.294
5.25	3.62	0.276
5.5	3.85	0.260
5.75	4.09	0.245
6	4.35	0.230

^{123}I

Hours	Precalibration decay factor	Postcalibration decay factor
2	1.11	0.900
4	1.23	0.811
6	1.37	0.730
8	1.52	0.657
10	1.70	0.591
12	1.88	0.533
14	2.08	0.479
16	2.32	0.432
18	2.57	0.389
20	2.86	0.350
22	3.17	0.315
24	3.53	0.284
26	3.92	0.255
28	4.35	0.230
30	4.83	0.207
32	5.37	0.186
34	5.96	0.168
36	6.62	0.151
38	7.36	0.136
40	8.17	0.122
42	9.07	0.110
44	10.08	0.992
46	11.20	0.893
48	12.43	0.804
50	13.81	0.724

^{131}I

Days	Precalibration decay factor	Postcalibration decay factor
1	1.09	0.918
2	1.19	0.8
3	1.29	0.773
4	1.41	0.709
5	1.54	0.651
6	–	0.597
7	1.82	0.548
8		0.503
9		0.461
10		0.423
11		0.388
12		0.356
13		0.327
14		0.300
15		0.275
16		0.253
17		0.232
18		0.213
19		0.195
20		0.179
21		0.164
22		0.151
23		0.138
24		0.127

^{133}Xe

Days	Precalibration decay factor	Postcalibration decay factor
0.25	1.03	0.968
0.5	1.07	0.936
0.75	1.10	0.905
1	1.14	0.876
1.25	1.18	0.848
1.5	1.22	0.820
1.75	1.26	0.794
2	1.30	0.768
2.25	1.35	0.743
2.5	1.39	0.719
2.75	1.44	0.695
3	1.49	0.673
3.25	1.54	0.651
3.5	1.59	0.630

^{133}Xe *Continued*

Days	Precalibration decay factor	Postcalibration decay factor
3.75	1.64	0.609
4	1.70	0.589
4.25	1.75	0.570
4.5	1.81	0.552
4.75	1.87	0.534
5	1.94	0.516
5.25	2.0	0.500
5.5	2.07	0.483
5.75	2.14	0.468
6	2.21	0.453
6.25	2.28	0.438
6.5	2.36	0.424
6.75	2.44	0.410
7	2.52	0.397
7.25	2.61	0.384
7.5	2.69	0.371
7.75	2.78	0.359
8	2.88	0.347
8.25	2.98	0.336
8.5	3.08	0.325
8.75	3.18	0.315
9	3.29	0.304
9.25	3.40	0.295
9.5	3.51	0.285
9.75	3.63	0.276
10	3.75	0.267

^{201}Tl

Hours	Precalibration decay factor	Postcalibration decay factor
5	1.04	0.954
10	1.10	0.910
15	1.15	0.868
20	1.21	0.828
25	1.27	0.790
30	1.33	0.754
35	1.40	0.719
40	1.46	0.686
45	1.53	0.654
50	1.60	0.624
55	1.68	0.595
60	1.76	0.568
65	1.84	0.542
70	1.94	0.517
75	2.03	0.493
80	2.13	0.470
85	2.23	0.449
90	2.34	0.428
95	2.45	0.408
100	2.57	0.389

Appendix C

Recommended adult doses

Radiopharmaceutical	Procedure	Dose	
		MBq	mCi
$^{99m}TcO_4^-$	Thyroid, Meckel's diverticulum	74–185	2–5
	In vivo RBC labeling	555–925	15–25
	Dacyocystography	3.7	0.100
	Parathyroid	74	2
	Testicular imaging	37–370	1–10
	Salivary imaging, brain death	370–555	10–15
^{99m}Tc-*d*, *l*-HMPAO	Cerebral perfusion	555–740	15–20
^{99m}Tc-*l*, *l*-ECD	Cerebral perfusion	370–740	10-20
^{99m}Tc-MRP 20	Cerebral perfusion	555–925	15-25
^{99m}Tc-MAA	Lung perfusion	55.5–111	1.5–3
^{99m}Tc-HAM	Lung perfusion	74–111	2–3
^{99m}Tc-DTPA aerosols	Lung ventilation	74–111	2–3
^{99m}Tc-RBCs	Cardiac blood pool studies	555–925	15–25
^{99m}Tc-sestamibi	Myocardial perfusion	370–1110	10–30
	Parathyroid imaging	74	2
^{99m}Tc-teboroxime	Myocardial perfusion	555	15
^{99m}Tc-tetrofosmin	Myocardial perfusion	140–170	3.7–4.7
^{99m}Tc-MDP			
^{99m}Tc-PYP	Bone imaging	555–740	15–20
^{99m}Tc-HMDP			
^{99m}Tc colloids	Liver and spleen imaging	185	5
	Bone marrow	370–555	10–15
	GI bleeding	370	10
	Cystogram	37	1
	Esophageal reflux	11.1–18.5	0.3–0.5
	Lymphoscintigraphy	37–74	1–2
	Inflammation	185–340	5–10
^{99m}Tc colloid–chicken liver	Motility of solid meal	22.2	0.6
^{99m}Tc-mebrofenin			
^{99m}Tc-disofenin	Hepatobilliary imaging	150–185	4–5
^{99m}Tc-EHIDA			
^{99m}Tc-DTPA	Renal imaging	185–370	5–10
	Brain imaging	555–740	15–20
	Angiography and GI bleeding	740	20

Radiopharmaceutical	Procedure	Dose	
		MBq	mCi
^{99m}Tc-DMSA	Renal imaging	37–185	1–5
	Imaging of medullary carcinoma of thyroid	370	10
^{99m}Tc-glucoheptonate	Renal imaging	370–555	10–15
	Brain imaging	740–925	20–25
^{99m}Tc-MAG_3	Renal imaging	37–370	1–10
^{99m}Tc-HSA	Blood flow studies	18.5–185	0.5–5
	Cardiac blood pool studies	185–925	5–25
	Placental visualization and lymphatic channels	37	1
$^{123}I^-$ ion	Thyroid imaging	7.4–11.1	0.2–0.3
$^{131}I^-$ ion	Thyroid uptake rest	0.37–0.925	0.01–0.025
$^{131}I^-$ ion	Treatment of hyperthyroidism	74–1110	2–30
$^{131}I^-$ ion	Treatment of thyroid carcinoma and its metastases	1110–7400	30–200
^{123}I-*o*-hippuran	Renal imaging	185	5
$^{131}I^-$-hipuran	Renal imaging	11.1	0.300
^{123}IMP	Cerebral perfusion	185	5
^{123}I-HIPDM	Cerebral perfusion	185–370	5–10
^{123}I-mIBG	Adrenal imaging	370	10
^{67}Ga citrate	Tumor imaging	74–370	2–10
^{111}In-DTPA	CFS leakage	18.5	0.5
^{111}In-oxine/tropolone leukocytes	Imaging infection	18.5–37	0.5–1
	Leukocyte survival	3.7	0.1
^{111}In-oxide/-tropolone platelets	Thrombus and renal transplant	11.1–18.5	0.3–0.5
	Platelet survival	1.85–3.7	0.05–0.1
$^{201}Tl^+$ion	Myocardial perfusion imaging (peak exercise) and for rest imaging if required	74–111 37	2–3 1
	Parathyroid imaging	74	2
	Tumor imaging	111–148	3–4
^{111}In-antimyosin	Infarcted myocardial imaging	55.5–74	1.5–2
^{111}In-anti-CEA	Tumor imaging and evaluation of therapeutic treatment	37–74	1–2
^{111}In-anti-TAG/B72.3	Imaging colorectal and ovarian cancer	185	5
^{123}IBZM	Imaging D_2 dopamine receptor density in neuropsychiatric conditions	185	5
^{111}In-octreotide	Visualization of somatostatin tumor-positive tissues	185–259	5–7
$^{127/133}$Xe ^{81m}Kr	Lung ventilation	296–555	8–15

Radiopharmaceutical	Procedure	Dose	
		MBq	mCi
^{18}FDG	Cerebral and myocardial glucose utilization and CNS tumors	74–370	2–10
$^{15}O_2$	Measuring oxygen metabolism		
^{15}O-CO_2	Measuring oxygen metabolism and blood flow	37	1
^{15}O-CO	Measuring blood volume		
$^{13}NH_3$	Myocardial perfusion	370–555	10–15
^{51}Cr-RBCs	Red cell mass	0.74–1.11	0.02–0.03
	Red cell survival	2.96–3.7	0.08–0.1
^{57}Co-vitamin B_{12}	B_{12} absorption	0.018–0.137	0.0005–0.001
^{58}Co-vitamin B_{12}			
^{59}Fe citrate	Iron absorption study	0.074–0.185	0.002–0.005
	Ferrokinetic studies	0.185–0.370	0.005–0.01
^{125}I-fibrinogen	Deep vein thrombosis	3.7–5.55	0.1–0.15
^{32}P-sodium phosphate	Treatment of polycythemia vera, leukemia, bone metasis	330–660	8.9–17.8
^{89}Sr chloride	Palliation of pain from osseous metastases	1.5–2.0/kg	0.04–0.06/kg
^{153}Sm-EDTMP	Palliation of pain from osseous metastases	10–37/kg	0.27–1/kg
^{186}Re-HEDP	Palliation of pain from osseous metastases	990–1300	24.3–35.13

Appendix D

Recommended pediatric dose as a fraction of the adult dose

Weight (kg)	Fraction of adult dose	Weight (kg)	Fraction of adult dose	Weight (kg)	Fraction of adult dose
3	0.10	22	0.50	42	0.78
4	0.14	24	0.53	44	0.80
6	0.19	26	0.56	46	0.82
8	0.23	28	0.58	48	0.85
10	0.27	30	0.62	50	0.88
12	0.32	34	0.68	52–54	0.90
14	0.36	36	0.71	56–58	0.92
16	0.4	38	0.73	60–62	0.96
18	0.44	40	0.76	64–66	0.98
20	0.46			68	0.99

Appendix E

Build-up factors at various times following previous elution of the ^{99}Mo–^{99m}Tc generator

Hours	Factor	Hours	Factor	Hours	Factor
1	0.094	9	0.579	17	0.788
2	0.179	10	0.615	18	0.804
3	0.256	11	0.648	19	0.818
4	0.324	12	0.678	20	0.831
5	0.386	13	0.705	21	0.843
6	0.442	14	0.729	22	0.853
7	0.492	15	0.751	23	0.863
8	0.538	16	0.771	24	0.871

Appendix F

Conversion to SI units

Conversion from Curies to Becquerels

μCi mCi Ci	Kbq MBq BGq	μCi mCi Ci	MBq GBq TBq
0.1	3.7	30	1.11
0.2	7.4	40	1.48
0.25	9.25	50	1.85
0.3	11.1	60	2.22
0.4	14.8	70	2.59
0.5	18.5	80	2.96
1	37	90	3.33
2	74	100	3.70
2.5	92.5	125	4.62
3	111	150	5.55
4	148	200	7.4
5	185	250	9.25
6	222	300	11.1
7	259	400	14.8
8	296	500	18.5
9	333	600	22.2
10	370	700	25.9
12	444	750	27.75
15	555	800	29.6
20	740	900	33.3
25	925	1000	37.0

Conversion from Rads to Grays

1 rad/mCi = 0.27 mGy/MBq

1 millirad (mrad)	=	10 microgray (μGy)
1 rad	=	10 milligray (mGy)
1 rad	=	1 centigray (CGy)

Conversion from Rems to Sieverts

1 millirem (mrem)	=	10 microsievert (μSv)
1 rem	=	10 millisievert (mSv)
1 rem	=	1 centisievert (cSv)

Appendix G

Decay schemes for commonly used radionuclides

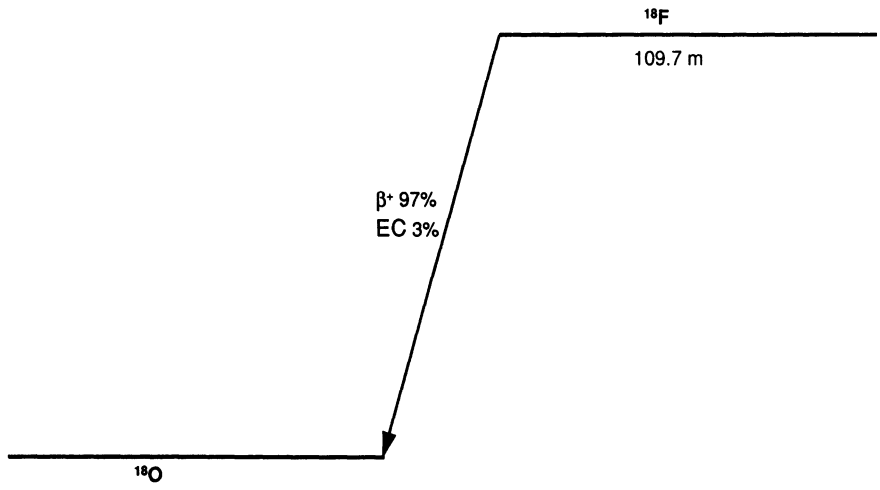

Figure G.1 Decay scheme of ^{18}F. Useful gamma energy for imaging: 0.511 MeV.

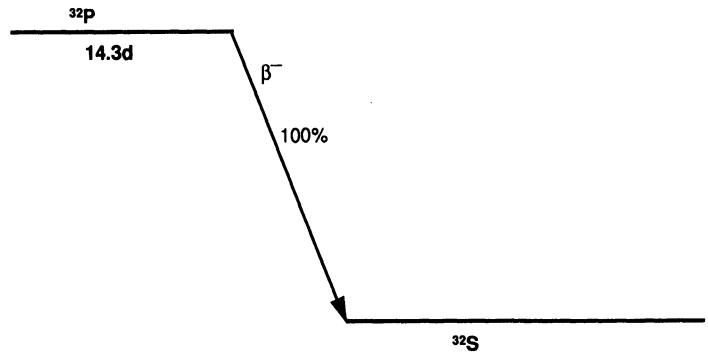

Figure G.2 Decay scheme of ^{32}P. Useful beta energy for therapy: E_{max} 1.71 keV.

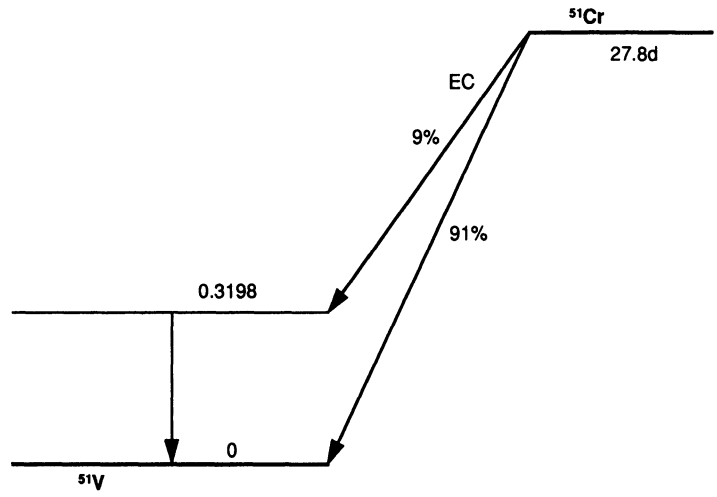

Figure G.3 Decay scheme of ^{51}Cr. Useful gamma energy for counting: 320 keV.

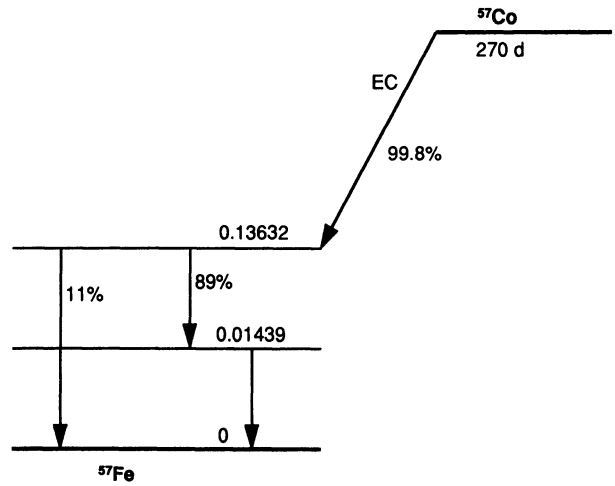

Figure G.4 Decay scheme of ^{57}Co. Useful gamma energy for counting: 122 keV.

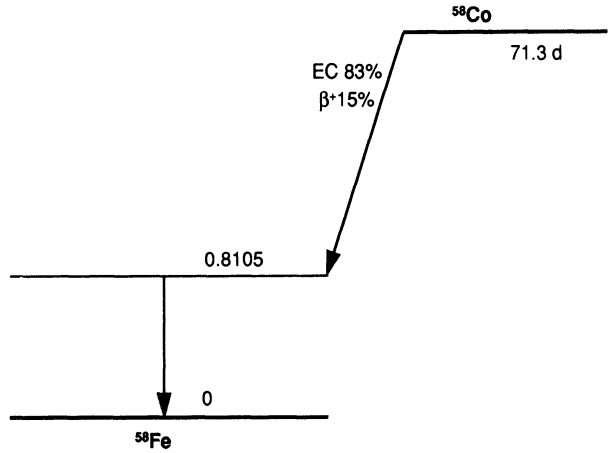

Figure G.5 Decay scheme of ^{58}Co. Useful gamma energy for counting: 810 keV.

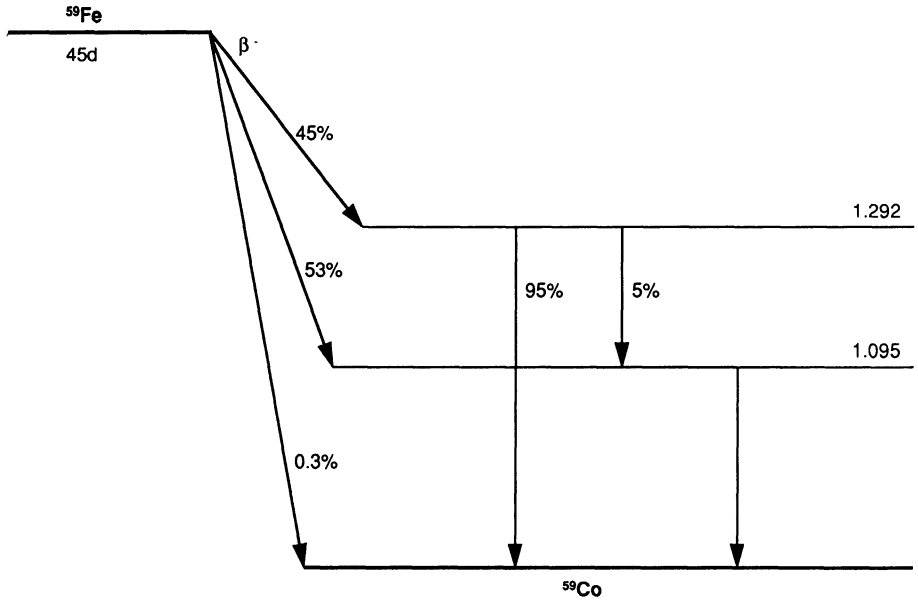

Figure G.6 Decay scheme of ^{59}Fe. Useful gamma energies for counting: 1.095 and 1.292 MeV.

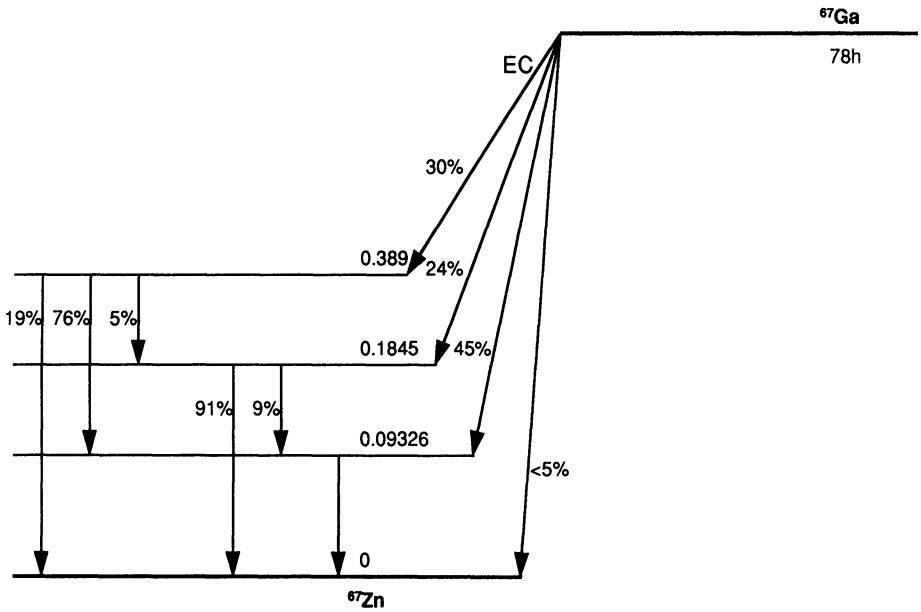

Figure G.7 Decay scheme of ^{67}Ga. Useful gamma energies for imaging: 93, 184 and 296 keV.

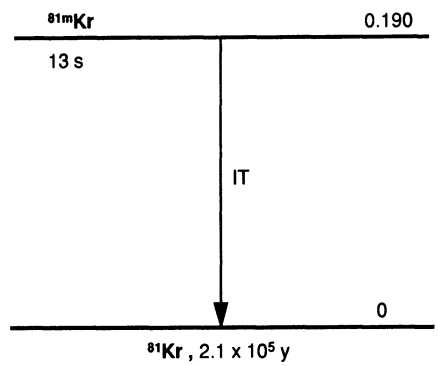

Figure G.8 Decay scheme of ^{81m}Kr. Useful gamma energy for imaging: 190 keV.

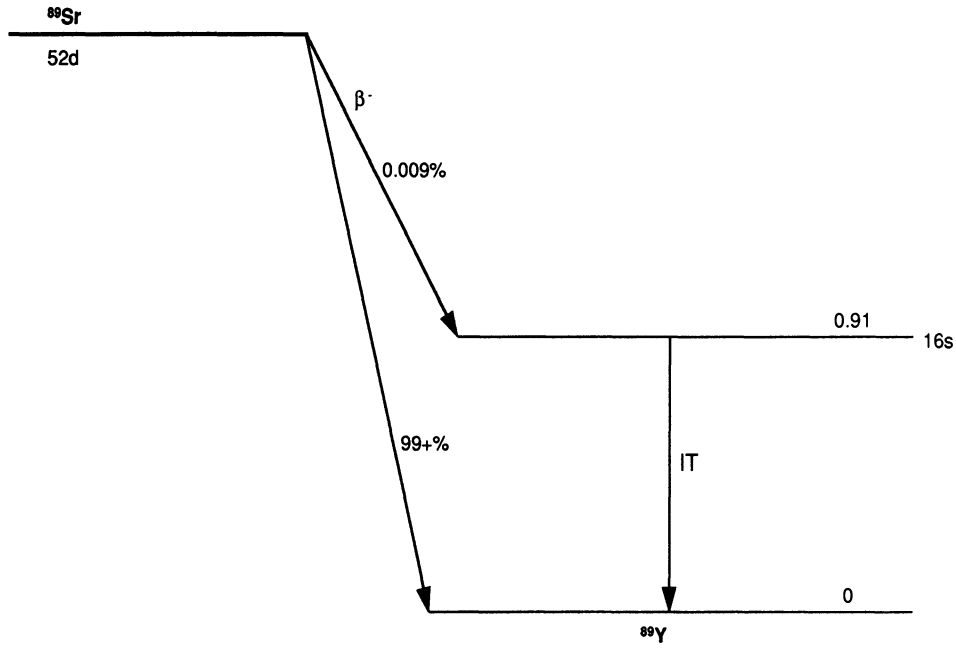

Figure G.9 Decay scheme of ^{89}Sr. Useful beta energy for therapy: E_{max} 1.46 MeV.

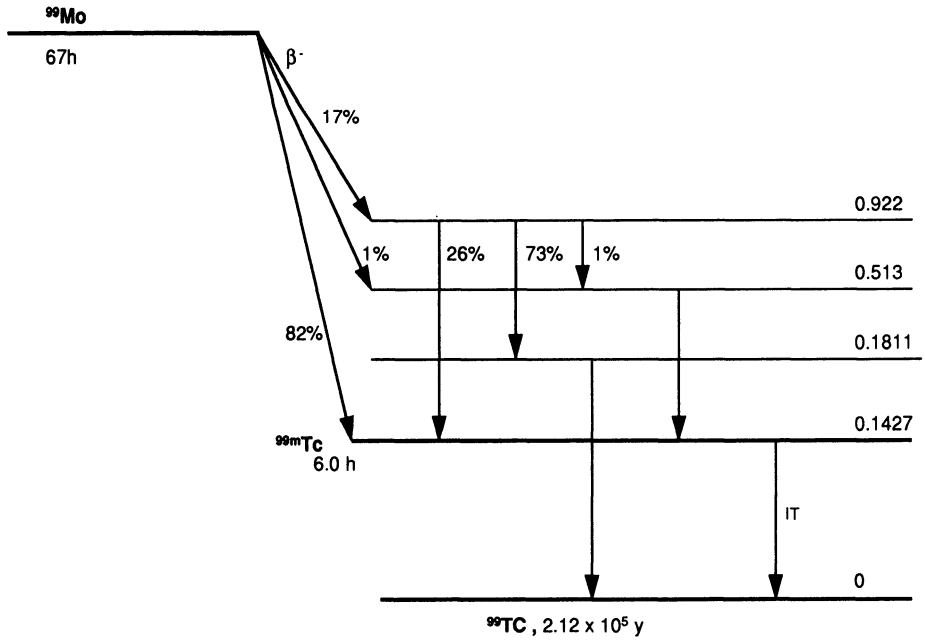

Figure G.10 Decay schemes of ^{99}Mo and ^{99m}Tc. (Note that approximately 13% of ^{99}Mo decays directly to ^{99}Tc). Useful gamma energy for imaging: 143 keV.

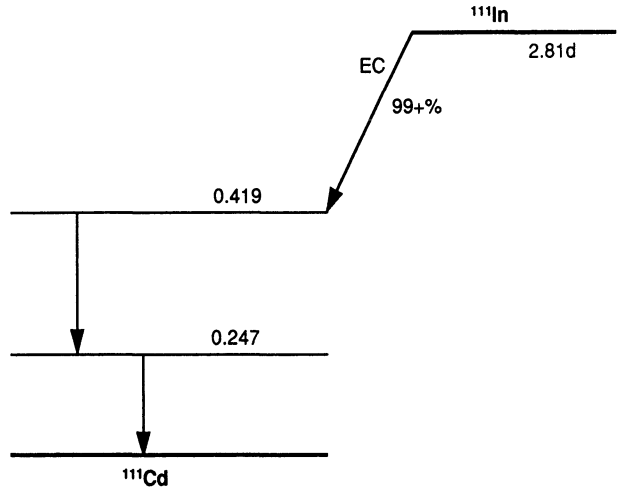

Figure G.11 Decay scheme of ^{111}In. Useful gamma energies for imaging: 172 and 247 keV.

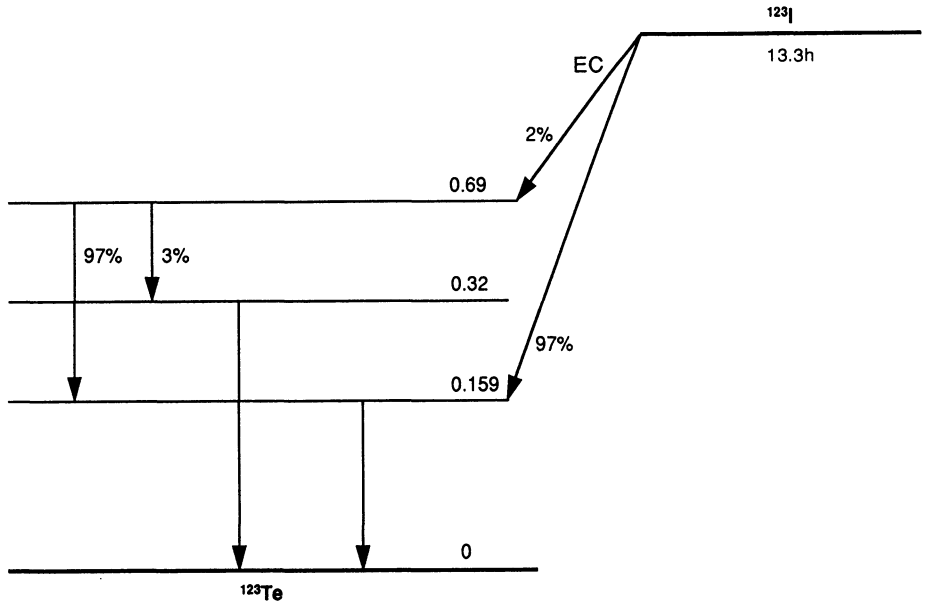

Figure G.12 Decay scheme of ^{123}I. Useful gamma energy for imaging: 159 keV.

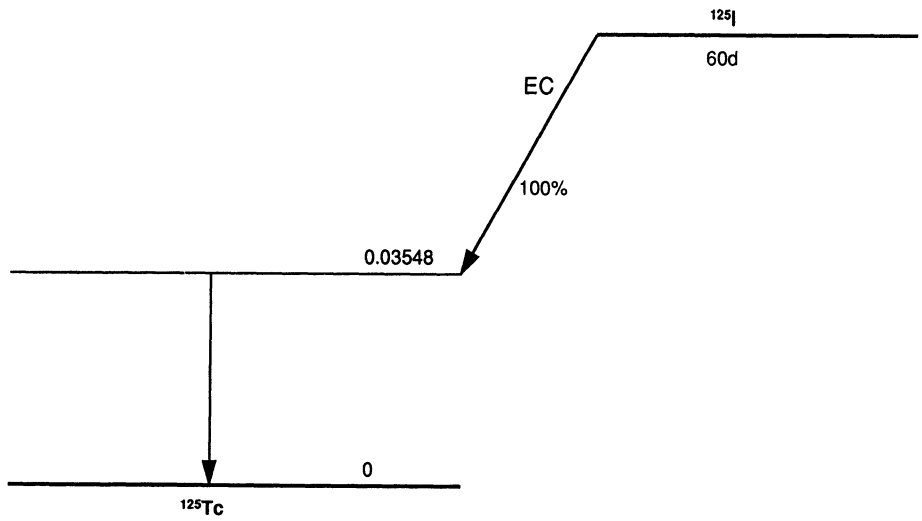

Figure G.13 Decay scheme of ^{125}I. Useful gamma energy for counting: 35 keV.

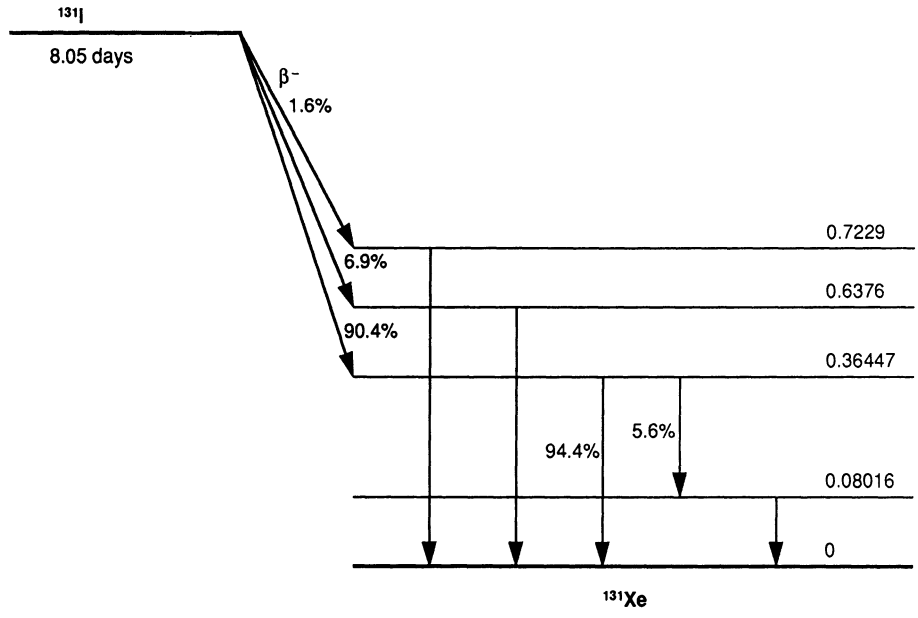

Figure G.14 Decay scheme of ^{131}I. Useful gamma energy for imaging: 364 keV. Useful energies for therapy: E_{max} 0.25, 0.33, 0.47, 0.61 and 0.81 MeV.

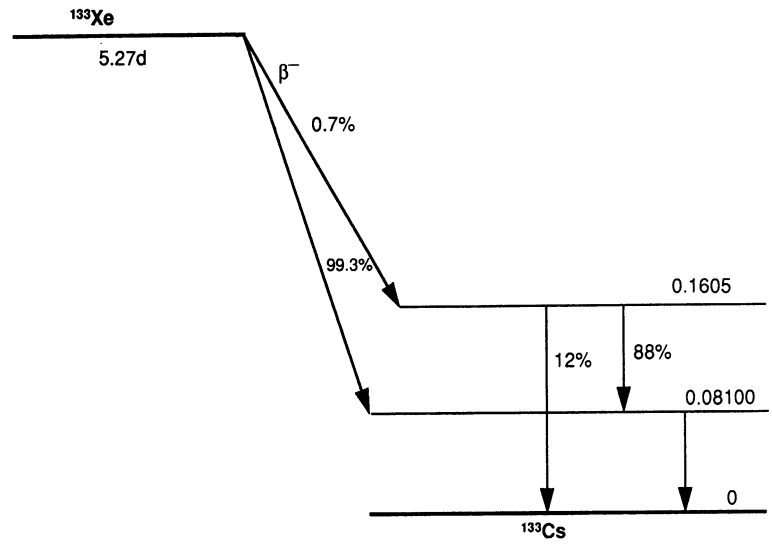

Figure G.15 Decay scheme of ^{133}Xe. Useful gamma energy for imaging: 81 keV.

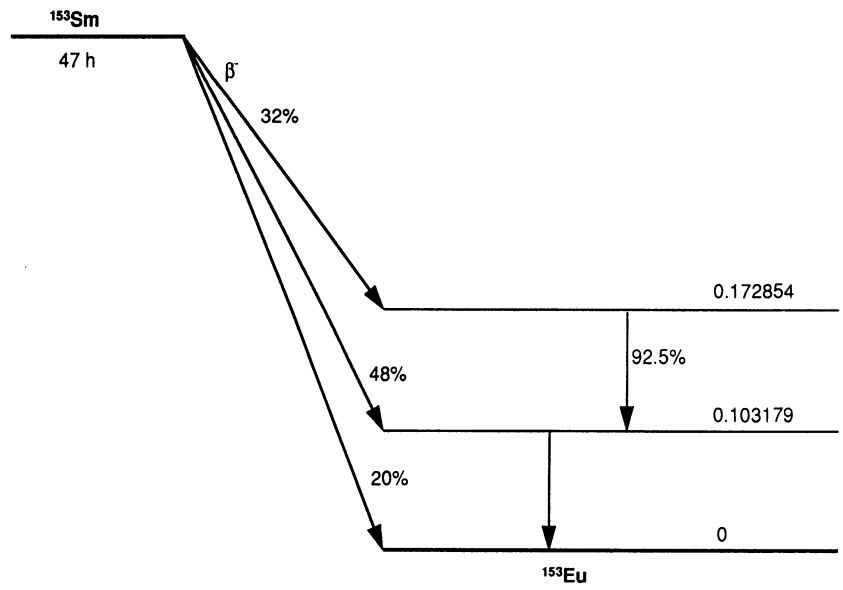

Figure G.16 Decay scheme of ^{153}Sm. Useful gamma energy for imaging: 103 keV. Useful beta energies for therapy: E_{max} 640, 710 and 810 keV.

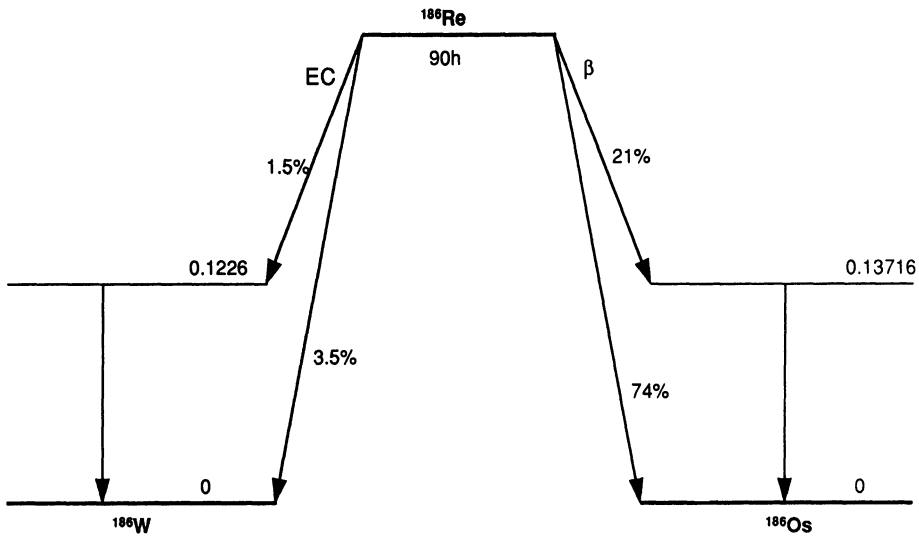

Figure G.17 Decay scheme of ^{186}Re. Useful gamma energy for imaging: 137 keV. Useful beta energy for therapy:E_{max} 1.07 MeV.

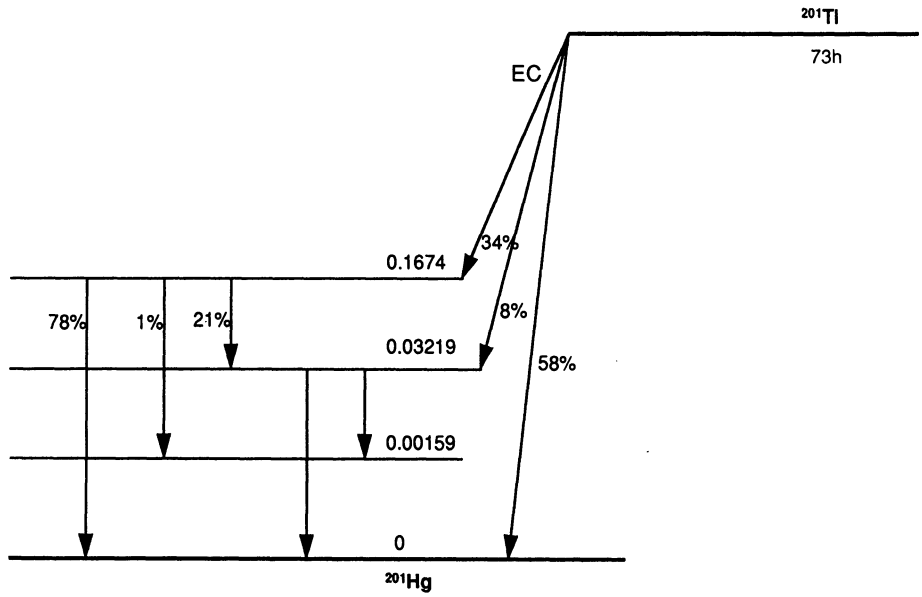

Figure G.18 Decay scheme of ^{201}Tl. Useful X-ray energy for imaging: 72 keV from Hg.

Appendix H

Physical properties and production modes of reactor-produced radionuclides

Radionuclide	Physical half-life	Decay mode	Principal gamma energy (keV) and abundance (%)	Production nuclear reaction
^{32}P	14.3 days	β^-	–	$^{32}S(n,p)^{32}P$
^{51}Cr	27.8 days	EC	320 (9%)	$^{50}Cr(n,\gamma)^{51}Cr$
^{59}Fe	45 days	β^-	1095 (56%), 1291 (44%)	$^{58}Fe(n,\gamma)^{59}Fe$
^{75}Se	120 days	EC	121 (17%), 136 (57%), 265 (60%), 280 (25%), 401 (12%)	$^{74}Se(n,\gamma)^{75}Se$
^{90}Y	64 h	β^-	–	$^{89}Y(n,\gamma)^{90}Y$
^{99}Mo	67 h	β^-	181 (7%), 740 (12%) 780 (4%)	$^{98}Mo(n,\gamma)^{99}Mo$ $^{235}U(n,f)^{99}Mo$
^{113}Sn	118 days	EC	390 (γ from ^{113m}In)	$^{112}Sn\ (n,\gamma)^{113}Sn$
^{125}I	60.2 days	EC	35(7%), 27 (X-rays 138%)	$^{124}Xe(n,\gamma)^{125}Xe$ $^{125}Xe \xrightarrow[17h]{EC} {}^{125}I$
^{131}I	8.05 days	β^-	284 (5.4%), 364 (82%) 637 (6.8%), 723 (1.6%)	$^{130}Te(n,\gamma)^{131}Te$ $^{235}U(n,f)^{131}I$
^{99m}Tc	6 h	IT	144 (90%)	$^{99}Mo \rightarrow {}^{99m}Tc$
^{133}Xe	5.3 days	β^-	81 (37%), Cs X-rays	$^{132}Xe(n,\gamma)^{133}Xe$
^{137}Cs	30 years	β^-	662 (85%), Ba X-rays	$^{235}U(n,f)^{137}Cs$
^{153}Sm	46.8 hours	β^-	70 (5.4%), 103 (28%)	$^{152}Sm(n,\gamma)^{153}Sm$
^{186}Re	89 hours	β^-, EC	137 (9%), Os X-rays	$^{185}Re(n,\gamma)^{186}Re$
^{198}Au	2.7 days	β^-	412 (95%)	$^{197}Au\ (n,\gamma)^{198}Au$

Appendix I

Physical properties and production modes of cyclotron-produced radionuclides

Radionuclide	Physical half-life	Decay mode	Principal gamma energy (keV) and abundance (%)	Production nuclear reaction
^{11}C	20.3 min	β^+	511 (200%)	$^{11}B(p,n)^{11}C$ $^{10}B(d,n)^{11}C$
^{13}N	10.0 min	β^+	511 (200%)	$^{12}C(d,n)^{13}N$ $^{16}O(P,\alpha)^{13}N$
^{15}O	123 s	β^+	511	$^{14}N(d,n)^{15}O$
^{18}F	109.7 min	β^+	511 (194%)	$^{16}O(\alpha,pn)^{18}F$ $^{16}O(^3He,n)^{18}F$
^{52}Fe	8.2 h	β^+, EC	511 (112%), 165 (100%)	$^{50}Cr(\alpha,2n)^{52}Fe$ $^{52}Cr(^3He,3n)^{52}Fe$
^{57}Co	270 days	EC	127 (87%), 136 (9%)	$^{56}Fe(d,n)^{57}Co$
^{58}Co	72 days	EC, β^+	551 (30%), 810 (99%)	$^{55}Mn(\alpha,n)^{58}Co$
^{67}Ga	77.9 h		93 (40%), 184 (24%) 296 (22%), 388 (7%)	$^{67}Zn(p,n)^{67}Ga$ $^{65}Cu(\alpha,2n)^{67}Ga$
^{68}Ga	68 min	β^+ EC (12%)	511 (176%)	^{68}Ge – decay $^{68}Zn(p,n)^{68}Ga$
^{68}Ge	275 days	EC	Ga-X-rays	$^{64}Zn(\alpha,n)^{68}Ga$
^{81m}Kr	13 s	IT	190 (65%)	^{81}Rb – decay
^{81}Rb	4.7 h	β^+ (13%) EC (87%)	253 (26%), 450 (26%), 511 (26%)	$^{79}Br(\alpha,2n)$
^{111}In	2.8 days	EC	173 (89%), 247 (94%)	$^{111}Cd(p,n)^{111}In$ $^{109}Ag(\alpha,2n)^{111}In$
^{123}I	13.3 h	EC	159 (83%)	$^{122}Te(d,n)^{123}I$
^{201}Tl	74 h	EC	80 (95% Hg X-rays) 167 (8%)	^{201}Pb decay $^{203}Pb(p,3n)^{201}Tl$

Index

Radionuclides are placed as the *element* is spelled: thus ^{51}Cr will be found before Cisplatin, and ^{59}Fe after Iodine.
Some radiopharmaceuticals are double-entered: e.g. ^{198}Au is found under both A and G.